Experimental Study and Computational Analysis of Piano Key Weir

A Thesis Submitted

in partial fulfilment of the requirements for the award of the degree of

DOCTOR OF PHILOSOPHY

In

CIVIL ENGINEERING

By

DEEPAK SINGH

(Roll. No. - 2K18/Ph.D./CE/02)

Under the supervision of

Prof. Munendra Kumar

DEPARTMENT OF CIVIL ENGINEERING

DELHI TECHNOLOGICAL UNIVERSITY

SHAHBAD DAULATPUR, BAWANA ROAD, DELHI - 110042 (INDIA).

2022

DELHI TECHNOLOGICAL UNIVERSITY

(Formerly Delhi College of Engineering, Since 1941)

Shahbad Daulatpur, bawana road, Delhi- 110042

DECLARATION

I hereby declare that the research work presented in this thesis entitled "Experimental study and Computational Analysis of Piano Key Weir" is original and carried out by me under the supervision of Prof. Munendra Kumar, Professor, Department of Civil Engineering, Delhi Technological University, Delhi, and being submitted for the award of Ph.D. degree to Delhi Technological University, Delhi, India. The content of this thesis has not been submitted either in part or whole to any other university or institute for awarding any degree or diploma.

Date: 18/08/2022 **(Deepak Singh)**

Place: DTU, Delhi. **Roll. No.– 2K18/Ph.D./CE/02**

DELHI TECHNOLOGICAL UNIVERSITY

(Formerly Delhi College of Engineering, Since 1941)

Shahbad Daulatpur, bawana road, Delhi- 110042

Date: - 18/08/2022

CERTIFICATE

This is to certify that the Ph.D. thesis entitled "Experimental study and Computational Analysis of Piano Key Weir" is being submitted by Mr. Deepak Singh, for the fulfillment of the requirements for the award of the degree of Doctor of Philosophy in Civil Engineering to the Department of Civil Engineering, Delhi Technological University, Delhi, India. He has a bonafide record of original research work carried out by him under my guidance and supervision. The results embodied in this thesis have not been submitted to any other university or institution for the award of any degree or diploma.

Prof. Munendra Kumar

Supervisor

Department of Civil Engineering

Delhi Technological University

Delhi – 110042.

ACKNOWLEDGEMENTS

I am grateful to my thesis advisor Prof. Munendra Kumar, Professor, Department of Civil Engineering, Delhi Technological University, for his sincere admonishment, indelible inspiration, consistent encouragement, and guidance, as well as his enormous patience and support throughout the investigation of the current research and the preparation of this manuscript. Words cannot express my heartfelt gratitude for his benevolent guidance, wholehearted encouragement, critical appreciation in the execution of my work, and all the trust he had in my ability, which is primarily responsible for my current accomplishment. It is no exaggeration to say that sir is like a true friend, motivator, and philosopher and guided me at all essential and crucial stages during my degree program.

With stupendous ecstasy and profundity of complacency, I pronounce utmost gratitude to Sh. Kewal Singh, retired senior lab technician, Mr. Anil Agnihotri, Mr. Sunil Tirkey, lab technician, and Nitesh, Inder Singh, lab attendant, Department of Civil Engineering, for their valuable help. I also express my gratitude to my colleagues Saurabh Sah, Dinesh Kumar Reddy, Rahul Kumar Meena, Inderjeet Singh, Abhishek Paswan, Ruchika Dabas, Geeta Devi, Vijay Kaushik, Gaurav Kumar Nain, Vishal Pandey, Shailesh Kumar Gupta, Neha Rani, and Noopur Awasthi for providing me helpful advice, kind cooperation, and friendly discussion at various stages of the work.

My inexplicable gratitude goes to the Head of the Civil Engineering Department (Prof. Vijay K. Minocha), the DRC Chairman (Prof. K.C. Tiwari), and all the faculty members, especially Prof. Nirendra Dev, Prof. A. K. Shrivastava, Dr. Shilpa pal, Prof. Raju Sarkar, Dr. Ritu Raj, and Mr. Hrishikesh Dubey for providing me sensible guidance, faultless planning, helpful advice, and kind cooperation at various stages of the work. I am also thankful to the lab staff and office staff of the Civil Engineering Department for providing the kind cooperation and necessary facilities to carry out the study and grateful to the University for providing financial assistance and support during my degree program.

Finally and most importantly, I would like to express my love and thanks to my parents for their encouragement and support, who stood by me like a rock and provided constant motivation during the years. My family members have been extremely patient throughout this process and have cheerfully sacrificed time that was rightfully theirs.

At the end of this Ph.D. research, I want to thank all the people who helped, supported, and encouraged me all these four years.

Delhi **(Deepak Singh)**
August, 2022 **Author**

ABSTRACT

Piano Key Weir (PKW) is a further development of the well-known nonlinear labyrinth weir. Thus PKW is a similar type of labyrinth weir, which has a zig-zag shape in the plan, except that PKWs have a repeating rectangular profile. It replaces linear overflow structures by increasing the unit discharge at the same head and channel or spillway width. As a result, it is a viable option for newly constructed hydraulic systems and can significantly increase the evacuation and storage capacity of several existing hydraulic structures at a low cost. The hydraulic structures used as discharge measuring devices during flood release or open channel applications are free-to-flow spillways or weirs. PKW is a cost-effective solution for rehabilitation and new dam projects with a high level of constraints, for instance, limited space, small reservoir level, high specific flood discharge, etc. It has several advantages for preferring this structure instead of the labyrinth weir: it has less footprint area than other rectilinear labyrinth weirs, making it suitable for installation on top of existing or new gravity dams. It also has the inclined bottom of the keys instead of the horizontal-vertical arrangement of labyrinth weirs, improving their hydraulic efficiency.

The main objective of this study is to examine the effect of the different geometrical parameters associated with PKW on its discharge carrying capacity by experimental and computational investigation. The study also deals with the various aspects of PKWs, including the energy dissipation, aeration performance, and other geometrical elements across the different types of the PKW. Moreover, soft computing techniques used the experimental data to generate the empirical equation to estimate the discharge capacity of the PKW correctly. A total of 60 laboratory-scale model configurations were examined and assessed to understand better the effects of PKW geometry on discharge efficiency, energy dissipation across the weir, and weir aeration performance. As a result, the impact of the following PKW geometries and modifications on discharge efficiency has been partially isolated: magnification ratio, inlet-to-outlet key slopes ratio, inlet-to-outlet key width ratio, upstream and downstream apex overhangs, and raising the crest elevation via a parapet wall. Based on the findings of this study, it was concluded that the discharge efficiency of the PKW increased or decreased with geometrical variations. Furthermore, the hydraulic performance of various types of PKW in terms of energy dissipation and aeration performance was investigated. It was concluded that Type-C dissipates more energy than type-A and type-B, but type-A has a higher aeration efficiency than type-B and type-C. However, type-B PKW has shown the most efficient PKW among the three.

TABLE OF CONTENTS

DECLARATION……ii

CERTIFICATE……..iii

ACKNOWLEDGEMENTS……...iv

ABSTRACT……v

TABLE OF CONTENTS…… vi

List of Figures……ix

List of Tables……....xii

List of Abbreviations……xiii

CHAPTER 1 INTRODUCTION……1

1.1 General……..1

1.2 Spillways ……..1

1.2.1 Service Spillways……....2

1.2.2 Auxiliary Spillways……2

1.2.3 Emergency Spillways……..3

1.3 Weirs……3

1.4 Piano Key Weirs……3

1.5 Types of Piano Key Weirs……5

1.6 Objectives of the Present Study……6

1.7 Organization of Thesis……..7

2 CHAPTER 2 REVIEW OF LITERATURE……..8

2.1 General……8

2.2 Piano Key Weir (PKW)……9

2.3 Physical Modelling……..11

2.4 Numerical Modelling……..22

2.5 Computational Analysis/ Machine Learning Techniques……...23

2.6 Literature GAP……25

2.7 Motivation for Present Work……..26

2.8 Conclusion……..27

CHAPTER 3 MATERIALS AND METHODOLOGY…….....28

3.1 General……28

3.2 Materials and Methods……28

3.2.1 Experimental Setup……..28

3.2.2 Model Fabrication……30

3.3 Hydraulic Behaviour of PKW…….30

3.3.1 Geometric Parameters……..31

3.3.2 Discharge Equations……32

3.3.3 Dimensional Analysis……..33

3.4 Design Methodologies/Parameters……..33

3.4.1 Proposed standard reference designs by the researchers based on physical modeling.34

3.5 Computational Analysis……..38

3.5.1 Application of GEP……..39

3.5.2 Fitness function and selection……..39

3.5.3 Replication……...41

3.5.4 Mutations……..41

3.5.5 Transposition and insertion sequence elements……...41

3.5.6 Recombination……42

3.6 Some other Important Design Aspects……42

3.6.1 Parapet walls, crest shape, and nose……42

3.6.2 Energy Dissipation over the PKW……..43

3.6.3 Aeration……..46

3.7 Conclusion……..47

CHAPTER 4 RESULTS AND DISCUSSION…….....……...48

4.1 General……48

4.2 Experimental Results and Discussion……48

4.2.1 Flow Behaviour of PKW……..48

4.3 Geometric Influences on the Discharge Capacity of PKWs……..49

4.3.1 Magnification ratio (*L/W*)…….50

4.3.2 Wier Height (*P*)……53

4.3.2.1 Effect of the PKW's sloping key bottom on its discharge capacity with Horizontal Bed……54

4.3.2.2 Effect of the PKW's sloping key bottom on its discharge capacity with Sloping Bed……61

4.3.3 Inlet to outlet key width ratio (W_i/W_o)……65

4.3.4 Overhangs portions (B_i, B_o)……75

4.3.5 Numbers of Cycles (*N*)……76

4.4 Energy Dissipation capacity……79

4.4.1 Effects of the cyclic variation (*N*) on energy dissipation…….80

4.4.2 Effects of the relative length (*L/W*) on energy dissipation……91

4.4.3 Effects of the relative width ratio(W_i/W_o) on energy dissipation…….106

4.4.4 Sensitivity Analysis……109

4.5 Aeration Capacity of the PKW……..115

4.6 Conclusion……121

CHAPTER 5 SUMMARY AND CONCLUSIONS .....…….…….122

5.1 SUMMARY……..122

5.2 RECOMMENDATION FOR FURTHER WORK……...125

LIST OF PUBLICATIONS……126

References……...127

List of Figures

Figure: 1.1 PKW types Type-A, Type-B, Type- C and Type- D (Adapted *from Lempérière et al. 2011*)…….....6

Figure: 3.1 (a) & (b) Schematic plan and side view of the experimental setup……..29

Figure: 3.2 Fundamental parameters of a PKW – 3D view (*Pralong et al. 2011*)…….31

Figure: 3.3 Fundamental parameters of a PKW – plan view (left) and cross-section (right) (Pralong et al. 2011)……...31

Figure: 3.4 Reference design for PKW Type-A – plan view (left) cross sections (right) (ICOLD 2010)……...34

Figure: 3.5 The flow chart of the Gene Expression Algorithm (Adapted from (Ferreira 2001))……40

Figure: 3.6 Schematic plot for total energy head measurement……44

Figure: 4.1 Flow patterns over PKW. ……...49

Figure: 4.2 C_{DL} vs. H_t/P for different L/W ratios of different types (type-A, type-B and type-C) PKW.……52

Figure: 4.3 (a) &(b) Variation of discharge [Q] with [H_t/P] and [H_t]……56

Figure: 4.4 Surface tension effects to jet trajectory formation from (a) to (d) on Largest models and from (i) to (iv) on Smallest models…….57

Figure: 4.5 (a) & (b) Variation of discharge coefficient [C_{DL}] with [H_t/P] and [Q]……58

Figure: 4.6 Variation of discharge enhancement ratio [r] with [H_t/P]……59

Figure: 4.7 Comparison of discharge computed using an equation given by *Machiels et al. (2011c)* and experimental results of the present study……60

Figure: 4.8 Variation of discharge enhancement ratio [r] with various inlet-outlet key slopes [S_i=S_o] of PKW…….61

Figure: 4.9 Variation of coefficient of discharge [C_{DL}] with [H_t/P] on different bed slopes for different inlet-outlet key slopes……64

Figure: 4.10 Fabricated model Geometry of PKW (a) Plan view (b) PKW with constant Parapet Wall……..66

Figure: 4.11 Variation of discharge Q [L/s] with [H_t/P] and [H_t]……68

Figure: 4.12Variation of discharge coefficient of discharge [C_{DL}] with [H_t /P]……69

Figure: 4.13 Variation of discharge coefficient [C_{DL}] with the inlet to outlet width ratio [W_i/W_o]……..70

Figure: 4.14 Expression Tree (*ET*) for GEP formulation……...73

Figure: 4.15 Comparison between observed and predicted discharge coefficient for the different data phases (training and testing phases)…….74

Figure: 4.16 Comparison curve among the discharge efficiencies of the different types of PKWs……76

Figure: 4.17 Comparison curve between the C_{DL} vs. H_t/P of the different types (Type-A, Type-B and Type-C) of PKWs for different cyclic variations…….79

Figure: 4.18 (i)Relative energy dissipation [E_L=(E_1-E_2)/E_1] with respect to the (a) headwater ratio [H_t/P] and (b) the unit discharge [q] for different cycles [for L/W=5] for Type-A……82

Figure: 4.18 (ii) Relative residual energy [E_2/E_1] with respect to (c) the headwater ratio [H_t/P] and (d) the unit discharge [q] for different cycles [for L/W=5] for Type-A……83

Figure: 4.19 (i) Relative energy dissipation [E_L=(E_1-E_2)/E_1] with respect to the (a) headwater ratio [H_t/P] and (b) the unit discharge [q] for different cycles [for L/W=6] for Type-A……84

Figure: 4.19 (ii) Relative residual energy [E_2/E_1] with respect to the (c) headwater ratio [H_t/P] and (d) the unit discharge [q] for different cycles [for L/W=6] for Type-A……..85

Figure: 4.20 (i) (Relative energy dissipation [E_L=(E_1-E_2)/E_1] with respect to (a) the headwater ratio [H_t/P] and (b) the unit discharge [q]) for [L/W=5] for Type-B…….....86

Figure: 4.20 (ii) (Relative residual energy [E_2/E_1] with respect to (a) the head water ratio [H_t/P] and (b) the unit discharge [q] for [L/W=5] for Type-B……87

Figure: 4.21 (i) (Relative energy dissipation [E_L=(E_1-E_2)/E_1] with respect to (a) the head water ratio [H_t/P] and (b) the unit discharge [q] for [L/W=6] for Type-B…….88

Figure: 4.21 (ii) (Relative residual energy [E_2/E_1] with respect to (a) the head water ratio [H_t/P] and (b) the unit discharge [q] for [L/W=6] for Type-B……..89

Figure: 4.22 (i) Relative energy dissipation [($\Delta E/E_1$] with respect to (a) the head water ratio [H_t/P] and (b) the unit discharge [q] for diffirent cycles (N).……...94

Figure: 4.22 (ii) Relative residual energy [E_2/E_1] with respect to (a) the headwater ratio [H_t/P] and (b) the unit discharge [q] for different cycles (N)……97

Figure: 4.23 (i) (Relative energy dissipation [$E_L=(E_1-E_2)/E_1$] with respect to (a) the head water ratio [H_t/P] and (b) the unit discharge [q] for [L/W=5, 6]……..100

Figure: 4.23 (ii) (Relative residual energy [E_2/E_1] with respect to (a) the head water ratio [H_t/P] and (b) the unit discharge [q] for [L/W=5, 6]……103

Figure: 4.24 (i) (Relative energy dissipation [$E_L=(E_1-E_2)/E_1$] with respect to (a) the head water ratio [H_t/P] and (b) the unit discharge [q] for [L/W=5, 6]……..104

Figure: 4.24 (ii) (Relative residual energy [E_2/E_1] with respect to (a) the head water ratio [H_t/P] and (b) the unit discharge [q] for [L/W=5, 6]……105

Figure: 4.25. (i) Relative energy dissipation [$E_L=(E_1-E_2)/E_1$] with respect to (a) the head water ratio [H_t/P] and (b) the unit discharge [q] for different Wi/Wo ratios for Type-A…..107

Figure: 4.25. (ii) Relative energy dissipation [$E_L=(E_1-E_2)/E_1$] with respect to (a) the head water ratio [H_t/P] and (b) the unit discharge [q] for different W_i/W_o ratios for Type-B…..108

Figure: 4.26 (i) & (ii) Type-A and Type-B PKW after using the steps at the outlet key, respectively (a) Laboratory model (b) Sectional view……110

Figure: 4.27 Flow regimes above stepped weir: (a) Nappe Flow, (b) Transition Flow & (c) Skimming Flow……...111

Figure: 4.28 (i) (Relative energy dissipation [$E_L=(E_1-E_2)/E_1$] with respect to (a) the head water ratio [H_t/P] and (b) the unit discharge [q] for type-A……113

Figure: 4.28 (ii) (Relative energy dissipation [$E_L=(E_1-E_2)/E_1$] with respect to (a) the head water ratio [H_t/P] and (b) the unit discharge [q] for type-B……114

Figure: 4.29 Laboratory Schematic PKW Aeration Apparatus……...115

Figure: 4.30 Flow pattern over PKW……116

Figure: 4.31 Variation in Aeration Efficiency with Discharge and Drop height for (a)Type-A, (b) Type-B, and (c) Type-C Piano Key Weirs……118

Figure: 4.32 Comparison of aeration efficiency curves of various PKWs models with drop heights……120

List of Tables

Table 3. 1 Different parameters related to the PKW……...36

Table: 4. 1 Range of Data collected for different *L/W* ratios of Different types of PKWs….50

Table: 4.2 Range of data collected for different inlet-outlet key bed slopes [type-A PK weirs]…….55

Table: 4.3 Q comparison for corresponding Ht between the present section and published data by *Machiels et al. (2011c)*……..60

Table: 4. 4 Range of Data collected for different Wi/Wo ratios……67

Table: 4. 5 Functional set and operational parameters used in the GEP model……72

Table: 4.6 Performance evaluation of predicted E_2/E_1 by GEP model for training and testing dataset……75

Table: 4.7 Range of Data collected for different overhang (B_i/B_o) ratios…….76

Table: 4.8 Range of Data collected for different cyclic count (N) of different types of PKWs……77

Table: 4. 9 Range of data collected for energy dissipation of different types (type-A, type-B & type-C) of PKWs……81

Table: 4. 10 Ranges of data were collected for aeration performance of different types of PKWs……..117

List of Abbreviation

A	Surface area associated with the volume (V) of water over which the transfer occurs
B	Length of side weir ($B_i + B_b + B_o$)
B_b	Base length
B_i	Length of overhang portions at the inlet side
B_o	Length of overhang portions at the outlet side
C	DO concentration
CC	Correlation Coefficient
C_d	DO concentration d/s of hydraulic structure
C_{DL}	Coefficient of discharge along developed crest length
C_S	DO concentration at the saturation level
C_u	DO concentration u/s of hydraulic structure
E	Oxygen transfer or aeration efficiency
E_i	Specific energy at section 'i'
F_r	Froude Number
g	Gravitational Acceleration
H	Downstream water pool height
h_s	Height of the one step
H_t	Total head
h	Drop/fall height
h_t,	Piezometric head
K_L	Coefficient of liquid-mass transfer
l_s	Length of one step
L	Total developed crest length
L_{cy}	Developed crest length of one cycle
m	Oxygen deficit ratio
MAE	Mean absolute error
$MAPE$	Mean absolute percentage error
N	Number of cycles
P	PKW height

P_d	Dam height
Q	Discharge over the PKW
Q_{PKW}	Discharges flow over the Piano Key Weir
r	Enhancement Ratio
R	Height of parapet wall
R^2	Determination coefficient
R_e	Reynolds Number
$RMSE$	Root mean square error
S_i	Inlet key slope
S_o	Outlet key slope
t	Time
T	Temperature during measurement in ^{0}C.
T_s	Thickness of the Piano Key Weir sidewall
V_t	Average Velocity
$V_t^2/2g$	Approach velocity head
W	Channel width/ Width of PKW
W_{cy}	Width of one cycle
W_e	Weber Number
W_i	Inlet Key Width
W_o	Outlet Key Width
X	Distance of measurement section from the lateral centreline of the PKW.
ρ	density of flowing fluid,
μ	dynamic viscosity, and
σ	surface tension of flowing fluid

CHAPTER 1 INTRODUCTION

1.1 General

Free flow spillways and weirs are the hydraulic structures that can be used as discharge measuring devices on existing as well as newly constructed dam structures, during flood release or for open channel applications. The control of floods generally assures the passage or release of floods without creating any hazardous incidents on dam structures. Nevertheless, its cost represents a significant part of the total cost of the dam.

Dams play an indispensable role in the betterment of any country. It is a multipurpose structure that contributes to supplying water for domestic purposes, generation of hydroelectric energy, navigation, and irrigation, as well as helps in flood control during the rainy season. Most of the dams in India are 30 to 40 years old and require rehabilitation because their storage capacity has been decreasing day by day due to siltation or sedimentation of the reservoir. Some of them face the problem of submerging. Thus, the issue of storage loss owing to the siltation can be addressed by heightening the sill of spillways that permit additional storage space. As far as the problem of submerging is concerned, building an ungated spillway or a weir over the dam structure can be an effective remedy. There are numerous ways to remedy the downstream hazardous but ungated spillway, and weirs are the essential hydraulic structures over the dams.

1.2 Spillways

A spillway serves as a control structure and is usually constructed perpendicular to the direction of water flow in a dam site. Spillways operate as safety valves for dams. Thus, it becomes imperative that they be appropriately designed and have sufficient capacity to effectively dispose of the entire quantity of surplus water, despite the arrival of the worst design flood. They regulate the water flow on the downstream side of the wall and prevent the dam from overtopping and possible failure, especially at the time of wet periods or flooding. Spillway design considers the allowance of excess water to dispose of from the upstream side of the dam to the downstream without threatening any damage or hazard to the main body of the dam structure. Spillways release the surplus water that exceeds the whole reservoir level (FRL) of the dam structure, thus safeguarding the dam's downstream face against erosion resulting from flowing waters. The high velocity of water flowing over the spillway, owing to the dams' energy head, significantly contributes to damage and erosion

downstream. To ensure that this does not happen, the design of these hydraulic structures should have a provision for energy dissipaters and stilling basins. These are crucial points that one should bear in mind while designing or building such kinds of hydraulic structures. **(SK. Garg, 2010; Subramanya, 2010)**

Based on the frequency of use, there are three primary categories of spillways that are typically employed by Reclamation:

a) Service spillways

b) Auxiliary spillways

c) Emergency spillways

Here, service spillways are those designed to pass floods with a common or frequent occurrence. The auxiliary spillways are those designed to operate once the size of the flood exceeds those passable by a service spillway.

1.2.1 Service Spillways

A service spillway provides continuous or frequent release from a reservoir without incurring significant damage to the dam body due to releases up to and including the maximum design discharge. Typically very strong, these spillways are erosion-resistant structures that mostly consist of cast-in-place reinforced concrete and riprap channel protection. Service spillways may operate alone or be supplemented by an auxiliary spillway. They may be gated or ungated, allowing for greater control of the flow downstream, and can contribute to an effective reduction of the flood peaks when early warnings are available in the case of a gated service spillway. On the other hand, ungated spillways are generally favored for their greater reliability; However, the condition of the project depends on what is downstream of the dam. (**US. Bureau of Reclamation August 2014)**

1.2.2 Auxiliary Spillways

An auxiliary spillway is a secondary spillway that is used infrequently (enhancing a service spillway discharge capacity). During their operation, auxiliary spillways could undergo significant erosion or structural damage due to the water releases. They may be less solid and erosion-resistant. They may either accompany service spillways or be built in conjunction with flooding outlets (in which case, the requirement of service spillways is not there). Auxiliary spillways are especially useful in case of the failure of the service spillway. (**SANCOLD, 1991**).

As per their characteristic features, the various kinds of spillways are listed below **(Vischer and Hager, 1998; Garg, 2010)**:

- Free over fall or straight drop spillway
- Ogee or overflow spillway
- Chute spillway
- Side channel spillway
- By wash spillway
- Labyrinth spillway and
- Piano Key Weir

1.2.3 Emergency Spillways

Emergency spillways offer additional protection against the overtopping of a dam body. They are designed to serve during unusual or extreme conditions. This may include misoperation of the service spillway or outlet works during extensive, small floods (such as the Probable Maximum Flood) or other emergency conditions. As with auxiliary spillways, there could be some significant structural damage during operation, and erosion may be expected due to water releases. It has the least strong and erosion-resistant structure.

1.3 Weirs

Weirs are similar to notches but have a considerable amount of thickness in the flow direction; thus, their discharge coefficient is less than that of a notch. A weir is an artificial barrier that regulates or measures the flow rate and water depths in a watercourse. The construction of a weir structure across any water body enhances the water surface level on the upstream side and hence increases the storage capacity of the watercourse. The capacity of a given weir or spillway refers to the capable discharge for a given head of flow over its crest. There are various uses of the weir or spillway across any water body. We can manage the water level, measure the rate of flow over the crest, create a pool from which to pump or divert water and help channel stabilization, etc. **(Ghare *et al.* 2008)**

1.4 Piano Key Weirs

The search for an optimal shape of free-flow spillways or weirs, which possesses a high degree of performance at a low cost, is continuously going on. Numerous studies have aimed at reducing the submergence problem by using different shapes of weirs. In some studies,

researchers have made use of a modified shape of the weir, named the Labyrinth, which has resulted in the conception of a new shape of a nonlinear weir. A special category of the labyrinth weir, which can serve as a side weir, is at the core of research investigations from the last decade. This new shape of the weir, designated as Piano Keys Weir (PKW), is a modification of the well-known nonlinear labyrinth weir, having a zig-zag shape in the plan, except that PKWs have a repeating rectangular shaped profile in the plan. Most experimental models are studied to determine the coefficient of discharge. The zig-zag shape of the Piano Key Weir permits multiplying the crest length of a given spillway length, increasing discharge capacity without expanding the submergence area on the dam's upstream side. Piano Keys Weir (PKW) is the replacement of linear overflow structures by increasing the unit discharge at the same head and same channel or spillway width; thus, it represents an effective alternative for most newly constructed dam structures and can increase the capacity of evacuation and or the stocking of several existing dams at the low cost. It (PKW) has several advantages over the labyrinth weirs are:

1. It has less footprint area than other rectilinear labyrinth weirs, making it convenient for installation on top of new or existing gravity dams and earth dams. **(Lempérière and Ouamane 2003)**
2. It offers a higher discharge capacity, mainly due to the fact that the development crest length is greater than the weir width in the transverse direction. In addition, it has the inclined bottom of the keys, as opposed to the horizontal-vertical arrangement observed in the case of Labyrinth Weirs, it enhances their hydraulic efficiency **(Laugier *et al.,* 2009, Anderson and Tullis, 2011, 2012).**
3. It has a less complex structure, is easy to construct using local resources available in all regions, and it requires less quantity of reinforcement relative to labyrinth weirs.

The best alternative for improving the coefficient of discharge (C_d) of the PKW is to increase the length of the weir crest without altering the channel width. Labyrinth and PKWs are folded in plan-view, and they offer this advantage and can be used as a side weir.

The concept of the PKW was explicitly developed for free-surface flow control structures having a spillway footprint that was relatively small. There isn't a significant or standard design procedure that is available or widely accepted. This is because many researchers addressed the problem of hydraulic design of PKWs on tests performed on scale models (physical) and numerical simulations contributed to increased knowledge. Several studies have been carried out in the last ten to fifteen years **(Anderson and Tulli, 2011; Kabiri-**

Samani & Javaheri, 2012; Erpicum *et al.*, 2014; Machiels *et al*., 2014 & Crookston *et al*., 2019) based on geometric development to identify the hydraulic behavior of PKW, and now it is well understood. The different worldwide studies based on the geometric evolution and hydraulics of PKW have been summarised by **Erpicum *et al.* (2011, 2013 & 2017)** with three reference books. However, the transient behaviour of PKWs is not so well comprehended and is the major focus of several ongoing studies.

1.5 Types of Piano Key Weirs

Preliminary models have been used in experiments performed at the LNH Laboratory, France (1999) and at the Roorkee University, India, and Biskra University, Algeria, in 2002. Thereafter, a few shapes of the weir models were chosen based on the rectangular layout that somewhat resembled the shape of piano keys; they were termed "Piano Key Weir." It has a bottom that is inclined at the upstream and downstream parts (the part where the flow enters is known as the inlet, and the other part the outlet) and reduced width of the elements. In 2003, a detailed study at the Biskra University involved several tests that were carried out on selected shapes, while some of the tests used a very wide flume at the LNH Lab. This research on various shapes helped lay the groundwork for optimizing flow growth in accordance with the ratios between the length, breadth, depth, and shape of the components, particularly in accordance with the ratio (length of walls/length of spillway). To select the most attractive solutions, they also studied the impact of various overhangs, particularly structural design and construction facilities. **Lempérière and Ouamane (2003)** presented two solutions based on the Hydraulic and structural data. Type-A, having similar upstream and downstream overhangs, favors using precast concrete elements, suitable for specific flow up to 20 $m^3/s/m$.

For this reason, this solution is preferred for improving many existing spillways. The Type-B solution only has the upstream overhang. Relevant savings fair at approximately ten percent higher than solution Type-A and the structural loads are observed to be less for high specific flows. It could, thus, serve as a very lucrative choice for many large dams in the future.

Although other designs based on the same principles may be more efficient, the relative cost savings probably won't be very different. According to local conditions within each country, employing one or two essential solutions could be intriguing, and then standardizing the drawing for various specific flows. Type-A has upstream and downstream overhangs, while Type-B has no downstream overhang but a larger upstream one. This solution has two advantages and one drawback:

1. The specific flow is higher than model A, keeping the length, height, and cost as same.
2. The structural stresses are relatively lower for upstream overhangs. This is because the weight of the concrete reduces the impact of the water pressure added to it. However, model B does not favor using precast elements.

Type-B is likely more attractive for new dams having large existing spillways and high specific flows. After that, many researchers classified the PKWs based on geometry, mainly into four types (Type A, B, C, and D). A Type-A PKW has symmetrical keys relative to a transverse centerline axis. Type-B features cantilevered apexes on the upstream (outlet keys) and vertical apex walls on the downstream (inlet keys). Type-C is the opposite of Type B, with the cantilevered apexes downstream. Type-D is a rectangular labyrinth weir (vertical apex walls) **Anderson 2011, Leite Ribeiro *et al*. 2012).**

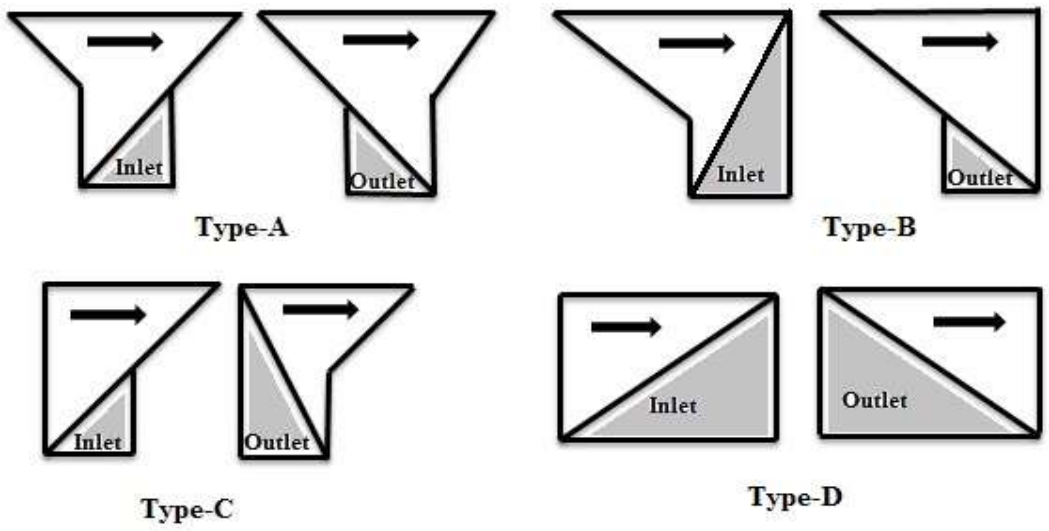

Figure: 1.1 PKW types Type-A, Type-B, Type- C and Type- D (Adapted from Lempérière et al. 2011)

1.6 Objectives of the Present Study

The primary aim of this study is to investigate the performance of PKW with the help of experimental research and compare the results using computational analysis. The specific objectives of this study are as follows:

1. To develop discharge vs. head relationship for different cycles and shapes of Piano Key Weir from the hydraulic point of view.
2. To examine the flow patterns of the approach flow for different geometries of Piano Key Weir.
3. To study the downstream energy dissipation of different types of Piano Key Weir.

4. To examine the aeration performances of the different types of the Piano Key Weir.

1.7 Organization of Thesis

This thesis contains five chapters: **Chapter 1** presents a brief introduction to the different types of hydraulic structures and Piano Key Weir, along with the objective and scope of the present study. **Chapter 2** presents a review of relevant literature dealing with the design and evaluation of the Piano Key Weir. **Chapter 3** describes the materials used in fabricating the PKW models, the experimental setup, detailed specifications, and the design considerations related to the PKW. Then the developed relationship between the coefficient of discharge vs. head and various design aspects that influence the discharge efficiency of the weir is also presented. **Chapter 4** contains the present study's findings and their practical application based on multiple goals, i.e., the hydraulic behavior of PKW, the various geometrical parameters affecting hydraulic behavior and design aspects of the PKW, energy dissipation, and aeration performance of the PKW. The last chapter discusses the summary and conclusions of the thesis, and what could be further possibilities were also mentioned in **Chapter 5**.

2.1 General

The Piano Key Weir (PKW) represents an effective solution for the increase in the storage capacity and the capacity to evacuate floods from the majority of the existing dams and newly constructed hydraulic structures. Many researchers found that the PKW weir is an optimal shape for free-flow spillways or weirs, which possesses a high degree of performance at a low cost. This concept of a new weir considerably reduces the global price of the new dams and enhances the storage capacity and safety of many existing reservoirs.

In recent times, researchers have given due consideration to making scale models for their experimental studies by considering the economy and hydraulics of different weirs. Free-crest spillways have an appreciable hydraulic efficiency and are safe while operating over dams or other hydraulic structures, owing to the fact that their discharge capacity is proportional to the developed crest length. The traditional labyrinth weir spillways have been studied and utilized for a long time among these structures, as their hydraulic performance and the effect of the geometrical parameters are known quite well. The recently introduced PKWs have comparably greater hydraulic performance and lesser construction costs than the classical labyrinth weirs. The small footprint area makes the PKW an efficient and cost-effective alternative to raise the flood release capacity at existing concrete gravity dams. The research is still going on this complex hydraulic structure because preliminary design procedures are available that cannot yet be generalized. Currently, no well-accepted standard PKW design procedure is available. Despite this, over the last few years, numerous PKW prototypes have been successfully installed on existing dams that efficiently increase the flood release capacity.

Spillways play an essential role in releasing the flood and ensuring the flood safety of dams. One-third of all dam failure has been caused due to insufficient spillway capacity. For a given upstream head, the discharge capacity of a free fall spillway is directly proportional to the crest length of the weir. The spillway crest length can be raised using undulated or corrugated, curve-shaped weirs as opposed to straight linear weirs. Consequently, the flow rate increases at a similar head. Nevertheless, the waterway downstream of the weir must also have appropriate evacuation capacity. So far, the following weir crest shapes have been devised with the goal of maximizing crest length:

a) Duckbill spillway or bath-tube spillway (in case of parallel side walls)

b) Fan spillway

c) Type Y spillway

d) Daisy-shape (marguerite), morning glory spillway (**Schleiss, 2011)**

2.2 Piano Key Weir (PKW)

Piano Key Weir (PKW) is a further step of the labyrinth spillways that were developed starting in the thirties of the last century. The year 2000 saw the introduction of the PKW as a modified form of the traditional labyrinth weirs. Developed as a novel weir type by **Blanc and Lempérière (2001) and Lempérière and Ouamane (2003),** the PKW offers the advantages of a labyrinth weir having overhangs in order to facilitate the weir location on the crest of a dam. **Schleiss (2011) and Lempérière *et al.* (2011)** gave a brief historical review on the design and development of labyrinth weirs and PKWs.

The installation of the first PKW was done in the year 2006 at the Golours Dam, France **(Laugier, 2007)**. Since then, PKWs have been used to increase the flood discharge capacity of three other EDF dams: St. Marc (2008), Etroit (2009), and Gloriettes (2010). (2010). PKW spillways may be easily integrated with stepped chutes, resulting in greater downstream energy dissipation **(Bieri *et al.,* 2009)**. The essential learnings from these four PKW spillways' designs are given by **Laugier *et al.* (2009)** and **Vermenten *et al.* (2011)**. A further study of PKW developments was carried out in Vietnam **(Hien *et al.,* 2006)**, India **(Sharma & Singhal, 2008),** and France **(Gage, Malaria, and La Raviege Dam)**. Thanks to the early fruitful collaboration between academia and industry, the concept developed fast and has been rapidly applied in the field to increase the discharge capacity at existing gravity dams in France **(Laugier *et al*., 2017)** or as an impressive alternative to gated weirs for diversion structures in Vietnam **(Ho Ta Khanh, 2017)**.

Since 2011, the regular organization of specific international workshops where knowledge is freely exchanged in an open and friendly environment facilitates the connection of all these actors, forming an international nonlinear weirs community and resulting in the publication of three reference books summarizing the current state of the art **(Erpicum *et al*., 2011; 2013 and 2017).** Since the 2006 Goulours dam first PKW commissioning in France, more than 35 PKWs have been built worldwide **(Crookston *et al.*, 2019),** and research continues throughout the globe. Interestingly, in addition to the developments mentioned above focused on using PKW as a frontal weir for flood release, the concept has been recently shown to be attractive inside weirs applications **(Karimi *et al*., 2018).** PKW is a nonlinear

overflow structure that induces complex and three-dimensional flow patterns in its vicinity. It behaves similarly to a standard linear weir with a very long crest length at the low head. However, the additional velocity and longitudinal flow momentum at the inlet section at the slightly higher head cause flow over the lateral crest to deviate from this normal/average vector. Consequently, the flow efficiency over the side crest decreases marginally, and only the key to the inlet and outlet comes into play.

The unit discharge approaching through the PKW crest directly determines the relative width of the inlet key. Most researchers presented that the optimal inlet to outlet ratio is 1.2 **(Barcouda *et al*., 2006; Hien *et al*., 2006; Lempérière and Jun 2005 and Ouamane and Lempérière, 2006)**. Further, **Lempérière (2009)**, **Lempérière *et al*. (2011)**, and **Machiels *et al*. (2014)** claimed the optimal width ratio (W_i/W_o) = 1.25. **Anderson (2011)** found that the maximum discharge efficiency is achieved when the width ratio (W_i/W_o) lies between 1.25-1.5. **Leite Ribeiro *et al*. (2012a)** and **Machiels *et al*. (2011a)** recommended that the inlet to outlet key width ratio be approximately 1.5.

Depending on the upstream reservoir's characteristics, only a few studies have looked at the downstream components of PKWs so far. As a result, additional research in this area is recommended to supplement the preliminary work of **(Eslinger and Crookston 2020);(Jüstrich *et al*., 2016); (Silverstri *et al*., 2013);** and **(Singh and Kumar, 2022)**. Numerical models may reproduce the complex flow conditions downstream of PKWs with acceptable accuracy, allowing their utilization to validate the design of the downstream structure or investigate energy dissipation. Therefore, it is essential to research energy dissipation and downstream scouring near the toe of PKW.

At present, many researchers have been working on the sediment transport upstream and downstream of the PKWs. Several researchers have also focused on the downstream scouring and ridge generation near the PKW's toe. **Jüstrich *et al*. (2016)** assessed the scour and the generation of the adjacent ridge in a systematical physical model study. The results of the study demonstrate that the maximum scour hole relies on the discharge, the head difference, sediment size, and tailwater depth.

Further, **Noseda et al. (2019)** carried out an experiment involving the passage of sediments over a PKW driven uniquely by the flow. A systematic physical model test was carried out to study the behavior of upstream riverbeds and the passage of sediments over the PKW. Interestingly, in addition to the above-mentioned developments focused on using PKW as a frontal weir for flood release, the concept has been recently shown to be interesting inside

weirs applications **(Karimi *et al.* 2018)**. Recently, **Zhao *et al.* (2020), Yazdi *et al.* (2021), Kumar *et al.* (2021), Laiadi *et al.* (2017), and (Kumar and Ahmad 2022)** examined the ridge and dip formation attributed to plunging and impinging jets originating from the inlet and outlet keys or the weir geometry effects on the scour development downstream of the PKW.

Recently **(Abhash and Pandey 2020) and** (**Singh and Kumar 2021**) presented a detailed review on the hydraulic design and analysis of the PKWs. Several design methodologies are available for the hydraulics of PKWs based on the prototype structure's model tests. Therefore, it is essential to find out the optimal geometry and design criteria for the PKWs; in addition, more research is needed on energy dissipation and downstream scouring near the toe of PKW.

The hydraulic performance of the weirs depends on the nappe geometry and aeration conditions **(Crookston and Tullis 2012)**. For PKW, the flow over the sideways and downstream inlet key crests forms a continuous curtain with a contained air pocket, i.e., a nappe **(Denys 2017)** (**Denys *et al.* 2017**; **Lombaard 2020; Hien *et al.*, 2006; Laugier *et al.*, 2013)**. The air pocket behind the nappe was found to serve only as an amplification and stabilization factor, and it does not affect the incidence of vibrations **(Lodomez *et al.* 2018)**. By estimating the fall height, one can determine the nappe thickness. When there are high flows or narrow outlet keys, the opposite lateral ridges collide, but they are unlikely to affect discharge efficiency significantly (**Machiels 2012**). Three typical nappe behaviors are observed for PKWs (free-flow conditions). They can all coincide along the lateral crests for a specific flow **(Machiels *et al.* 2009, 2011).**

2.3 Physical Modelling

Many researchers have discussed a brief review of the studies on PKWs. Among them, most of the studies are based on the experimental or physical modeling of PKWs, and their main motive is to enhance the capacity of PKWs.

Lempérière and Ouamane (2003) were the first researchers to propose the concept of a new shape of non-rectilinear weir, regarded as Piano Keys Weir tests of type A and B. Hydro-coop France developed its collaboration with the Laboratory Hydraulic Developments and Environment of the Biskra University, Algeria. The concept of modern Piano Keys Weir was born in the 19th century because most new dams guaranteed their safety.

Barcouda *et al.* (2006) studied the behavior of PKW flow for a sharp-crested linear weir having the same channel width in terms of a magnification ratio. **Ouamane and Lempérière (2006)** demonstrated that the PKW has B_i/B_o= 2, 12% more efficient than B_i/B_o = 0 (Type-B). A B_i/B_o = 1 (Type-A) PKW is 7% more efficient (H_t/P < 0.4). In the review studies, it was found that all of the researchers agreed that the Type-B geometry of the PKW offers a higher discharge efficiency relative to Type-A.

Hien et al. (2006) have found that the geometries or shapes of PKW perform better at nappe aeration than trapezoidal labyrinth weirs because of the cantilever or overhang at the outlet or inlet key.

Leite Riberio et al. (2007) studied three different PKW crest geometries: a downstream quarter round, an upstream quarter round, and a flat crest, and noticed that the upstream quarter round is the most efficient of the three; they also carried out a model study of the PKW at Saint-Marc and discovered that nappe aeration is required on the PKW structure to prevent undesirable vibrations in the weir structure.

Leite Ribeiro *et al.* (2009) presented an influence of a parapet wall on top of the PKW (the height of the PKW was raised without increasing the overhangs' length); they found that upon increasing the PKW height with the vertical parapet wall increased the discharge efficiency of the same PKW design without the parapet wall.

Pralong *et al.* (2011) described the various geometrical parameters related to the PKWs and defined all the standard notations. These are the most typically utilized parameters, revealing enough to offer an overall description of the PKWs.

Noui and Ouamane (2011) presented a dimensional analysis relation between the discharge capacity and different geometrical parameters of PKWs and suggested that different geometrical parameters influence flow over the PKW. On increasing the height of the weir, 25 % higher performance can be achieved for a low head; only 5 % can achieve for the medium head.

Leite Ribeiro *et al.* (2011) studied in detail how numerous dimensionless parameters affect the PKW. For instance, the effect of relative key widths W_i/W_o, the relative developed crest length L/W, the vertical to horizontal shape P_i/W_i ratio, and the vertical dam height relative to PKW height P_d/P_i on the discharge capacity of type A PKW. They also stated that the discharge is directly proportionate to P_i for bottom slopes of 0.3 to 0.6 ($V: H$). They

concluded that the relatively developed crest length ratio *L/W* is the most influencing parameter on PKW capacity.

Anderson and Tullis (2011) stated that the overhang plays an indispensable positive effect on the PKW discharge capacity. The overhangs on the upstream side of PKW increase the inlet flow area and wetted perimeter, reducing energy losses.

Ho Ta Khanh *et al.* (2011) analyzed the outcome of experimental studies conducted in Vietnam between 2004 and 2010. They mainly focused on the following topics: determining the discharges vs. the nappe depths for different shapes and sizes of the labyrinth and PKWs, under free-flow and submerged flow conditions. Observing the aeration of the flow, energy dissipation, and measurement of the scour at the dam toe. This study shows the main results of these tests to compare with the results of other hydraulic laboratories, particularly in France and Algeria, and provides useful information for the projects of PKWs under design and construction in Vietnam. They noticed that for the low dams, a smooth downstream face and a short stilling basin are generally sufficient to dissipate the energy of the flow, even with the higher specific discharges. A stepped downstream face, combined with a short stilling basin and an end sill raising the downstream water level, appears to be a good solution for medium and high dams on the entire height or only on the lower part.

Machiels *et al*. (2011a) and Machiels *et al.* (2011c) presented the effect of slopes on the capacity of PKW s. In this study, the models' geometry was kept constant, and only the slopes of the alveoli (wide range of slope from 0.25 to 1.5, height over length) were varied. They found that increasing the inlet slope enhances the release capacity of the weir. However, increasing the slope over a limit near 1.2 does not change the weir's release capacity. **Machiels *et al*. (2011a)** and **Leite Ribeiro *et al.* (2012)** recommended an inlet width to outlet width ratio of approximately 1.5**.**

Machiels *et al.* (2011b), based on the extrapolation of existing experimental outcomes, presented a systematic preliminary design method to develop one or more available projects for improving the PKW efficiency.

Machiels *et al.* (2011d) conducted experimental work on the 1:10 scale model to enhance understanding of the flow over PKWs and ascertain the flow features along the weir as per the upstream head. They characterized the flow conditions in terms of specific discharge, pressure, velocity, water level, and streamlines' pattern along the weir. They discovered that wall thickness and weir shape have a vital role in discharge capacity, decreasing the discharge efficiency for low head and increasing the hydraulic head's

efficiency. They also investigated the formation and position of the critical section or control section. They did so as the appearance of the control section along the inlet was showing a reduction in the discharge coefficient with the head, owing to the decrease in the effective length of the weir crest. Therefore, the author proposed some geometric changes to prevent the control section's formation along the inlet, such as increasing the width of the inlet, height of the weir, or the length of the upstream overhang, so as to raise the discharge capacity of PKWs.

Leite Ribeiro *et al.* (2012) identified some essential key points: a PKW offers high efficiency for low heads. As the hydraulic head increases, the PKW's efficiency decreases rapidly. They also analyzed that the capacity of PKWs primarily relies on crest length and hydraulic head, the vertical and horizontal shapes of the PKWs. Further, the ratio of inlet and outlet key width and height, length of the overhang, and parapet wall's height significantly influence the capacity of the PKW.

Kabiri-Samani and Javaheri (2012) provided a global approach for estimating free and submerged flow discharge coefficients over PKWs. To determine the rating curve of PKWs, the first general equations that used the Poleni equation were presented and expressed in terms of the discharge coefficient. They ran comprehensive model testing in a 12 m long, 0.4 m broad channel having specific discharges ranging from 25 to 175 l/s/m. The PKWs evaluated were sharp-crested of types A, B, and C.

Leite Ribeiro *et al.* (2012a) performed extensive model tests on numerous type-A Piano Key Weirs having a half-circular crest sectional setup. They thoroughly analyzed the equation relating to the head-discharge ratio and established that the conditions downstream had no effect on the head-discharge relationship.

Anderson and Tullis (2012) assessed the A-Type PKW head-discharge behavior for reservoir approach and in-channel flow conditions using a laboratory-scale physical model and tested it with varying flow approach depths upstream apron slopes and abutment details in their study. They concluded that increasing the depth of approach flow, steeper approach aprons, and improved abutment designs boosted discharge efficiency while reducing the impact of flow separation.

Anderson and Tullis (2012a) demonstrated the comparison between Piano Key Weir and rectangular labyrinth weir hydraulics, concluding that the PKW had relatively higher efficiency. They proposed that enhanced weir discharge capacity is connected to the higher

wetted perimeter, lower inlet velocity, and the concomitant reduction in entry losses due to the PKW inlet key design.

Dabling and Tullis (2012) performed an experimental assessment on the influence of tailwater submergence on the PKW's head-discharge relationship. The outcomes were then compared to previously published data for the labyrinth and linear, sharp-crested linear weirs. They discovered that PKWs need a lesser upstream head relative to the labyrinth and linear weirs, subject to the same discharge value for low submergence.

Leite Ribeiro *et al.* (2013) demonstrated that relative to linear weirs, non-linear weirs are observed to be more effective. However, such behaviour holds for low upstream water heads only. The relative benefit reduces asymptotically as the water level increases in proportion to the height of the weir. For this reason, the design of PKWs is suitable for operating on lower heads only. Although tests involving a range of upstream heads ($0 < H_t/P < 3$) have been conducted on PKWs, none have been constructed that are suitable for operating greater than the H_t/P value of 0.66. The design of the majority of the prototypes allows for discharging the maximum flows at around $H_t/P = 0.3$.

Sharma and Tiwari (2013) observed the role of the Z-component of the velocity of water; as the flow approaches towards the PKW, the Z-component of the velocity in lower levels is seen as increasing, which can be useful for maintaining a significant quantity of sediment in suspension even at a low discharge value and enhance the flushing capacity.

Noui and Ouamane (2013) suggested that if a traditional flip bucket is utilized in the outlet key, the discharge capacity of the PKW may be reduced. Alternatively, a concrete apron downstream of the weir paired with an end-sill (for example, a stilling basin) is an excellent technique to avoid scouring.

Anderson and Tullis (2013) compared the relative head-discharge efficiency of trapezoidal labyrinth weir and PKW s concerning footprint restrictions and crest length.

Michael and Schleiss (2013) presented a general design equation for A-type PKWs and derived the rating curve of PKWs, expressed in terms of the discharge coefficient.

Machiels *et al.* (2013) presented a global effect of the parapet walls over PKW, either increasing or keeping the total weir height constant. It was observed that the parapet walls considerably impact the rise in the inlet height and, hence, decrease the value of longitudinal velocity, raising the lateral discharge. However, the parapet wall height needs to be limited to keep the interest of overhang use, limiting the head losses at the entrance of the inlet key.

Silvestri *et al.* (2013a) performed tests to investigate energy dissipation under flutter flow circumstances on a downstream stepped spillway of a PKW, drawing comparisons with the theory of stepped spillway of the regular ogee-crested weir.

Silvestri *et al.* (2013b) performed a systematic experimental study to compare the residual energy at different lengths of a stepped spillway's toe. A classical OCW and two different PKWs were employed at the top of the structure. It was observed that conditions of uniform flow, i.e., flow energy at the toe of the spillway independent of the spillway length, are reached on considerably shorter spillways at downstream of a PKW relative to downstream of an OCW. However, the energy of the uniform flow is not the same depending on the weir type.

Ramakrishnan *et al.* (2014) determined the discharge coefficient for PKW s of varying geometry. They concluded that the discharge (*Cd*) value coefficient depends on geometrical parameters such as inlet width, outlet width, floor slope, and parapet wall. They tested three different geometrical models with varying slopes (inlet slope = outlet slope) 45^0, $60^{0,}$ and 45^0(without parapet wall), and they found a high *Cd* value at slope 45^0 with parapet wall.

Erpicum *et al.* (2014) demonstrated the changes in a given value of crest length, magnification ratio, and discharge capacity of weir having varying geometric parameters and overhang positions. A standard linear weir's theoretical rating curve was taken for drawing comparison, and the analysis showed that the key widths and overhang lengths ratios significantly impact the efficiency of PKW, although less than the weir height, so the height of the weir is of primary importance.

Oertel and Tullis (2014) determined the coefficient of discharge for numerous types of PKW experimentally and made a comparative analysis with a numerical 3D Volume-of-Fluid (VOF) model, observing that the VOF Code showed good consent and applicability in their study.

Lade *et al.* (2015) presented two physical PKW models with different sill geometries of PKWs, one with a triangular sill and the other with a sloping sill. The experimental results found that the discharge coefficient (*Cd*) for triangular sill and sloping sill are 0.264 and 0.243, respectively. The discharge coefficient of the aforesaid models did not demonstrate a significant improvement in discharge coefficient when compared to the regular PKW. However, it may be more efficient at more significant discharges.

Khassaf and Al-Baghdadi (2015) studied the hydraulic behavior of non-rectangular PKW where the sidewall angle or the sidewall inclination angle is greater than zero. This study investigated the sidewall angle α and the sidewall inclination angle β separately on a conventional rectangular type–A PKW. Each time the value of either α or β was altered, keeping all geometrical parameters constant. It was observed that modifying these angles to approximately 10° has a negative effect on the capacity of discharge. Altering them around 5° can raise the discharge capacity when the appropriate change in the inlet and outlet keys widths ratio.

Ali and Mansoor (2015) compared the performance of PKW s to the normal sharp-crested weirs with the help of an experimental study and analyzed using regression analysis. It was found that the PKWs perform doubly w.r.t a normal weir at the same head over the weir crest.

Oertel M. (2016) presented a sensitivity analysis for PKW experimentally, and the author suggested that the sensitivity analysis provides a guideline for measurement purposes on experimental work within laboratories.

Jüstrich *et al.* (2016) developed a mathematical model that focused on assessing scouring and the adjacent ridge generation in a loose riverbed downstream of a PKW in their study. They proposed that their work contributes significantly to determining a suitable foundation depth for a PKW built on a moving riverbed.

Khassaf *et al.* (2016) evaluated, by conducting laboratory experiments, the effects of the geometry of a type-B PKW on the coefficient of discharge under free-flow conditions.

Hotaki and Hailkar (2017) compared laboratory-scale physical models of rectangular labyrinth (RL) weir and PKW based on their hydraulic efficiency, designed based on the Froudian similarity, and established and analyzed the head-discharge relation, coefficient of discharge relation for the different models.

Denys (2017) discussed some essential standard design principles and flow-induced vibrations related to the PKW spillway. **Denys *et al.* (2017)** presented a sensitivity analysis of the PKW regarding pressure fluctuations.

Laugier *et al.* (2017) suggested that the crest's shape plays a significant role in the weir's efficiency, which is observed mainly at low water levels. During the field operation, the crest shape of PKWs was studied, and downstream key portions were seen to have a minimal effect on lesser length. They suggested that the upstream crest may be rounded

(quarter round on its upstream side), and the downstream crest may be sharp-crested to maintain the uniform flow pattern. The curvature of the rounded shape may lie from 0.5 T_s to 1.0 T_s. Due preference should be for half-rounded or quarter-rounded shapes by considering construction aspects related to formwork and durability concerns.

Tiwari and Sharma (2017) presented the turbulence study in the vicinity of the PKW and said that many researchers had investigated it. The utilization of PKW is known to raise the capacity of discharge owing to the increased length of the weir crest and thus, needs to be studied for local sediment behavior. In open channels, sediment transport has been observed to be in direct link with turbulence structures. It is related to the PKW's design criteria. For an open channel included with PKW, turbulence proves to be a complex phenomenon and requires comprehensive laboratory experiments: relevance, instrumentation, parameters, and methods.

Karimi *et al.* (2018) compared different types of weirs in an experimental study. They employed twenty-one weirs, consisting of three linear weirs, nine piano key side weirs, and nine rectangular labyrinth side weirs having identical crest prints. They used De Marchi's model for the coefficient of discharge calculation. The main focus of the study was how the surface flow characteristics varied over the different types of weirs. This study found that the discharge coefficients for the folded shape side weirs were significantly higher than the linear side weirs. Although the authors saw no considerable variation in the coefficient of discharge between the rectangular labyrinth side weirs and the piano key weir, the latter was found to be the better alternative for overcoming space or other limitations of the construction site.

Saghari *et al.* (2019) examined the effect of using one or two cycles in Trapezoidal Piano Key Side Weirs (TPKSWs) on the capacity of discharge while maintaining the same upstream-downstream length and total width. All those dimensionless parameters were determined, which influenced the coefficient of discharge related to the developed length (C_{DL}) of TPKSWs placed in a curved channel. In addition, an empirical relation for C_{DL} based on the experimental outcomes was proposed. The measured data was in good agreement with the estimated data. The results demonstrated that the coefficient of discharge related to the total width of a TPKSW is 1.7 to 5.6 times higher compared to that of a Curved Rectangular Side Weir (CRSW). Also, the value of C_{DL} for a one-cycle TPKSW was observed to be 1.4 to 2 times larger relative to that of a two-cycle TPKSW.

Kumar *et al.* (2019) assessed various methodologies given by different researchers. They have used four equations for the data sets to compare the methods developed by the

other researchers, i.e., **Kabiri-Samani and Javaheri (2012); Leite Ribeiro *et al.* (2013)**; **Crookston et al. (2018)** and **Cicero and Delisle (2013).** The authors determined that the methods suggested by **Crookston et al. (2018)**; **Cicero and Delisle (2013)** offer a better prediction of the discharge coefficient in comparison to other equations for the data sets used in this present study. 97% of results lie within ±20% error lines for these two equations.

Crookston *et al.* (2019) surmised the 100 years of evolution over advancements and hydraulics of Labyrinth and PKWs and pointed out future needs.

Mehri et al. (2020) examined the rectangular PKW's applicability as side weirs at 120^0 and 180^0 in a curved channel plan. The authors found that at two ends of the RPKSWs, the specific energy was the same, but the discharge efficiency of the type-B side PKW was observed to be 9.9 % more relative to other types of weirs.

Lombaard (2020) investigated the impact of aeration on the capacity of discharge due to the flowed-induced vibrations of Piano Key Weir Spillways. They observed that the introduction of air behind the nappe did seem to have a somewhat stabilizing effect on the air pressure fluctuations near the tip of the sidewall cavity; however, the data did not produce enough evidence to confirm this finding.

Eslinger and Crookston (2020) performed an experimental study on the type-A PKW to know the energy dissipation capacity of the PKW. It was observed that the energy dissipation rate is non-linear and is most significant at a lower value of heads.

Crookston (2020) illustrated the energy dissipation behavior of labyrinth and PKW and observed that more energy dissipation occurs at low head discharges. They also noticed that the energy dissipation over such type of nonlinear weirs depends on the weirs' geometry.

Ghanbari and Heidarnejad (2020) presented the experimental and numerical flow analysis of the different plan shapes of the PKW. They concluded that relative to the rectangular PKWs, the discharge coefficient for triangular PKWs was 25% higher.

Kumar and Ahmad (2020) examined the scour pattern at the downstream side of outlet and inlet keys, with as well as without having a solid apron. It was found the falling and impinging jet that originates from the inlet and outlet keys is responsible for developing a dip and ridge at the weirs downstream. The scour depth and length of scouring were also found to be high for a higher discharge and lower tailwater.

Tullis *et al.* (2020) evaluated the scaling effects in free-flow head-discharge relationships over the different types of nonlinear weirs. This study found variations in head-discharge performance between prototype and model.

Tullis *et al.* (2021) evaluated the hydraulic behavior of a labyrinth weir with outlet ramps configurations on flow surging and water surface levels and fluctuations in a relatively steep stepped chute. They noticed that installing ramped floors in labyrinth weir downstream cycles helps redirect the flow into the chute, reducing flow turbulence and potentially minimizing the maximum flow depth in the stepped chute.

Lantz *et al.* (2021) examined how the use of aprons and cut-off walls impacts the scour at PKWs. The authors found that a considerable reduction in scours depth is observed for an apron length that is 1.5 times the height of the weir, while marginal benefits were observed by using longer aprons.

Mishra and Ahmad (2021) conducted an experimental study over type-A PKW to see the effect of the shape of the outlet key slope on the discharge capacity of PKW. To do this, they tested two models with straight and curvature slopes. They found that the discharge efficiency of PKW-CL became moderately higher than PKW-L.

Kumar *et al.* (2021) investigated the mechanics of the flow of single quartz gravel and coarse sand riverbed particles upstream and over the Type-A PKW models' inlet key. They discovered that silt typically slows down as it moves upstream toward the inlet key and then accelerates rapidly at the key entry.

Yazdi *et al.* (2021) investigated the scouring phenomenon by considering the different geometry (trapezoidal and rectangular-shaped PKWs). They found that, on average, the dimensionless ratios for maximum scour depth, maximum scour depth distance, and length of scour hole for TPKW were 6%, 13%, and 11% lower than the corresponding values for the rectangular PKW.

Sangsefidi et al. (2021) illustrated the hydrodynamics and hydraulic behavior of different plan shapes of PKW under free-flow conditions. They concluded that for a trapezoidal PKW, the discharge efficiency is highest across the studied domain ($B/W_u \geq 2$ and $H_o/P > 0.25$). It can enhance discharge efficiency by approximately 5% while having a body volume close to 7% smaller than a traditional rectangular PKW. But in the case of high-head and low-length conditions ($H_o/P > 0.5$ and $B/W_u = 1$), a rectangular PKW is better than the other shapes.

Singh and Kumar (2021) presented a detailed review of the aeration performances of the PKW and compared it with its alternatives. They observed that the PKW has an excellent oxygen transfer rate.

Alizadeh Sanami *et al.* (2021) examined the hydraulic characteristics of a D-type triangular PKW, with or without considering the downstream ramp. They also proposed two prediction equations for predicting the discharge coefficient of the D-type PKWs, with a downstream ramp and without a downstream ramp.

Bekheet *et al.* (2022) assessed the flow efficiency of various PKW shapes (trapezoidal, Rectangular, and triangular PKWs) for various inlet and outlet key width ratios (W_i/W_o). The flow efficiency of the trapezoidal PKW is the best of the three investigated forms, according to the experimental data, followed by the rectangular PKW. Because the triangular PKW had the lowest flow efficiency, it is not recommended for usage.

Lantz *et al.* (2022) evaluated the local scouring downstream of Type A PKW in non-cohesive sediments. They concluded that scour at PK weirs can significantly exceed the structure's height under particular hydraulic conditions and suggested that the scouring morphology's intensity, depth, and evolution depend on particle characteristics, Q, and downstream water depth (or tailwater depth). A decrease in particle size and water level downstream results in more scour, whereas an increase in Q results in more scour.

Singh and Kumar (2022) presented a detailed review of the hydraulic design and analysis of the PKW. They demonstrated different geometrical impacts on the hydraulic behavior of the PKW. Further, **Singh and Kumar (2022a)** examined the various geometrical influence on the energy dissipation of the type-B PKW. They found that energy dissipation decreases as the head over the weir increases. The energy dissipation was found to decrease with the increasing magnification ratio and relative width ratio; however, the energy dissipation was found to increase with increasing cycle number (for a constant-width channel).

Singh and Kumar (2022b) examined the aeration performance of type-A, type-B, and type-C PKWs with the discharges and drop height. The authors determined that the type-A PKW shows an aeration rate 22–28% higher than the type-C PKW at a drop height of 0.20–0.40 m. When compared with a type-B PKW at the same drop height, the type-A PKW showed a 23-56% higher rate of aeration.

2.4 Numerical Modelling

There have been few studies that use numerical modelling of PKWs.

The first simplified 1D-numerical model for the PKW was presented by **Erpicum *et al.* (2011a)**. It is based on a distinct 1D model of the inlet and outflow, with a single upstream reservoir and flows interacting via mass and momentum exchange along the lateral crest. The comparison of the numerical findings with many experimental data has proved the numerical model's ability to forecast the release capacity of a PKW fairly throughout a wide range of reservoir heads, regardless of geometry (not too low or too high).

Mario Oertel (2015) compared the discharge coefficients from experimental models to the numerical 3D simulations for various PKW types. An experimental model was built or designed in such a way to measure flow depths for discharges varying up to 100 l/s. The author found that the CFD accurately produces the experimental flow depth model. However, for calculating the discharge coefficient, a satisfactory reproduction was observed only for more significant discharge events ($H_T/P > 0.15$). A significant deviation of the experimental model results could be found for $H_T/P < 0.15$. The author also carried out numerical 3D CFD simulations for reproducing water surface profiles and discharge coefficients. The data collected with this simulation model was compared with the data from the literature.

Cicero *et al.* (2016) gave a new experimental program to enhance the knowledge of a few secondary parameters such as the crest shape, the overhangs, and the dam's height. The program was tested for rectangular and trapezoidal shapes (Type-A, Type-B, and Type-C) of PKWs under free-flow and submerged conditions. They used the experimental data to validate empirical correlations and FLOW-3D numerical models and concluded that type C is lesser sensitive than type A, which is less sensitive than type B in the submergence case. They also concluded that the overhang affected the efficiency of weirs, and type-B was five to fifteen percent more efficient than type-A, which was fifteen percent more efficient than type C.

Ujeniya *et al.* (2016) focused on the optimization model of PKWs, based on outlet key to inlet key ratio, increasing discharge and interference of nappe in outlet key.

Denys and Basson (2018) studied the transient features of complex flow patterns around a PKW, considering numerical and physical modeling. The transient data collected from the physical model were used to compare or verify the numerical modeling. They analyzed unique transient hydrodynamics in both the inlet and outlet keys and observed how the pressure fluctuated upstream and downstream sides of the wall.

Bremer and Oertel (2018) considered their study's first assessment of mesh quality and meshed independence. They used different mesh sizes to check the effect of mesh in the velocity magnitude for a specific area and mesh dependence related to the coefficient of discharge of PKW. They compared the velocity magnitude of different mesh sizes for different discharges for numerical PKW simulations with the Grid Convergence Method (GCI).

Al-Baghdadi (2019) presented a 2D simulation for pressure distributions and flow velocity over the individual outlet and inlet keys under varying discharges using Flow-3D software. In this study, the author identified the areas having extreme pressures and velocities over the PKWs, allowing the hydraulic engineers to consider them while going through the design process.

Ghanbari and Heidarnejad (2020) presented experimental and numerical modeling over two shapes of PKWs: rectangular and triangular PKW. The authors studied the impact of the triangular notch on the discharge coefficient of PKWs physically, while the FLOW-3D software was employed for simulating the rate of discharge and the impact of each model on the flow field over the weirs. The results showed that relative to the rectangular PKWs, the coefficient of discharge for the triangular PKWs was 25% higher.

2.5 Computational Analysis/ Machine Learning Techniques

Many researchers have applied the GEP in the various field of hydraulics to predict the accurate estimates of the different hydraulics characteristics **(Azamathulla et al., 2013); (Karbasi and Azamathulla, 2016)**; **(Azamathulla et al. (2018). Shivashankar et al. (2022)** describe the different methodologies for estimating the velocity phenomenon. This study proposed a hybrid generalized reduced gradient-genetic algorithm (hybrid GRG-GA) to assess the fall velocity. The hydraulic performance of the trapezoidal labyrinth-shaped stepped spillways was investigated by **Ghaderi et al. (2020).** Sediment characteristics, discharge, residual energy, and tailwater level all have a role in determining the scour depth and volume of sediment removed at the toe of PK weirs.

Bashiri *et al.* (2016) made use of an artificial neural network (ANN) along with multiple linear and nonlinear regression analyses to determine a new design equation for the discharge capacity of PKWs. They evaluated how parameters such as weir height, width of inlet and outlet keys, water head, overhangs' length, and length of side crest affected the discharge capacity of PKW models and made a comparison based on RMSE and R^2. The

model results were also validated with experimental results and other existing equations, and found that H/P, B_i/P, and B_o/P have more impact than other parameters in the MLR model. Also, H/P, P/W_u, W_i/W_o, and B/P significantly influenced the discharge capacity in the MNLR model. For ANN, it is H/P and W_i/W_o.

Karbasi and Azamathulla (2016) used Gene Expression Programming (GEP) to predict the characteristics of a hydraulic jump over a rough bed. They compared it with the standard artificial intelligence (ANN and SVR) techniques. They found that the artificial intelligence techniques indicated that the performance of these models is slightly better than the GEP model, but the application of the GEP model due to derivation of explicit equations is easier for practical purposes. Further, **Azamathulla et al. (2018)** used the GEP to predict the atmospheric temperature in Tabuk, Saudi Arabia.

Bremer and Oertel (2018) assessed the discharge coefficient by numerical modeling, specifically considering the mesh size. This is because sufficiently maximum mesh sizes with the Grid Convergence Method (GCI) demonstrated a better accuracy in results.

Kashkaki *et al.* (2018) investigated the feasibility of using Artificial Neural Networks (ANN) to estimate the coefficient of discharge for the Circular Piano Key Spillway. The authors conducted lab tests on three Circular Piano Key Spillway models with 45, 60, and 90 degrees angles. The data collected from these trials were then validated with the test stages of the ANN models. They discovered that the 90-degree circular PKW demonstrated optimum capacity, evident by comparing statistical indicators for various models employed in the test step. Their investigation used a Multilayer Perceptron (MLP) network with a Levenberg-Marquardt backpropagation method. The following statistical parameters assessed the ANN's performance: Mean absolute error (MAE), mean fundamental percentage error (MAPE), root mean square error (RMSE), and coefficient of determination (R^2). They reported that ANN predicts the discharge coefficient of the circular piano key spillway with exceptional accuracy.

Zounemat-Kermani and Mahdavi-Meymand (2019) used artificial intelligence data-driven models (ANFIS & MLPNN) embedded with several meta-heuristic algorithms (GA, PSO, FA & MFO) to simulate the passing flow over PKW, and compared the results. General results indicated that the ANFISs and MLPNNs could simulate the discharge coefficient of the PKW more accurately than empirical relations.

Akbari *et al.* (2019) presented the experimental and numerical modeling over a gated inlet key type of the PKW. They concluded that the gate increased the hydraulic performance

of PKW. In this study, the authors have applied many soft computing techniques to estimate the discharge coefficient (C_d) using MLP, GPR, SVM, and GRNN. The GPR model shows effective results.

Pandey *et al.* (2021) suggested some critical points to Mohammad Najafzadeh and Ali Reza Kargar for their article on "gene-expression programming, evolutionary polynomial regression, and model tree to evaluate local scour depth at culvert outlets." Despite numerous significant experimental and computational investigations on energy dissipation across the labyrinth and PKWs, designers lack the knowledge to predict using traditional empirical models. As a result, new and precise approaches are still in high demand.

Singh and Kumar (2022c) used gene expression programming (GEP)for computing energy dissipation over the type-B PKW, and the performances of the GEP model were compared with empirical equations based on statistical factors, i.e., determination coefficient (R^2) and root mean square error (RMSE). The computed values of the relative residual energy using the proposed models are within ±5% of the observed ones. Results indicate that the proposed GEP model predicted the relative residual energy satisfactorily with the coefficient of determination (R^2 = 0.9979 for training, 0.9980 for testing) and root mean square error (RMSE) of 0.0099, 0.0092 for training and testing datasets, respectively.

2.6 Literature GAP

Based on the above discussion, the following shortcomings were observed:

1. The limited solution is given by the different researchers for the discharge vs. head from the hydraulic point of view for the different cycles and shapes of the PKW.
2. There is limited literature available on the approach flows over the different types of PKW (scaling effects).
3. Only a few researchers have focused on the downstream energy dissipation system.
4. There is no significant case study or literature on the balance between the pressure-related forces on the upstream and downstream sides of the sidewall (wall effects).
5. A few studies have focused on the aeration performance of the PKW.
6. There is limited literature available on the erosion/ sediment transport study over the PKW.

7. A few studies have focused on the computational analysis of PKWs. Also, no one has presented a significant correlation between experimental and computational research in any study hitherto.

2.7 Motivation for Present Work

The hydraulic behavior of PKW is highly intricate due to its three-dimensional flow nature. Hence, most prototype activities were planned, designed, or developed based on physical demonstration to understand better the hydraulic behavior of the PKW **(Laugier 2007, Cicero *et al.*, 2011, Ho Ta Khanh, 2013**, **Dugue *et al.* 2011, Leite Ribeiro *et al.* 2012; Erpicum *et al.* (2011; 2013 & 2017), Erpicum *et al.* 2013a, Hu *et al.*, 2018, Li *et al.*, 2019).** Several studies have been carried out in the last ten to fifteen years **(Anderson & Tullis, 2011) (Erpicum *et al.*, 2014) (Machiels *et al.*, 2014) (Kabiri-Samani & Javaheri, 2012)** based on geometric development to identify the hydraulic behavior of PKW, and now it is well understood. The different worldwide studies based on the geometric evolution and hydraulics of PKW have been summarised by **Erpicum *et al.* (2011; 2013 & 2017)** with three reference books. However, the transient behavior of PKWs is not so well comprehended and is the major focus of several ongoing studies.

Similarly, the downstream flood characteristics of a PKW have not been thoroughly investigated; to date, only several studies have discussed the downstream aspects of PKWs. **Bieri *et al.* (2009)** showed that PKW or spillways could effortlessly join with stepped chutes, decreasing downstream energy dissipation. The PKW's energy dissipation is not linear and more at a low head **(Eslinger and Crookston 2020); (Singh and Kumar 2022a); (Singh and Kumar 2022c)**. According to **Jüstrich *et al.* (2016)**, residual flow energy will result in a scour in an alluvial river bed if a prevention structure (such as a dissipation basin) is not constructed downstream of the flow control structure. Furthermore, **Pfister *et al.* (2017)** examined the scouring behavior at PKW's toe. They found that if a rock foundation is not possible, scouring occurs at the PKW's toe, which is relevant to weir stability during the flood. The efficient passage of sediment is critical in preventing floods upstream of the PKW and ensuring the waterway's navigability **(Noseda *et al.* 2019)**.

Sedimentation effects on the PKW are not yet well defined, but it is being studied. Different institutions have conducted the majority of PKW research in regions where rivers transport relatively little sediment. **(Tiwari & Sharma, 2017)** presented in their study that PKW tends to self-cleaning behavior. However, the effect may be too localized to allow the weir to behave regularly, sediment-free.

Interestingly, in addition to the developments mentioned above focused on using PKW as a frontal weir for flood release, the concept has been recently shown to be interesting inside weirs applications **(Karimi *et al.*, 2018)**. Recently **(Mehboudi *et al.*, 2017; Gebhardt *et al.,* 2018; Abhash and Pandey, 2020; Singh and Kumar, 2022)** summarised the PKW's geometrical and hydraulic evaluation over the last decade. **Yazdi et al. (2021)** examined the weir geometry effects on the scour development downstream of the PKW. They stated that the scour characteristics depend on the weir's geometry and the discharge rate. **Zhao et al. (2020)** found an increase in the saltation height and length if the particle shape is not spherical. Moreover, **Kumar et al. (2021)** investigated sediment movement over type-A PKWs and noticed that the sediment generally slows down as it moves upstream toward the inlet key and primarily accelerates instantly near the key entrance. The ridge and dip formation was attributed to plunging and impinging jets originating from the inlet and outlet keys **(Kumar and Ahmad, 2022)**. In addition, the scouring near the hydraulic structures affects aeration over the hydraulic systems **(Pandey et al. 2020a); (Pandey et al. 2020b)**. Aeration will not influence the shape of the scouring pit; it mitigates the scouring and the effect of air concentration on scouring depth **(Pandey et al., 2019)**. The aeration influences the scour hole's shape mainly by decreasing the scour depth. Scour depth depends on bed material and tailwater depth and is affected very little by the air concentration itself in the test range **(Pandey et al. 2021); (John et al. 2021a); (John et al. 2021b)**. The suspended sediment transport usually ranges from dilute to hyper-concentrated during flooding, depending on the local flow and ground conditions **(Pu et al., 2021)**.

2.8 Conclusion

This chapter clearly shows that much experimental (Physical modeling) work has been done based on the design and analysis of the PKWs. Many PKWs physical models were tested by many researchers and compared their results with linear weirs as well as labyrinth weirs of the exact dimensions. Only a few researchers have used numerical modeling for the analysis of PKWs. This literature review clearly demonstrates the need for developing a computational or numerical analysis for PKWs. In the case of physical modeling, it is difficult to determine the transient behavior of PKWs, so numerical modeling/computational study of PKWs is beneficial for that.

3.1 General

The primary objective of this study consists of examining the performance of the Piano Key Weir (PKW) with the help of experimental work. So it is essential to check the hydraulic performance of PKWs models physically (experimentally) as well as computationally. This chapter deals with the various aspects of the PKWs, including the last decade's evolution of the weir, multiple design methods and approaches, and some other essential designing aspects such as inlet to outlet slope effects, inlet to outlet width effects, number of cycles variations, effects of the magnification ratio, the impact of noses and parapet walls, pressure distribution at the upstream and downstream side of sidewalls, energy dissipation across the different types of PKWs, advantages, and disadvantages associated with the use of a PKWs.

3.2 Materials and Methods

3.2.1 Experimental Setup

A specific experimental facility has been built in the "Fluid Mechanics and Hydraulics Research Laboratory" at Delhi Technological University, Delhi, India, to perform all the scale model tests depicted hereafter. A straight rectangular channel, 10 m long, 0.6 m deep, and 0.516 m wide, has been used to carry out a range of scale model tests depicted hereafter. A series of pipes of 4-inch supply coupled to a 20.0 Horse Power (HP) pump is used to feed the channel, providing discharges up to a value of 50 L/s. The upstream of the flume's entry has been fitted with a metal grid along with a synthetic membrane to ensure uniform alimentation conditions. The Plexiglas plate sheets are facilitated up to 6.5 m flume sidewalls allowing for a phenomenal assessment of the flow patterns on the whole channel height. The supply line of the flume is calibrated using an orifice meter (having an uncertainty of 0.25%) along with a flow regulating valve to control the discharge. A 4-20mA electromagnetic flowmeter (uncertainty ± 0.2%) is fitted with a supply pipe for the discharge measurement **(see Figure: 3.1)**. In addition, the flume is fitted with a 4-20 mA ultrasonic level sensor (with an accuracy of ± 0.2 % ±1 mm) instrumentation carriage and a pointer gauge of least count ± 0.1 mm, which are utilized to measure the height of the water surface and crest elevations in various sections. The channel has massive tilting arrangements with a longitudinal slope of 2.5 % of the main channel. The discharge channeled over the weir is selected as the main variable of this study. For every test, the depth of flow over the weir was measured at a location (X= 2 x P) upstream of the weir crest (where P denotes the height of the weir). Readings for transient pressures on

the weir's downstream face were noted as well. The experiments of the present study were conducted using the channel flow approach (i.e., over PKW models in a laboratory flume); thus, this study primarily covered PKWs installed at river barrages or as a control structure in a canal.

An Acoustic Doppler Velocimeter (ADV) was utilized for the measurement of average flow velocities. ADV is enormously dependable to catch the turbulence attributes in an open channel stream in the laboratory's research facility. In the present case, the sampling rate was 25 *Hz*, and the sampling volume was located 5 cm from the probe for the 1-minute duration of collecting the sampling data. The mean velocity V_t was calculated as the average velocity measured at the same cross-section at 0.25, 0.5, and $0.75W$ across the flume width W, each for one-minute records using a Sontek ADV. The results of the velocity analysis revealed agreement between these average cross-sectional velocities and mean approach velocities (by ADV), yielding a difference in H_t of less than 5% for the Q ranges.

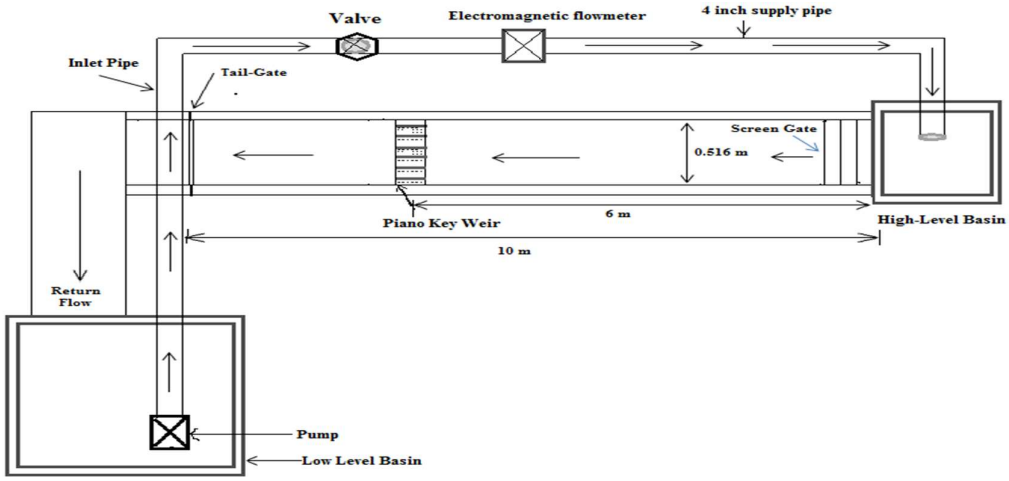

(a)

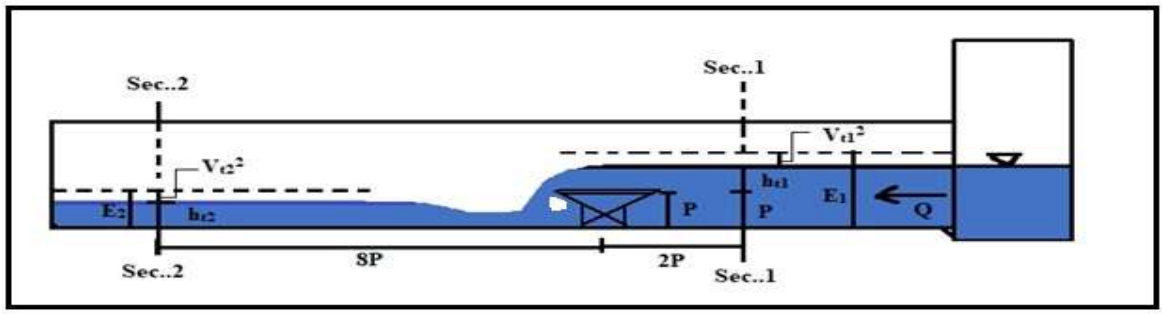

(b)

Figure: 3.1 (a) & (b) Schematic plan and side view of the experimental setup

ADV (Acoustic Doppler Velocimeter) is based on the Doppler shift principle. Using this principle, velocity is measured in three dimensions. A transmitting probe sends acoustic signals in the water of a particular frequency. The receiver probe receives the returned signal after striking the particulate in the water. The change in the frequency of the received signal help in calculating the instantaneous velocity at a point.

3.2.2 Model Fabrication

In this study, the models are fabricated using a 0.008 m thick transparent acrylic sheet and affixed with the help of chloroform. The models were assembled so that the inlet-outlet width ratio varies between $1.0 \leq W_i/W_o \leq 1.5$. The magnification ratio (L/W) ratio varies between 4 and 6, and the height of the model changes from 0.075 m to 0.35 m (or key slopes $0.3 \leq (S_i=S_o) \leq 1.4$) without increasing the overhang portions (**see Table:1**). The inlet and outlet key slopes for Type-A varies from $0.3 \leq (S_i=S_o) \leq 1.4$, $S_i=1$, *&* $S_o=0.37$ for Type-B, and $S_i=1$, *&* $S_o=3.2$ for Type-C. The two overhang portions are such that $B_i=B_o$, are alike for Type-A, whereas $B_i=0$, $B_o= 2/3\ B$, for Type-B, and $B_i=2/3\ B$, $B_o=0$, for Type-C (**see Table: 1 and Figures: 3.1 & 3.2**).

The data collected over the tested models under free-flow conditions are as follows: $0.005\text{m}^3/\text{s} \leq Q \leq 0.05\text{m}^3/\text{s}$; $0.042 \leq H_t/P \leq 1.2$, $0.0072\text{ m} \leq H_t \leq 0.145\text{ m}$, $B_i/P= B_o/P = 0.76$; for Type-A; $0.088 \leq H_t/P \leq 1.16$, $0.013\text{ m} \leq H_t \leq 0.174\text{ m}$, $B_i/P=0$, $1.1 \leq \{B_o/P\} \leq 1.89$; for Type-B; and $0.09 \leq H_t/P \leq 0.95$, $0.0167\text{m} \leq H_t \leq 0.175\text{ cm}$, $B_o/P =0$, $1.16 \leq \{B_i/P\} \leq 1.89$; for Type-C (**see Table: 1**). However, the flow measurement data ranges under the submerged conditions are slightly different that as follows: $0.01\text{m}^3/\text{s} \leq Q \leq 0.03\text{m}^3/\text{s}$; $0.11 \leq H_t/P \leq 0.80$, $0.0165\text{ m} \leq H_t \leq 0.08\text{ m}$, for Type-A; $0.09 \leq H_t/P \leq 1.1$, $0.0135\text{ m} \leq H_t \leq 0.081\text{ m}$, for Type-B; and $0.075 \leq H_t/P \leq 0.075$, $0.0132\text{ m} \leq H_t \leq 0.079\text{ m}$, for Type-C (**see Table: 2**).

3.3 Hydraulic Behaviour of PKW

The PKW is a nonlinear overflow structure; that establishes complex and three-dimensional flow patterns in their vicinity. It behaves in a manner similar to that of a standard linear weir having a very long crest length at a low head, although, at a slightly higher head, the longitudinal momentum of flow in the inlet key and the additional velocity result in flow over the side crest to deviate from this normal vector. Due to this, flow efficiency over the side crest gets slightly reduced, and only inlet and outlet keys come into play. From a hydraulic point of view, the width of the inlet key plays an important role, and thus its dimension needs to be shaped so that the flow velocity within it remains as smooth and subcritical as possible. On the other hand, the outlet key revolves around local submergence in the key. When, at a

particular location, the water level rises above the crest level of the weir, a considerable portion of the side crest encounters submergence effects, thereby resulting in a reduction of discharge efficiency of the weir as a whole.

3.3.1 Geometric Parameters

Many geometrical parameters influence the discharge behavior of PKWs. **Pralong *et al.* (2011)** described the most commonly used parameters related to the PKWs, revealing sufficient to provide the weir's overall description. The parameters are divided into various categories depending on whether they represent length, width, height, or thickness. The key parameters associated with physical dimensions are depicted in **Figures: 3.2** and **3.3**.

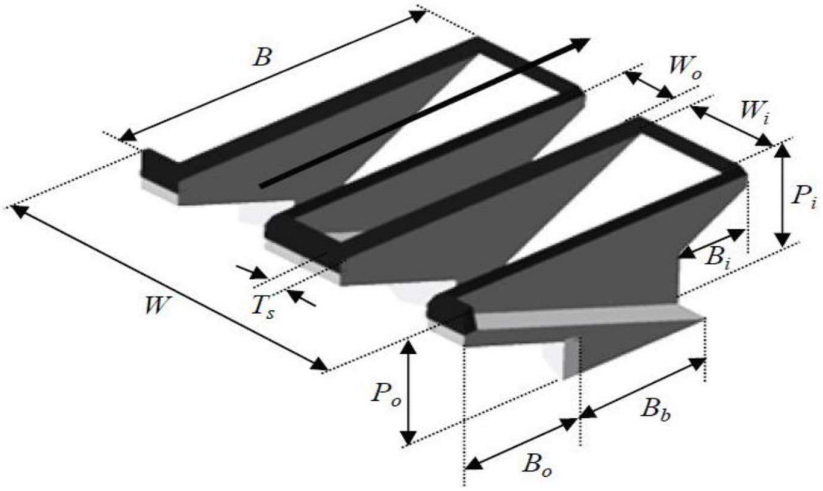

Figure: 3.2 Fundamental parameters of a PKW – 3D view (Pralong et al. 2011)

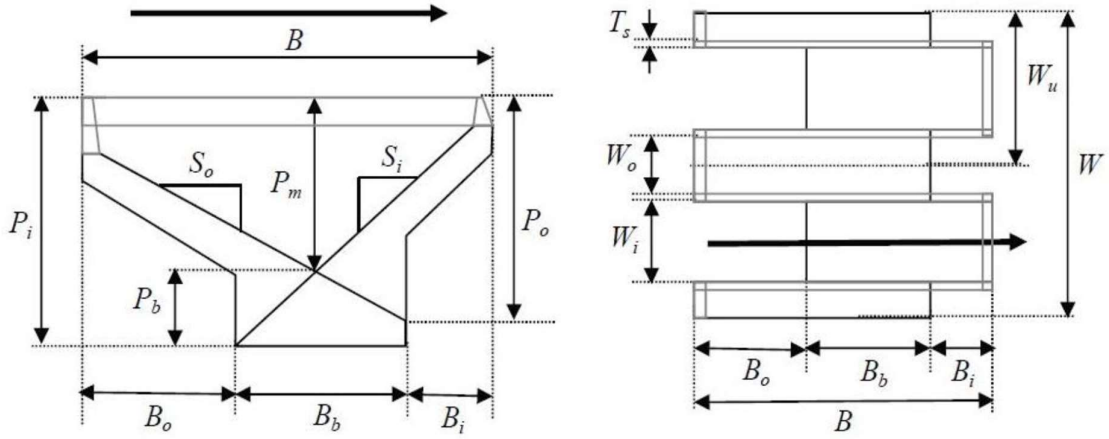

Figure: 3.3 Fundamental parameters of a PKW – plan view (left) and cross-section (right) (Pralong et al. 2011)

3.3.2 Discharge Equations

A PKW is a nonlinear ungated structure that causes a complex flow pattern. In this study, the main aim is to provide an overflow development length that is much longer than conventional linear weirs for raising the discharge capacity of PKWs at a given upstream head compared to linear weirs. The total discharge over a PKW is a function of numerous parameters, as indicated by Eq. (3.1) given below:

$$Q_{PKW} = f\ (\rho, g, \mu, \sigma, V_t, H_t, L, P, P_b, W, W_i, W_o, B, B_i, B_o, B_b, S_i,\ S_o, T_s, R, N) \quad (3.1)$$

where Q_{PKW} represents the total discharge flow over the PKW, ρ is the density of flowing fluid, μ denotes the dynamic viscosity, and σ represents the fluid's surface tension. 'g' = acceleration of gravity, T is the temperature of flowing fluid and H_t is denoted the total upstream hydraulic head. The other parameters are related to the geometry of the PKW: where L = total developed length of weir crest; W = total width of the PKW ; P = height of PKW, P_b = depth of approach flow; W_o and W_i = widths of outlet and inlet keys sections, respectively. $B = (B_i + B_b + B_o)$ represents the side weir's length; B_o and B_i are the lengths of the overhang portions at the downstream and upstream side, respectively, and B_b is the base length. S_o and S_i = outlet and inlet key slopes, respectively, α is the angle between inlet/outlet key crest and side weir of the PKW, T_s = thickness of the PKW sidewall, R = radius of crest curvature, and N= number of cycles.

To determine the discharge of a PKW for conditions of free-flow, numerous researchers have made use of the general equation of discharge for rectangular sharp-crested weir, which is as follows:

$$Q = \frac{2}{3}\ C_{DW}\ W\sqrt{2\ g}\ {H_t}^{3/2} \quad (3.2)$$

Where C_{DW} is the discharge coefficient, the W subscript denotes the discharge is calculated using the linear width of the PKW. However, some researchers express discharge coefficient related to PKW developed length as follows:

$$Q = \frac{2}{3}\ C_{DL}\ L\ \sqrt{2\ g}\ {H_t}^{3/2} \quad (3.3)$$

Where C_{DL} is the discharge coefficient, the L subscript of the discharge coefficient refers to the estimated discharge using the developed crest length of the PKW. In order to improve the performance of labyrinth and PKWs, several recent past experimental studies have been done based on the geometrical aspect of these weirs. So the performance or flow behavior over the weir depends on the hydraulic as well as geometric aspects of the weir. The benefit of the longer crest is to increase the discharge capacity of the weir. Many researchers presented it

as estimated using numerical modeling for several overflow structures in their study. They ascertained that the nonlinear weirs exhibited a much higher efficiency than linear weirs. However, this behavior was limited to low upstream heads only. With the rise in the water level, the relative benefit decreased asymptotically with the weir's height. For this reason, PKWs need to be designed for operating at lower heads only. Though tests on PKWs have been conducted at a range of upstream heads ($0 < H_t/P < 3$), none are built to operate larger than $H_t/P = 0.66$. Most of the prototypes have been designed so that their maximum flows are discharged at approximately $H_t/P = 0.3$. **(Leite Ribeiro *et al.* 2013).**

3.3.3 Dimensional Analysis

Discharge over the PKW depends on the hydraulic as well as the geometrical parameters. So to better understand the effects of the hydraulic and geometrical parameters on the capacity of the PKW, the dimensionless parameters are derived. Using the Buckingham theorem as a dimensional analysis technique and considering the ρ, g, and P as repetitive parameters (**Eqns. (3.4, 3.5, and 3.6)**), the dimensionless parameters are derived **Eqn. (3.7).**

$$\prod_1(H_t) = \frac{H_t}{P}\ \ \prod_2(L) = \frac{L}{P},\ \ \prod_3(P_b) = \frac{P_b}{P},\ \ \prod_4(W) = \frac{W}{P},\ \ \prod_5(W_i) = \frac{W_i}{P},\ \ \prod_6(W_o) = \frac{W_o}{P},\ \prod_7(B) = \frac{B}{P},\ \prod_8(S_i) = S_i\ ,\ \prod_9(S_o) = S_o,\ \ \prod_{10}(R) = \frac{R}{P},\ ,\ \prod_{11}(T_s) = \frac{T_s}{P} \text{ and } \prod_{12}(V_t) = \frac{V_t}{\sqrt{gP}} = F_r, \prod_{13}(\mu) = \frac{h_s}{P} \quad (3.4)$$

$$\prod(L) \times \frac{1}{\prod(W)} = \frac{L}{P} \times \frac{P}{W} = \frac{L}{W}\ , \prod(W_i) \times \frac{1}{\prod(W_o)} = \frac{W_i}{P} \times \frac{P}{W_o} = \frac{W_i}{W_o}, \prod(S_i) \times \frac{1}{\prod(S_o)} = \frac{S_i}{S_o}, \prod(h_s) \times \frac{1}{\prod(l_s)} = \frac{h_s}{l_s} \quad (3.5)$$

$$\prod(L) \times \frac{1}{\prod(L_{cy})} = \frac{L}{L_{cy}} = N = \prod(W) \times \frac{1}{\prod(W_{cy})} = \frac{W}{W_{cy}} = N \quad (3.6)$$

By combining or rearranging these parameters, the discharge coefficient (C_{DL}) of the PKW is the function of various geometrical and hydraulic parameters and can define as follows:

$$C_{DL} = f\left(\frac{H_t}{P}, \frac{L}{W}, \frac{W_i}{W_o}, \frac{S_i}{S_o}, \frac{P}{P_b}, \frac{B_i}{B}, \frac{B_o}{B}, \frac{T_s}{R}, F_r, R_e, W_e\right) \quad (3.7)$$

The discharges over the different PKWs have been calculated in the present study by considering the (based on **Eqn 3.3**.) total development crest length. The head over the weir has considered the total hydraulic head [$H_t = h_t + (V_t^2/2g)$].

3.4 Design Methodologies/Parameters

Despite its complex nature, the PKW's hydraulic behavior and the numerous variables that influence it are now understood reasonably well. **Table 3.1** shows some geometrical limits used by researchers in their studies as well as what the author considered in the present study.

3.4.1 Proposed standard reference designs by the researchers based on physical modeling

Several theories are proposed as a reference for standard design for PKWs, but they did not consider all the parameters in their design procedure; only a few parameters have been considered. There is little research theory we discussed here.

A good estimate of the realistic concerns related to the standard shape of PKW was first introduced in 2010. **(ICOLD 2010)**. This shape was considered to be near to the hydraulic optimum; however, it most likely does not represent an economic optimum **(Lempérière *et al.*, 2011).** The reference shape has been depicted in **Figure: 3.4.**

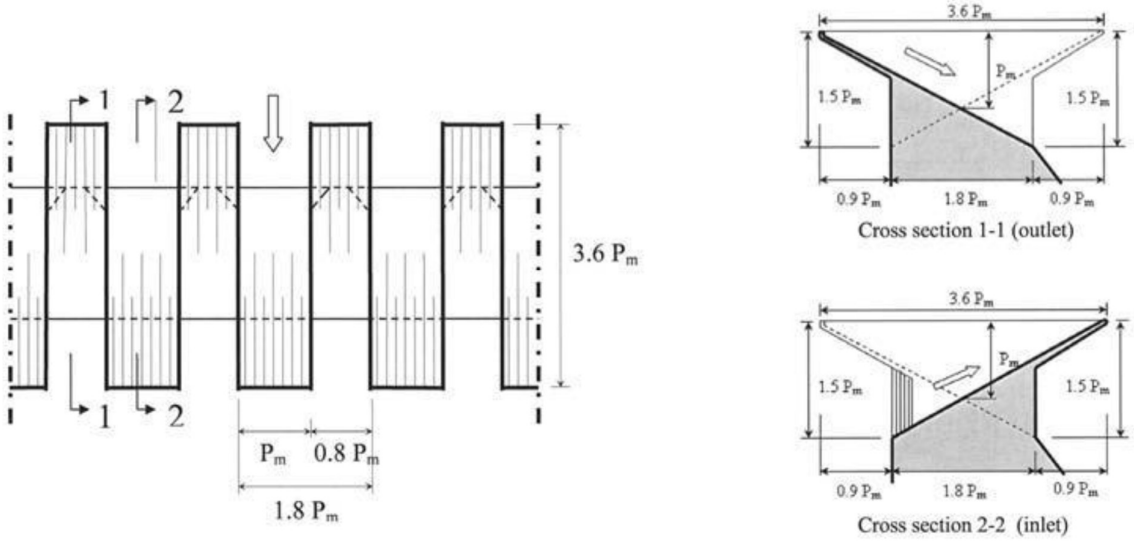

Figure: 3.4 Reference design for PKW Type-A – plan view (left) cross sections (right) (ICOLD 2010)

Lempérière (2009, 2013) accounted that with the standard geometry mentioned above; the unit discharge could be calculated within the specified limits of: $0.4P_m \leq H \leq 2\ P_m$ using the following relationship:

$$q = 4.3\ H\ \sqrt{P_m} \tag{3.8}$$

This linear proportionality ($Q \propto H$) contrasts sharply with the typical equation for a standard nonlinear weir ($Q \propto H^{3/2}$). Moreover, the constant value of 4.3 represents a fixed-value discharge coefficient which changes typically as per the overflow depth. Despite this, Anderson and Tullis (2013) established that although the formula is valid, it is applicable only for the given reference geometry.

Kabiri-Samani & Javaheri (2012) conducted an experimental investigation over-scaled physical model of Type A, B, and C of PKW having the specific discharge ranging

between 25 to 175 l/s/m at the Isfahan University of Technology, Iran. They carried out the experiments under both free as well as submerged flow conditions; however, the equation below applies only to the condition of free overflow. The metzhodology was developed by utilizing sharp-crested PKWs and therefore can be generally applied to them. The method is based on the ogee crest overflow equation:

$$Q = \frac{2}{3} C_d W \sqrt{2\, g\, H^3} \tag{3.9}$$

Where C_d, is the discharge coefficient and defined as a function of the various relevant geometrical parameters:

$$C_d = \left[0.212 \left(\frac{H}{P}\right)^{-0.675} \times \left(\frac{L}{W}\right)^{0.377} \times \left(\frac{W_i}{W_o}\right)^{0.426} \times \left(\frac{B}{P}\right)^{0.306} \times e^{1.504\frac{B_o}{B} + 0.093\frac{B_i}{B}}\right] + 0.606 \tag{3.10}$$

Where H represents the head over the PKW (m), H_d is the downstream head above the crest, P is the height of the weir (m), L is the development crest length (m), and W represents the total width of the weir, W_i and W_o represent the width (m) of inlet and outlet keys respectively, B is the length of the PKW along with the flow (m). B_i and B_o are the length (m) of the overhang portion inlet and outlet sections, respectively. Then **Eqn. (3.10)** subjected the limitations as follows: H>30mm, $0.1 \leq H/P \leq 0.6$, $2.5 \leq L/W \leq 7$, $1 \leq B/P \leq 2.5$, $0.33 \leq W_i/W_o \leq 1.22$, $0 \leq B_i/B \leq 0.26$, $0 \leq B_o/B \leq 0.26$ *and* $H_d/H \leq 0.6$.

In order to calculate the discharge coefficient of PKW under submerged conditions as flows:

$$C_s = \left[1 - 0.858 \left(\frac{H_d}{H}\right) + 2.628 \left(\frac{H_d}{H}\right)^2 - 2.489 \left(\frac{H_d}{H}\right)^3\right] \times \left(\frac{L}{W}\right)^{0.055} \tag{3.11}$$

Subjected to the limitations; $2.5 \leq L/W \leq 6$, $1 \leq B/P \leq 2.5$, $0.33 \leq W_i/W_o \leq 1.22$, $0 \leq Bi/B \leq 0.26$, $0 \leq B_o/B \leq 0.26$ *and* H_d/H >0.6.

Leite Ribeiro *et al.* (2012) also carried out systematic tests on physical models at the Laboratory of Hydraulic Constructions, Ecole Polytechnique Fédérale de Lausanne, Switzerland. Tests involved subjecting a Type-A PKW to free overflow conditions while the values of specific discharge ranged between 26 to 440 l/s/m.

Table 3. 1 Different parameters related to the PKW

Parameter → / Reference ↓		$\frac{L}{W}$	$\frac{H_t}{P}$	$\frac{W_i}{W_o}$	$\frac{B}{P}$	$\frac{B_i}{B}, \frac{B_o}{B}$	$\frac{P}{W_u}$	$\frac{B_i}{P}, \frac{B_o}{P}$	$S_i = S_o$
Lempérière and Ouamane (2003)		6	*	1	*	*	*	*	0.75:1-1.5:1
Ouamane and Lempérière (2006)		4-8.5	*	0.67-1.49	*	*	*	*	*
Lempérière (2009)		5	*	1.25	*	*	*	*	1.8:1- 1.8:1
Anderson (2011)		8	0.05-0.95	0.67-1.5	2.2-2.6	*	*	*	
Noui & Ouamane (2011)		4-8	0.1-0.9	0.7-1.5	1.6-4.1	*	0.59-1.2	*	*
Kabiri and Javaheri (2012)		2.5- 7.0	0.1-0.6	0.33-1.22	1.0-2.5	0.0-0.26	*	*	*
Leite Ribeiro *et al.* (2012b)		3.0- 7.0	0.1-2.8	0.50-2.00	1.5-4.6	0.07-1.2	0.29-0.65	0.25-4.00	*
Machiels (2012)		4.2- 5.0	0.1-5.0	0.50-2.00	1.0-6.0	*	0.33-2.00	0.0-2.67	*
Machiels *et al.* (2014)		5	0.06-3.2	0.46-2.18	1-6	*	0.33-2.0	0-2.67	*
Mehboudi *et al.* (2017)		2.8-6.5	0.07-1.11	1.33-4	1-7	0.1	0.128-0.178	0.3-2.33	*
Laiadi *et al.* (2017)		6	0.09-0.52	1.2-1.5	1.99-2.7	0.12-.36	0.9-1.24	0.24-1.0	*
According to present study	**Type-A**	4.0- 6.0	0.042-1.2	1.0-1.5	0.5-7.0	0.25-0.33	0.5-3.5	0.28-1.6	0.3-1.4
	Type-B	4.0- 6.0	0.088-1.16	1.0-1.5	0.5-7.0	0, 0.66	0.5-3.5	0, 1.1-1.89	1, 0.37
	Type-C	4.0- 6.0	0.09-0.95	1.0-1.5	0.5-7.0	0.66, 0	0.5-3.5	1.16-1.89, 0	1, 3.2

This methodology was formulated through, and therefore generally applies to, PKWs having crests of half-circular rounded shape. The discharge enhancement ratio, Q_{PKW}/Qs, is the ratio of discharge over a PKW compared to discharge for a linear sharp-crested weir, and it is used to define the output rating curve.

$$r = \frac{Q_{PKW}}{Q_s} = \frac{Q_{PKW}}{0.42\, W \sqrt{2g\, H^3}} \tag{3.12}$$

The ratio was found to vary primarily due to four key parameters: the overflow length (L), overflow depth (H), the weir height (P_i), and the weir width (W). Secondary parameters were also included to account for the effects of overhang lengths, key widths, and parapet walls.

$$r = 1 + 0.24 \left(\frac{(L-W)\, P_i}{W\, H}\right)^{0.9} wpba \tag{3.13}$$

where $w = \left(\frac{W_i}{W_o}\right)^{0.05}$ is used to define the influence of the inlet and outlet key ratio, $p = \left(\frac{P_o}{P_i}\right)^{0.25}$ to reflect any difference in the height of the inlet and outlet keys, $b = \left(0.3 + \frac{B_i+B_o}{B}\right)^{-0.5}$ to specify the influence of the overhang lengths and, $a = 1 + \left(\frac{R_o}{P_o}\right)^2$ to stipulate the presence of any parapet walls.

Machiels (2012) conducted an extensive parametric study on PK weirs and developed a methodology for discharge calculation based on an analytical approach applicable to flat-topped PK weirs. He divided the discharge flowing over the PK weirs into three parts. The discharge is released from the upstream overhangs, the downstream overhangs, and the lateral sides.

$$Q = q_{upstream} \frac{W_o}{W_u} + q_{downstream} \frac{W_i}{W_u} + q_{lateral} \frac{2B}{W_u} \tag{3.14}$$

Where Q represents the total gross discharge flowing over the PK weir (l/s), $q_{upstream}$, $q_{downstream}$ and $q_{lateral}$ are the discharges (l/s) flowing over the outlet, inlet, and side crest, respectively. W_u is the unit width (m), W_i and W_o represent the inlet-outlet key widths (m), respectively, and B represents the width of the PKW along with the flow (m). He estimated each of the specific discharges over PK weir elements as follows

$$q_{upstream} = 0.374 \left(1 + \frac{1}{1000H^{.6}}\right) \left(1 + 0.5 \left(\frac{H}{H+P_T}\right)^2\right) \sqrt{2gH^3} \tag{3.15}$$

$$q_{downstream} = 0.445\left(1 + \frac{1}{1000H+1.6}\right)\left(1 + 0.5\left(\frac{H}{H+P}\right)^2\right)\sqrt{2gH^3} \quad (3.16)$$

$$q_{lateral} = 0.41\left(1 + \frac{1}{833H+\ .6}\right)\left(1 + 0.5\left(\frac{0.833H}{0.833H+\ _e}\right)^2\right)\left(\frac{P_e^{\alpha}+\beta}{(0.833H+\ _e)^{\alpha}+\beta}\right)\sqrt{2gH^3} \quad (3.17)$$

The discharges over different segments of the PKW are calculated based on these three different equations. It is noted that each equation has a different weir height; here, P is the height of the weir (m). According to the analysis, he suggested that the downstream crest discharge depends on the ratio between water head and weir height; In the case of upstream discharge, he considered weir crest height is the summation of weir height and dam height ($P_T = P + P_d$), and for lateral discharge height of weir considered as follows: $P_e = P_T\frac{B_o}{B} + \frac{P}{2}\left(1 - \frac{B_o}{B}\right)$, B_o is the length of the overhang portion on the upstream side (m). The parameters α and β define the influence of the inlet key slope as follows:$\alpha = \frac{0.7}{S_i^2} - \frac{3.58}{S_i} + 7.55$, and $\beta = 0.029e^{-\frac{1.446}{S_i}}$.

Where H represents the overflow depth (m), P_T represents the height of the upstream crest (m), P_d is the height of the dam (m), and S_i is the slope of the inlet key. In the present study, the authors follow the methodology developed by **Leite Ribeiro *et al.* (2012)** and **Machiels (2012)** discussed in previous sections.

3.5 Computational Analysis

In this study, the computational analysis was done using Gene Expression Programming (GEP). Gene Expression Programming (GEP) is an evolutionary algorithm of the linear chromosomes encoded GEP computer programs introduced by (**Ferreira, 2001a, 2001b)**. It incorporates aspects of Genetic Programming and Genetic Algorithm. In GEP, chromosomes of different sizes and shapes can code in a simple graph 2001a, 2001b and begin with randomizing early population chromosomes, like other evolutionary methods. The early population's chromosomes are then estimated using a fitness function and its value.

In the GEP model, various fitness functions, such as mean squared error (MSE), root mean square error (RMSE), relative standard error (RSE), and root relative squared error (RRSE), can be used **(Ferreira 2001)**. The best chromosomes are more likely to be passed down to the next generation. Genetic operators repeat these acts with slight variations after selecting the best chromosomes. The applications of the GEP were covered in more detail in the subsections that followed.

3.5.1 Application of GEP

The GEP model must be configured in several stages, and the process starts with randomly generating the initial population's chromosomes. The chromosomes are then expressed, and the fitness of each individual is assessed. Individuals are then chosen to reproduce with modification based on fitness, resulting in progeny having new traits. The same developmental process is then subjected to the individuals of this new generation: genome expression, selection environment confrontation, and reproduction with modification. The process is repeated until a solution is found or until a certain number of generations have passed.

In the case of the present study, the modeling process is adopted as the target parameter and the independent parameters on which the target parameter depends. Then select the basic operators for developing the GEP models based on the target parameters. For achieving a GEP model that is uncomplicated and sensible, the functions were chosen on the basis of their coherence to the quiddity of the problem. The general sampling strategy chose 30 chromosomes, three genes, and eight head sizes in this study.

The flowchart for the gene expression algorithm (GEA) is illustrated in **Figure: 3.5.** It is important to note that reproduction encompasses replication and the actions of genetic operators having the capability to generate genetic diversity. A copy of the genome is made and then transmitted to the next generation during the process of replication. However, the process of repetition alone is unable to introduce variation: genetic variation is introduced into the population only through the actions of the remaining operators. These operators choose the chromosomes to be modified at random. Therefore, in GEP, a chromosome may either be simultaneously limited by one or more operators, or not be modified at all. The chromosome or genome in GEP is a linear, symmetrical string having a fixed length of one or more genes. It shall be demonstrated that even though they have fixed lengths, the GEP chromosomes are capable of coding ETs of various shapes and sizes.

3.5.2 Fitness function and selection

A fitness function can be regarded as an objective function that summarizes how precise a given design solution is in achieving the set objectives in terms of a single figure of merit. These functions are employed in genetic programming and algorithms for steering the simulations in a way that leads to optimal design solutions. A problem's success relies on how the fitness function has been designed: the goal needs to be defined in a clear and correct manner to make the system evolve in that direction.

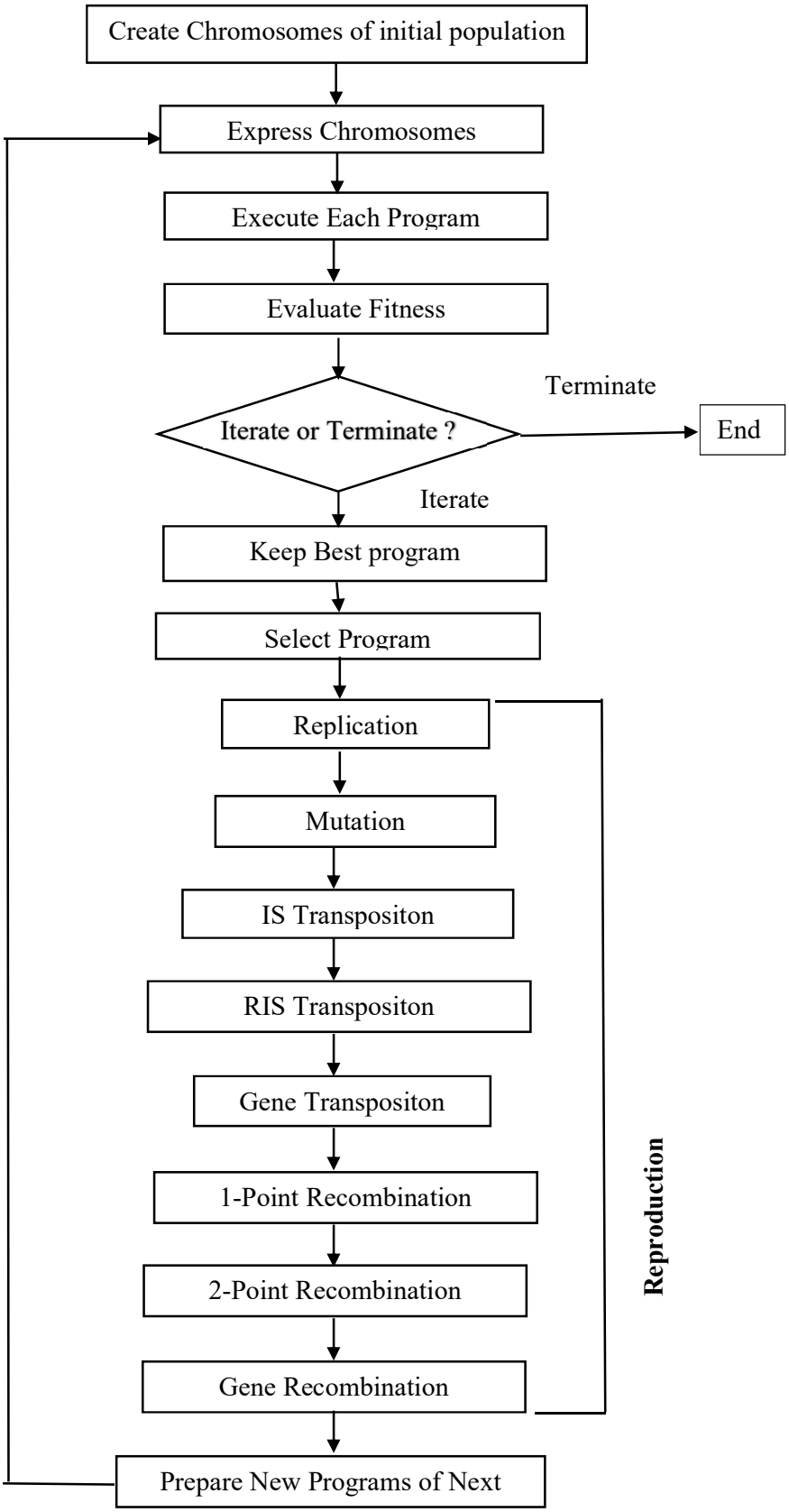

Figure: 3.5 The flow chart of the Gene Expression Algorithm (Adapted from (Ferreira 2001))

The purpose of symbolic regression or function finding of the GEP is to determine an expression that is capable of performing well for the entire range of fitness cases within a certain error of the true value. Small relative or absolute errors can help you find a perfect solution in a few mathematical applications. However, for an overly narrow range of selection, the population evolution rate is very slow and thus is unable to determine a correct solution. At the same time, if the range of options is expanded, the various solutions having maximum fitness are far from satisfactory.

Several selection schemes are available, including a roulette wheel selection with and without elitism, a tournament selection with and without elitism, and various deterministic selections with and without elitism. However, there is no discernible difference between them in terms of ensuring the cloning of the best individual (results not shown). A few schemes outperform others in one problem while excelling in another. However, roulette wheel selection with elitism appears best for more complex issues.

3.5.3 Replication

According to the roulette's luck and fitness, individuals are chosen for reproducing along with modification, thus generating the required genetic diversification to allow evolution in the long run. Although vital, replication is the least interesting operator alone; it does not contribute anything to the process of genetic diversification. (Combined together with selection, it can only result in genetic drift.)

3.5.4 Mutations

Mutations can take place at any location in the chromosome. Having said that, the chromosomes' structural organization needs to remain intact. In the tails, terminals can only be modified into terminals. While in the heads, any of the symbols can change into another (terminal or function); This maintains the chromosomes' structural organization and ensures all the new individuals generated as a result of mutation are structurally correct programs.

3.5.5 Transposition and insertion sequence elements

GEP transposable elements are genome fragments that can be activated and jump to a different chromosome location. In GEP, there are three types of transposable elements. (1) Short fragments with a function or terminal in the first position transpose to the head of genes, except for the root (insertion sequence elements or IS elements). (2) To the root of genes, transpose short fragments with a function in the first position (root IS elements or RIS elements). (3) Entire genes that transpose to the beginning of chromosomes.

3.5.6 Recombination

Three kinds of recombinations are there in GEP: one-point, two-point, and gene recombination. In each case, two-parent chromosomes are chosen at random and paired to exchange some material.

3.5.6.1 One-Point Recombination

The chromosomes cross over an arbitrarily chosen point during one-point recombination, resulting in two daughter chromosomes.

3.5.6.2 Two-Point Recombination

The chromosomes are paired in two-point recombination, and the two recombination points are chosen at random. The material between these points is then exchanged among the two chromosomes, forming two new daughter chromosomes.

3.5.6.3 Gene Recombination

Gene recombination involves the exchange of an entire gene. The exchanged genes are selected randomly and occupy the same position on the parent chromosomes.

3.6. Some other Important Design Aspects

In this section, PKW's capability is to be checked regarding the energy dissipation, aeration performance of the different types of the PKW, and scouring aspects near the toe of the PKW. A discharge over a PKW almost depends on the various geometrical and hydraulic parameters. Several additional factors could change the PKW's discharge capacity and should be considered during the design process. The PKW's capabilities in terms of energy dissipation, scouring at the weir's toe, aeration performance, and other factors are described below:

3.6.1 Parapet walls, crest shape, and nose

Parapet walls: The parapet wall is a short vertical wall mounted on the PKW's crest. It raises the height as well as the length of the weir's keys. The PKW design with parapet walls on the inlet keys can primarily improve the with relatively low heads. However, implementing PKW with parapet walls on the outlet keys does not affect performance **(Machiels *et al*., 2013).** As investigated by some researchers, only a minimal benefit is there to a parapet on the inlet key's downstream crest; however, a significant benefit is observed when one is placed on the outlet key's upstream crest **(Machiels *et al.* 2013).** With a larger volume, the outlet key can operate under undrowned conditions for a longer time relative to the side crest operating at its free-flowing efficiency.

Crest shape: The crest shape has a significant role in the efficiency of any spillway, especially at low water levels. **(Falvey, 2003)** conducted the tests on the crest shape over labyrinth weir and said this study could be applied entirely to PKWs. The PKW's crest shape is more influenced at low H_t/P values, but this effect decreases considerably as $H_t/P > 0.3$. **Cicero & Delisle (2013)** studied the impact by utilizing scaled physical models and observed that a quarter-round or half-round crest on the lateral (side) crest encountered the most considerable effect relative to a flat-topped crest.

In addition, it was observed that the crest shape on the downstream and upstream portions of the keys had negligible effect, possibly owing to their short length. Nonetheless, the downstream crest must be sharp-crested for smoother flow lines while the upstream crest is rounded (quarter round on its upstream side). **(Laugier *et al.*, 2017).**

Nose: The nose placement on the upstream (outlet key) overhang portion plays a vital role in guiding the flow to the inlet keys; either side has been found to be a good design feature **(Philips & Lesleighter 2013).** Their presence causes smoother flow lines, lower energy losses, and fewer vortexes to shed, resulting in increased PKW discharge efficiency. Noses can be made in any convenient shape rounded, triangular, or tapered; it depends on the structure's overall stability, especially Type-A PKWs, which are self-stable without these noses **(Laugier *et al.*, 2017).** Many researchers have investigated the nose impact on PKW behavior, but none has been incorporated into the design equations. They suggested that the nose is recommended, but their quantified effect can only be determined by physical or numerical modeling.

3.6.2 Energy Dissipation over the PKW

The PKW represents an effective solution for increasing the storage capacity and evacuation capacity of floods during the rainy season. Any hydraulic structure tends to discharge water at high efficiency; in that case, the high energy dissipation occurs downstream of the weir. Particular attention should be taken to dissipative structures downstream of a PKW to prevent undesirable aspects such as scour and cavitation. Many experimental studies have shown that the scour depth or scour volume downstream of a PKW depends not only on the sediment characteristics, head differences, the discharge, and the tailwater depth but also on the downstream overhang length of the weir **(Jüstrich *et al.*, 2016).**

Recently **(Truong and Ho Ta Khanh, 2017) (Eslinger and Crookston 2020); (Singh and Kumar 2022a), and (Singh and Kumar 2022c)** examined the energy dissipation

flow over the PKW and found the energy dissipation grater at the low head. As the discharge/head increases, the energy dissipation capacity of the weir decreases.

In the present study, the experiments were performed under free-flow conditions as well as in submerged situations. In the case of submerged flow, the tailgate controls the downstream water depth. The following is the calculation of the upstream and downstream specific energy across the PKW:

$$E_i = P + h_{ti} + \frac{{V_{ti}}^2}{2g} \tag{3.18}$$

Where E represents the specific energy at section i, P represents the height of the weir in (m) (for downstream of the weir, P=0 m), h_t represents the head at section i, V_t is the velocity at section i, and i represents the section (i.e., i =1, 2…, Section 1 was considered upstream, and section 2 was considered downstream as shown in the **Figure: 3.6.**

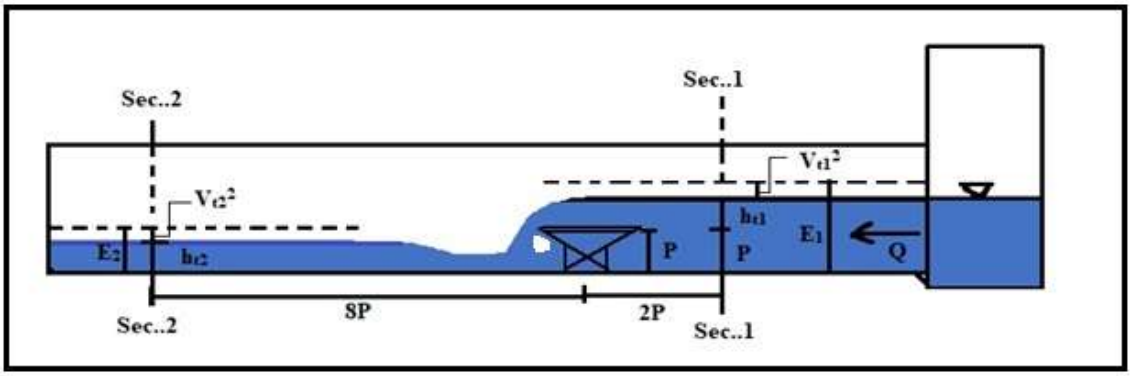

Figure: 3.6 Schematic plot for total energy head measurement.

Upstream flow depth (P+ h_{t1}) and downstream flow depth h_{t2} were measured carefully with a 4-20 mA ultrasonic level sensor as well as a pointer gauge of ± 0.1 mm (accuracy ± 0.2 % ±1 mm) after the water surface had been allowed to steady-state for at least 3 to 5 minutes or it can increase for the higher flow rate) were taken in such a way that the flow or water level has been stabilized. In general, a more stabilization time is required for a higher discharge rate through the channel. With the help of ADV, the mean approach flow velocity V_{ti} was measured for one-minute records at the same section where the head h_{ti} values were measured. The heads over the PKWs were measured at a distance upstream X= 2 x P, where X is the distance from the lateral centreline of the PKWs **(Oertel 2016)**. The downstream site head was measured at a distance of $8P$ from the lateral centreline of the PKWs, after the downstream water level approximately stabilized, as shown in **Figure: 3.6.**

Further, the values of E_1 and E_2 were used to compute the relative energy dissipation based on **Eqn. (3.19)** and relative residual energy (E_r=E_2/E_1) is calculated considering the total energy downstream is equal to 100 %.

$$E_L = \frac{(E_1 - E_2)}{E_1} \times 100 = \left(1 - \frac{E_2}{E_1}\right) \times 100 \tag{3.19}$$

and,

$$E_r = 1 - E_L = \frac{E_2}{E_1} \tag{3.20}$$

Where E_L denotes total relative energy dissipation or energy dissipation ratio, and E_r (=E_2/E_1) is the relative residual energy downstream of the PKW.

Hydraulic and geometrical parameters involved in energy dissipation are arranged in **Eqn. (3.21)** to determine those that affect energy dissipation over the PKW.

$$E_L = f\left(\rho, g, V_t, H_t, L, L_{cy}, P, W, W_i, W_o, W_{cy}, S_i, S_o, R, h_s, l_s\right) \tag{3.21}$$

In which ρ is the density of flowing fluid, g is the acceleration of gravity, and H_t is the total upstream hydraulic head (h_t+V_t^2/2g) over the PKWs. The other geometrical parameters are as follows: L = the length of the crest developed; L_{cy} = crest length of one cycle; P = height of PKW, W = width of PKW; W_i and W_o = widths of inlet and outlet keys sections, respectively W_{cy} = width of one cycle and S_i and S_o represents the inlet and outlet key slopes variation, respectively, R = height of parapet wall, l_s and h_s = length and height of the steps, and N = number of cycles. Using the Buckingham theorem as a dimensional analysis technique and considering the ρ, g, and P as repetitive parameters **(Eqns. (3.22, 3.23, 3.24),** the dimensionless parameters are derived as **Eqn. (3.25).** Usually, the flow regime upstream of weirs constructed perpendicular to the river course is always subcritical; hence, the Froude number is not considered in evaluating their hydraulic properties **(Haghiabi *et al.*, 2021)**. Therefore, **Eqn. (3.25)** can be rewritten as **Eqn. (3.26).**

$$\prod_1(H_t) = \frac{H_t}{P},\ \prod_2(L) = \frac{L}{P},\ \prod_3(L_{cy}) = \frac{L_{cy}}{P},\ \prod_4(W) = \frac{W}{P},\ \prod_5(W_i) = \frac{W_i}{P},\ \prod_6(W_o) = \frac{W_o}{P},$$
$$\prod_7(W_{cy}) = \frac{W_{cy}}{P},\ \prod_8(S_i) = S_i,\ \prod_9(S_o) = S_o,\quad \prod_{10}(R) = \frac{R}{P},\ \text{and}\quad \prod_{11}(V_t) = \frac{V_t}{\sqrt{gP}} = F_r,$$
$$\prod_{12}(l_s) = \frac{l_s}{P}, \prod_{13}(h_s) = \frac{h_s}{P} \tag{3.22}$$

$$\prod(L) \times \frac{1}{\prod(W)} = \frac{L}{P} \times \frac{P}{W} = \frac{L}{W}, \prod(W_i) \times \frac{1}{\prod(W_o)} = \frac{W_i}{P} \times \frac{P}{W_o} = \frac{W_i}{W_o}, \prod(S_i) \times \frac{1}{\prod(S_o)} = \frac{S_i}{S_o},$$
$$\prod(h_s) \times \frac{1}{\prod(l_s)} = \frac{h_s}{l_s} \tag{3.23}$$

$$\prod(L) \times \frac{1}{\prod(L_{cy})} = \frac{L}{L_{cy}} = N = \prod(W) \times \frac{1}{\prod(W_{cy})} = \frac{W}{W_{cy}} = N \quad (3.24)$$

By combining or rearranging these parameters, the relationship is obtained:

$$\frac{E_L}{E_1} = f\left(\frac{H_t}{P}, \frac{L}{W}, \frac{W_i}{W_o}, \frac{S_i}{S_o}, \frac{h_s}{l_s}, N, F_r, \frac{R}{P}\right) \quad (3.25)$$

For subcritical flow

$$\frac{E_L}{E_1} = f\left(\frac{H_t}{P}, \frac{L}{W}, \frac{W_i}{W_o}, \frac{S_i}{S_o}, \frac{h_s}{l_s}, N, \frac{R}{P}\right) \quad (3.26)$$

3.6.3 Aeration

The flow over the weir is naturally aerated, according to most physical models of PKWs. It is only valid for the relatively low head. The air pocket under the nappe becomes isolated at the higher head, and sub-atmospheric pressure conditions may occur. This negative pressure enhances the discharge efficiency of the weir; however, its influence on the structure's stability remains unclear.

Aeration efficiency depends on the quality of air intake in the state of water. DO is incongruent with an entirely liquid-controlled gas-water transfer rate. Thus **Gameson (1957) and Gulliver *et al.* (1990)** stated that the concentration rate of oxygen changes over time in the air-water phase system as water passes over hydraulic structures and can be expressed as,

$$\frac{dC}{dt} = K_L \frac{A}{V}(C_S - C) \quad (3.27)$$

Where C = DO concentration; K_L= Coefficient of liquid-mass transfer; A = Surface area associated with the volume of water (V) over which the transfer occurs; C_S = Saturation concentration at the equilibrium with the air phase is achieved; and t is the time. By integrating the **Eqn. (3.27)** we get the aeration efficiency.

$$E = \frac{C_d - C_u}{C_s - C_u} = 1 - \frac{1}{m} \quad (3.28)$$

E= oxygen transfer or aeration efficiency, C_d = DO concentration d/s of hydraulic structure, C_u = DO concentration u/s of hydraulic structure, C_s = DO at a saturated level for a given ambient condition, and m = oxygen deficit ratio. Aeration efficiency E = 1.0 indicates that complete exchange up to the saturation value occurred at the structure, while E = 0.0 indicates no transfer occurred. Typically, the saturation concentration is calculated using charts or equations and is set to the local atmosphere value.

The temperature profoundly affects aeration efficiency, so researchers use a temperature correction factor to estimate aeration efficiency. **Gameson *et al.* (1958)** specified the most

commonly used temperature correction factor for hydraulic structures. **Gulliver *et al.* (1990)** developed the mass exchange comparability relationship to adjust aeration efficiency to 20^0C and signified it as E_{20}.

$$E_{20} = 1 - (1 - E)^{1/f} \tag{3.29}$$

Where exponent *f* depends on the in-situ temperature and is expressed as follows:

$$f = 1 + 0.02103(T - 20) + 8.261 \times 10^{-5}(T - 20)^2 \tag{3.30}$$

Where T = temperature during measurement in ^{0}C.

In the present study, the above methodology has been adopted to examine the aeration performance of the three different types (type-A, type-B, and type-C) of PKW models. The study results demonstrated that the aeration performances of the PKW depend on the drop height and the flowing discharge (**Singh and Kumar, 2022b)**. **Vermeulen et al. (2017)** proposed a method of air demand emphasis on air driven by a rectangular channel stream dropping into a volume of free water surface.

3.7 Conclusion

As discussed, free flow spillways and weirs serve as hydraulic structures for discharge measurement on existing and newly constructed dam structures during flood release or open channel applications. Efficient hydraulic systems are vital in controlling and releasing the flood water without harming the dam structures and protecting the towns and cities farther down the river. The PKW can be an efficient solution for rehabilitation and new dam projects with various constraints, such as limited space, a small reservoir level, a high value of specific flood discharge, and so on. This chapter deals with the different methodologies developed by researchers over the past fifteen to twenty years and various geometric and hydraulic aspects that influence the efficiency of the PKW. The findings of the present study are presented in the next chapter.

4.1 General

Chapter 3 presents the experimental setup, model fabrication, used methodologies, and Piano Key Weir's design requirements (PKW). This chapter presents the results of the various objectives and the impacts of the different parameters on the hydraulic behavior of the PKW. The findings of this study are based on multiple goals, i.e., hydraulic behavior of PKW, energy dissipation, aeration performance, and the various geometrical parameters affecting hydraulic behavior and design of the PKW, which are presented and discussed in the following sections.

PKW, as previously demonstrated, is an intriguing structure for dam rehabilitation, enhancing magnitudes of probable maximum storm events, reservoir water storage, and the ongoing need for dam safety; many existing spillways are undersized and require replacement. The utilization of PKW for new dams and barrages is intriguing because, as with gated spillways, they maximize the Full Supply Level (FSL) and minimize the Maximum Water Level (MWL), with a possible rapid drawdown just after the floods due to the high PKW capacity for low nappe depth. Gated or non-gated weirs are commonly used as the flow control structure in reservoir spillways because they allow more discharges than ogee-crested weirs for the same water head. These advantages are much appreciated in Vietnam, with several small power plants at the toe of low dams and flat rice fields **(Ho Ta Khan, 2017)**. Moreover, the PKW presents many advantages compared with the gates. They can thus totally or partially replace the gates in many situations with the possibility to be easily installed on all types of concrete structures.

4.2 Experimental Results and Discussion

4.2.1 Flow Behaviour of PKW

The basic concept of the flowing discharge over the PKW is that flow converges into the inlet key and diverges away from the outlet key **(Machiels 2012).** The total flowing discharge over the weir summarizes three discharges, discharge through the inlet keys, discharge through the outlet keys and discharge through the side crest walls. All the three modes of the flow of discharges meet consequently in an intricate flow **(Khassaf *et al.* 2015)**. The flow through the PKW is highly aerated and three-dimensional, with splash and spray regions within the outlet keys and at the base of the structure (**see Figure: 4.1**). The area of spray and sprinkling only increased marginally proportional to the trajectory of H_t and the

planar jet that started downstream on the crest. But the aeration region increased significantly with H_t, partly because the local speed increased, resulting in greater advection levels and turbulent mixing. The nappes passing over the PKW crest are patterned as three planar jets conversing over a slanting surface **(see Figure: 4.1)**, with opposing nappes creating a water surface conflict zone, a crossing region, and small wakes near the upstream apexes.

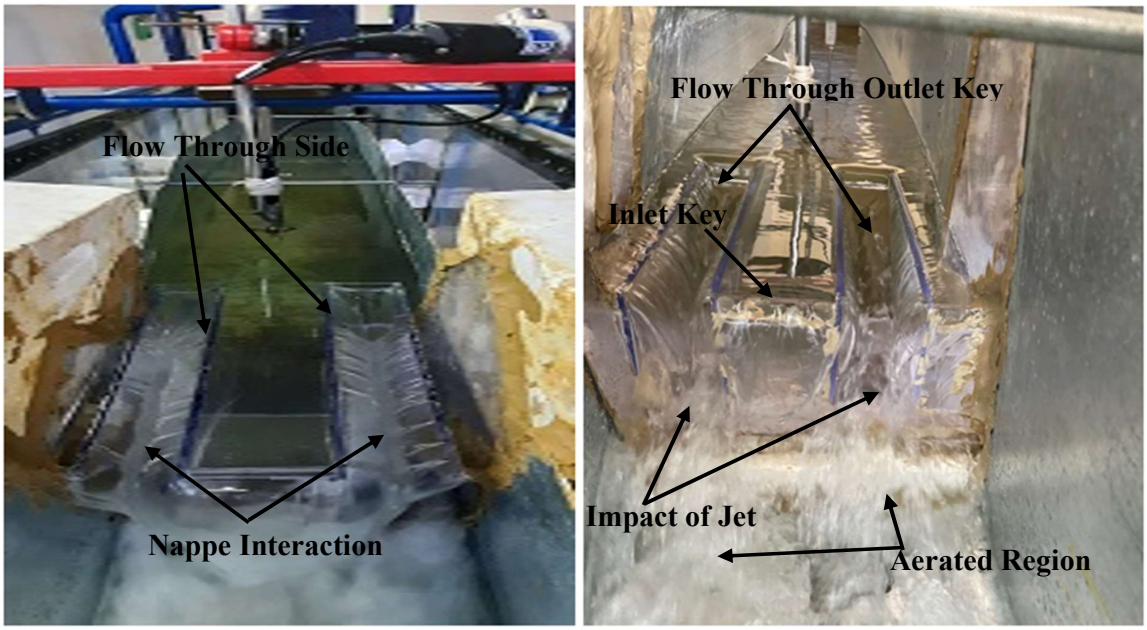

Figure: 4.1 Flow patterns over PKW.

4.3 Geometric Influences on the Discharge Capacity of PKWs

The PKW is a complex structure that involves a large number of geometrical and hydraulic parameters. From the experimental results and the observations of the different types of model studies and the flow behavior of the PKW almost depends on the L/W and H_t/P ratios, several additional factors could change the PKW's discharge capacity and should be considered during the design process. The development crest length (L), the slope of the inlet-outlet keys (S_i & S_o), weir height (P), inlet and outlet key width (W_i & W_o), unit width (W_u), number of unit width, base length (B), lengths of inlet and outlet overhang portions (B_i & B_o), and wall thickness are the main influencing geometrical parameters (T_s). The PKW unit is the central component of the PKW. It is a small-scale replica of a complete structure consisting of two sidewalls, an inlet key, and half of the outlet keys on both sides **(Pralong *et al.*, 2011).** There are some of the most discharge influencing parameters that are discussed in detail below:

4.3.1 Magnification ratio (*L/W*)

The magnification ratio is the most significant parameter which directly influences PKW's discharge capacity. According to, **Machiels *et al.* (2011)**, the development crest length to width ratio (L/W) = 5, height to unit width ratio (P/W_u) = 1.3, overhangs length ratio B_i/B_o= 3, and the ratio of key width (W_i/W_o) = 1.25 shows the highest discharge capacity and this finding is steady with those of **Lempérière *et al.* (2011)** and **Leite Ribeiro *et al.* (2012)**. **Lempérière and Jun (2005)** stated that the L/W ratio for effective PKW design must lie between 4 to7. The value for L/W= 6 is recommended as near to optimal by **Barcouda *et al.* (2006)**. In order to have a large L/W ratio, more the PKW's efficiency **(Ouamane and Lempérière, 2006)**.

The present study tested the magnification ratio (L/W) range of 4-6 and examined their hydraulic behaviour by conducting an experimental investigation of different types of PKWs (i.e., type-A, type-B & type-C). The model's configurations are as follows: the relative width ratio (W_i/W_o) is 1.28. The height of all models (P) is 0.15 m. The inlet-outlet key slopes are 45^0 (S_i=S_o=1) for Type-A, S_i =1, & S_o =0.37 for Type-B, and S_i =1, & S_o =3.2 for Type-C. The two overhang portions are such that B_i=B_o, are alike for Type-A, whereas B_i=0, B_o= 2/3 B_b, for Type-B, and B_i=2/3 B_b, B_o=0, for Type-C. The testing discharges were varied over the model between 0.005 $m^3/s \leq Q \leq 0.05 m^3/s$. The ranges of the data collected in the present study are shown in **Table: 4.1.**

Table: 4. 1 Range of Data collected for different L/W ratios of Different types of PKWs

S. No.	W_i/W_o	L/W	S_i, S_o	H_t(m)	Q(L/s)	$B_i/P= B_o/P$	Number of readings
Type-A	1.28	4	1.08	0.0144-0.1187	5.13-50.16	0.69	15
	1.28	5	1.08	0.0141-0.1235	5.10-50.26	0.69	15
	1.28	6	1.08	0.0139-0.1198	5.16-50.07	0.69	15
Type-B	1.28	4	1, 0.37	0.0134-0.1257	5.25-50.21	0, 1.49	15
	1.28	5	1, 0.37	0.0131-0.1335	5.14-50.06	0, 1.49	15
	1.28	6	1, 0.37	0.0137-0.1388	5.06-50.17	0, 1.49	15
Type-C	1.28	4	1, 3.2	0.0140-0.1087	5.03-50.36	1.49, 0	15
	1.28	5	1, 3.2	0.0137-0.1215	5.20-50.16	1.49, 0	15
	1.28	6	1, 3.2	0.0143-0.1098	5.09-50.11	1.49, 0	15

For maximum discharge efficiency, the development crest length of the PKW should be several times the weir width. Indeed, this ratio demonstrates how effectively a design maximizes the crest length L by maximizing the available width W. The flow control section must then be located along the crest to maximize the developed crest length L discharge. This means that the inlet should not constrain flow over the developed crest, and flow conditions

in the outlet should not cause it to submerge. At this point, it is necessary to concentrate on the economic aspects of the PKW.

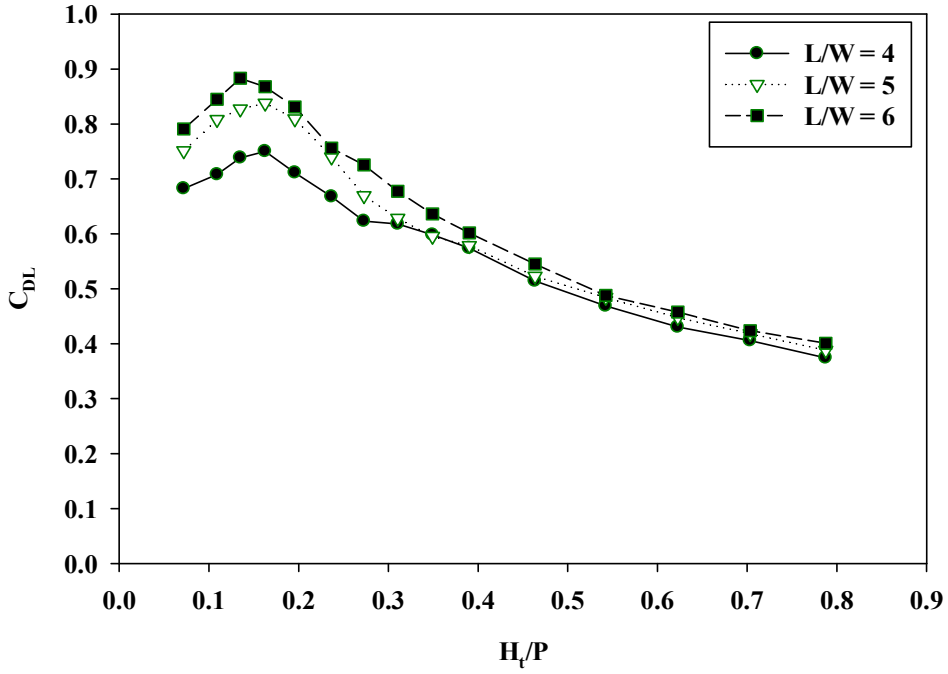

Type- A

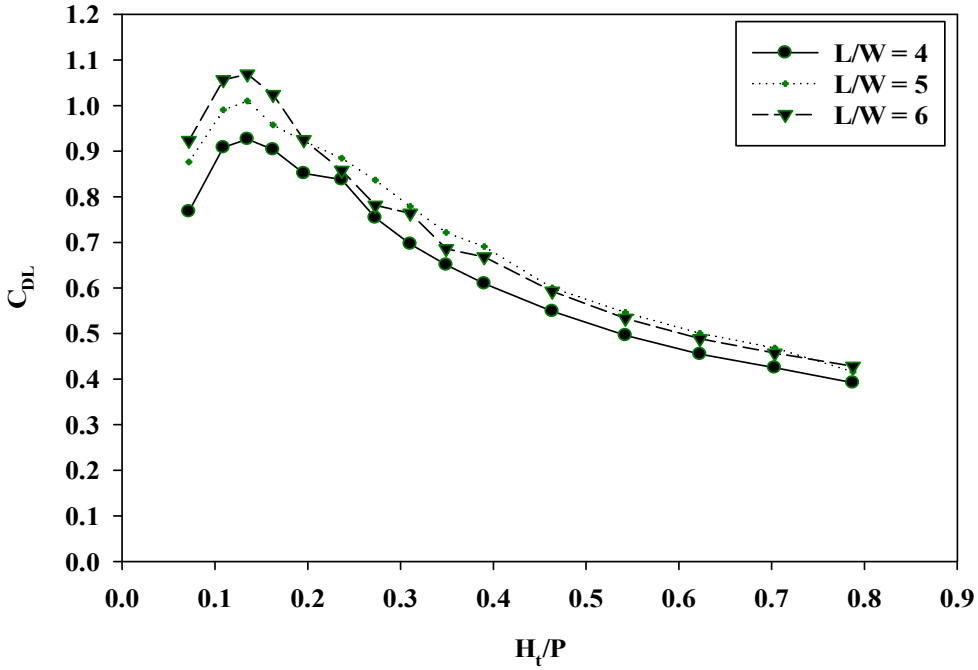

Type-B

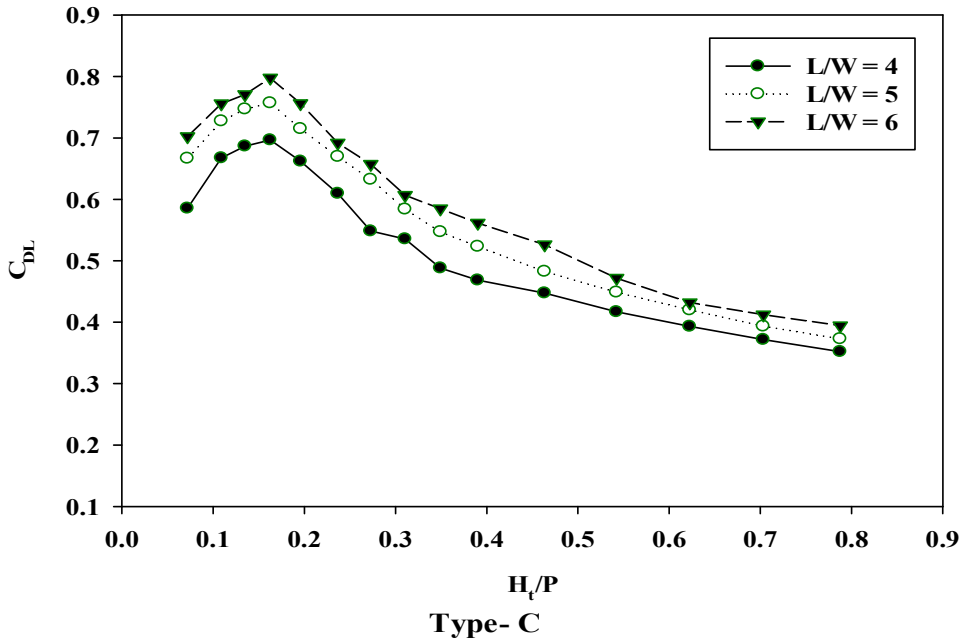

Figure: 4.2 C_{DL} vs. H_t/P for different L/W ratios of different types (type-A, type-B and type-C) PKW.

Figure: 4.2 concludes that the *L/W* ratio equal to 6 shows more efficiency than the *L/W* = 4 in all the types of PKW. *L/W* = 6 has 12-16 % more efficiency than the *L/W* = 4 for the type-A PKW models. The type-B PKW has shown a 16% - 22% higher discharge efficiency rate at *L/W* = 6 than the *L/W* = 4. Type-C at *L/W* = 6 has shown a 10-14 % higher discharge efficiency than the *L/W* = 4. The variation of the crest length affects the discharge carrying capacity of PKW at a significant level; this may be due to the *L* varies with the head as the effective crest length decreases with expanding heads because of local submergence on the upstream apex. Flow drowning and lateral jet overcrossing occur as the head increases, increasing the discharge efficiency of the PKW. **Lempérière (2009)** recommended that the *L/W* ratio equal to 5 was close to efficient. According to **Hien *et al.* (2006)**, for smaller H_t/P values, the *L/W* ratio equal to 7 is more effective, and for larger H_t/P values, the optimal value of the *L/W* ratio lies between 5 to 6. According to **(Lempérière *et al.*, 2011); and (Leite Ribeiro *et al.*, 2013)**, the *L/W* ratio for most PKWs installed to date ranges from 4 to 8; however, a ratio of 5 seems to be the most cost-effective and has been implemented in most existing PKWs. The *L/W* ratio values of 6 or 7 will optimize discharge versus substantial quantity, improving project economics, according to **Laugier *et al.* (2017)**. But according to the present study findings, the discharge efficiency increases as the *L/W* ratio increases because the constant width of the weir or channel *L* should be maximized to release or discharge more flow.

4.3.2 Wier Height (*P*)

The PKW's height is also the most influencing parameter for the inlet and outlet key slopes; without increasing the overhang's potion length. **Lempérière and Jun (2005)** stated that the minimum ratio of the floor slope for the inlet to outlet key should be 2:1. Further, **Barcouda *et al.* (2006)** reported that by increasing the floor slope from 2:1 to 3:2, the discharge efficiency is increased by 20% for large H_t/P values, and it was found to uniform for both types A and B of PKW (where H_t head over the weir and P represents the weir height). **Ouamane and Lempérière (2006)** tested three different PKW models with varying height P and, consequently, changes in floor slope (inlet-outlet key slope), with other parameters held constant. They found that an increasing the height by 25%, the efficiency increased by 6%. It is unclear whether the height P is more predominant for improving the efficiency or floor slope because two parameters are changing simultaneously. **Lempérière (2009)** recommended that the inlet-outlet key slope of PKWs be 1.8:1 (horizontal: vertical). Increasing the weir height for the low head, 25%, and for the medium head, 5 % higher performance can be achieved **(Noui and Ouamane 2011)**.

The floor slope effect of the inlet-outlet key over the capacity of PKW was presented by **Machiels *et al.* (2011a)**, and they suggested that as the inlet key height increases, the evacuation capacity of the weir increases. However, **Machiels *et al.* (2011c)** indicate that a further rise in the slope for a slope more than 1.2 (*V: H*) increases the slope and does not significantly change discharge efficiency. **Erpicum *et al.* (2014)** stated that the efficiency of PKW is influenced by parameters such as inlet and outlet key widths and overhang length ratio (B_i/B_o) but is highly affected by the weir height as primary importance. **Ramakrishnan *et al.* (2014)** found a high *Cd* value of the discharge coefficient at slope 450 with a parapet wall.

Most past studies on PKW height (or slope of inlet-outlet key bottoms) are based on experimental and analytical approaches. Few studies were based on numerical simulation. Therefore, there is a need to develop numerical simulation or CFD analysis and validate the results with experimental data to understand PKWs geometry better. PKW is influenced by parameters such as inlet and outlet key widths and overhang length ratio (B_i/B_o) but is highly affected by the weir height as primary importance. **Ramakrishnan *et al.* (2014)** found a high *Cd* value of the discharge coefficient at slope 450 with a parapet wall. Most past studies on PKW height (or slope of inlet-outlet key bottoms) are based on experimental and analytical approaches. Few studies were based on numerical simulation. Therefore, there is a need to

develop numerical simulation or CFD analysis and validate the results with experimental data to understand PKWs geometry better.

In general, the literature indicates that as the height and slope of key floors of the PKW are increased, the discharge efficiency of the PKW increases. Including the parapet wall over the top of PKW is vital in upgrading the weir height and storage capacity without expanding the overhangs **(Leite Ribeiro *et al.*, 2009; Machiels *et al.*, 2013)**. Few studies have shown that placing a parapet wall of a certain size on the upstream crest of the outlet key increases the discharge capacity of PKWs, while adding the parapet wall on the downstream crest of the inlet key has a marginal effect on PKW discharge efficiency **(Machiels *et al.*, 2013)**. In addition, **Leite Ribeiro *et al.* (2009)** presented a model-based study on the Etroit dam. They concluded that by enhancing PKW's height, roughly 1 m (in the prototype) with a parapet wall, the discharge capacity increased up to 15 %.

This study aims to determine the optimal slopes for the inlet-outlet key bottom of the PKW and compare the findings to previously published data. To this end, 12 laboratory-scaled PKW models were tested with a horizontal channel bed as well as a sloping bed (all 12 models were tested for six different bottom slopes (S_b= 0%, 0.025%, 0.5%, 0.75%, 1.0%, and 1.25 %)), and the discharge coefficients were calculated using **Eqn. (3.3).** The flowing rate (Q) was varied (0.0025 - 0.050) m^3/s, the head and head to weir height ratio ranged 0.0072 m $\leq H_t \leq$ 0.11m, $0.04 \leq H_t/P \leq 1.2$, respectively, and other parameters were varied $0.28 \leq \{B_i/P = B_o/P\} \leq 1.6$. The data collected in the present section is presented in **Table: 4.2.** After assessing data, results were plotted and analyzed between the various design characteristics parameters, as shown in **Figures: (4.3 to 4.8).**

4.3.2.1 Effect of the PKW's sloping key bottom on its discharge capacity with Horizontal Bed

In the current study, the hydraulic head-to-weir height ratios ranged from $0.04 \leq H_t/P \leq 1.2$, at which some H_t readings are smaller than 0.03 m (**Erpicum *et al.*, 2016: Novak *et al.*, 2010)**, implying that the scale effect plays a role in these critical area's values. In that case, more than one model law comes into the picture (i.e., Reynolds number (R_e), as well as Weber number (W_e), have also come along with Froude number (F_r) to influence the discharge capacity of weir structures). **Erpicum *et al.* (2016)** presented a detailed study about the scale effects consideration over PKWs. Large-scale variables are considered when developing physical models (small dimensional models). The flow characteristics of such models may be affected- by unscaled parameters such as atmospheric pressure, water viscosity, and surface

tension. Weir crests at low overflow depths will show scale effects due to viscosity and surface tension that is very difficult to scale. As a result, scaling fails to achieve model-to-prototype similarity. These variations are referred to as size-scale effects. These variations can affect the stage-discharge correlation, nappe course, and air entrainment **(Tullis *et al.*, 2020)**. **Tullis *et al.* (2020)** evaluated that the total head over the PKW and scaled-to-prototype (for scale-ratio 1:3) head thresholds are (*Ht/P*) 0.09. In the present study, the head-to-weir height ratio H_t/P is divided into three categories to identify the impact of surface tension and viscous effects on PKW; (i) Low head ratio ($0.04< H_t/P \leq 0.09$), (ii) Medium head ($0.10 \leq H_t/P \leq 0.35$) (iii) High head ratio ($H_t/P > 0.35$), and to see the hydraulic performance of the weir in terms of flow initiation, nappe aeration, and trajectory behaviors. The detailed discussion follows in the subsections that follow.

Table: 4.2 Range of data collected for different inlet-outlet key bed slopes [type-A PK weirs]

Model No.	Range of Q (m^3/s)	Range of H_t (m)	$S_i = S_o$	$\frac{W_i}{W_o}$	P (m)	$\frac{L}{W}$	B (m)	B_i (m)	B_o (m)	N (No. of cycles)	No. of runs for six-bed slopes
PKW-1	0.0025-050	0.0072-0.11	0.3	1	0.075	5	0.343	0.115	0.115	3	**14 runs per slope**
PKW-2	0.0025-050	0.0075-0.105	0.4	1	0.10	5	0.343	0.115	0.115	3	---do---
PKW-3	0.0025-050	0.0076-0.102	0.5	1	0.125	5	0.343	0.115	0.115	3	---do---
PKW-4	0.0025-050	0.0079-0.101	0.6	1	0.15	5	0.343	0.115	0.115	3	---do---
PKW-5	0.0025-050	0.0081-0.095	0.7	1	0.175	5	0.343	0.115	0.115	3	---do---
PKW-6	0.0025-050	0.0073-0.10	0.8	1	0.20	5	0.343	0.115	0.115	3	---do---
PKW-7	0.0025-050	0.0074-0.101	0.9	1	0.225	5	0.343	0.115	0.115	3	---do---
PKW-8	0.0025-050	0.0077-0.10	1.0	1	0.25	5	0.343	0.115	0.115	3	---do---
PKW-9	0.0025-050	0.0079-0.098	1.1	1	0.275	5	0.343	0.115	0.115	3	---do---
PKW-10	0.0025-050	0.0073-0.099	1.2	1	0.30	5	0.343	0.115	0.115	3	---do---
PKW-11	0.0025-050	0.0078-0.093	1.3	1	0.325	5	0.343	0.115	0.115	3	---do---
PKW-12	0.0025-050	0.0082-0.092	1.4	1	0.35	5	0.343	0.115	0.115	3	---do---

Figure: 4.3 depicts the stage-discharge relation (with head and relative head H_t/P) over the PKW weir crest for different inlet-outlet key slopped models. During the investigation, it was noticed that the surface tension effects have more prominent in the most miniature model than in larger models at low heads. Variations in air entrainment were also seen over the different key slopped models with varying the upstream head and noticed that the air entrainments influence the discharge capacity of the weir. Surface tension and viscous forces at the crest-water-air interface come into play at a shallow head ($H_t/P \leq 0.06$), and no discharge over the weir exists for a few seconds. Then later, for the same head, flow passes or is initiated (but limited) over the weir along with less air entrainment, and water adheres to the downstream of the inlet key. Similar flowing effects were observed by **Machiels (2012).**

When the head is sufficiently high to overcome surface tension everywhere, the entire crest is involved in discharge conveyance. Air entrainment increases at higher heads/discharges, and fully aerated nappe intermingling with leaping nappe is observed. The variation of the air entrainment for the different heads is shown in **Figure: 4.4.**

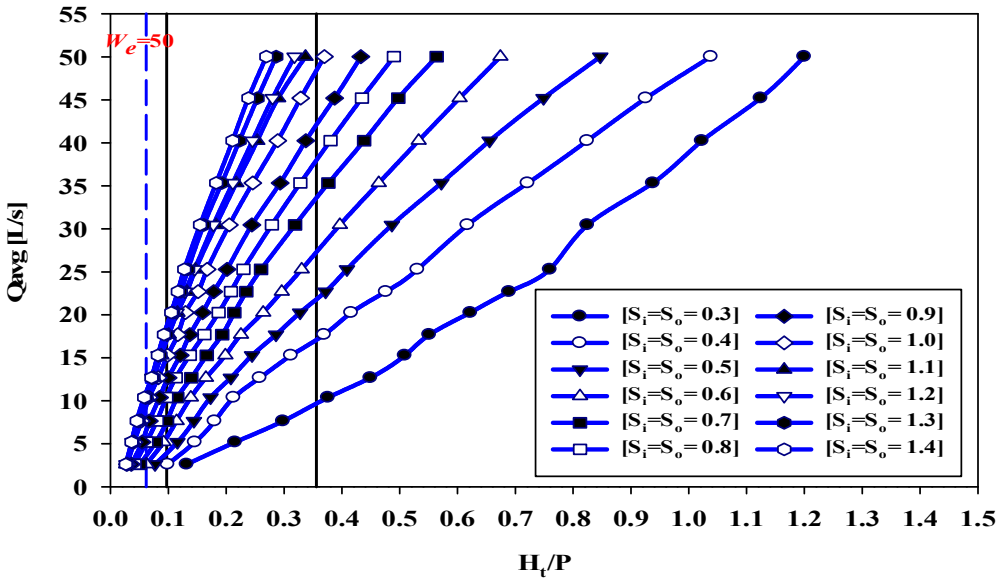

(a)

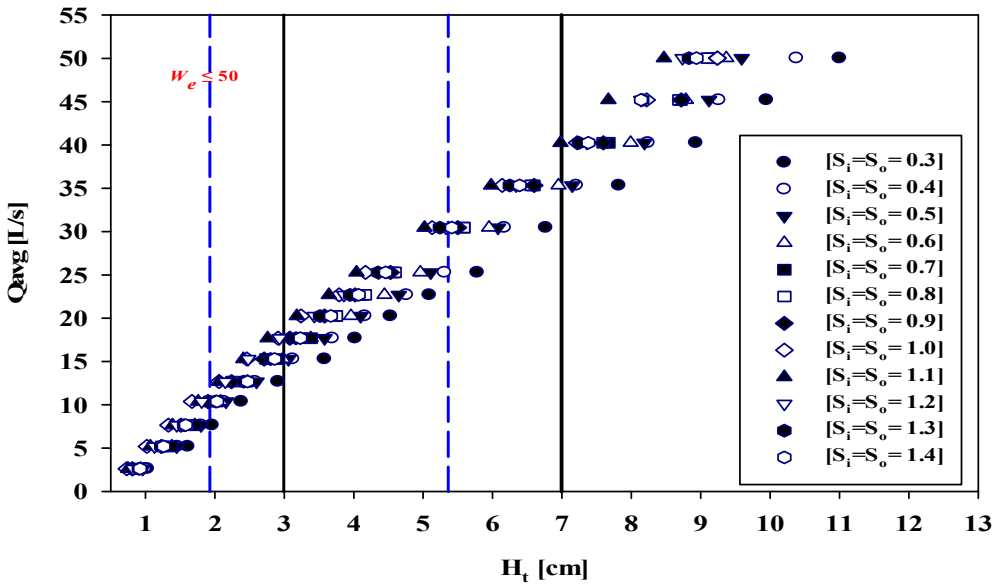

(b)

Figure: 4.3 (a) &(b) Variation of discharge [Q] with [H_t/P] and [H_t].

Figure: 4.4 Surface tension effects to jet trajectory formation from (a) to (d) on Largest models and from (i) to (iv) on Smallest models.

According to the current research, the minimum H_t/P at which the entire crest engaged to convey the discharge at a small shape of nappe with a radius of 0.005m-0.10 m was between 0.06-0.09 (or H_t ranges 0.02-0.03 m, because some models fully conveyed discharge at 0.02 m while others engaged fully at 0.03 m head). It means in the present study, the head threshold value above which the scale effect has been considered negligible is $H_t/P \geq 0.09$. The clear nappe or jet trajectory was visible at a minimum H_t/P ratio of 0.22-0.26 (H_t range 0.05-0.06 m), as illustrated in **Figures: 4.3 and 4.4**.

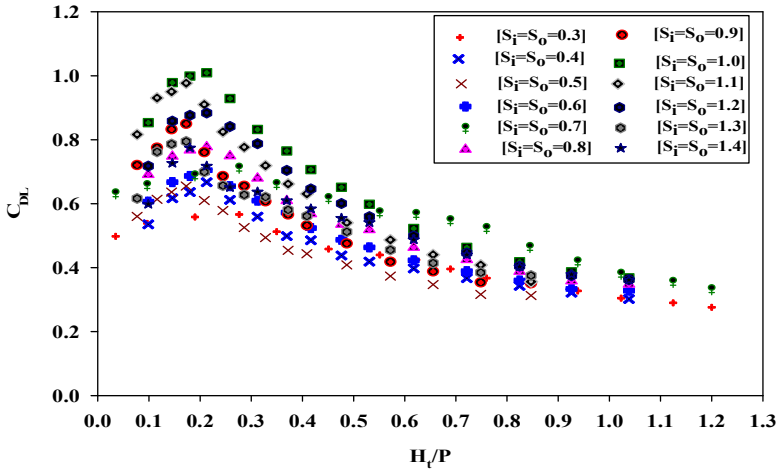

(a)

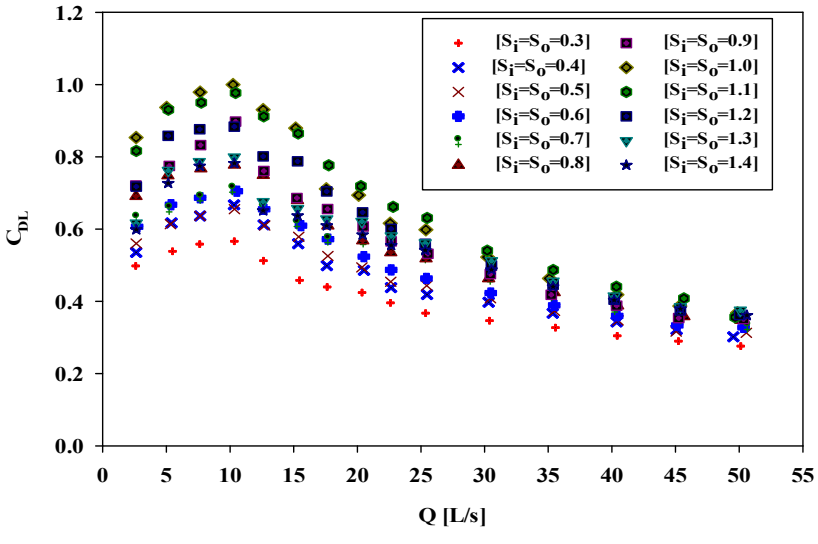

(b)

Figure: 4.5 (a) & (b) Variation of discharge coefficient [C_{DL}] with [H_t/P] and [Q].

The discharge coefficients (C_{DL}) for each weir setup have been evaluated over 0.042 ≤ H_t/P ≤1.2, as shown in **Figures: 4.5. [(a) & (b)].** The results demonstrate that as the inlet-outlet key's slope increases, the hydraulic efficiency of PKW increases to a certain slope and then starts decreasing. The PKW discharge efficiency increases at H_t/P<0.24 for all models, while decline trends were observed in almost all models at $H_t/P \geq 0.24$. However, a closer look at **Figure: 4.5 (a)** reveals that the peak is ranged between $0.2 \leq H_t/P \leq 0.25$. **Figure: 4.5 (b)** shows that the coefficient of discharge (C_{DL}) has a rising trend at low release and a decreasing trend at high discharge. The peak was observed corresponding to the discharge range between 10-15 L/s. This point concludes that the PKW is more efficient at low discharges/heads; as the discharges/heads increase, the efficiency gradually or abruptly decreases.

A comparison of rating curves between the sharp-crested weir and the PKW is required to improve efficiency in terms of enhancement ratio '*r,*' and the H_t/P ratio of the various key slopped PKW models shown in **Figure: 4.6.**

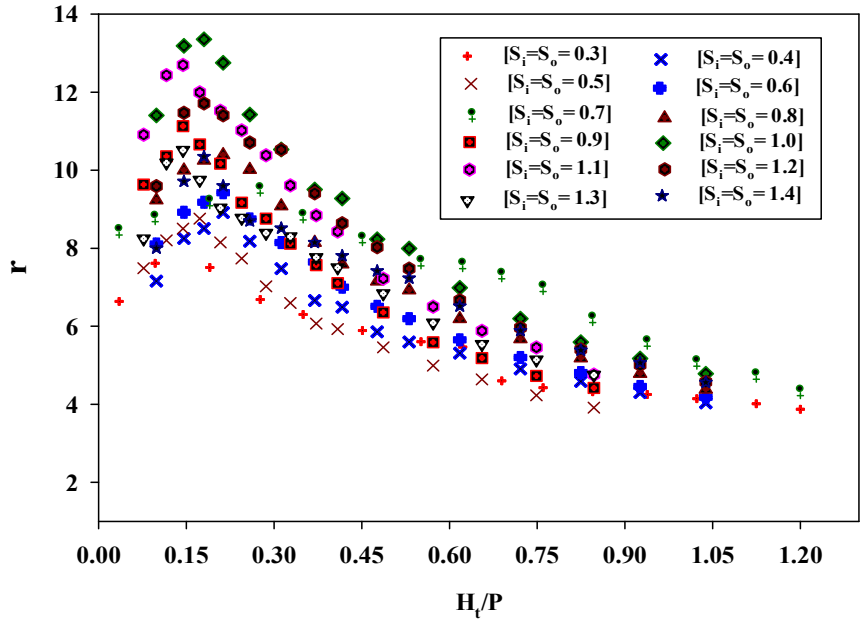

Figure: 4.6 Variation of discharge enhancement ratio [r] with [Ht/P].

During the investigation, it was noticed that the enhancement ratio increases up to a particular sloped value, then shows a declining trend. However, a closer look at **Figure: 4.6** reveals that the maximum enhancement ratio '*r*' is observed at $H_t/P \approx 0.18$, which corresponds to the key slope ($S_i = S_o = 1$), then follows the key slope ($S_i = S_o = 1.1$). The optimal range of

the key slopes lies between 1 and 1.1 and shows better efficiency than the sharp-crested weir for all the tested model sets (i.e., $r \geq 1$ for each model).

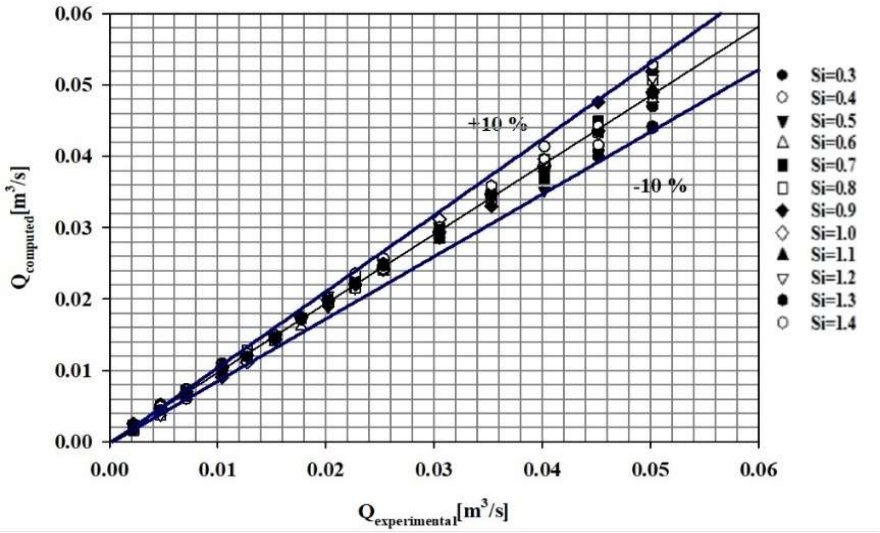

Figure: 4.7 Comparison of discharge computed using an equation given by Machiels et al. (2011c) and experimental results of the present study.

The test results were compared with the design equations or methodology developed by **Machiels *et al.* (2011c),** which tested seven different key sloped models. The first comparison of Q was computed with the help of equations developed by **Machiels *et al.* (2011)**, and Q was experimentally measured for the present study. It emphasizes that the analytical approach reaches the experimental results of the current research with an accuracy of within 10 % (**see Figure: 4.7**). Therefore, the present experimental study herein shows good agreement with the published data. The second comparison is specific to inlet-outlet key slopes, where the Q vs. H_t data collected for various slopped models herein were compared to a previously published study by **Machiels *et al.* (2011c)**. The mean absolute percentage error (MAPE), coefficient of determination (R^2), and root mean square error (RMSE) were used to compare Q for measured H_t values, as shown in **Table: 4.3.**

Table: 4. 3 Q comparison for corresponding H_t between the present section and published data by Machiels et al. (2011c).

S. No.	Models	S_i=S_o	MAPE	RMSE	R^2
1	PKW-1	0.3	7.50%	0.001	0.99
2	PKW-2	0.4	8.70%	0.001	0.998
3	PKW-3	0.5	9.50%	0.003	0.996
4	PKW-4	0.6	8.70%	0.006	0.99
5	PKW-5	0.7	6.70%	0.007	0.977
6	PKW-6	0.8	4.50%	0.008	0.973
7	PKW-7	0.9	5.80%	0.009	0.967

8	PKW-8	1	5.00%	0.007	0.985
9	PKW-9	1.1	5.20%	0.007	0.985
10	PKW-10	1.2	7.90%	0.008	0.978
11	PKW-11	1.3	8.40%	0.007	0.976
12	PKW-12	1.4	9.80%	0.008	0.971

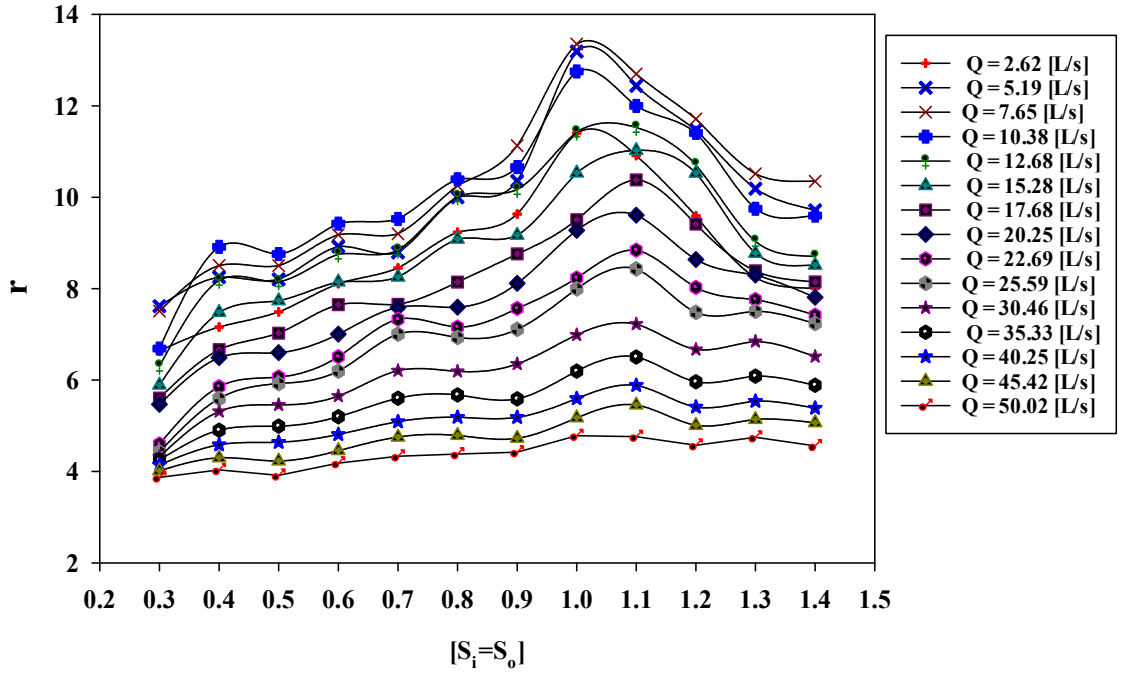

Figure: 4.8 Variation of discharge enhancement ratio [r] with various inlet-outlet key slopes [S_i=S_o] of PKW.

The results were plotted in terms of discharge enhancement ratio vs. key slopes, as shown in **Figure: 4.8.** In the present study, it was found that the optimal floor slopes for the inlet-outlet key ranged from 1-1.1 (or peaked at 1.04), whereas the optimal floor's slope was 1.2 (range 1.1-1.2) reported by **Machiels *et al.* (2011c).** During the investigation, it was noticed that as the floor slope of PKW increases, the efficiency of the weir increases (i.e., '*r*-value' increases) at a specific limit and then starts decreasing. However, the slope (S_i=S_o) range is different with or without parapet walls, making it a unique study.

4.3.2.2 Effect of the PKW's sloping key bottom on its discharge capacity with Sloping Bed

The second part of this section was to investigate the channel bed slope effects on the discharge efficiency of the PKWs. In order to analyse the effects of the bed slope of a channel on the efficiency of PKW, all 12 models were tested for six different bottom slopes (S_b= 0%, 0.25%, 0.5%, 0.75%, 1.0%, and 1.25 %). The tests of the present study were conducted by considering the channel flow approach; thus, the application of this investigation covers

mainly PKWs constructed as a control structure in a canal or river barrages, where the difference between crest and downstream is limited.

As literature said, the channel bottom slope study is essential to know the hydraulic behavior of the run-off river/stream or canal system where the difference between the weir crest and the downstream river is limited **(Ranga Raj, 2005)**. The channel slope plays a crucial role in assessing the relationship between the end depth and the flowing discharge over the weir. It also reveals the clear visibility of the consistent nappe appearances downstream of the weir (see Figure:4 (b)). According to **Carollo and Pampalone (2021)**, the channel bed slope is useful in discharge measurement at an upland basin outlet. A high slope is required to limit the negative effects of sediment load on discharge measurement.

Indeed, sediment settling caused by the presence of a horizontal or flat-bottomed could form a sediment layer upstream from the flume, resulting in relevant errors in water depth measurement and discharge. Moreover, it assists in forming the hydraulic jump, its location (including its length, which depends on the slope of the downstream apron) **(Ranga Raj, 2005)**, and enhancing energy dissipation downstream of the weir **(Al-Hashimi *et al.*, 2016)**. **Elyass (2012)** investigated the effect of channel bed slope on flow energy dissipation for a single-step broad-crested weir under free flow conditions. He discovered that the channel bed slope effect (S_b) was inversely proportional to energy dissipation for the same ratio (upstream to downstream weir height, i.e., P/P_1).

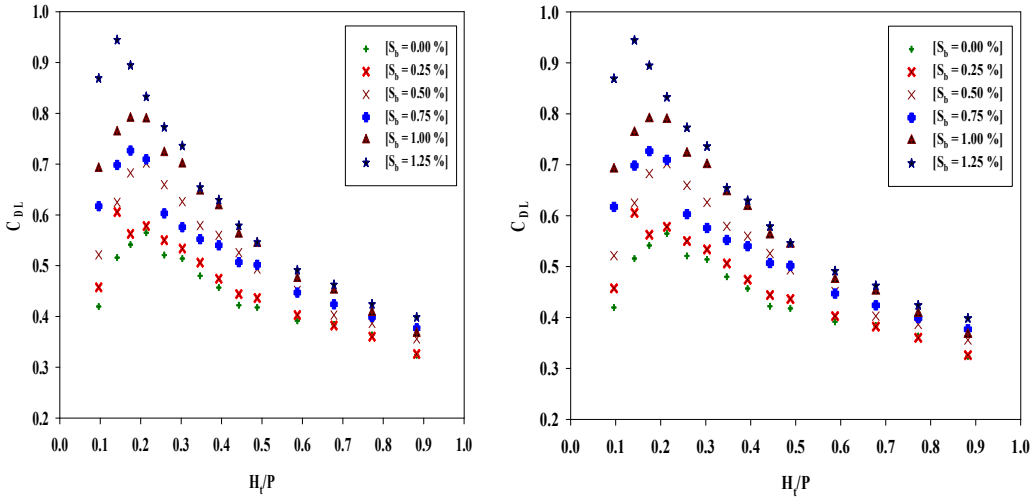

(a) **[S_i=S_o=0.3]** ***(b)*** **[S_i=S_o=0.4]**

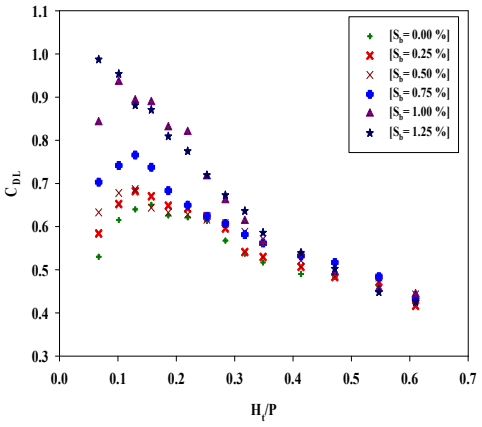

(c) [S_i=S_o= 0.5]

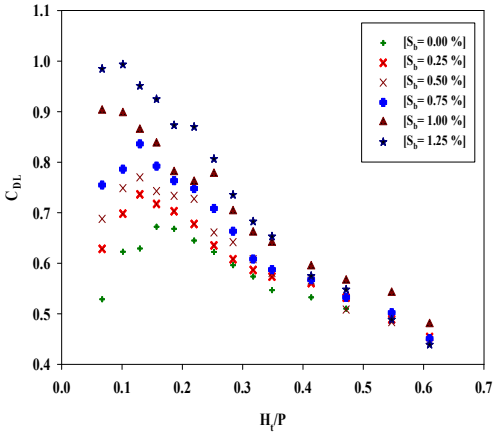

(d) [S_i=S_o= 0.6]

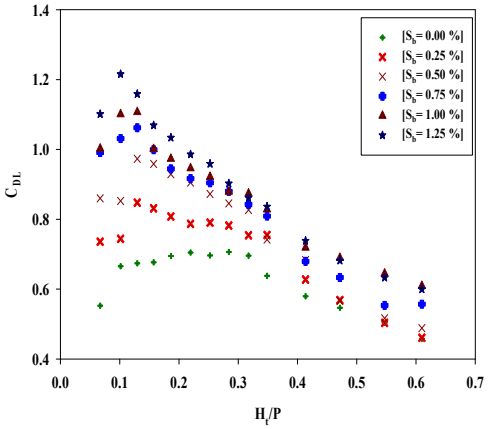

(e) [S_i=S_o= 0.7]

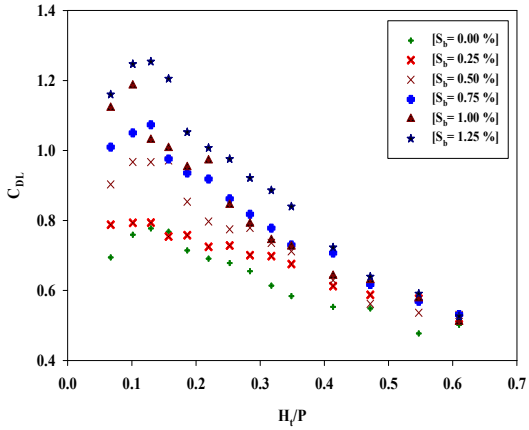

(f) [S_i=S_o= 0.8]

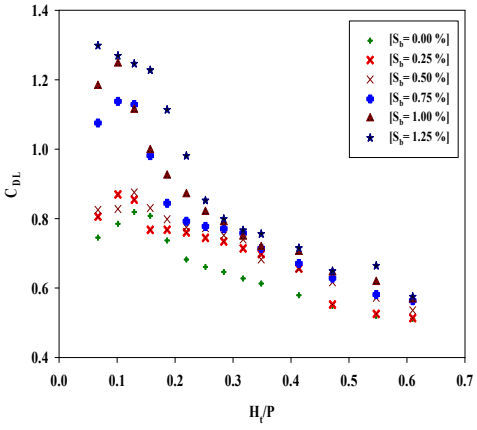

[S_i=S_o= 0.9]

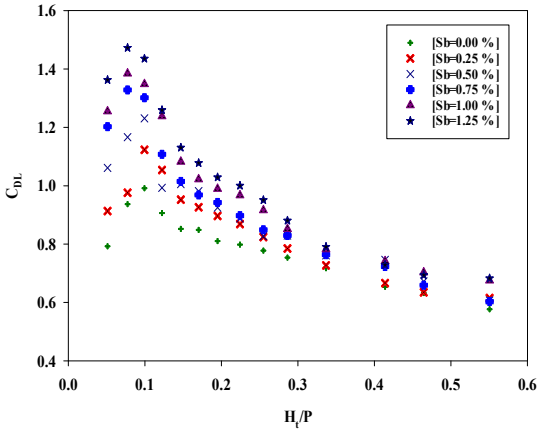

(h) [S_i=S_o= 1.0]

(g)

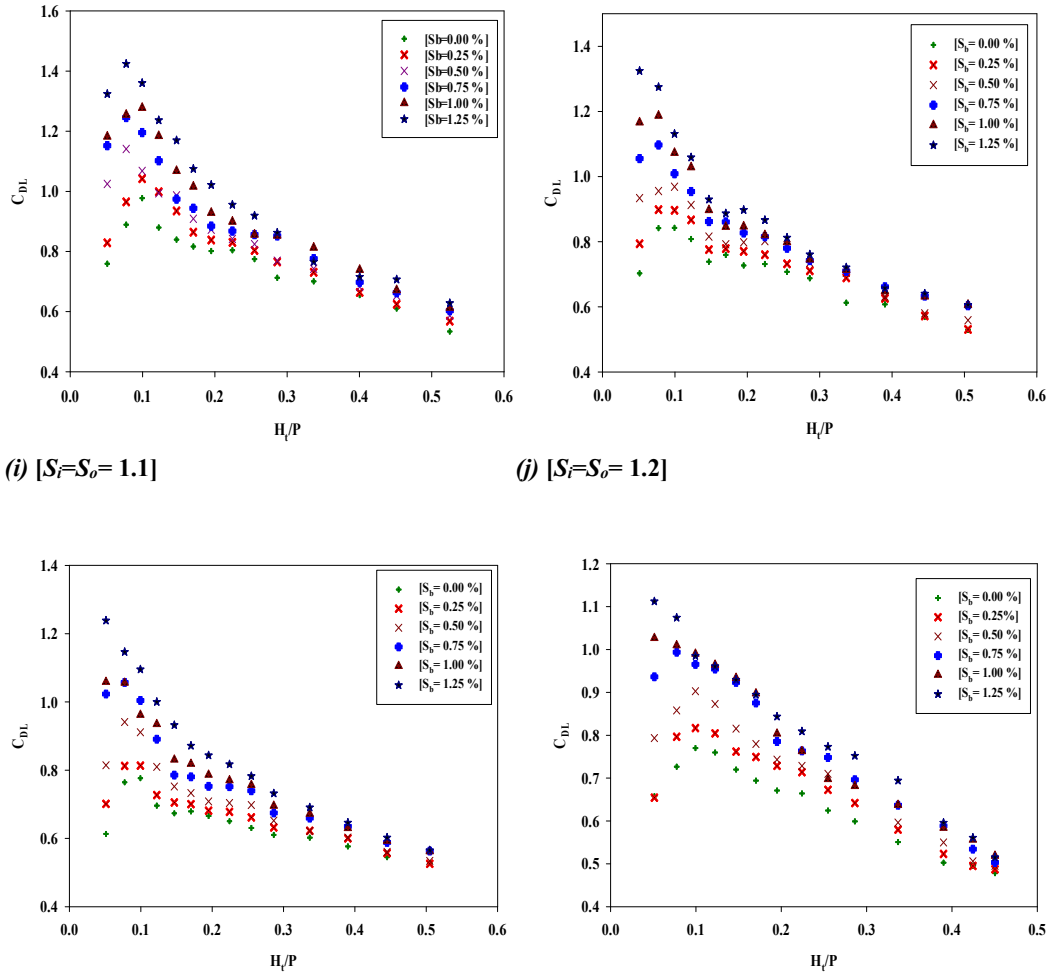

(i) **[S_i=S_o= 1.1]** *(j)* **[S_i=S_o= 1.2]**

(k) **[S_i=S_o= 1.3]** *(l)* **[S_i=S_o= 1.4]**

Figure: 4.9 Variation of coefficient of discharge [C_{DL}] with [H_t/P] on different bed slopes for different inlet-outlet key slopes.

The present study aims to understand better the channel bed slope effects on the discharge carrying capacity of the PKW and how the channel bed slope affects downstream energy dissipation. The test results indicate that, as the slope of the channel bed increases, the discharge efficiency of PKW increases significantly for a low H_t/P ratio. It enhances for higher values also but the slightly a lesser rate. In order to the lower discharge value as the slope of the bottom increases, the releasing capacity or coefficient of discharge of the PKWs increases significantly reason being the velocity of flow increases and the head of the flow decreases and theoretical discharge decreases; as a result, the discharge efficiency of the weir increases. However, at the higher discharges, the discharge coefficient shows a decreasing trend as the channel bottom slope increases, as shown in **Figure: 9**. This is due to the rise in the discharge and bed slope simultaneously; the head over the weir and velocity over the crest

increase, so theoretical discharge increases; thus, the discharge carrying capacity of the weir decreases.

Thus, the effect of the channel slope plays a significant role in the discharge carrying capacity of the PKW. For lower heads, the probability of the critical section is increased at the outlet crest at higher channel bed slopes. This is unfavorable, so avoid it at all costs. In contrast, no such significant sections were observed at higher heads and lower bottom slopes during the investigation. The present research findings demonstrated that the discharge efficiency of the PKW increases about 50-60% for a low H_t/P ratio, while 18-20% for higher H_t/P values when channel bed slopes change from 0.0% to 1.25 %.

4.3.3 Inlet to outlet key width ratio (W_i/W_o)

Inlet and outlet key width ratio is another critical parameter that significantly influences the PKW's discharge efficiency. Several experimental studies have found that having an inlet key that is larger than the outlet key improves discharge efficiency. A wide inlet key reduces energy losses and improves weir discharge efficiency. The width cannot be too large; it can create the submergence effect on the side of the outlet key, as results decrease the efficiency of the weir. The optimum value for this ratio (W_i/W_o) is not fixed, depending on other factors. Most researchers found that the optimum ratio lies anywhere from 1.0 to 1.5, but few assume this ratio equals 1.2 in their studies. The design equations described above have mainly captured the ratio's effects.

In order to know a better comprehension of the impact of the inlet to outlet key width proportion on discharge efficiency of PKW, the different W_i/W_o proportion models were built and tested under the free-flow condition in a laboratory. Under this section of the study, a total of 8 (PKW Type-A, **see Figure: 4.10**) models of different inlet-outlet key width proportions (W_i/W_o = 1.0, 1.1, 1.2, 1.25, 1.3, 1.35, 1.4, and 1.5) were fabricated by using T_s = 8 mm thick transparent acrylic sheet and affixed with the help of chloroform. The testing discharge values varied from 0.005 $m^3/s \leq Q \leq$ 0.050 m^3/s. The fabricated models have an inlet to outlet key slope (S_i=S_o) of 1.08, and L/W is 5, where L represents the length of the total developed crest of the PKWs, and W represents the model's width, which is equal to the width of the flume. The two overhang portions (B_i=B_o) are symmetric and identical to the half of the base length B_b of the model, and the height of the parapet wall is 2 cm for each model. In relative terms, the parameters variation included values $0.12 \leq H_t/P \leq 0.81$ and B_i/P=B_o/P=0.69. The data collected in the present study are shown in **Table: 4.4.**

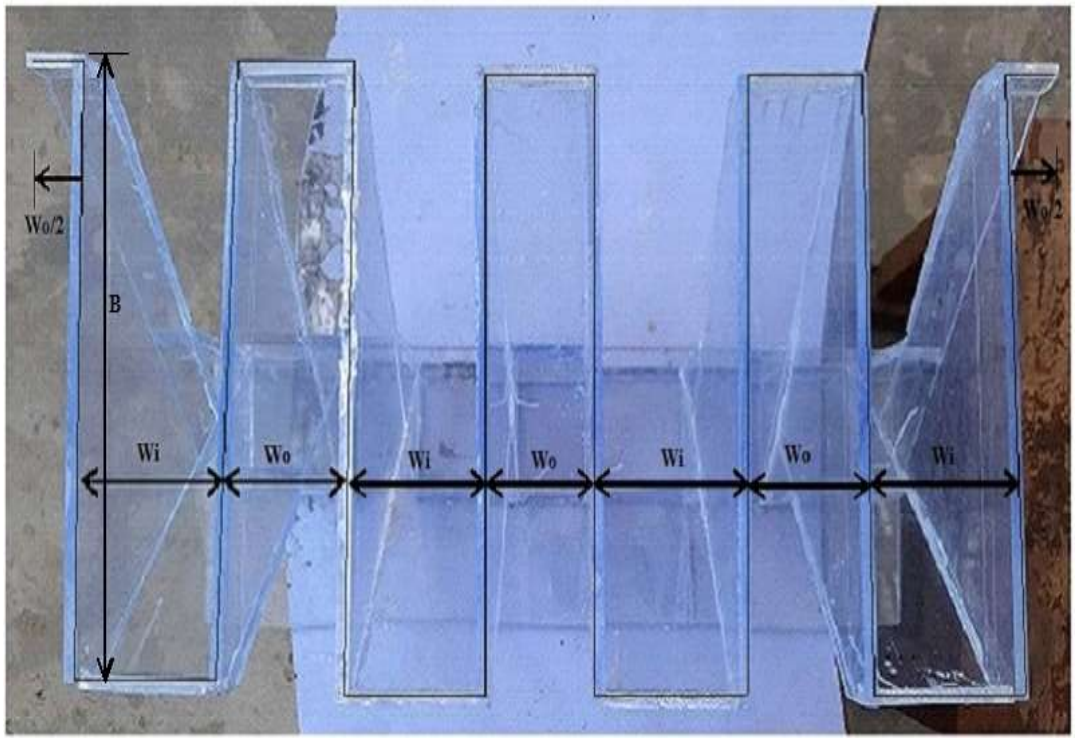

(a)

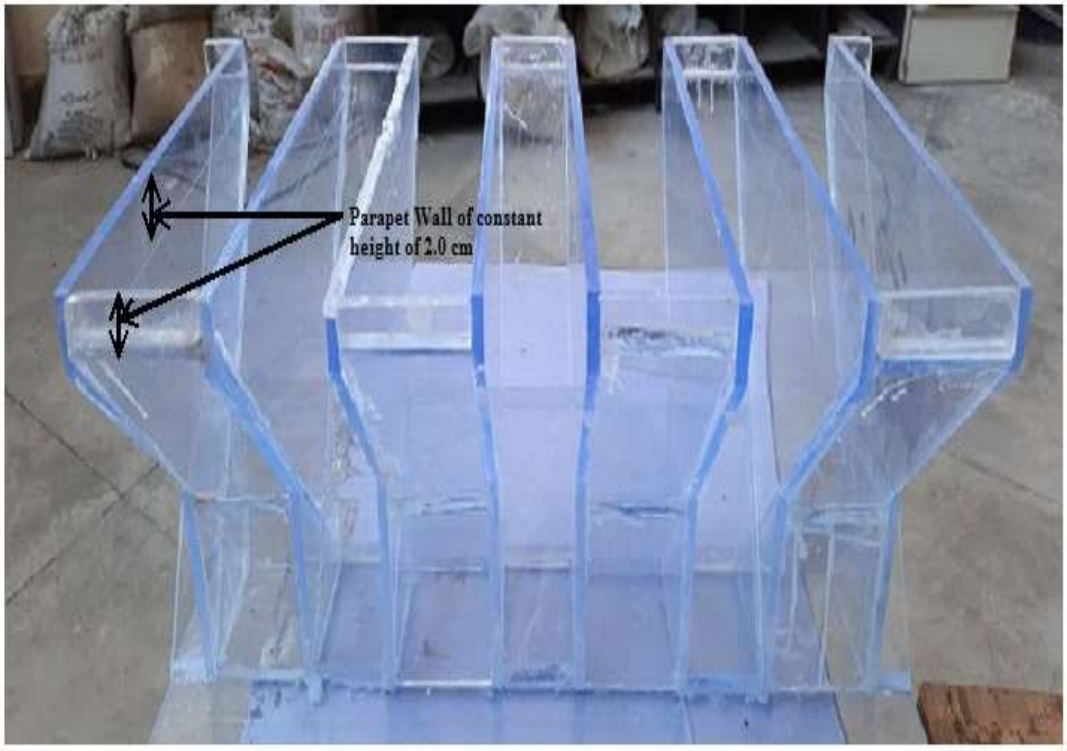

(b)

Figure: 4.10 Fabricated model Geometry of PKW (a) Plan view (b) PKW with constant Parapet Wall.

Table: 4. 4 Range of Data collected for different W_i/W_o ratios

S. No.	W_i/W_o	L/W	$S_i=S_o$	H_t(m)	Q(L/s)	$B_i/P= B_o/P$	Number of readings
1	1.00	5	1.08	0.0174-0.1007	5.13-50.16	0.69	18
2	1.10	5	1.08	0.0164-0.09014	5.10-50.26	0.69	18
3	1.20	5	1.08	0.0154-0.09981	5.16-50.07	0.69	18
4	1.25	5	1.08	0.0153-0.0842	5.25-50.18	0.69	18
5	1.30	5	1.08	0.0156-0.08561	5.06-50.00	0.69	18
6	1.35	5	1.08	0.0169-0.0870	5.11-50.07	0.69	18
7	1.40	5	1.08	0.0173-0.08254	5.31-50.13	0.69	18
8	1.50	5	1.08	0.0167-0.08315	5.15-50.45	0.69	18

All literature studies agreed that $W_i/W_o > 1.0$ has more significant discharge carrying efficiency than $W_i/W_o < 1.0$. With a relatively large value of the inlet key width (W_i), the flow has more space laterally, maintains the subcritical flow as possible, and reduces the losses **(Le Doucen et al. 2009)**. **Ujeniya et al. (2016)** investigated the effect of the outlet key to inlet key width ratio on the efficiency of a PKW. On the other hand, the less value of the outlet key declined local submergence near the outlet section of the PKW and reduced the efficiency of the weir. In general, hydraulic efficiency increases with an increasing W_i/W_o ratio up to a certain limit. In the outcome of expanding the inlet key width, the outlet key width diminishes (because the absolute width of the channel or weir is $W_i + W_o$ = constant). As the outlet key width decreases, the water split from the sidelong crest get in the outlet key is low as expected under the circumstances. So it releases water downstream without building up the neighborhood submergence or minimizing the submergence impacts in the outlet key section. Submergence impacts in the outlet keys can decrease the hydraulic efficiency of PKW. Until the two nappes mutually interact and form a solitary nappe, PKW tends to act like a linear weir. These are some reasons a balance of W_i/W_o exists **(Anderson and Tullis, 2011)**.

Because expanding the inlet key width decreases flow velocities along with the inlet key, it must also significantly increase PKW efficiency **(Eslinger and Crookston 2020).** However, for a given weir width and crest length, increasing the inlet width causes a decrease in the outlet width. Too narrow outlet key may be unable to evacuate the outlet flow under the supercritical conditions, therefore lowering the overall weir efficiency. A high W_i/W_o value improves the flow approach and distribution within the inlet keys and increases

submergence effects in outlet keys of PKWs. Thus, an optimal W_i/W_o ratio must be found by balancing inlet width increase and outlet resilience capacity.

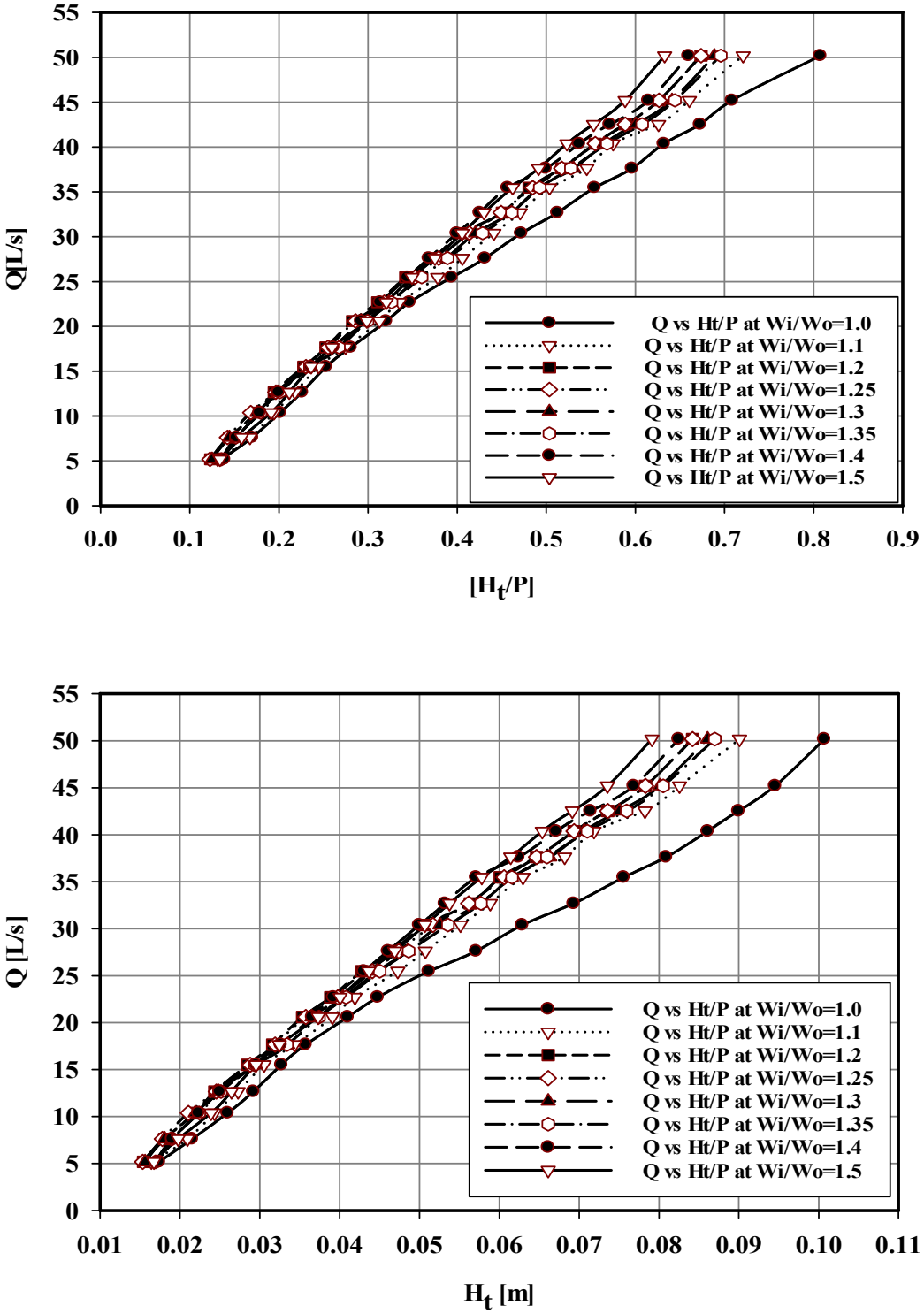

Figure: 4.11 Variation of discharge Q [L/s] with [Ht/P] and [Ht].

In order to compute the efficient analysis of the inlet to outlet key width ratio, the 18 tests comprising each model and a total of 144 tests have been conducted over eight models. The discharge coefficients were calculated using **(Eqn. 3.3)** over $0.12 \leq H_t/P \leq 0.81$ for each weir model arrangement. The stage-discharge relationship is the horoscope of each flow measurement structure and plotted between discharge vs. head, H_t/P ratio, as shown in **Figure: 4.11.** To distinguish the optimal range of inlet to outlet key width proportion (W_i/W_o), relating the most noteworthy C_{DL} esteems or most discharge proficiency, the test outcomes have been introduced in **Figure: 4.12**, C_{DL} as a component of H_t/P.

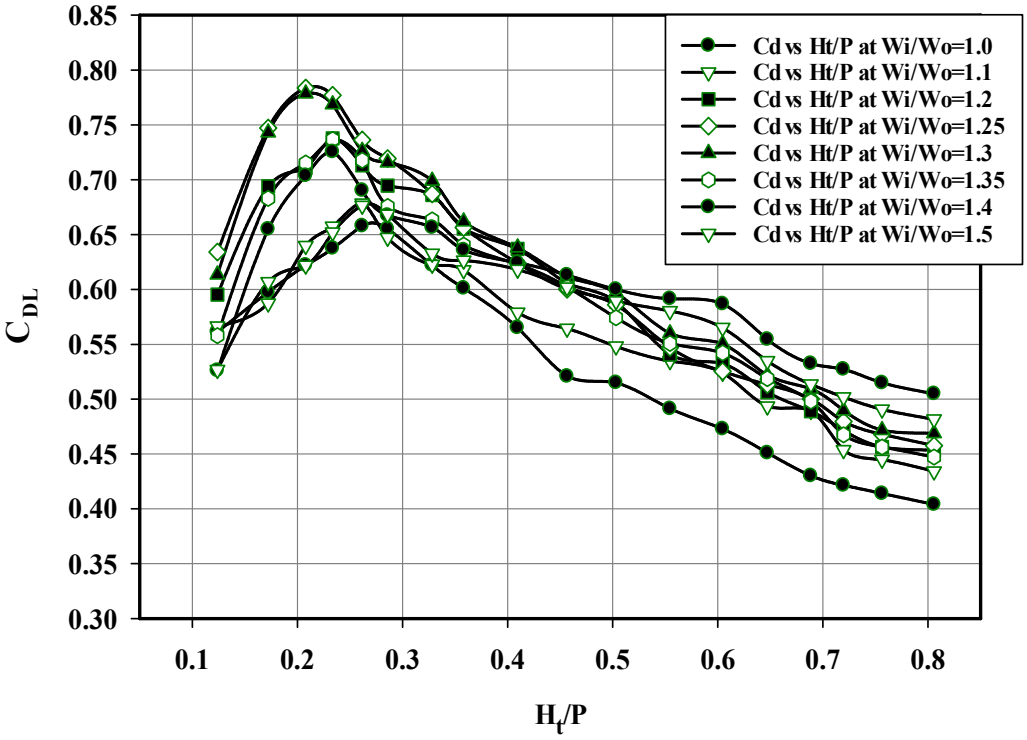

Figure: 4.12Variation of discharge coefficient of discharge [C_{DL}] with [H_t/P].

From **Figure: 4.12**, it is clear that the model W_i/W_o equal to 1.25 and 1.3 delivered the most significant release efficiency, followed by W_i/W_o= 1.2, 1.35, 1.4, 1.1, 1, and 1.5. It means the optimal discharge ranges lie between 1.25 to 1.3. Furthermore, the data in **Figure: 4.12** shows that W_i/W_o = 1.25 produce a respectively higher discharge efficiency than W_i/W_o = 1.3 for $H_t/P \leq 0.3$, and W_i/W_o = 1.3 produce a respectively higher discharge efficiency than W_i/W_o = 1.25 at $0.3 < H_t/P \leq 0.46$, however, the model W_i/W_o=1.4 produce the highest discharge capacity for the range of $0.46 < H_t/P \leq 0.81$. The PKW of W_i/W_o = 1.25 and W_i/W_o = 1.3 produce the (about 12 to 14 %) higher efficiency than to W_i/W_o = 1.0. So from the above

discussion, it is clear that the PKW is most sensitive to the low range of discharges; as the discharge increases, the efficiency of the PKW decreases rapidly or sometimes gradually.

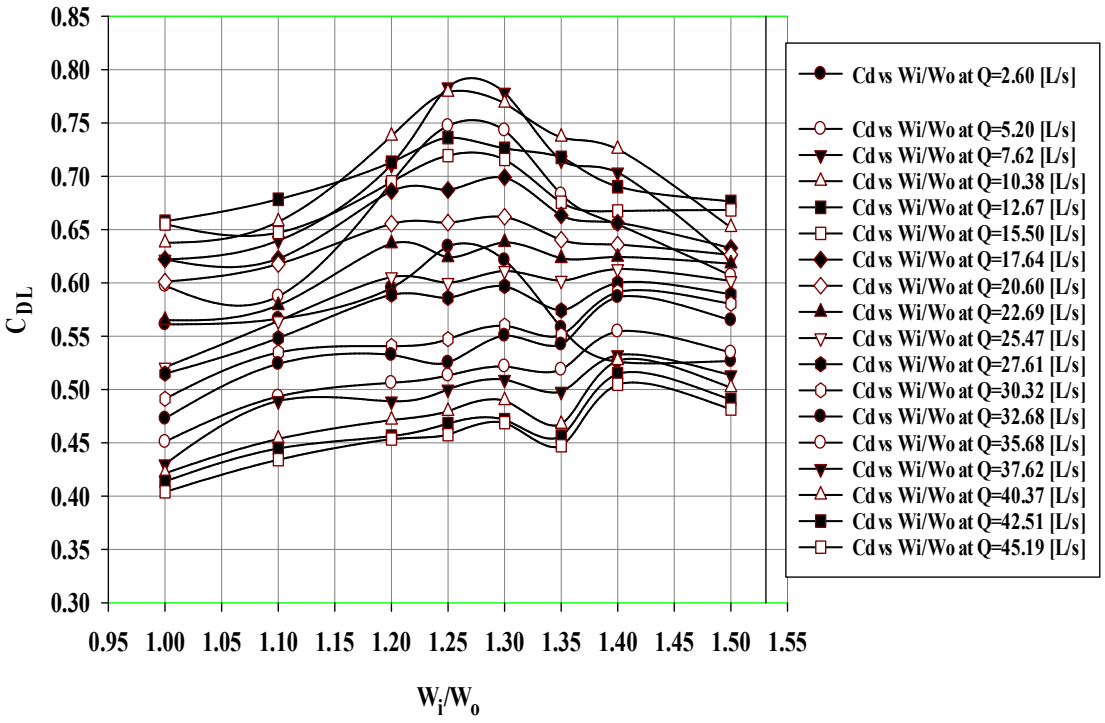

Figure: 4.13 Variation of discharge coefficient [C_{DL}] with the inlet to outlet width ratio [W_i/W_o].

Figure: 4.13 shows the maximum discharge efficiency at which the relative width ratio W_i/W_o in the range of 1.25 - 1.30 and the maximum efficiency observed corresponding to W_i/W_o = 1.275 ≈ 1.28; this width ratio shows the 15% and 20 % higher efficiency than the W_i/W_o = 1 and W_i/W_o = 1.5; respectively, however, the result of maximum previous studies varies between ranges 1-1.5 (**Anderson, 2011); (Anderson and Tullis, 2011)**. Some researchers suggested that the relative width (W_i/W_o) ratio ranges from 1.2 to 1.25 as close to optimal, but no data was presented to validate the claim. These findings are consistent with the result reported by **Ouamene and Lempérière (2006)**. **Anderson (2011)** proposed that enhancing the W_i/W_o ratio relative to 1.0 increases the discharge efficiency of PKW.

The optimal width ratio range is slightly different than previous studies, which may be due to the parapet wall. Because in most of the past studies, experiments have been performed on the flat top PKW models. In the present study, the experiments have been conducted with a parapet wall of constant height (2 cm) over each model. The recent past studies conducted over PKW suggested that the ratio for the inlet to outlet key width should

be greater than one because the relative width of the inlet key determines the unit discharge moving towards its crest, maintaining the subcritical flow as possible, and reducing the losses. On the other hand, the lesser value of the outlet key reduced the occurrence of local submergence.

The experimental data of the current study was used to develop the gene-expression programming (GEP) model by considering five non-dimensional parameters viz headwater ratio, magnification ratio, inlet to outlet width ratio, upstream Froude number, and the number of cyclic variations. The required dimensionless equation can be written as:

$$C_{DL} = f\left(\frac{H_t}{P}, \frac{L}{W}, \frac{W_i}{W_o}, F_r, N\right) \tag{4.1}$$

The above relationship describes the discharge coefficient of PKWs as the function of geometric and hydraulic parameters. The ranges of various parameters included in the present study are summarized in **Table: 4.4**. The GEP model is configured in stages, the first of which is to select a fitness function. As a result, the (RMSE) function is used in this study. The next step is to choose the set of terminals and functions that will be used to construct the chromosomes. The modeling process adopted in this study designates the discharge coefficient (C_{DL}) as the target value and the five independent parameters (H_t/P, L/W, W_i/W_o, F_r, and N) as input variables which are discussed in Eqn. (4). In the current study, a total of ten basic operators (+, −, ×, ⁄, ln, x^2, e^x, 1/x, $\sqrt[3]{x}$, Average) were used to develop the model (**see Table: 4.5**).

In order to achieve an uncomplicated and sensible GEP model, the functions were chosen based on their coherence to the quiddity of the problem. The general sampling strategy consisted of choosing thirty chromosomes, three genes, and eight head sizes (**see Table: 4.5**). A total of 144 data points were used in modeling and were distributed at random for the training and testing data phases. For the current work, about 80% of the data is used for training and the remaining 20% for testing. In GEP, the training and testing data were drawn randomly from the original dataset. GeneXpro Tools 5.0, a powerful soft computing software package, was used in this study. It runs efficiently on a personal computer. The analytical form of the proposed GEP model is expressed as:

Table: 4. 5 Functional set and operational parameters used in the GEP model

S. No.	Description of Parameter (1)	Setting of Parameter (2)
1.	Function Set	+, −, ×, ⁄, ln, x^2, e^x, 1/x, $\sqrt[3]{x}$, Avg.2
2.	Number of Chromosomes	30
3.	Head Size	8
4.	Number of Genes	3
5.	Gene Size	26
6.	Linking Function	Addition
7.	Fitness Function	RMSE
8.	Program Size	40
9.	Literals	13
10.	Number of Generations	2,70,151
11.	Constants per Gene	10
12.	Data Type	Floating-point
13.	Mutation	0.00138
14.	Inversion	0.00546
15.	Gene recombination rate	0.00277
16.	One-point recombination rate	0.00277
17.	Two-point recombination rate	0.00277
18.	Gene transposition rate	0.00277
19.	Insertion sequence (IS) transposition rate	0.00546
20.	Root insertion sequence (RIS) transposition rate	0.00546

$$C_{DL} = \left[\left(\left\{\frac{(-4.3420)-2.1086}{2.1086}\right\} - (-4.9214)^{1/3}\right) \times \left(\frac{\left(\left(\frac{H_t}{P}\right)-1.9430\right)+\frac{L}{W}}{2}\right)\right] +$$

$$\left[\left[\left\{\left(e^{e\left(\left(\frac{W_i}{W_o}\right)\times\left(\frac{H_t}{P}\right)\right)}\right)^{1/3} \times F_r\right\}^{1/3}\right]^{1/3}\right] + \left[\frac{\left[\left\{\left\{\left\{\left(\frac{H_t}{P}\right)\times\left(\frac{H_t}{P}\right)\right\}-N\right\}-F_r^2\right\}+\frac{\left[\left\{\left(\frac{L}{W}\right)+F_r\right\}+\{F_r+N\}\right]}{2}\right]}{2}\right] \quad (4.2)$$

Further, simplified the above equation as

$$C_{DL} = \left[(-1.3582) \times \left(\frac{\left(\left(\frac{H_t}{P}\right)-1.9430\right)+\frac{L}{W}}{2}\right)\right] + \left[\left[\left\{\left(e^{e\left(\left(\frac{W_i}{W_o}\right)\times\left(\frac{H_t}{P}\right)\right)}\right)^{1/3} \times F_r\right\}^{1/3}\right]^{1/3}\right] +$$

$$\left[\frac{\left[\left\{\left\{\left(\frac{H_t}{P}\right)^2-N\right\}-F_r^2\right\}+\frac{\left[\left\{\left(\frac{L}{W}\right)+F_r\right\}+\{F_r+N\}\right]}{2}\right]}{2}\right] \quad (4.3)$$

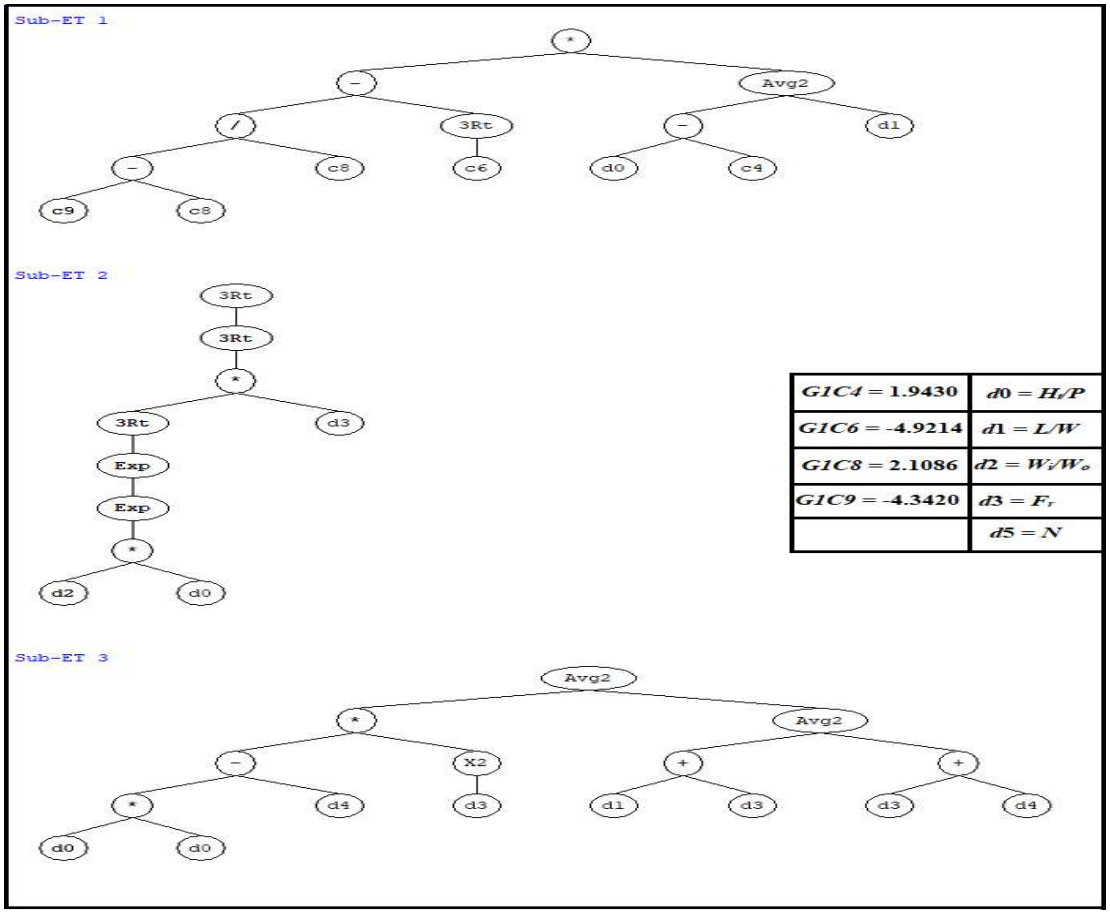

Figure: 4.14 Expression Tree (ET) for GEP formulation.

The above equation indicates that the GEP approach resulted in a highly nonlinear relationship between the discharge coefficient and the input parameters. An expression tree (ET) representation **Eqn. (4.2)** is shown in **Figure: 4.14**, representing the GEP model for estimating the discharge coefficient. In **Figure: 4.13**, $d0$ stands for H_t/P, $d1$ represents the L/W, $d2$ represents the W_i/W_o, $d3$ represents the F_r, $d4$ represents the number of cycles (N), and $G1c4$, $G1c6$, $G1c8$, and $G1c9$ represent the numerical constants used in the first gene of the model.

The GEP approach demonstrates a highly nonlinear relationship between discharge coefficient C_{DL} and the input parameters (H_t/P, L/W, W_i/W_o, F_r, N) with high accuracy and relatively low error for different geometrical variations.

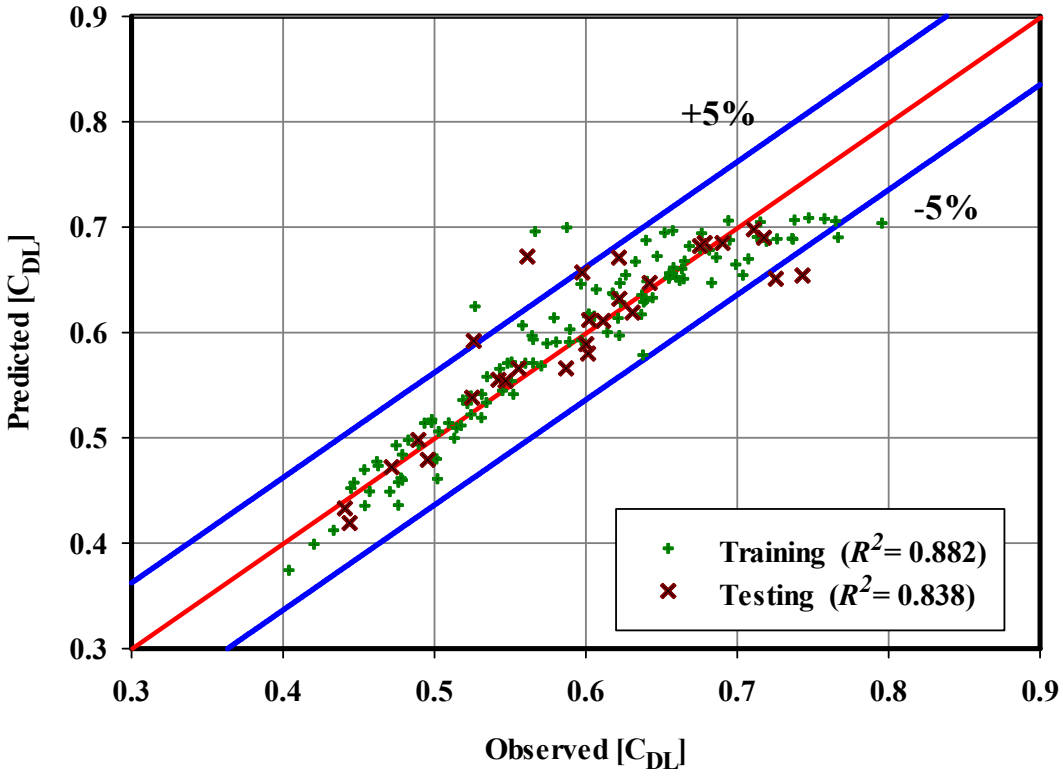

Figure: 4.15 Comparison between observed and predicted discharge coefficient for the different data phases (training and testing phases).

Figure: 4.15 depicts a closer examination of the performance matrices between the observed and predicted discharge coefficient (C_{DL}) achieved by the GEP approach **Eqn. (4.1)** for the training and testing data phases separately.

Table: 4.6 Performance evaluation of predicted E_2/E_1 by GEP model for training and testing dataset

Data Set	CC	R^2	MAE %	RMSE	MAPE %
Training	0.937	0.882	0.0224	0.0315	3.8
Testing	0.894	0.838	0.0250	0.0377	4.2

[1]CC =Coefficient of correlation; [2]R^2 =Coefficient of determination;[3]MAE== Mean Absolute Error; [4]RMSE = Root Mean Square Error; [5]MAPE= Mean Absolute Percentage Error.

The developed GEP model's performance was evaluated in terms of coefficient of correlation (*CC*), coefficient of determination (R^2), mean absolute error (MAE), root mean square error (RMSE), and mean absolute percentage error (MAPE), as shown in **Table: 4.6.** According to the author, the proposed nonlinear equation approximation may be adequate for conceptual designs and alternative analysis.

4.3.4 Overhangs portions (B_i, B_o)

Overhang portions of the PKW are equally crucial for developing and designing efficient PKW structures over the other main geometrical parameters. **Ouamane and Lempérière (2006)** suggested that the overhang length ratio B_i/B_o = 2 is 12 % less effective than type-B with B_i/B_o = 0 and 7% less effective than B_i/B_o = 1 of type-A PKWs. According to **Cicero et al. (2016)**, type-A has 15% more effective than type C but 5-15% less effective than type B. **Khassaf et al. (2016)** conducted laboratory experiments on the Type-B model of PKWs to learn about the various geometrical parameters influencing weir's discharge capacity under free-flow conditions. They found that the Type-B PKW has more efficient at low discharge. The larger overhangs on the upstream side increase the PKW efficiency because it increases the area of an inlet flow and reduces the energy losses **(Anderson and Tullis, 2011)**. This section tested and examined three different types (i.e., type-A, type-B & type-C) of PKW laboratory-scaled models to see the effects of the overhangs portion on the discharge carrying capacity. The models' configurations in the present sections are as follows: the relative width ratio (W_i/W_o) is 1.28. The L/W ratio is 5, and the height of all models (P) is 0.15 m.

The inlet-outlet key slopes are 45^0 (S_i=S_o=1) for Type-A, S_i=1, & S_o=0.37 for Type-B, and S_i =1, & S_o =3.2 for Type-C. The two overhang portions are such that B_i=B_o, are alike for Type-A, whereas B_i=0, B_o= 2/3 B_b, for Type-B, and B_i=2/3 B_b, B_o=0, for Type-C. The

testing discharges were varied over the model between 0.005 $m^3/s \leq Q \leq 0.05 m^3/s$. The data collected in the present study are shown in **Table: 4.7.**

Table: 4.7 Range of Data collected for different overhang (B_i/B_o)ratios

S. No.	$\frac{W_i}{W_o}$	$\frac{L}{W}$	S_i, S_o	$H_t(m)$	$Q(L/s)$	$B_i/P = B_o/P$	B (m)	B_i (m)	B_o (m)	Number of readings
Type-A	1.28	5	1.08	0.0141-0.1235	5.10-50.26	0.69	0.343	0.115	0.115	15
Type-B	1.28	5	1, 0.37	0.0131-0.1335	5.14-50.06	0, 1.49	0.343	0	0.229	15
Type-C	1.28	5	1, 3.2	0.0137-0.1215	5.20-50.16	1.49, 0	0.427	0.285	0	15

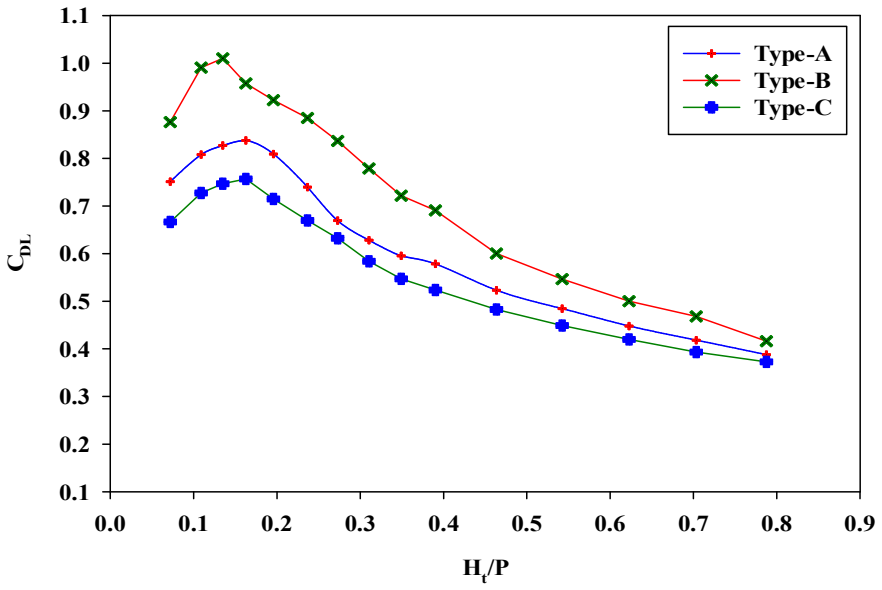

Figure: 4.16 Comparison curve among the discharge efficiencies of the different types of PKWs

Figure: 4.16 represents the comparison curve among the discharge efficiencies of the different types (i.e., type-A, type-B & type-C) of PKW models. The results demonstrated that the type-B PKW had shown maximum discharge efficiency from other PKW types. According to the present study findings, type-A has 5-13 % more effective than type C but 7-24% less effective than type B. In addition, the results show that the discharge efficiency of all PKW's models increases with increasing the discharge over the weirs at a certain release, then it starts decreasing.

4.3.5 Numbers of Cycles (*N*)

The smallest extent of a structure represents cycles or units and is composed of an entire inlet key with a sidewall and half an outlet key on both sides. It is also a critical

parameter that plays a vital role in enhancing the energy dissipation over the PKW. The number of cycles plays an essential role in influencing the discharge capacity when the width is limited or constrained. According to **Tullis et al. (2020a),** as increasing the number of units or cycles for fixed width, the discharge carrying capacity of the folded weir decreases. In general, hydraulic efficiency increases with an increasing W_i/W_o ratio up to a certain limit. In the outcome of expanding the inlet key width, the outlet key width diminishes (because the absolute width of the channel or weir is $W_i + W_o$ = constant). For a fixed channel width, the number of cycles varies in a PKW design depending on the allowable weir footprint in the streamwise direction (B) (where B is the length of the weir along the flow direction). As B gets smaller, the number of cycles must increase, and L_{cy} and W_{cy} of the cycle decrease for the weir to span W (where L_{cy} and W_{cy} represent the crest length and width of one cycle or unit).

In order to examine the effects of the cyclic variation of PKW on its discharge capacity, three different types (i.e., type-A, type-B & type-C) of PKW laboratory-scaled models were tested. The models' configurations in the present sections are as follows: the relative width ratio (W_i/W_o) is 1.28. The L/W ratio is 5, and the height of all models (P) is 0.15-0.185 m. The inlet-outlet key slopes are 45^0 (S_i=S_o=1) for Type-A, S_i=1, & S_o=0.37 for Type-B, and S_i =1, & S_o =3.2 for Type-C. The two overhang portions are such that B_i=B_o, are alike for Type-A, whereas B_i=0, B_o= 2/3 B_b, for Type-B, and B_i=2/3 B_b, B_o=0, for Type-C. The testing discharges were varied over the model between 0.010 $m^3/s \leq Q \leq 0.05 m^3/s$.

Table: 4.8 Range of Data collected for different cyclic count (N) of different types of PKWs

S. No.	W_i/W_o	L/W	S_i, S_o	H_t(m)	Q(L/s)	B_i/P= B_o/P	Number of Cycles	Number of readings
Type-A	1.28	5	1.08	0.0171-0.147	10.13-50.16	0.69	3	15
	1.28	5	1.08	0.0169-0.145	10.10-50.26	0.69	4	15
	1.28	5	1.08	0.0172-0.146	10.16-50.07	0.69	5	15
Type-B	1.28	5	1, 0.37	0.0133-0.165	10.25-50.21	0, 1.49	3	15
	1.28	5	1, 0.37	0.0132-0.164	10.14-50.06	0, 1.49	4	15
	1.28	5	1, 0.37	0.0135-0.174	10.06-50.17	0, 1.49	5	15
Type-C	1.28	5	1, 3.2	0.014-0.1087	10.03-50.36	1.49, 0	3	15
	1.28	5	1, 3.2	0.015-0.109	10.20-50.16	1.49, 0	4	15
	1.28	5	1, 3.2	0.011-0.108	10.09-50.11	1.49, 0	5	15

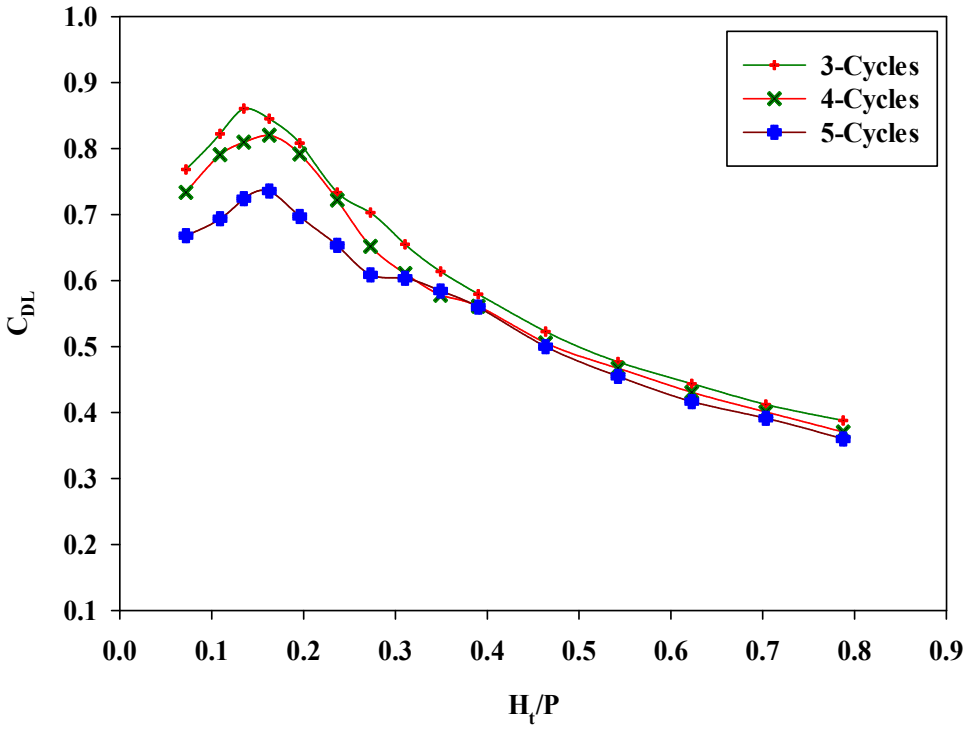
3-Cycles
4-Cycles
5-Cycles
C_{DL}
H_t/P
1.0
0.9
0.8
0.7
0.6
0.5
0.4
0.3
0.2
0.1
0.0
0.1
0.2
0.3
0.4
0.5
0.6
0.7
0.8
0.9

Type-A

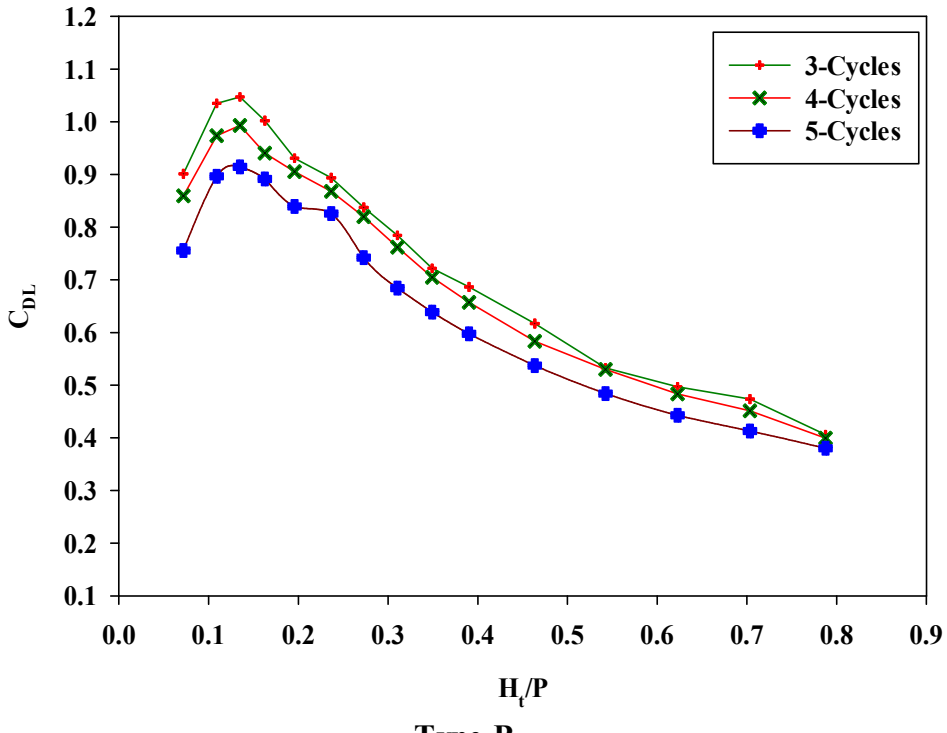
3-Cycles
4-Cycles
5-Cycles
C_{DL}
H_t/P
1.2
1.1
1.0
0.9
0.8
0.7
0.6
0.5
0.4
0.3
0.2
0.1
0.0
0.1
0.2
0.3
0.4
0.5
0.6
0.7
0.8
0.9

Type-B

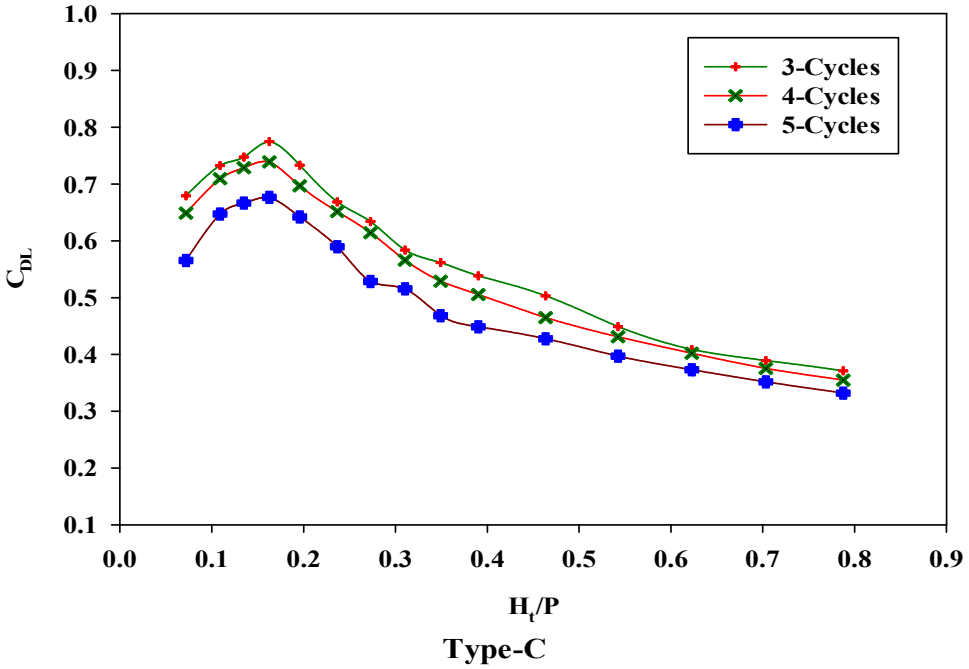

Figure: 4.17 Comparison curve between the C_{DL} vs. H_t/P of the different types (Type-A, Type-B and Type-C) of PKWs for different cyclic variations

The results of the present section indicate that as the number of cycles increases, the discharge efficiency decreases (**see Figure: 4.17**). For a specific channel width, total PKW length and discharge capacity/efficiency are maximized as the number of apexes and cycles is reduced. In many cases, however, other constraints (e.g., permitting-based limits on *B*) may become the key factor controlling PKW geometric design. As evaluated in this study, the number of cycle's dependency on PKW hydraulics is directly related to the influences of the height and width of the weir.

4.4 Energy Dissipation capacity

As the literature said, the hydraulic behavior of piano key weirs is complex and affected by various geometrical parameters directly or indirectly. Much literature was published to describe the hydraulic behavior; upstream structure design of the PKW. However, PKW's downstream structure design is prevented by a lack of systematic experimental studies and comprehensive data on flow conditions downstream of PKWs. As a result, additional research in this area is recommended to supplement the preliminary work of **Silvestri et al. (2013a), Jüstrich et al. (2016), and Eslinger and Crookston (2020).** The energy-dissipative properties of a hydraulic structure are critical. Currently, there is a scarcity of information and guidance, with previous energy dissipation studies of PKWs primarily for specific projects. Therefore, to document and quantify energy dissipation, a total of 26 PKW

models (12-type-A, 12-type-B, and 2-type-C) with different geometrical parameters were tested and examined, with 600 tests consisting of a new dataset along with detailed observations. The specifications of the various models are as follows: W_i/W_o=1.28; L/W=5-6; P = 0.15-0.20 m. (where W_i = width of inlet key, W_o = width of outlet key, W= total width of the channel, L= total developed crest length, and P = weir height). The inlet and outlet key slope are 45^0 (S_i=S_o=1) for Type-A, S_i=1, & S_o=0.37 for Type-B, and S_i=1, & S_o=3.2 for Type-C. The two overhang portions are such that B_i=B_o, are alike for Type-A, whereas B_i=0, B_o= 2/3 B_b, for Type-B, and B_i=2/3 B_b, B_o=0, for Type-C (**see Table: 4.9**).

As presented in the material and methods section, the flow energy dissipation over the PKWs are proportional to the various non-dimensionless parameters. In the present study, the values of the flow energy dissipation over the PKWs have been analyzed in three ways: the first one was to determine the effect of cyclic variation of the weir on energy dissipation over the PKW while keeping the L/W and W_i/W_o ratios were constant. The second aspect is comprehending the impact of varying the L/W ratio on energy dissipation by keeping the number of cycles and the W_i/W_o ratio constant. And the third aspect is to see how changing the inlet-outlet width (W_i/W_o) ratio affects the energy dissipation at the base of the PKW while keeping the L/W ratio and number of cyclic counts constant. The detailed discussion is described in the following subsections later on.

4.4.1 Effects of the cyclic variation (N) on energy dissipation

The primary consequence of the section of the present study is to find out the impacts of cyclic variation on energy dissipation. After investigating the experimental data, it was evident that the PKW shows significant energy dissipation variation with varying cycles or units. According to the current study's findings, the data for all the PKW models (type-A & type-B) show a convergence pattern in relative energy loss at both low and high values of H_t/P. The relative energy dissipation for the nonlinear weirs [E_L=(E_1-E_2)/E_1] has shown to be inversely proportional to H_t/P with a nonlinear pattern, as shown in **Figures: 4.18 (i), 4.19 (i), 4.20 (i) and 4.21 (i).**

Figures: 4.18 (i), 4.19 (i), 4.20 (i), and 4.21 (i) revealed that the lowest flow depth has the greatest energy dissipation, and the PKW is less effective at dissipating energy at higher heads. A marginal change in H_t/P results in a relatively significant difference in relative energy dissipation when the headwater ratio H_t/P is less than 0.38 for Type-A and 0.25 for Type-B.

Table: 4. 9 Range of data collected for energy dissipation of different types (type-A, type-B & type-C) of PKWs

Model No.		Range of Q (m^3/s)	Range of H_t (m)	$\frac{W_i}{W_o}$	W_i (m)	W_o (m)	P (m)	$\frac{L}{W}$	B (m)	B_i (m)	B_o (m)	Range of $\left(\frac{E_L}{E_1}\right)$	Range of $\left(E_r = \frac{E_2}{E_1}\right)$	N (No. of cycles)	No. of runs
Type-A	1	0.005-0.050	0.0170-0.165	1.0	0.078	0.078	0.20	5	0.28	0.093	0.093	0.8413-0.153	0.158-0.8419	3	20
	2	0.005-0.050	0.0168-0.167	1.1	0.082	0.075	0.20	5	0.28	0.093	0.093	0.8310-0.1460	0.1682-0.8504	3	20
	3	0.005-0.050	0.0169-0.164	1.2	0.085	0.071	0.20	5	0.28	0.093	0.093	0.8180-0.1531	0.189-0.853	3	20
	4	0.005-0.050	0.0168-0.154	1.3	0.089	0.068	0.20	5	0.28	0.093	0.093	0.8012-0.1601	0.198-0.843	3	20
	5	0.005-0.050	0.0171-0.151	1.4	0.091	0.065	0.20	5	0.28	0.093	0.093	0.7931-0.1476	0.206-0.852	3	20
	6	0.005-0.050	0.0168-0.160	1.5	0.094	0.063	0.20	5	0.28	0.093	0.093	0.7841-0.1301	0.215-0.861	3	20
	7	0.005-0.050	0.0171-0.147	1.28	0.088	0.069	0.15	5	0.343	0.115	0.115	0.8493-0.1671	0.1724-0.8329	3	20
	8	0.005-0.050	0.0169-0.145	1.28	0.064	0.05	0.15	5	0.259	0.086	0.086	0.860-0.1396	0.1512-0.8604	4	20
	9	0.005-0.050	0.0172-0.146	1.28	0.05	0.039	0.15	5	0.208	0.069	0.069	0.8731-0.1501	0.137-0.8498	5	20
	10	0.005-0.050	0.0172-0.145	1.28	0.088	0.069	0.15	6	0.427	0.142	0.142	0.833-0.1711	0.1924-0.8289	3	20
	11	0.005-0.050	0.0168-0.141	1.28	0.064	0.05	0.15	6	0.322	0.107	0.107	0.8456-0.1406	0.1757-0.8595	4	20
	12	0.005-0.050	0.0181-0.148	1.28	0.05	0.039	0.15	6	0.259	0.086	0.086	0.8597-0.1368	0.1555-0.8632	5	20
Type-B	1	0.005-0.050	0.0133-0.165	1.28	0.088	0.069	0.15	5	0.343	0	0.229	0.8110-0.1471	0.1889-0.8531	3	25
	2	0.005-0.050	0.0132-0.164	1.28	0.064	0.05	0.15	5	0.259	0	0.165	0.833-0.136	0.167-0.8642	4	25
	3	0.005-0.050	0.0135-0.174	1.28	0.05	0.039	0.15	5	0.208	0	0.139	0.8680-0.1667	0.1379-0.8333	5	25
	4	0.005-0.050	0.0132-0.174	1.28	0.088	0.069	0.15	6	0.427	0	0.285	0.8001-0.1302	0.199-0.869	3	25
	5	0.005-0.050	0.0135-0.172	1.28	0.064	0.05	0.15	6	0.322	0	0.214	0.8215-0.1492	0.179-0.8511	4	25
	6	0.005-0.050	0.0132-0.169	1.28	0.05	0.039	0.15	6	0.259	0	0.173	0.8439-0.1538	0.1574-0.8461	5	25
	7	0.005-0.050	0.0136-0.155	1.0	0.078	0.078	0.185	6	0.427	0	0.285	0.831-0.1531	0.1581-0.8465	3	20
	8	0.005-0.050	0.0138-0.157	1.1	0.082	0.075	0.185	6	0.427	0	0.285	0.822-0.146	0.1687-0.846	3	20
	9	0.005-0.050	0.0139-0.154	1.2	0.085	0.071	0.185	6	0.427	0	0.285	0.818-0.1535	0.182-0.84654	3	20
	10	0.005-0.050	0.0138-0.154	1.3	0.089	0.068	0.185	6	0.427	0	0.285	0.8012-0.1563	0.1987-0.8432	3	20
	11	0.005-0.050	0.0141-0.151	1.4	0.091	0.065	0.185	6	0.427	0	0.285	0.7834-0.1478	0.2165-0.8521	3	20
	12	0.005-0.050	0.0138-0.158	1.5	0.094	0.063	0.185	6	0.427	0	0.285	0.7743-0.1301	0.2256-0.8698	3	20
Type-C	1	0.010-0.050	0.015-0.109	1.28	0.088	0.069	0.15	5	0.427	0.285	0	0.898-0.2203	0.1220-0.7797	3	20
	2	0.010-0.050	0.011-0.108	1.28	0.088	0.069	0.185	6	0.322	0.214	0	0.8682-0.2191	0.1318-0.7809	3	20

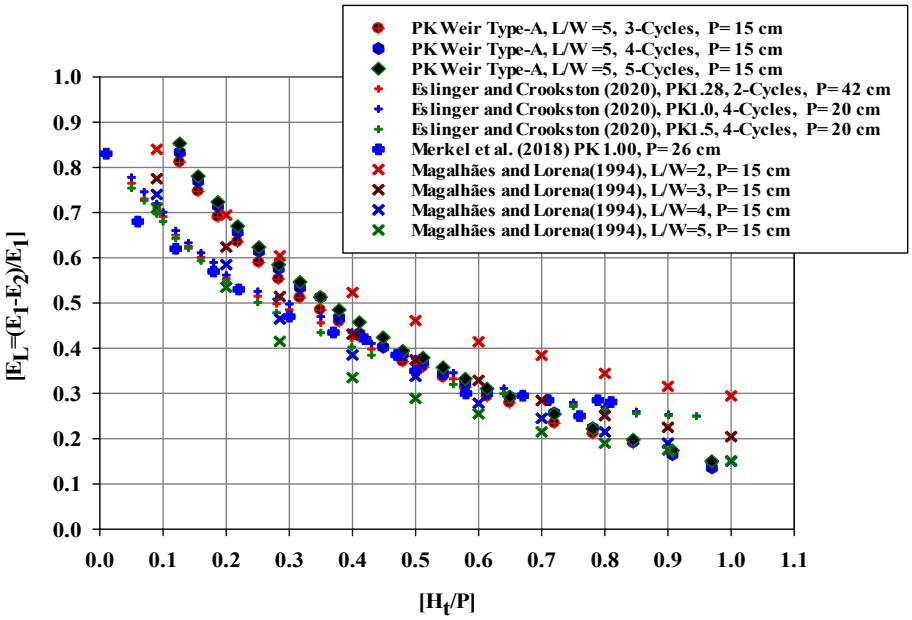

(a)

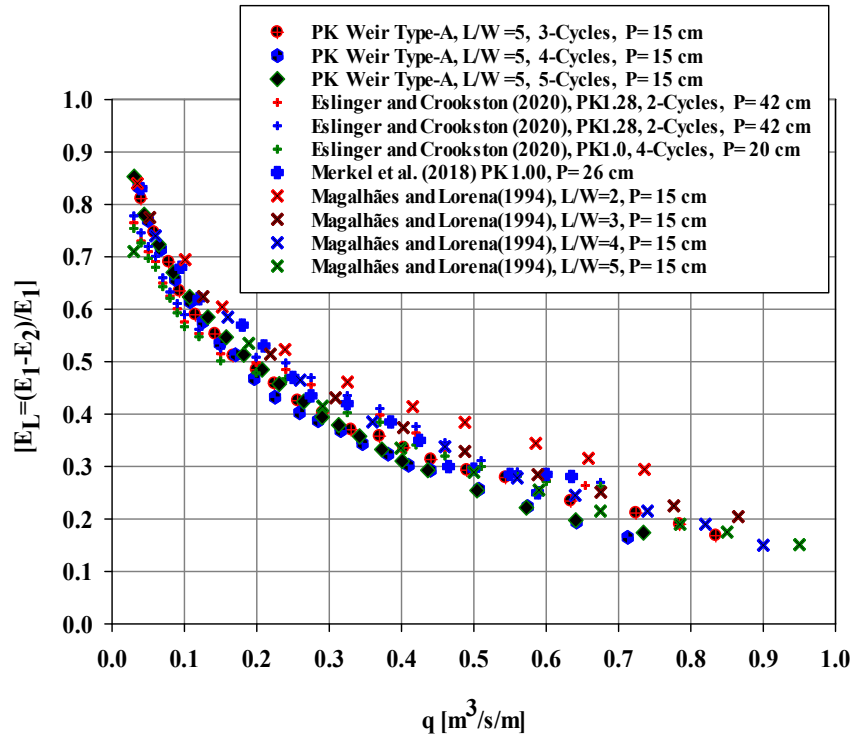

(b)

Figure: 4. 18 (i)Relative energy dissipation [$E_L=(E_1-E_2)/E_1$] with respect to the (a) headwater ratio [H_t/P] and (b) the unit discharge [q] for different cycles [for L/W=5] for Type-A.

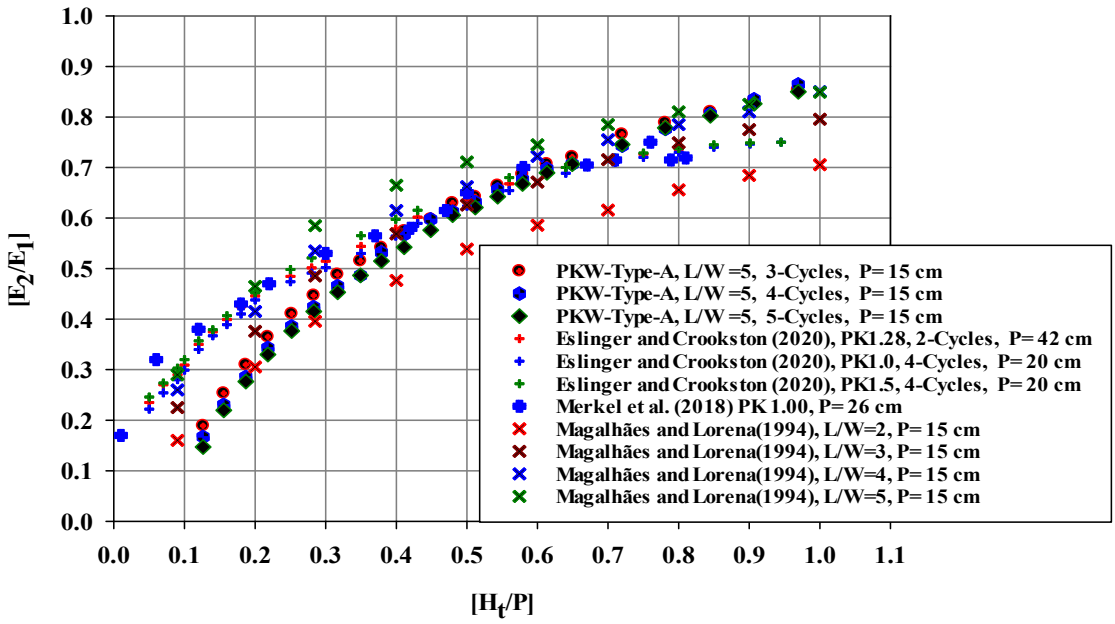

(c)

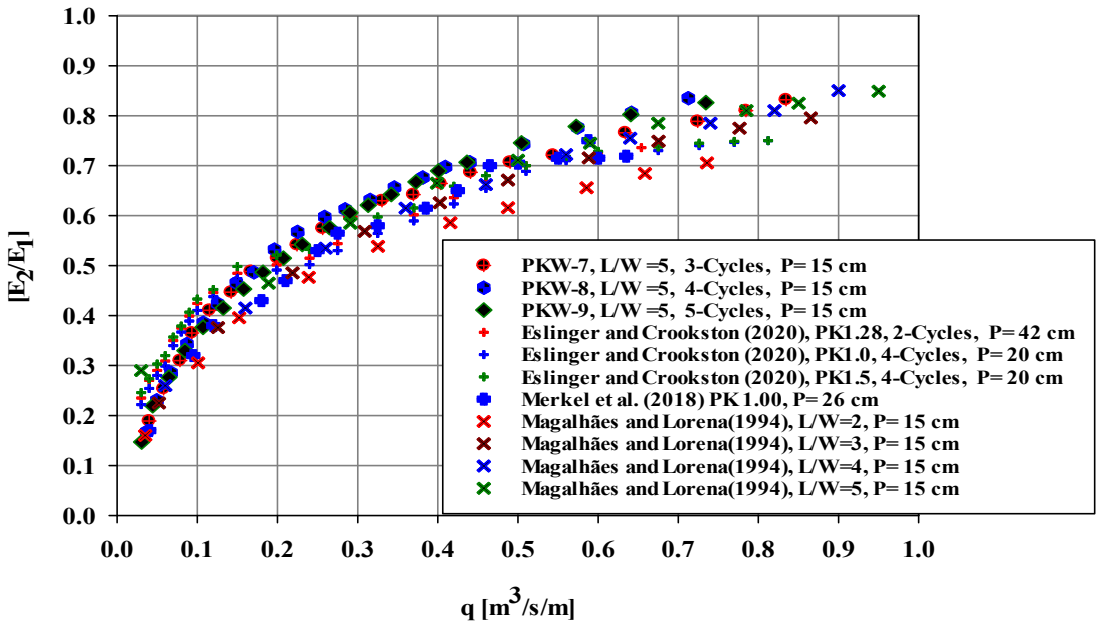

(d)

Figure: 4.18 (ii) Relative residual energy [E_2/E_1] with respect to the (c)headwater ratio [H_t/P] and (d) the unit discharge [q] for different cycles [for L/W=5] for Type-A.

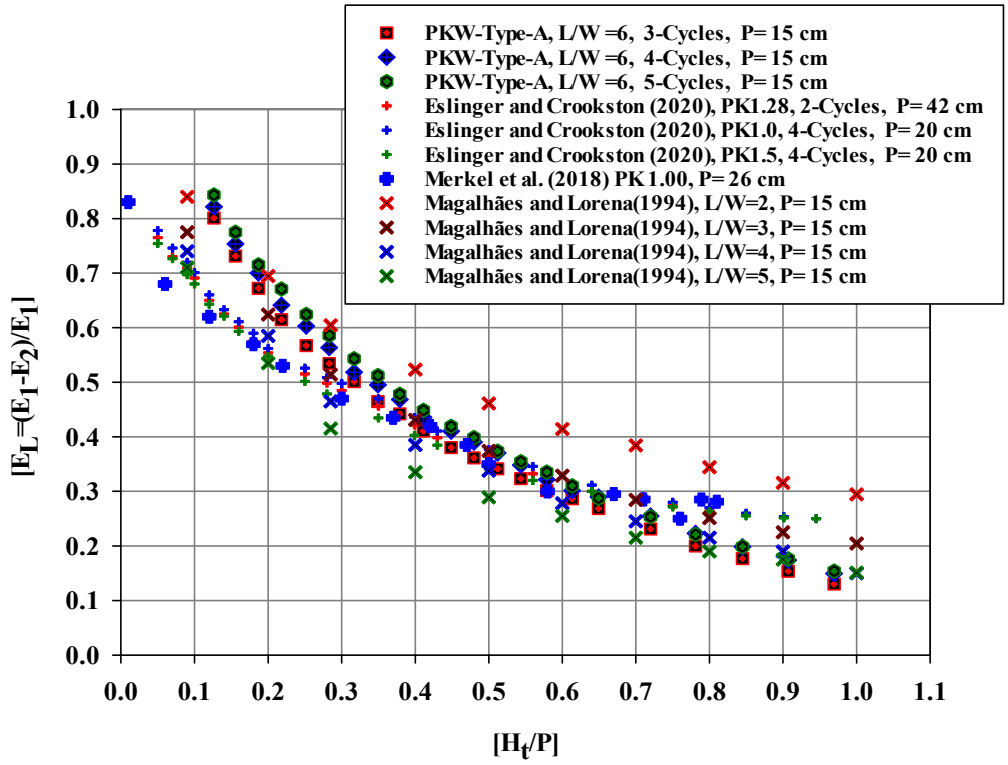

(a)

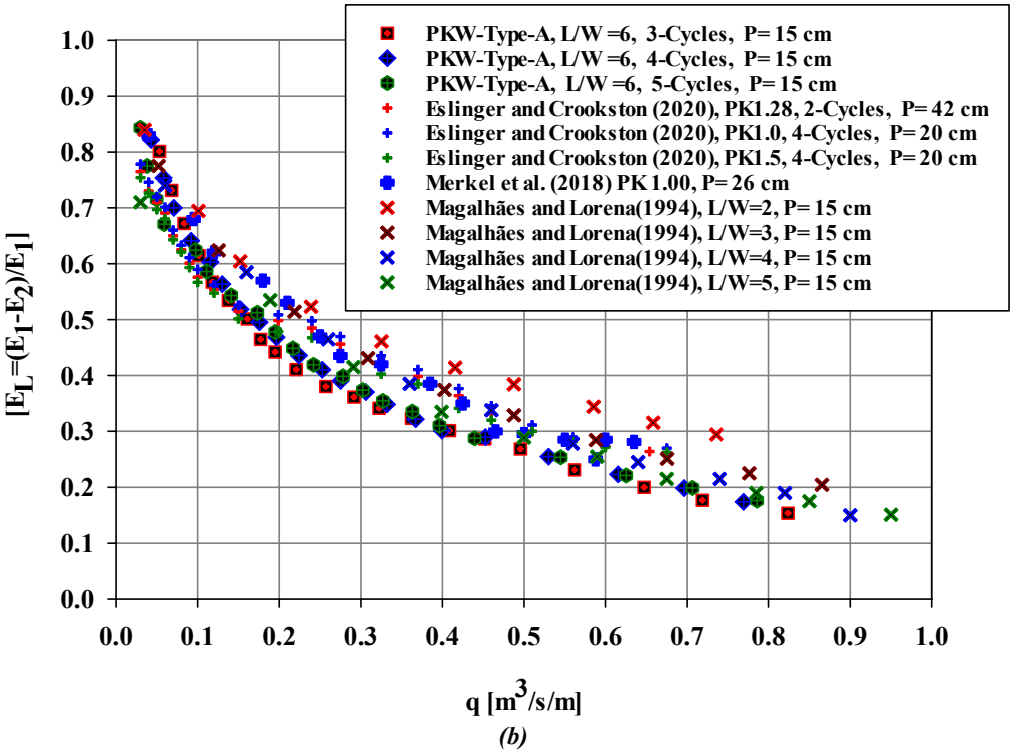

(b)

Figure: 4.19 (i) Relative energy dissipation [$E_L=(E_1-E_2)/E_1$] with respect to the (a) headwater ratio [H_t/P] and (b) the unit discharge [q] for different cycles [for L/W = 6] for Type-A.

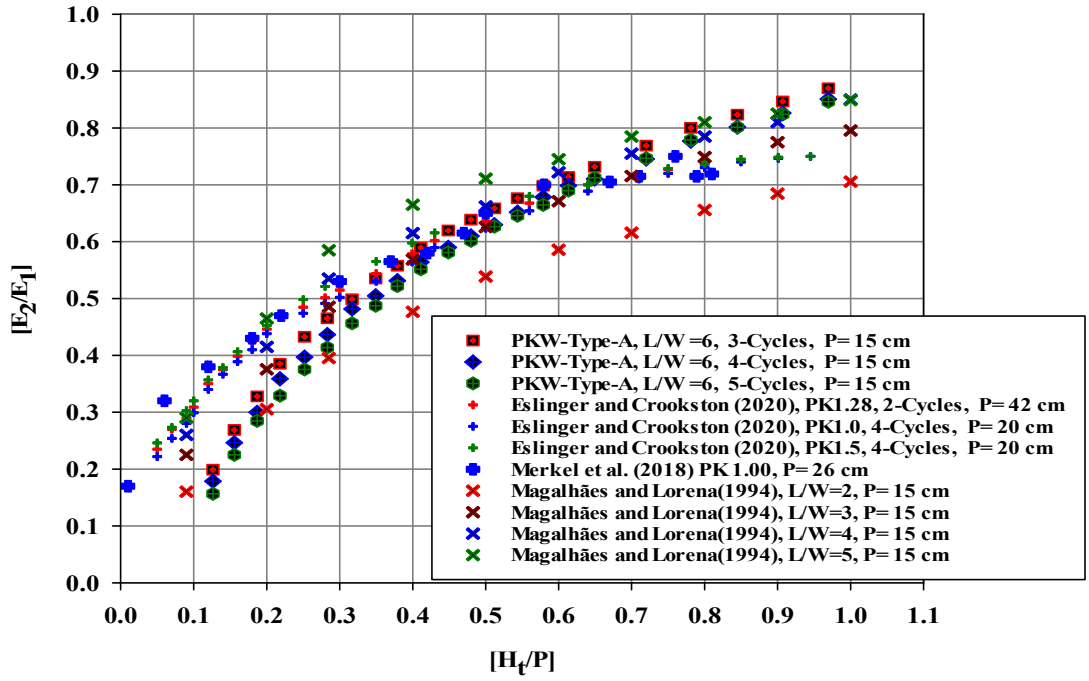

(c)

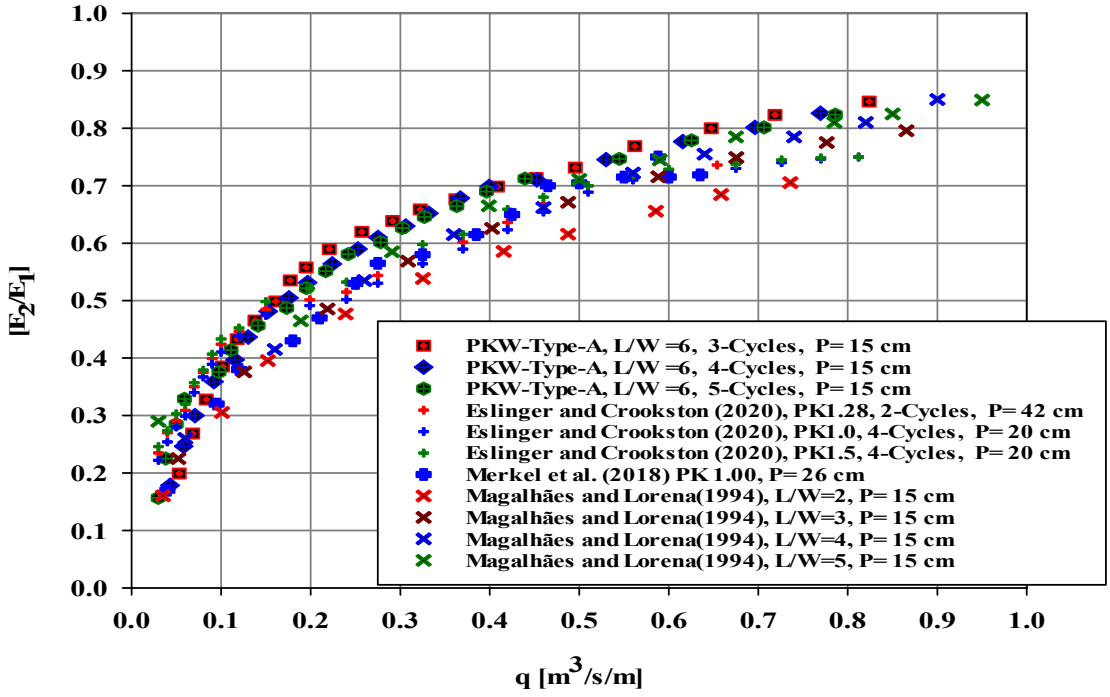

(d)

Figure: 4.19 (ii) Relative residual energy [E_2/E_1] with respect to the (c) headwater ratio [H_t/P] and (d) the unit discharge [q] for different cycles [for L/W=6] for Type-A.

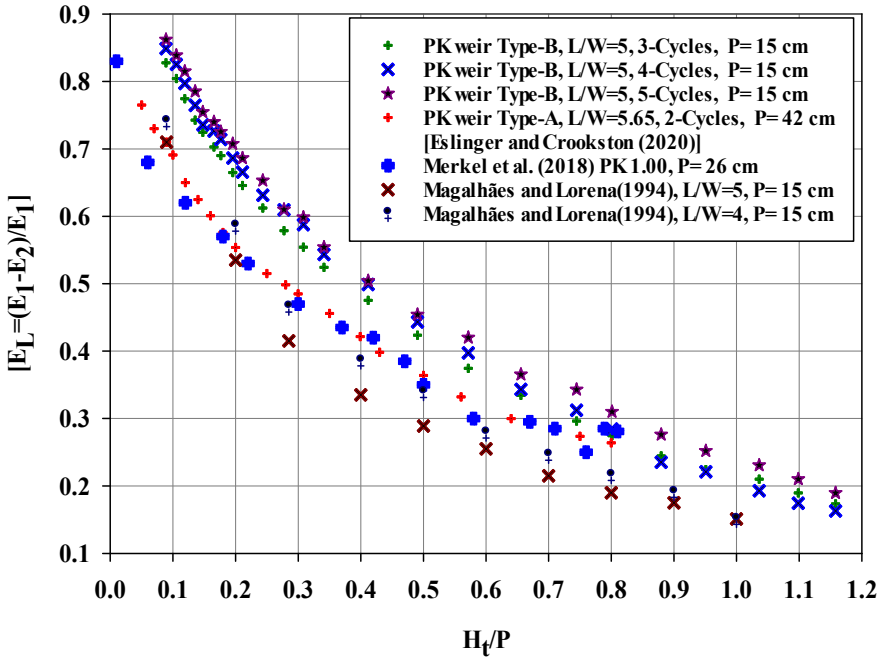

(a)

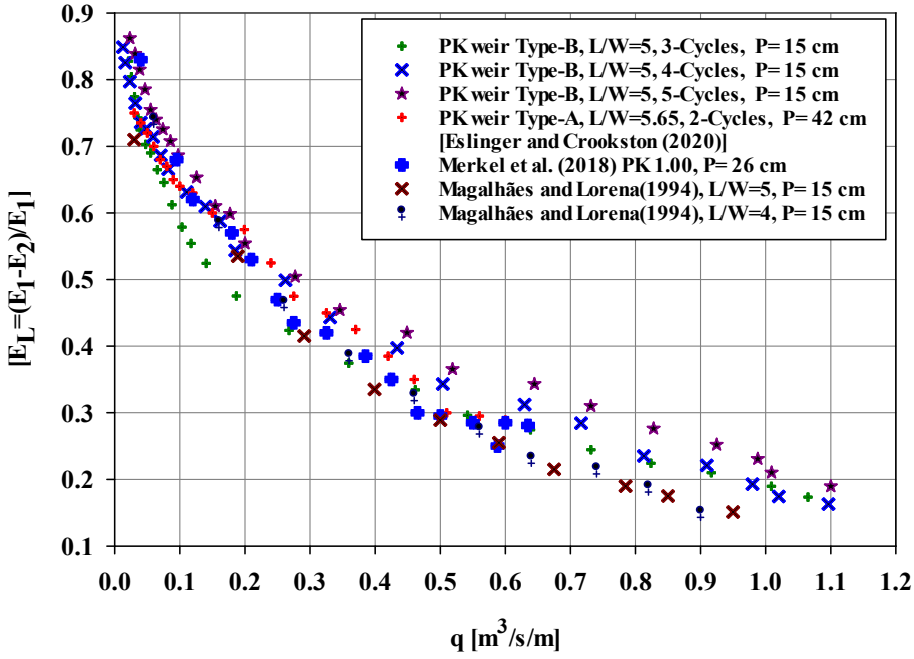

(b)

Figure: 4.20 (i) (Relative energy dissipation $[E_L=(E_1-E_2)/E_1]$ with respect to (a) the head water ratio $[H_t/P]$ and (b) the unit discharge [q]) for [L/W=5] for Type-B.

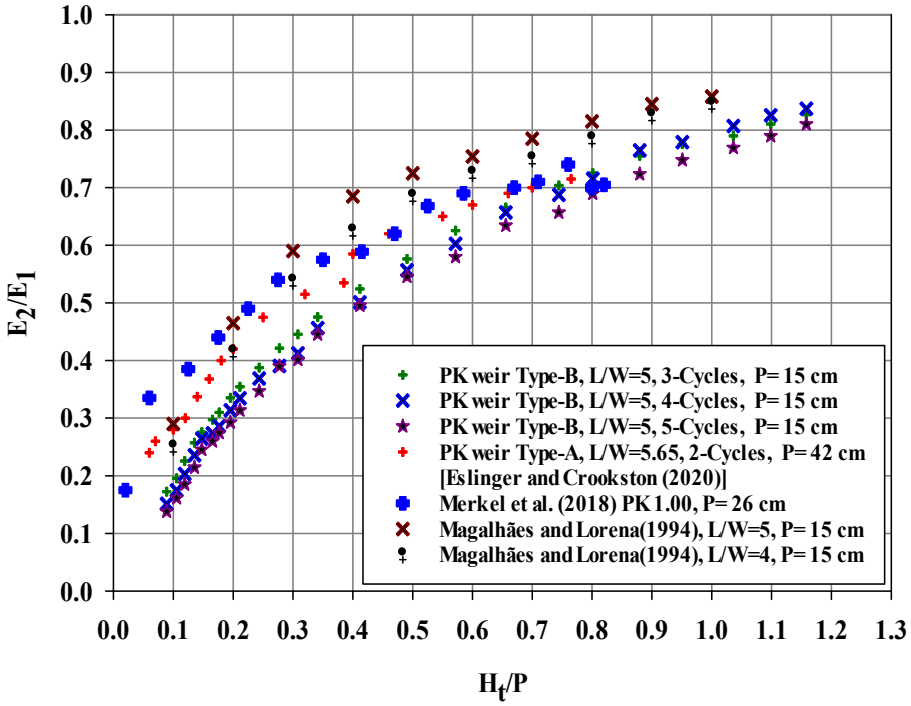

(a)

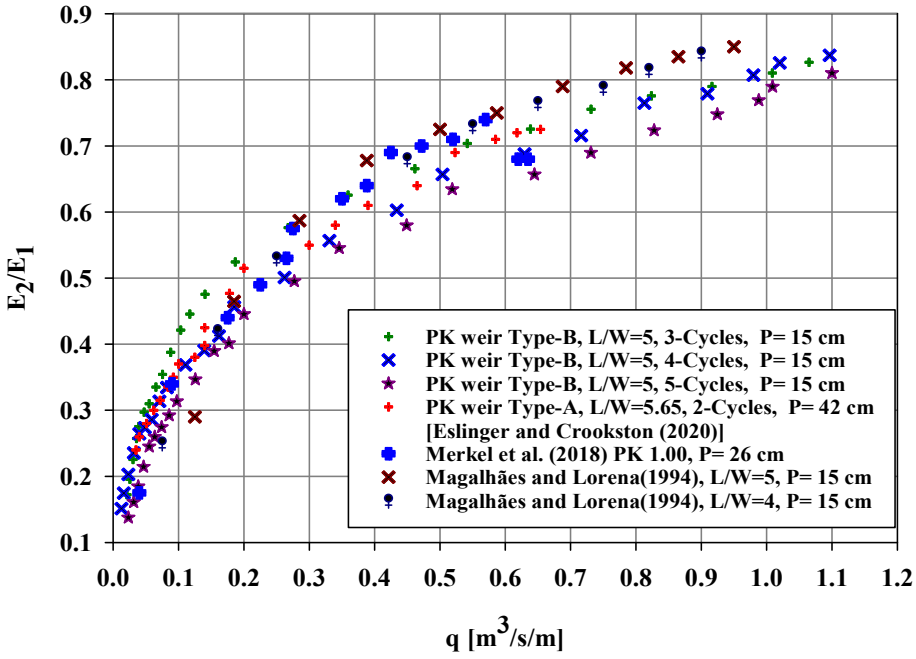

(b)

Figure: 4.20 (ii) (Relative residual energy [E_2/E_1] with respect to (a) the head water ratio [H_t/P] and (b) the unit discharge [q] for [L/W=5] for Type-B.

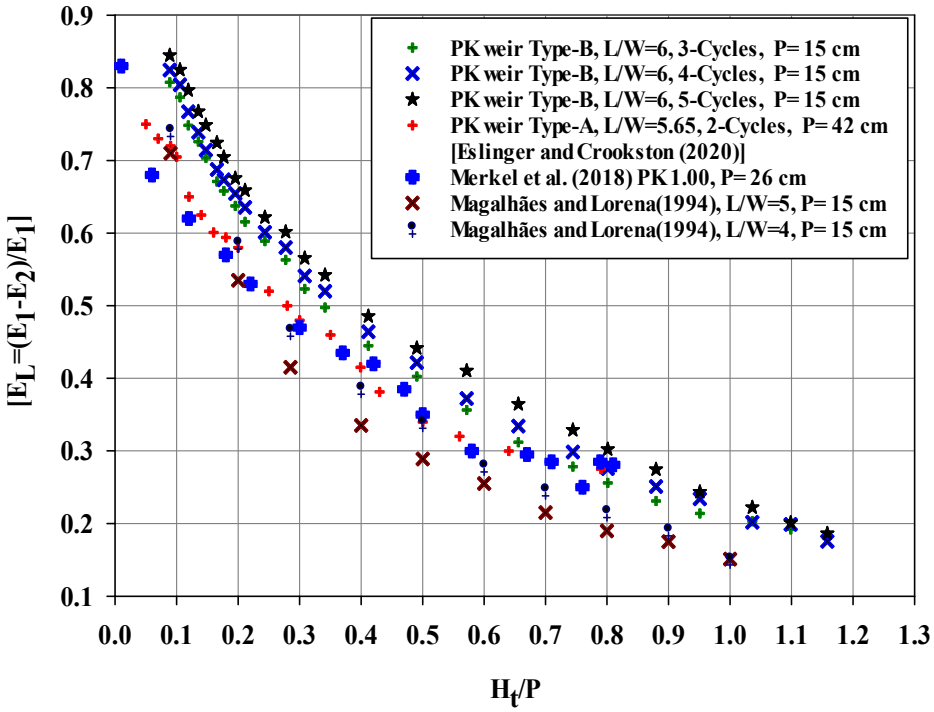

(a)

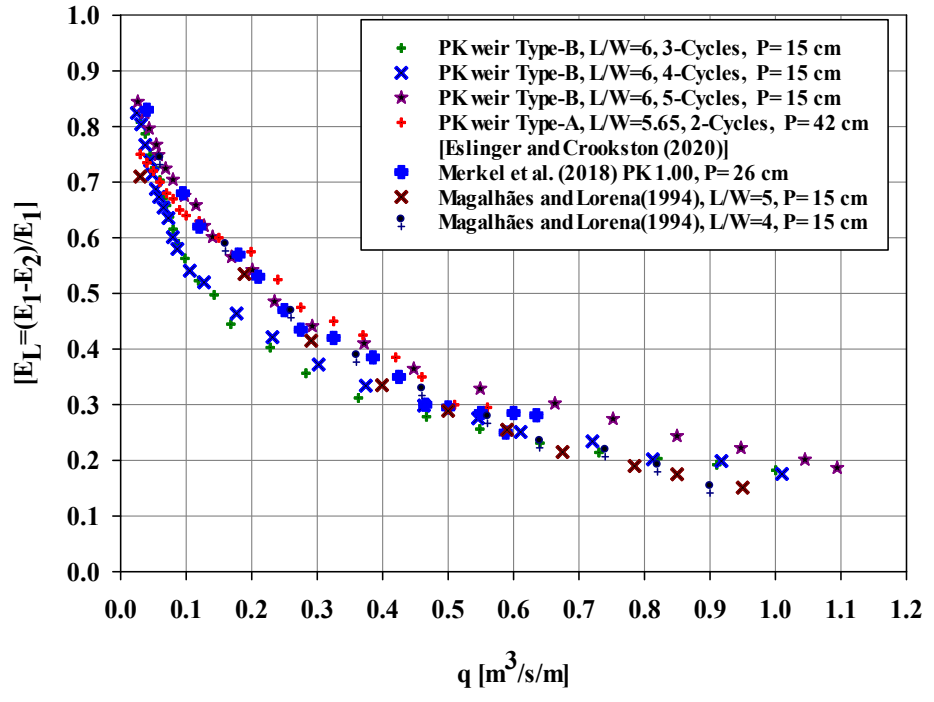

(b)

Figure: 4.21 (i) (Relative energy dissipation $[E_L=(E_1-E_2)/E_1]$ with respect to (a) the head water ratio $[H_t/P]$ and (b) the unit discharge [q] for [L/W=6] for Type-B.

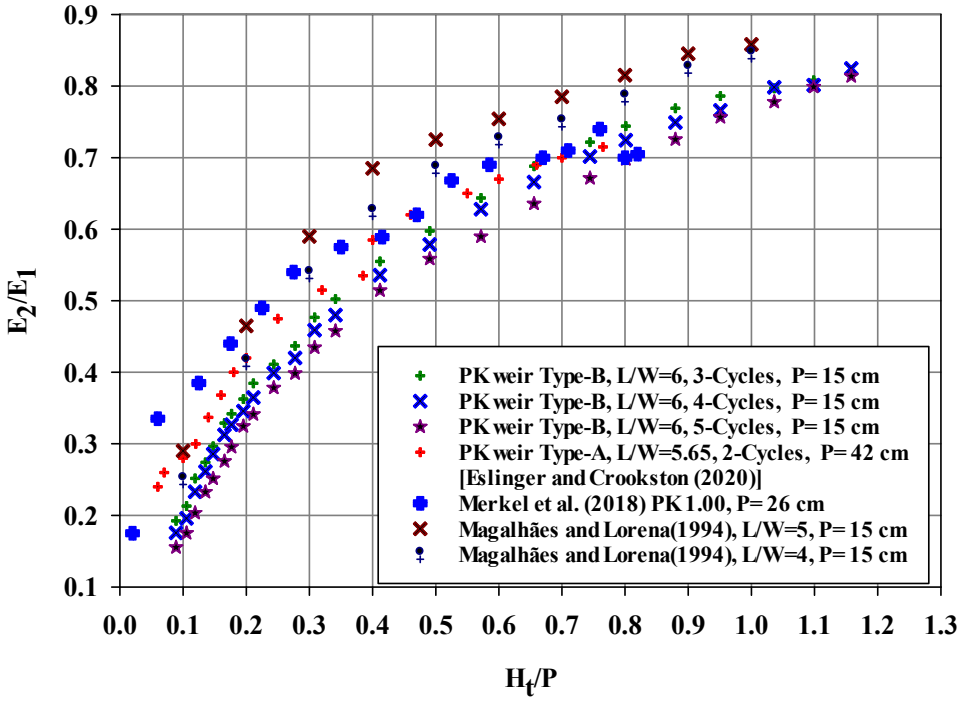

(a)

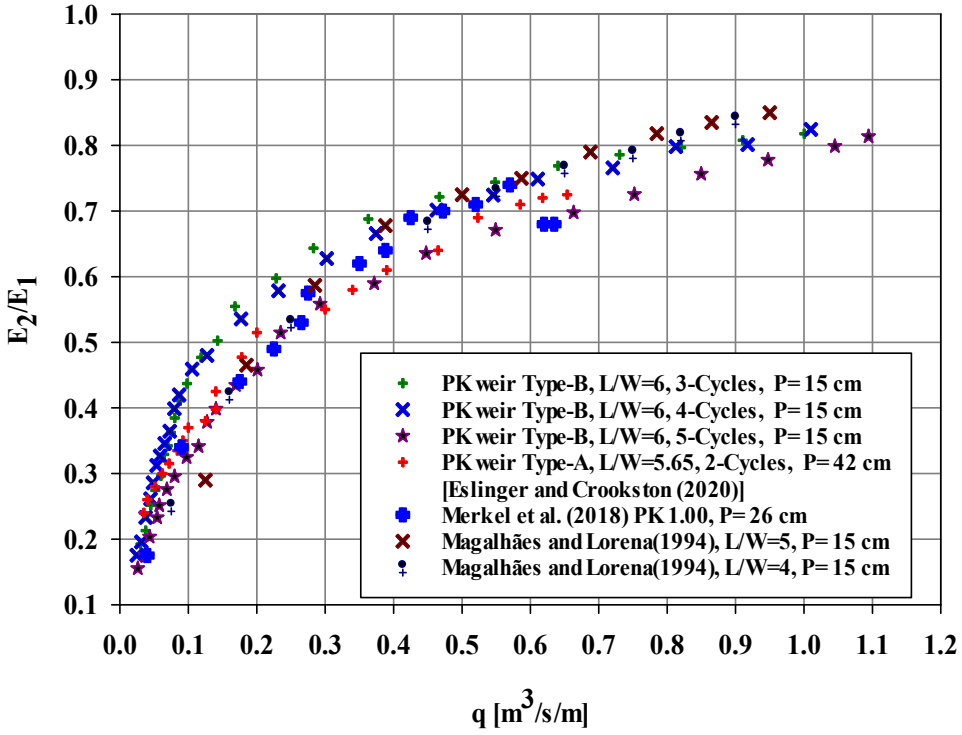

(b)

Figure: 4.21 (ii) (Relative residual energy [E_2/E_1] with respect to (a) the head water ratio [H_t/P] and (b) the unit discharge [q] for [L/W=6] for Type-B.

The relative energy dissipation was found to be constant at H_t/P >0.77 for Type-A, and H_t/P > 1.1 for Type-B and between $0.38 \leq H_t/P \leq 0.77$ for type-A and $0.25 \leq H_t/P \leq 1.1$ for type-B, the rate of $[E_L=(E_1-E_2)/E_1]$ relative energy dissipation steadily decreases as H_t/P increases. This is because the energy is dissipated in the outlet key section for small discharges, and the nappes are aligned partially laterally and partially in the flow direction. The water level in the keys rises for higher discharges due to local submergence effects **(Crookston and Tullis (2012)**, and the nappes are only aligned in the flow direction. As a result, energy dissipation decreases or remains nearly constant. This point concludes that the PKW represents the better relative energy dissipation efficiency at low discharges or low head level; an increasing the discharges or heads, its relative energy dissipation decreases gradually or sometimes rapidly.

The number of cycles plays an essential role in influencing the discharge capacity when the width is limited or constrained. According to **Tullis et al. (2020a)**, increasing the number of units or cycles for fixed-width decreases the discharge carrying capacity of the folded weir. The models were fabricated and tested in the current study while keeping the model's width constant. So, this section of the study is mainly focused on the influence of cyclic variation on the dissipating energy at the base of the different types of PKWs and found that for the same Magnification ratio (L/W), the relative energy dissipation $[E_L=(E_1-E_2)/E_1]$ at the base of PKWs increases with the number of cycles (units).

In addition, a closer look at **Figures: 4.18 to 4.21** reveals that the relative energy dissipation increases more with the number of cycles at low values of H_t/P (both the L/W ratio), and in contrast, for higher H_t/P values intermixing patterns of energy dissipation were observed. This is partly due to the gradual change in the nappe portion affected by neighborhood submergence. **(Crookston and Tullis, 2012a)**. The energy dissipation from jet collision and downstream impact is altered and thus reduced as the labyrinth or PKW nappe conditions transition from aerated to partially aerated and then drown (**Crookston and Tullis, 2012b)**. The trends mentioned above hold true when comparing relative energy dissipation to unit discharge (q) of dissimilar structures such as vertical drops and overflow weirs.

Figures: 4.18 (ii), 4.19 (ii), 4.20 (ii), and 4.21 (ii) show the variation of relative residual energy (E_2/E_1) downstream of the PKW with the H_t/P ratio, unit discharges (q). The maximum relative energy dissipation was observed in the present study corresponding to the highest cyclic count (i.e., $\Delta E/E_1$=.8831 or 88.31 percent for type-A and E_L= 0.8621 or 86.21% for type-B, which corresponds to L/W=5 and N=5). And the less energy dissipation for the

lowest cyclic counts (i.e., E_L =.8210 and 82.10 % for type-A and E_L= .8077 or 80.77% for type-B, correspond to L/W=6, and N=3) (**see Figures: 4.18 (ii), 4.19 (ii), 4.20 (ii), and 4.21 (ii)**). In the above discussion, PKWs depend on their key cycles (units) at $0.38 \leq H_t/P \leq 0.77$ for type-A, $0.25 \leq H_t/P \leq 1.1$ for type-B. Thus the number of cycles is a convenient parameter. Moreover, for comparison and reference, published data for laboratory-scale trapezoidal labyrinth weirs (**Magalhães and Lorena, 1994)**; rectangular labyrinth weirs **(Merkel et al., 2018);** and PKW **(Eslinger and Crookston, 2020)** were included. While the results were compared to previous studies within the accuracy of the measurements, all of these models had shown a very similar trend to other tested models. However, the minor differences in energy loss are due, in part, to experimental uncertainties and different experimental geometries.

4.4.2 Effects of the relative length (*L/W*) on energy dissipation

The second consequence of this study is to highlight the effects of the magnification ratio (*L/W*) on the relative energy dissipation of the different types (i.e., type-A, type-B & type-C) of PKW. The magnification ratio (*L/W*) is the most crucial parameter influencing the discharge carrying capacity of PKWs. According to **Leite Ribeiro et al. (2012)**, the discharge carrying capacity of the PKW enhances with the *L/W* ratio. However, the energy dissipation capacity of folded shape weir decreases with increasing the magnification ratio (*L/W*) **Magalhães and Lorena (1994)**.

Magalhães and Lorena (1994) investigated one-cycle trapezoidal labyrinth weirs with WES-type crest profiles for a different magnification ratio, and they noticed the residual energy (E_2/E_1) at the base of labyrinth weirs enhanced with the *L/W*. This trend may be highlighted because more significant flow rates are required for the same relative total upstream head (H_t/P) and magnification ratio (*L/W*). They also reported more relative residual energy for L/W = 5, which may be due to the difference between B and crest shape (overhanging profile) and cycle geometry. Finally, they concluded that the energy loss of labyrinth weirs is highly dependent on weir geometry.

In this section of the present study, the authors put effort into better understanding the effects of the magnification ratio on the energy dissipation capacity of the PKW and compared it with the previously published data. The test results indicated that the energy dissipation at the base of the PKW shows a decreasing trend with increasing the *L/W* ratio. In this approach, L varies with the head as the effective crest length decreases with increasing heads because

of local submergence on the upstream apex. Flow drowning and lateral jet overcrossing occur as the head increases, reducing the dissipation efficiency of the PKW.

The current study shows that the energy dissipation over the different PKWs is higher than its alternatives, except *L/W* =2 of the trapezoidal labyrinth weirs (**Magalhães and Lorena, 1994)**, but it follows the same trend.

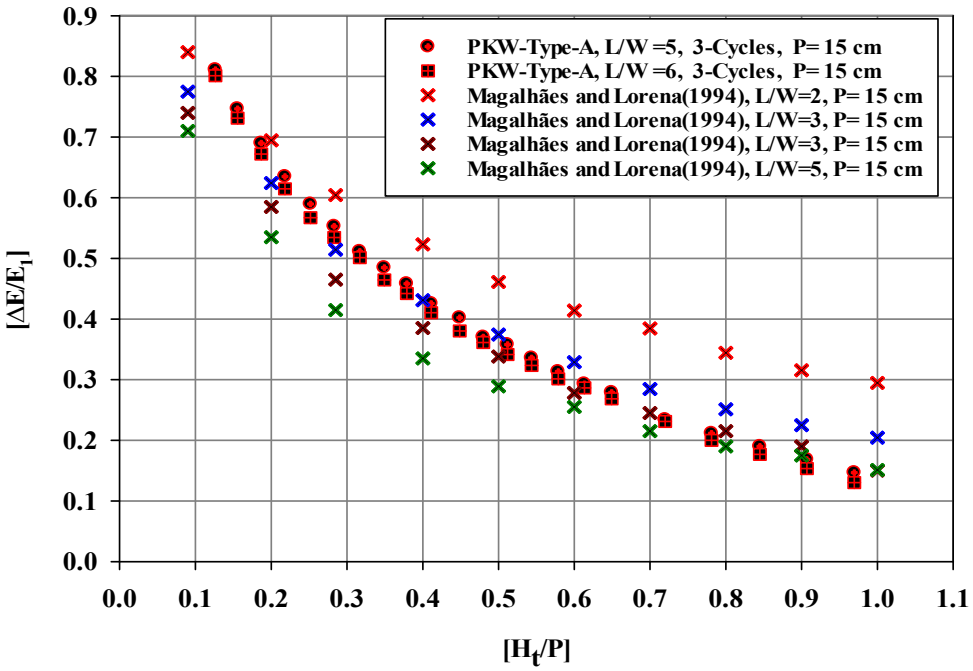

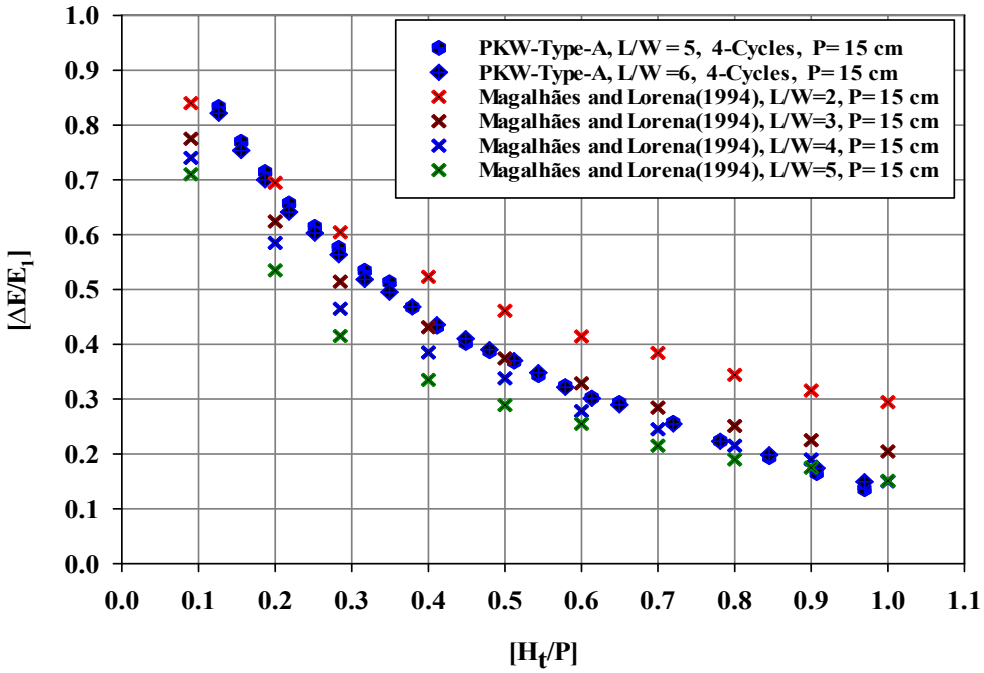

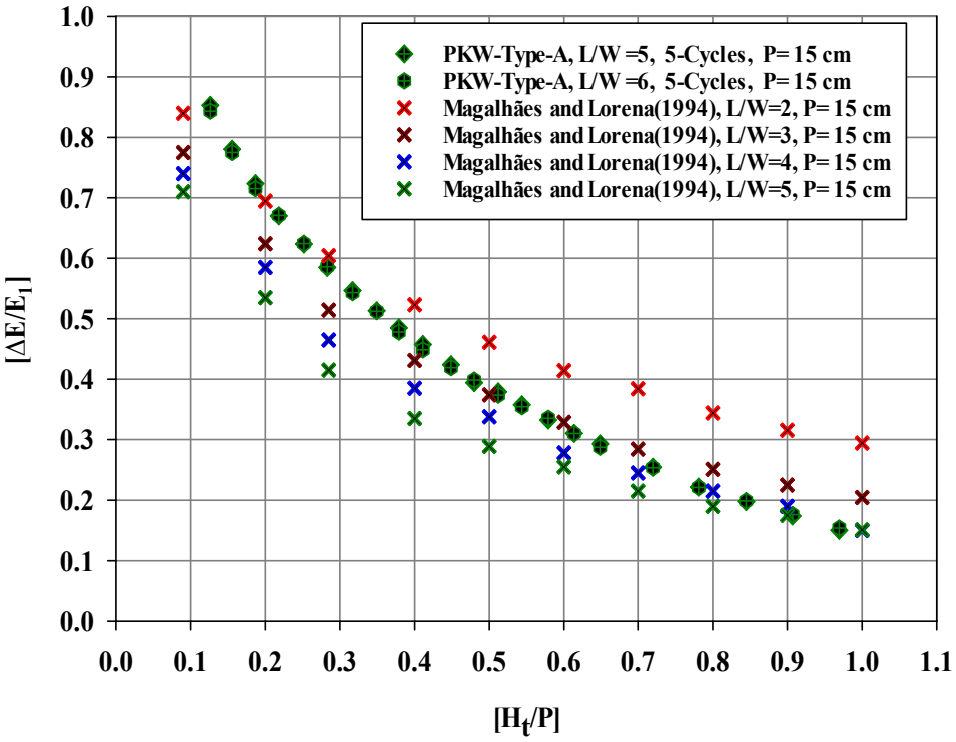
PKW-Type-A, L/W =5, 5-Cycles, P= 15 cm
PKW-Type-A, L/W =6, 5-Cycles, P= 15 cm
Magalhães and Lorena(1994), L/W=2, P= 15 cm
Magalhães and Lorena(1994), L/W=3, P= 15 cm
Magalhães and Lorena(1994), L/W=4, P= 15 cm
Magalhães and Lorena(1994), L/W=5, P= 15 cm
[ΔE/E1]
[Ht/P]
0.0
0.1
0.2
0.3
0.4
0.5
0.6
0.7
0.8
0.9
1.0
1.1

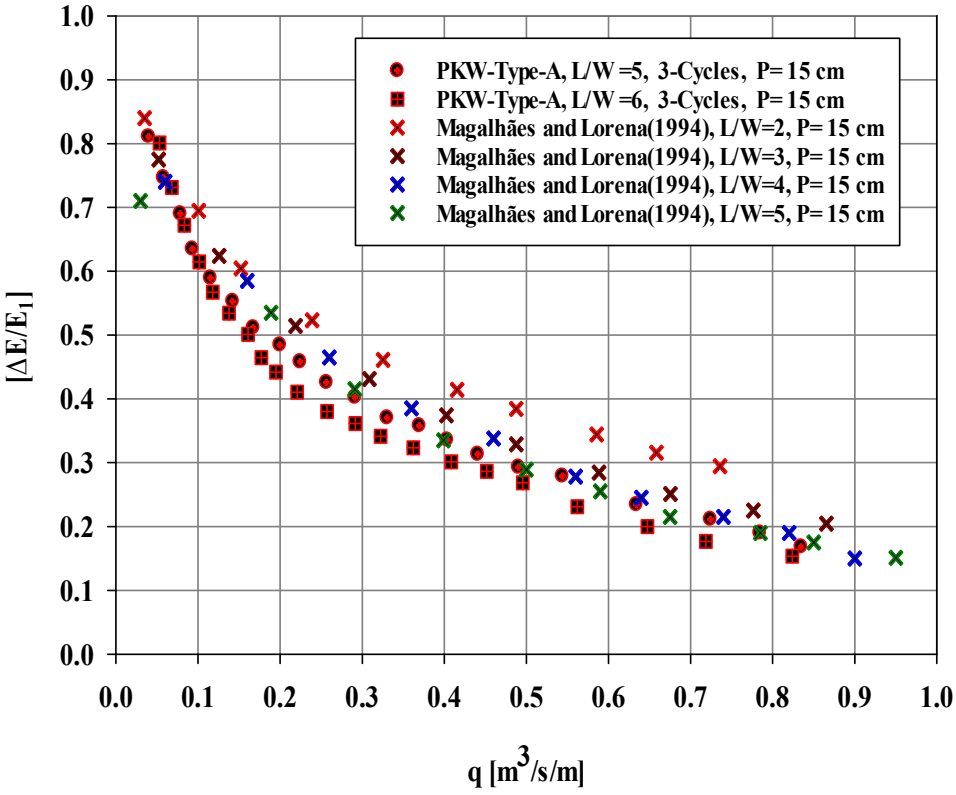
PKW-Type-A, L/W =5, 3-Cycles, P= 15 cm
PKW-Type-A, L/W =6, 3-Cycles, P= 15 cm
Magalhães and Lorena(1994), L/W=2, P= 15 cm
Magalhães and Lorena(1994), L/W=3, P= 15 cm
Magalhães and Lorena(1994), L/W=4, P= 15 cm
Magalhães and Lorena(1994), L/W=5, P= 15 cm
[ΔE/E1]
q [m3/s/m]
0.0
0.1
0.2
0.3
0.4
0.5
0.6
0.7
0.8
0.9
1.0

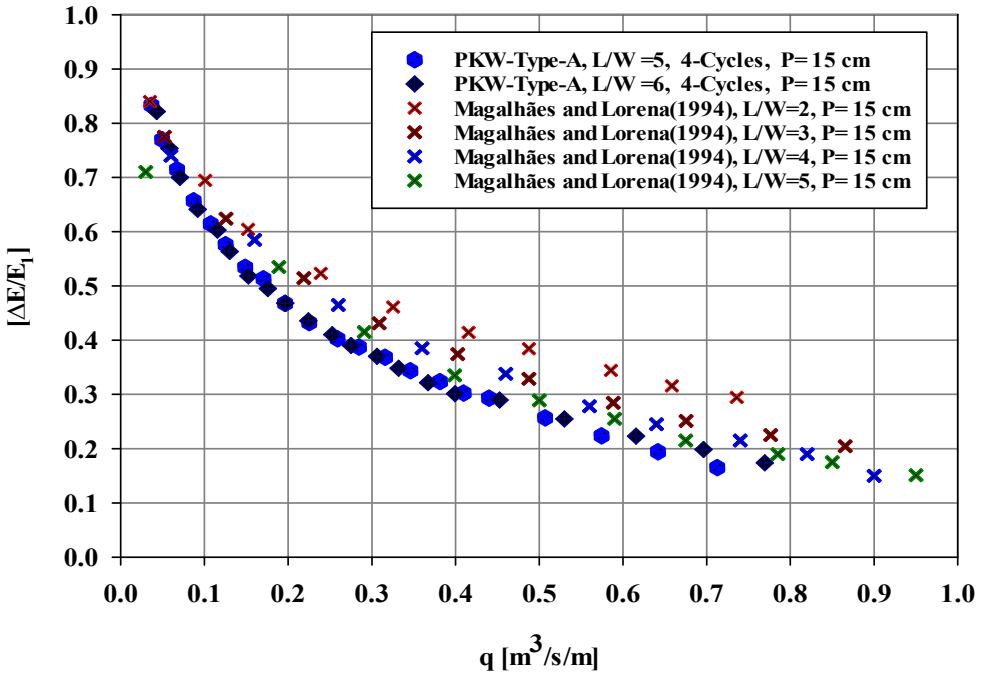

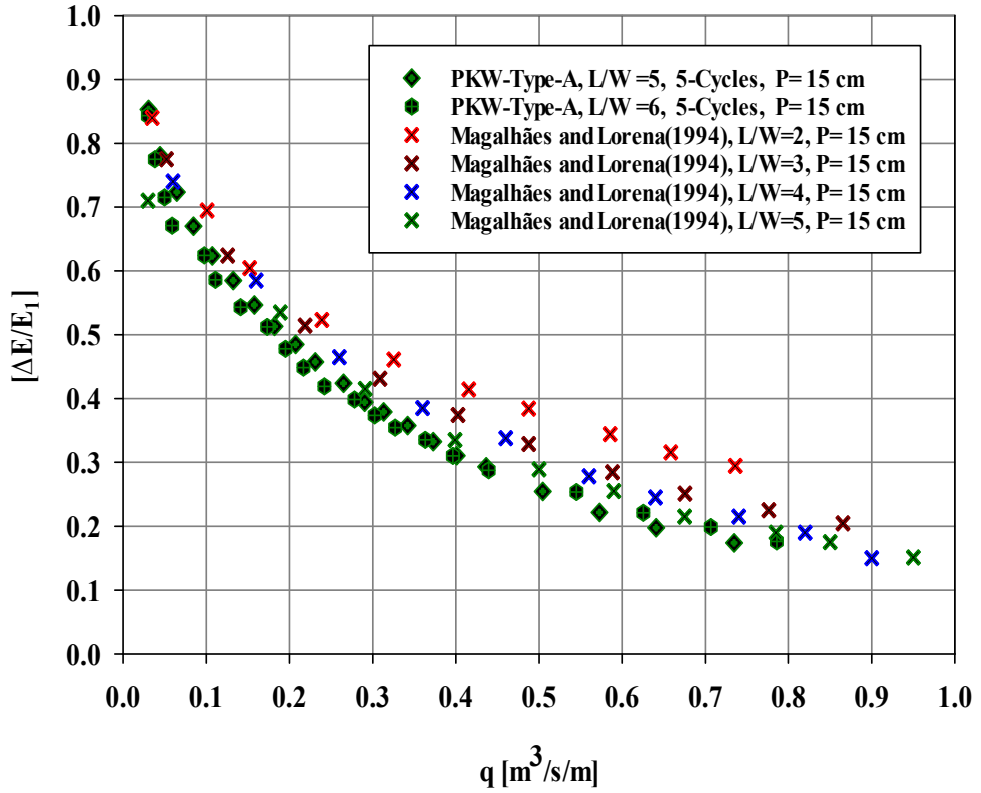

Figure: 4.22 (i) Relative energy dissipation [($\Delta E/E_1$] with respect to (a) the head water ratio [H_t/P] and (b) the unit discharge [q] for diffirent cycles (N).

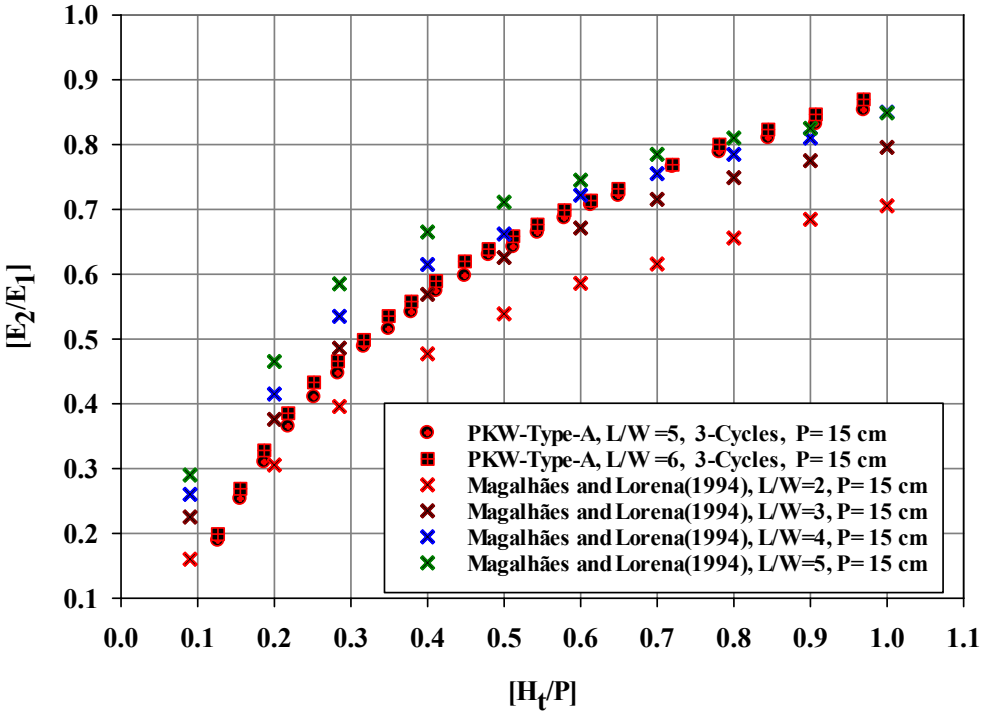
1.0
0.9
0.8
0.7
0.6
0.5
0.4
0.3
0.2
0.1
0.0
0.1
0.2
0.3
0.4
0.5
0.6
0.7
0.8
0.9
1.0
1.1
[E2/E1]
[Ht/P]
PKW-Type-A, L/W =5, 3-Cycles, P= 15 cm
PKW-Type-A, L/W =6, 3-Cycles, P= 15 cm
Magalhães and Lorena(1994), L/W=2, P= 15 cm
Magalhães and Lorena(1994), L/W=3, P= 15 cm
Magalhães and Lorena(1994), L/W=4, P= 15 cm
Magalhães and Lorena(1994), L/W=5, P= 15 cm

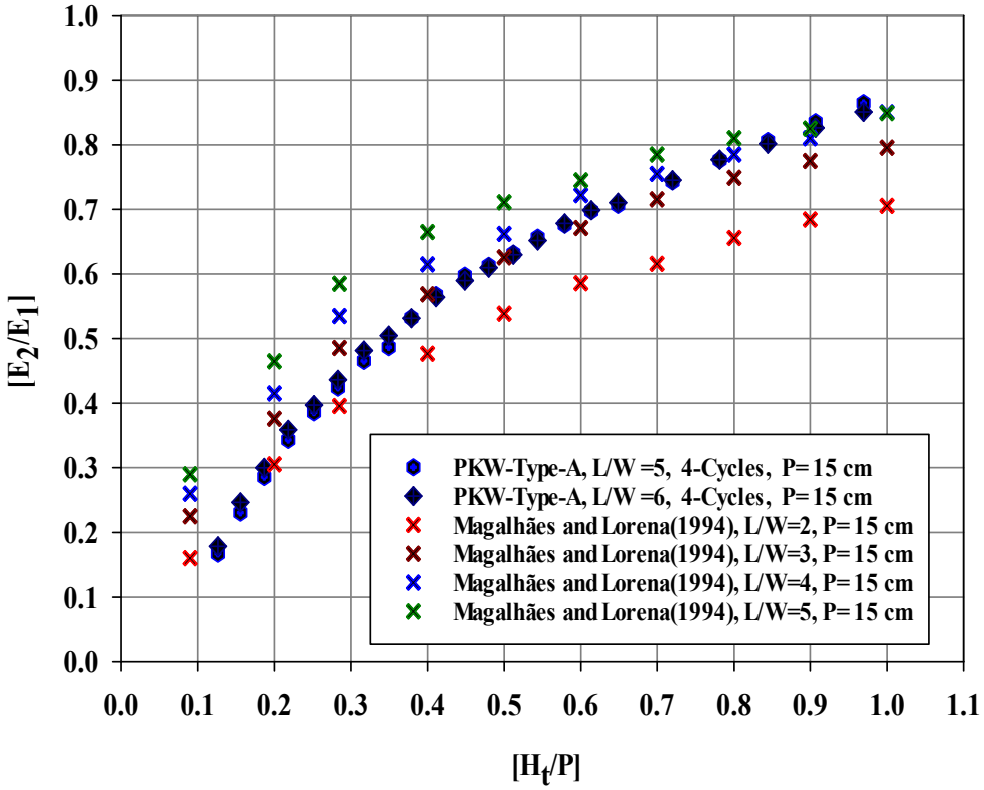
1.0
0.9
0.8
0.7
0.6
0.5
0.4
0.3
0.2
0.1
0.0
0.1
0.2
0.3
0.4
0.5
0.6
0.7
0.8
0.9
1.0
1.1
[E2/E1]
[Ht/P]
PKW-Type-A, L/W =5, 4-Cycles, P= 15 cm
PKW-Type-A, L/W =6, 4-Cycles, P= 15 cm
Magalhães and Lorena(1994), L/W=2, P= 15 cm
Magalhães and Lorena(1994), L/W=3, P= 15 cm
Magalhães and Lorena(1994), L/W=4, P= 15 cm
Magalhães and Lorena(1994), L/W=5, P= 15 cm

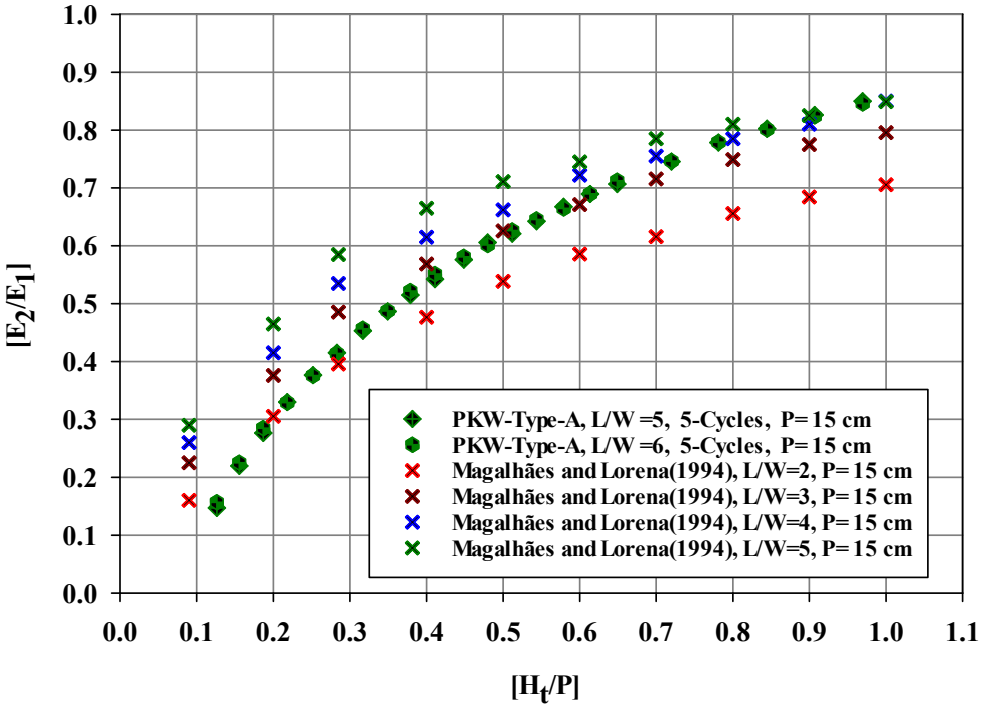
1.0
0.9
0.8
0.7
0.6
0.5
0.4
0.3
0.2
0.1
0.0
0.0 0.1 0.2 0.3 0.4 0.5 0.6 0.7 0.8 0.9 1.0 1.1
[E2/E1]
[Ht/P]
PKW-Type-A, L/W =5, 5-Cycles, P= 15 cm
PKW-Type-A, L/W =6, 5-Cycles, P= 15 cm
Magalhães and Lorena(1994), L/W=2, P= 15 cm
Magalhães and Lorena(1994), L/W=3, P= 15 cm
Magalhães and Lorena(1994), L/W=4, P= 15 cm
Magalhães and Lorena(1994), L/W=5, P= 15 cm

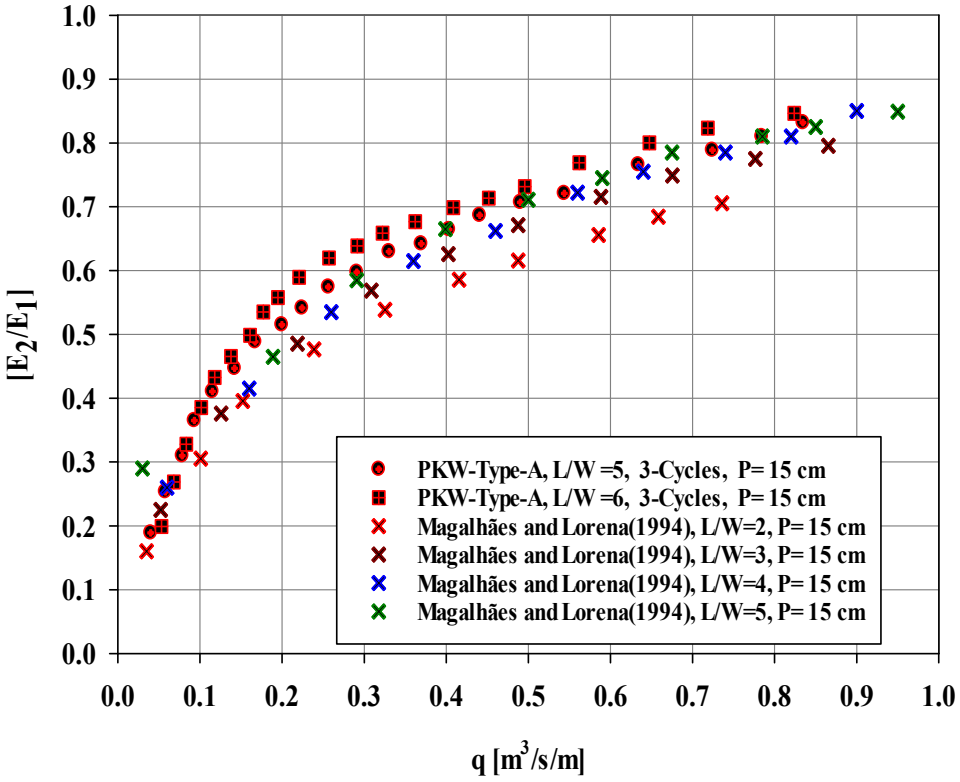
1.0
0.9
0.8
0.7
0.6
0.5
0.4
0.3
0.2
0.1
0.0
0.0 0.1 0.2 0.3 0.4 0.5 0.6 0.7 0.8 0.9 1.0
[E2/E1]
q [m3/s/m]
PKW-Type-A, L/W =5, 3-Cycles, P= 15 cm
PKW-Type-A, L/W =6, 3-Cycles, P= 15 cm
Magalhães and Lorena(1994), L/W=2, P= 15 cm
Magalhães and Lorena(1994), L/W=3, P= 15 cm
Magalhães and Lorena(1994), L/W=4, P= 15 cm
Magalhães and Lorena(1994), L/W=5, P= 15 cm

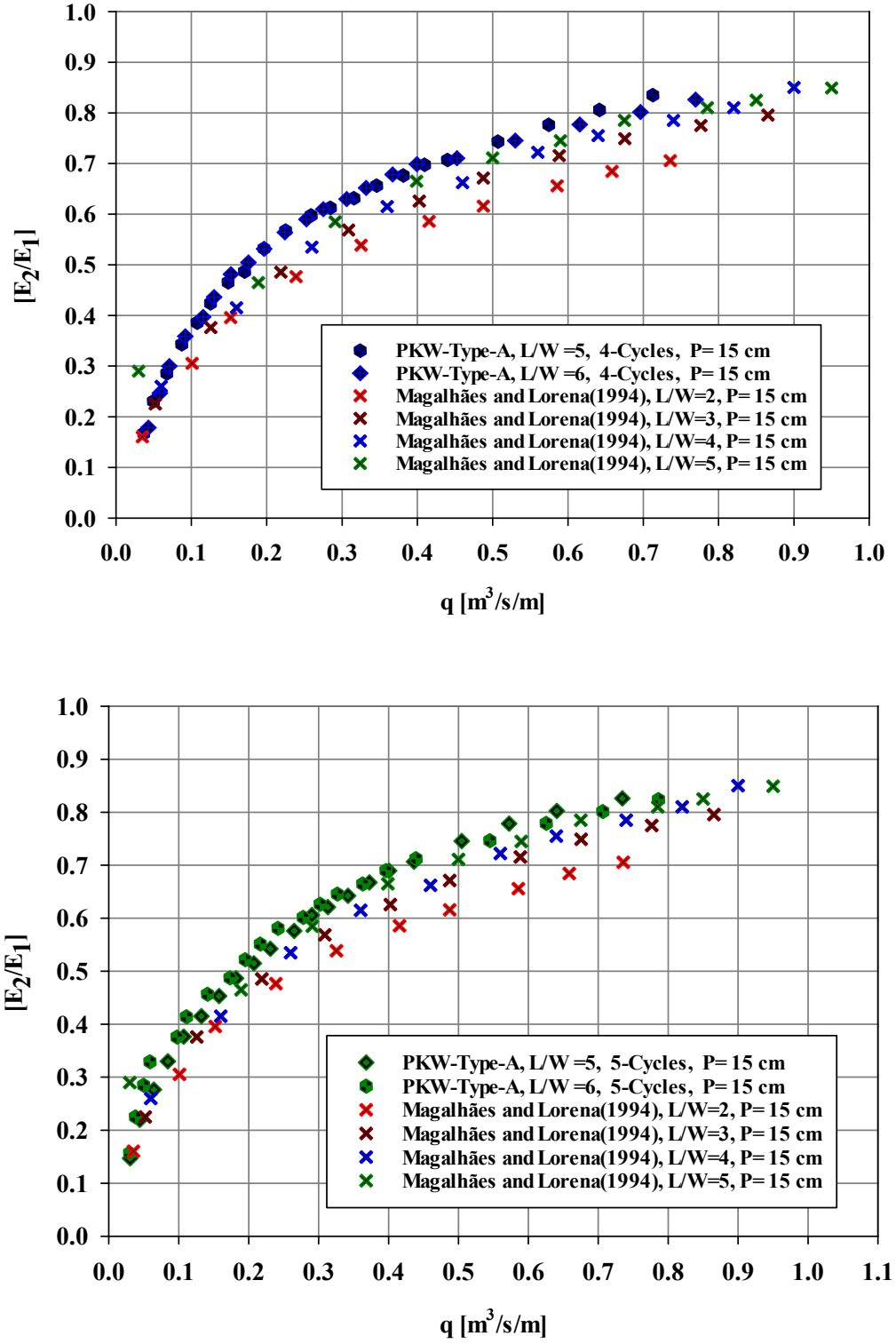

Figure: 4.22 (ii) Relative residual energy [E_2/E_1] with respect to (a) the headwater ratio [H_t/P] and (b) the unit discharge [q] for different cycles (N).

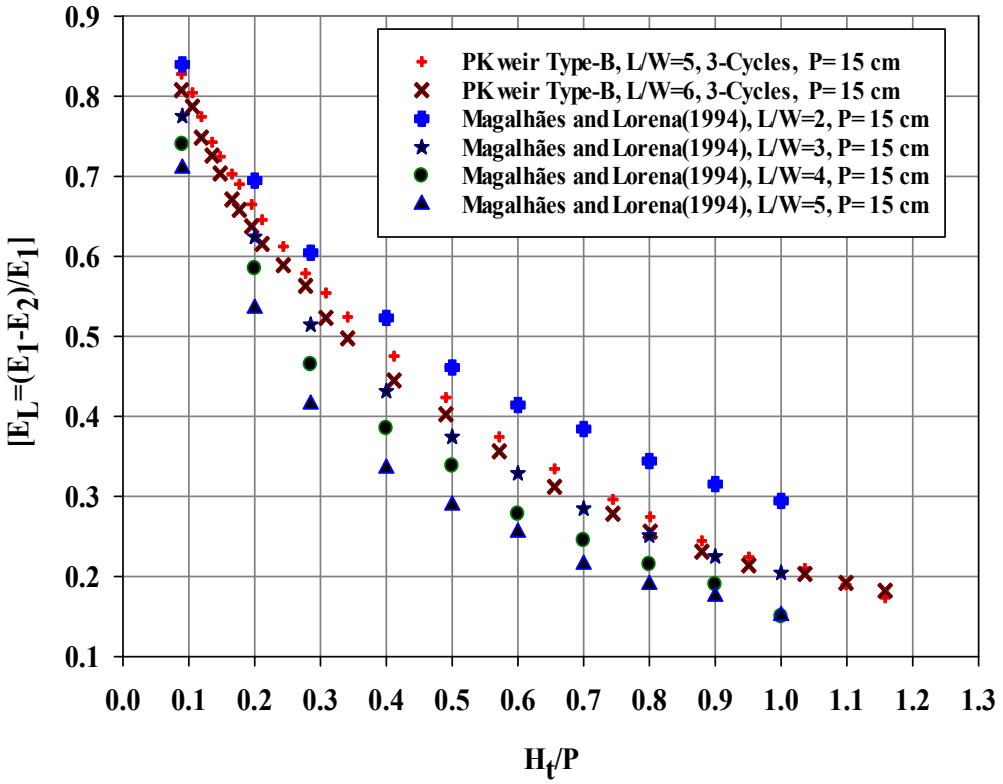
PK weir Type-B, L/W=5, 3-Cycles, P= 15 cm
PK weir Type-B, L/W=6, 3-Cycles, P= 15 cm
Magalhães and Lorena(1994), L/W=2, P= 15 cm
Magalhães and Lorena(1994), L/W=3, P= 15 cm
Magalhães and Lorena(1994), L/W=4, P= 15 cm
Magalhães and Lorena(1994), L/W=5, P= 15 cm
[E_L=(E_1-E_2)/E_1]
H_t/P
0.9
0.8
0.7
0.6
0.5
0.4
0.3
0.2
0.1
0.0 0.1 0.2 0.3 0.4 0.5 0.6 0.7 0.8 0.9 1.0 1.1 1.2 1.3

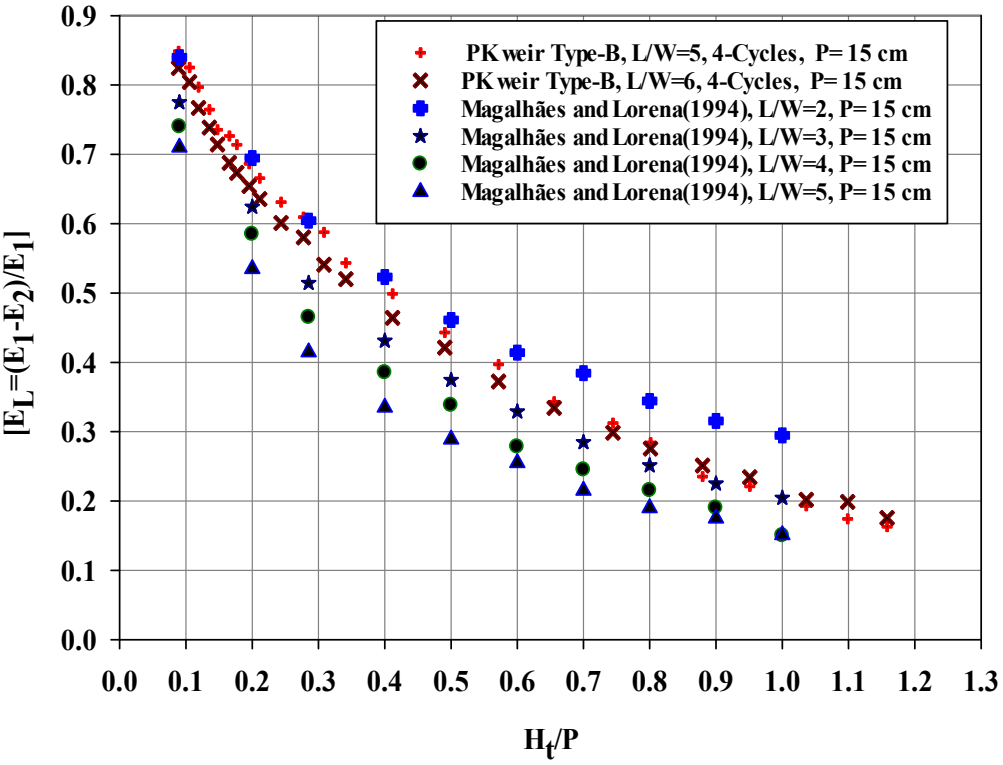
PK weir Type-B, L/W=5, 4-Cycles, P= 15 cm
PK weir Type-B, L/W=6, 4-Cycles, P= 15 cm
Magalhães and Lorena(1994), L/W=2, P= 15 cm
Magalhães and Lorena(1994), L/W=3, P= 15 cm
Magalhães and Lorena(1994), L/W=4, P= 15 cm
Magalhães and Lorena(1994), L/W=5, P= 15 cm
[E_L=(E_1-E_2)/E_1]
H_t/P
0.9
0.8
0.7
0.6
0.5
0.4
0.3
0.2
0.1
0.0
0.0 0.1 0.2 0.3 0.4 0.5 0.6 0.7 0.8 0.9 1.0 1.1 1.2 1.3

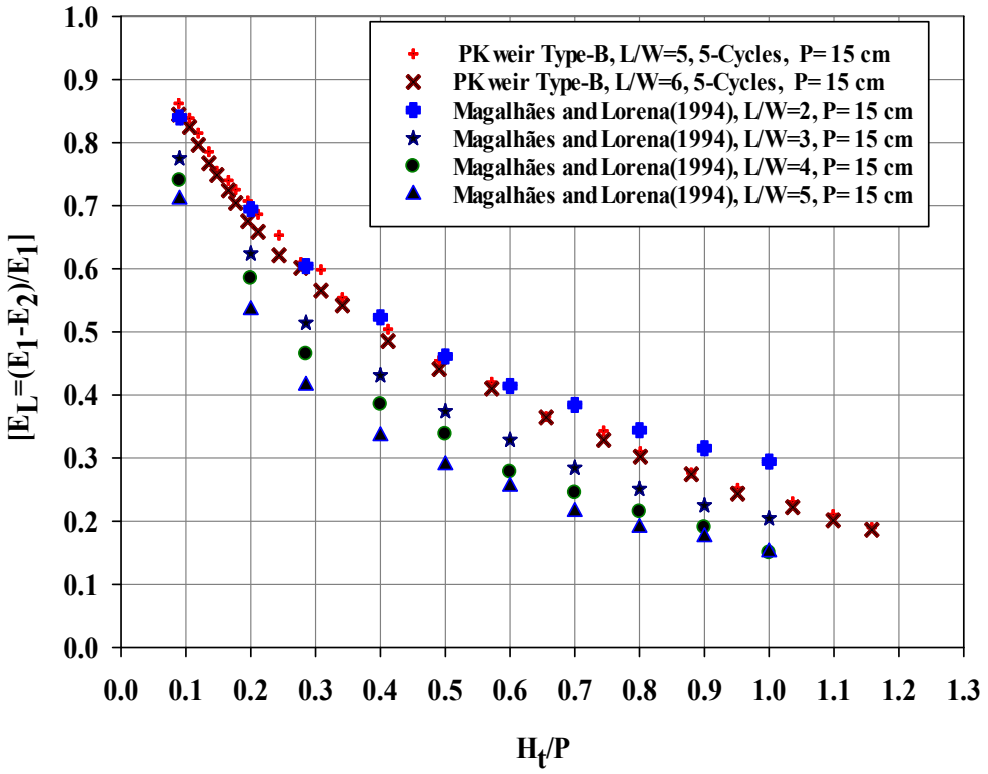
PK weir Type-B, L/W=5, 5-Cycles, P= 15 cm
PK weir Type-B, L/W=6, 5-Cycles, P= 15 cm
Magalhães and Lorena(1994), L/W=2, P= 15 cm
Magalhães and Lorena(1994), L/W=3, P= 15 cm
Magalhães and Lorena(1994), L/W=4, P= 15 cm
Magalhães and Lorena(1994), L/W=5, P= 15 cm
[EL=(E1-E2)/E1]
Ht/P

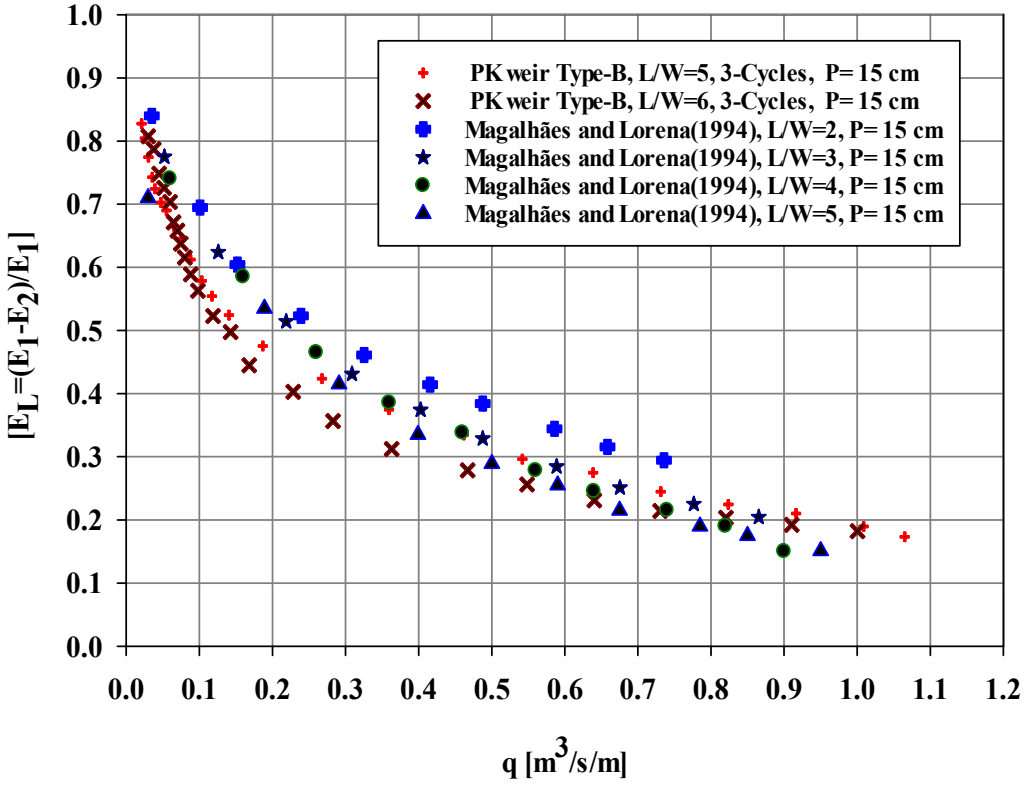
PK weir Type-B, L/W=5, 3-Cycles, P= 15 cm
PK weir Type-B, L/W=6, 3-Cycles, P= 15 cm
Magalhães and Lorena(1994), L/W=2, P= 15 cm
Magalhães and Lorena(1994), L/W=3, P= 15 cm
Magalhães and Lorena(1994), L/W=4, P= 15 cm
Magalhães and Lorena(1994), L/W=5, P= 15 cm
[EL=(E1-E2)/E1]
q [m3/s/m]

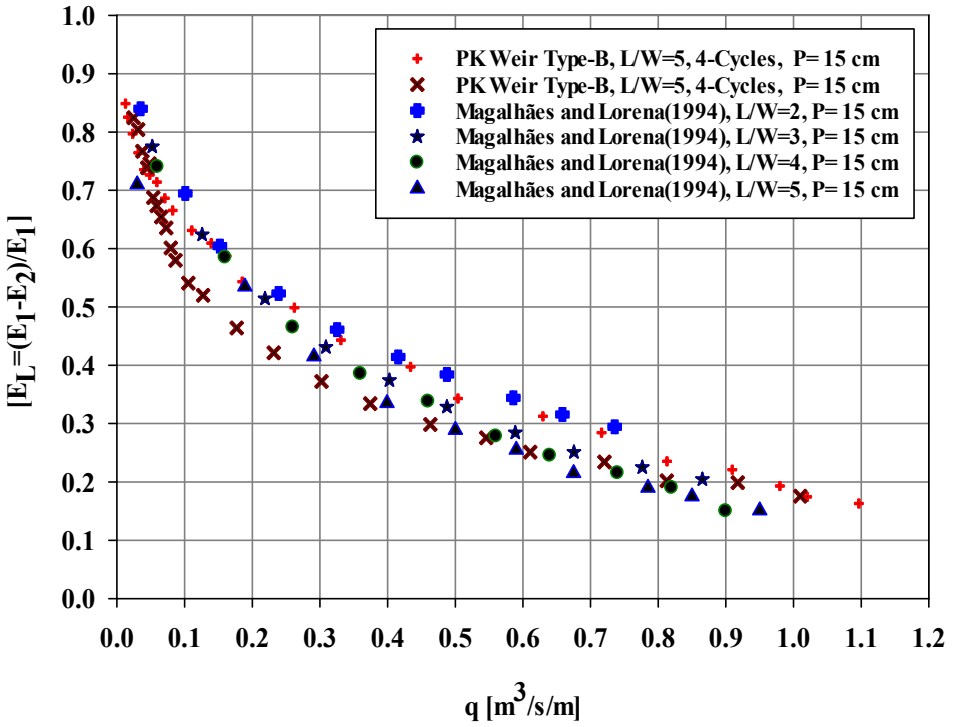

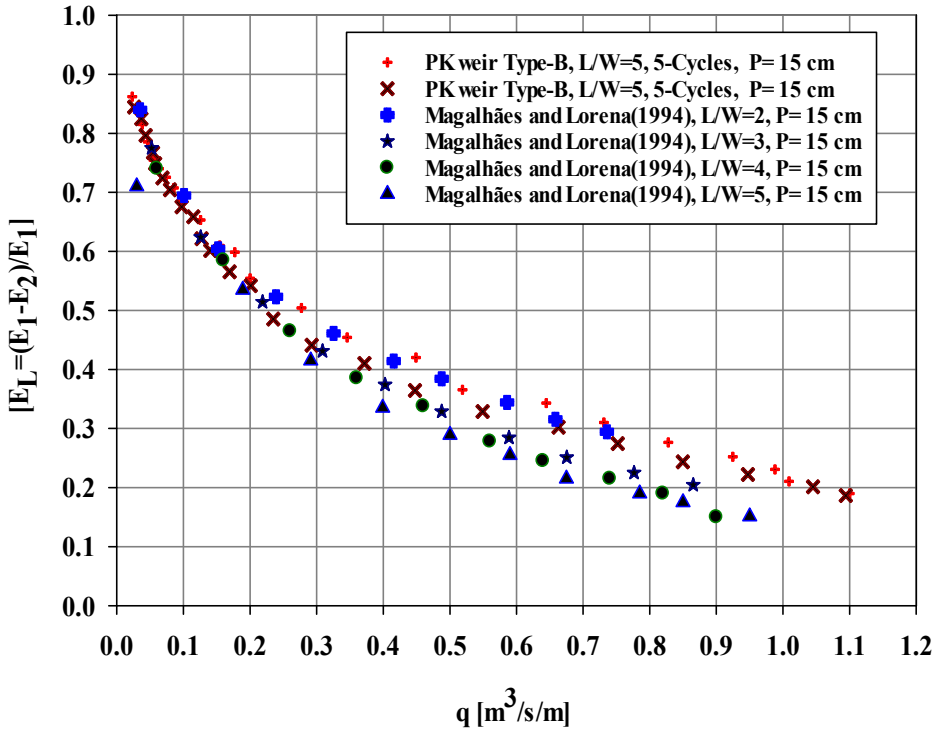

Figure: 4.23 (i) (Relative energy dissipation [$E_L=(E_1-E_2)/E_1$] with respect to (a) the head water ratio [H_1/P] and (b) the unit discharge [q] for [L/W=5, 6]

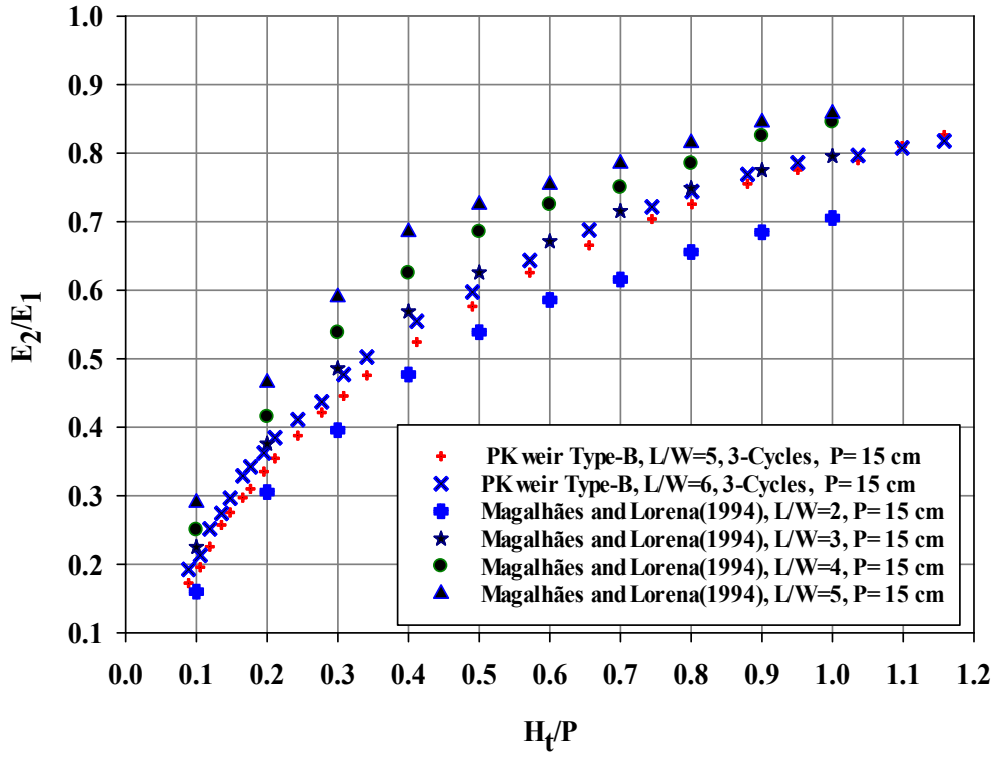
1.0
0.9
0.8
0.7
0.6
0.5
0.4
0.3
0.2
0.1
0.0
0.1
0.2
0.3
0.4
0.5
0.6
0.7
0.8
0.9
1.0
1.1
1.2
E2/E1
Ht/P
PK weir Type-B, L/W=5, 3-Cycles, P= 15 cm
PK weir Type-B, L/W=6, 3-Cycles, P= 15 cm
Magalhães and Lorena(1994), L/W=2, P= 15 cm
Magalhães and Lorena(1994), L/W=3, P= 15 cm
Magalhães and Lorena(1994), L/W=4, P= 15 cm
Magalhães and Lorena(1994), L/W=5, P= 15 cm

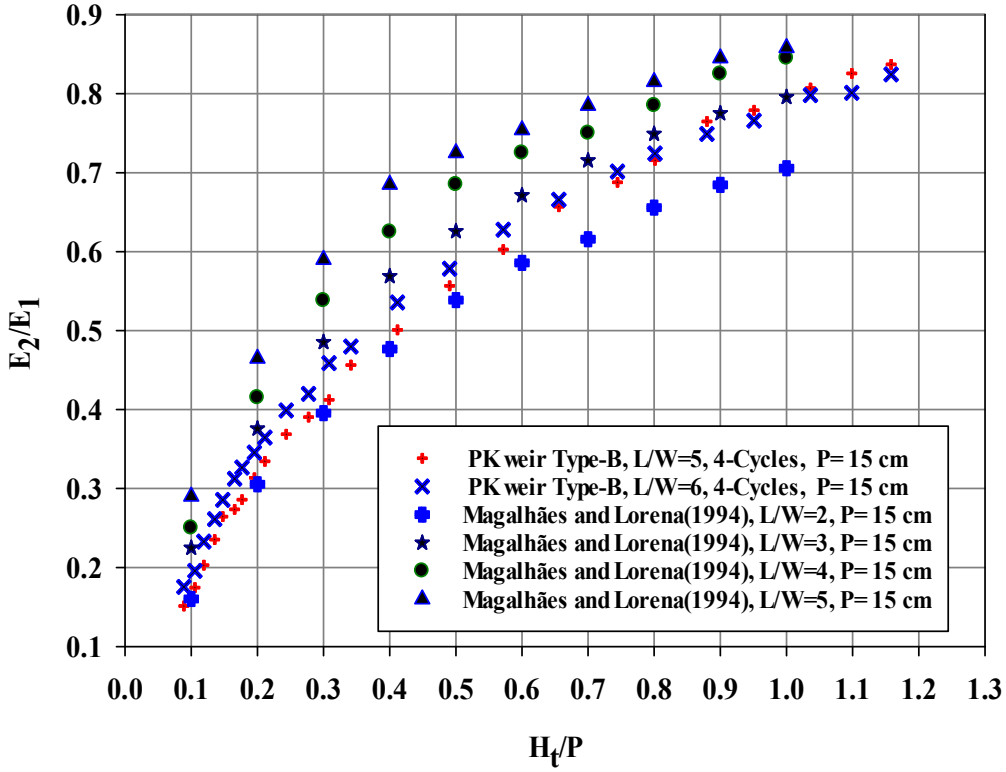
0.9
0.8
0.7
0.6
0.5
0.4
0.3
0.2
0.1
0.0
0.1
0.2
0.3
0.4
0.5
0.6
0.7
0.8
0.9
1.0
1.1
1.2
1.3
E2/E1
Ht/P
PK weir Type-B, L/W=5, 4-Cycles, P= 15 cm
PK weir Type-B, L/W=6, 4-Cycles, P= 15 cm
Magalhães and Lorena(1994), L/W=2, P= 15 cm
Magalhães and Lorena(1994), L/W=3, P= 15 cm
Magalhães and Lorena(1994), L/W=4, P= 15 cm
Magalhães and Lorena(1994), L/W=5, P= 15 cm

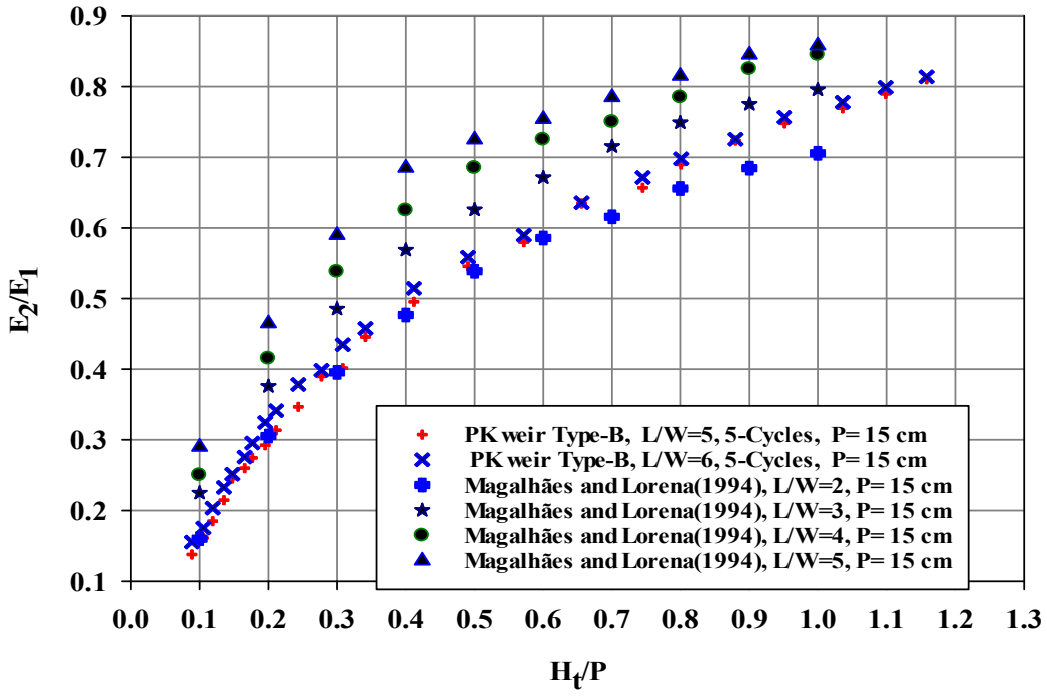
0.9
0.8
0.7
0.6
0.5
0.4
0.3
0.2
0.1
0.0 0.1 0.2 0.3 0.4 0.5 0.6 0.7 0.8 0.9 1.0 1.1 1.2 1.3
E2/E1
Ht/P
PK weir Type-B, L/W=5, 5-Cycles, P= 15 cm
PK weir Type-B, L/W=6, 5-Cycles, P= 15 cm
Magalhães and Lorena(1994), L/W=2, P= 15 cm
Magalhães and Lorena(1994), L/W=3, P= 15 cm
Magalhães and Lorena(1994), L/W=4, P= 15 cm
Magalhães and Lorena(1994), L/W=5, P= 15 cm

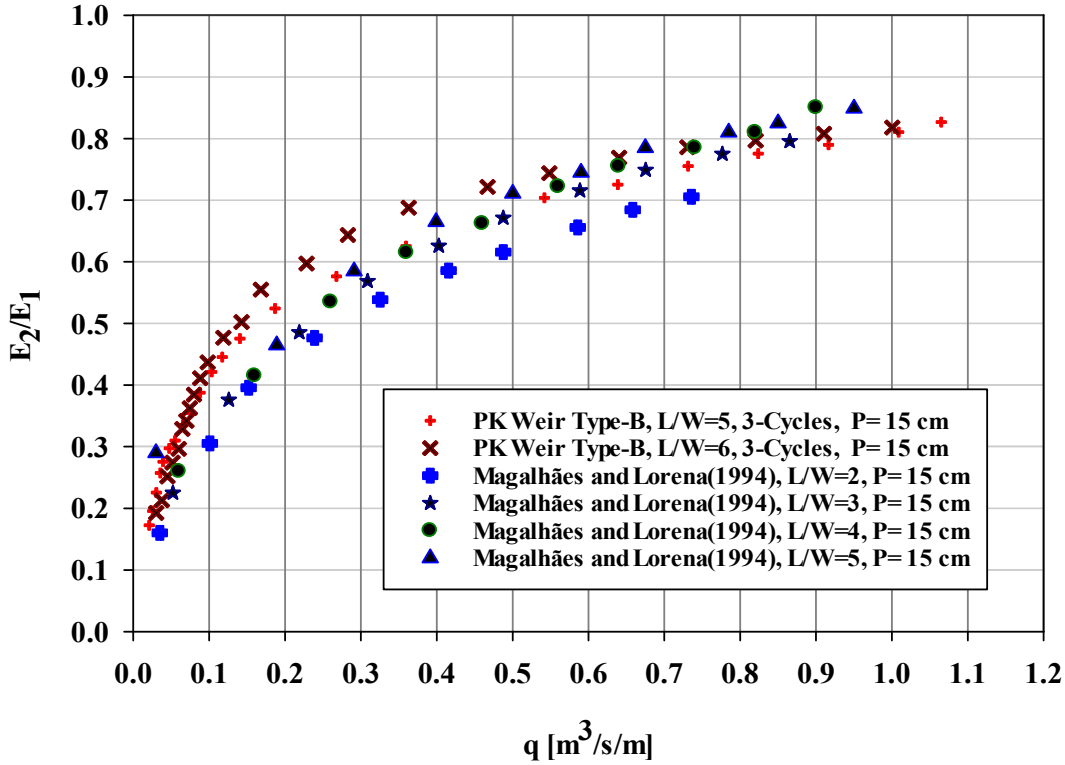
1.0
0.9
0.8
0.7
0.6
0.5
0.4
0.3
0.2
0.1
0.0
0.0 0.1 0.2 0.3 0.4 0.5 0.6 0.7 0.8 0.9 1.0 1.1 1.2
E2/E1
q [m3/s/m]
PK Weir Type-B, L/W=5, 3-Cycles, P= 15 cm
PK Weir Type-B, L/W=6, 3-Cycles, P= 15 cm
Magalhães and Lorena(1994), L/W=2, P= 15 cm
Magalhães and Lorena(1994), L/W=3, P= 15 cm
Magalhães and Lorena(1994), L/W=4, P= 15 cm
Magalhães and Lorena(1994), L/W=5, P= 15 cm

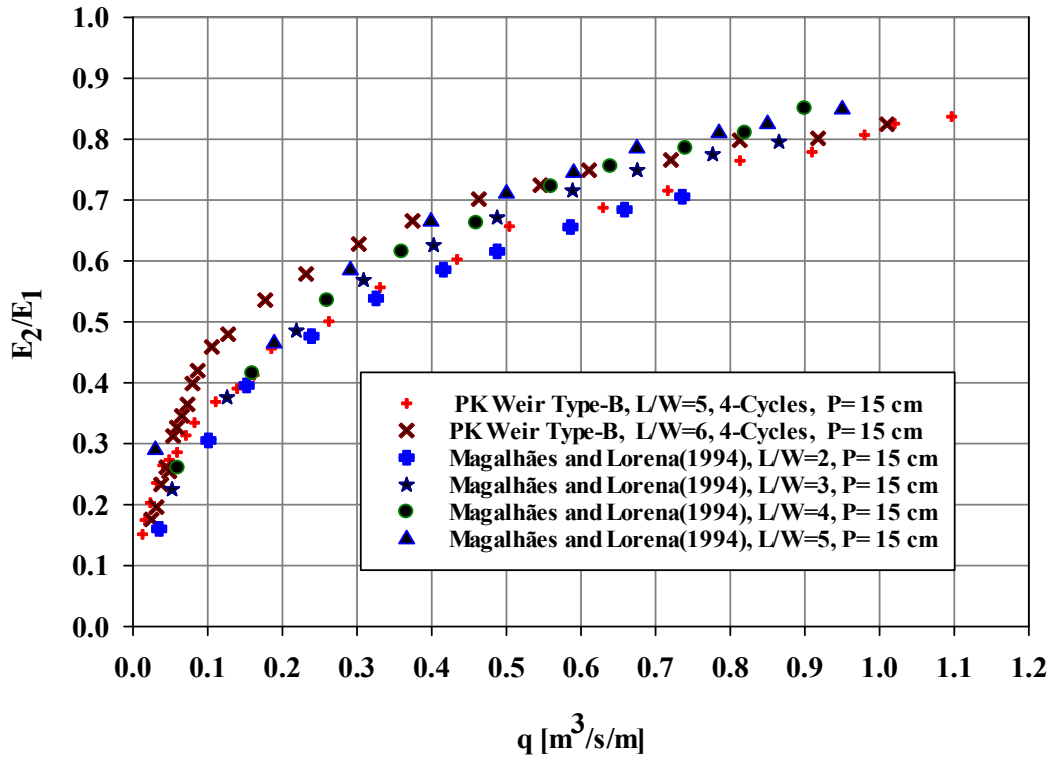

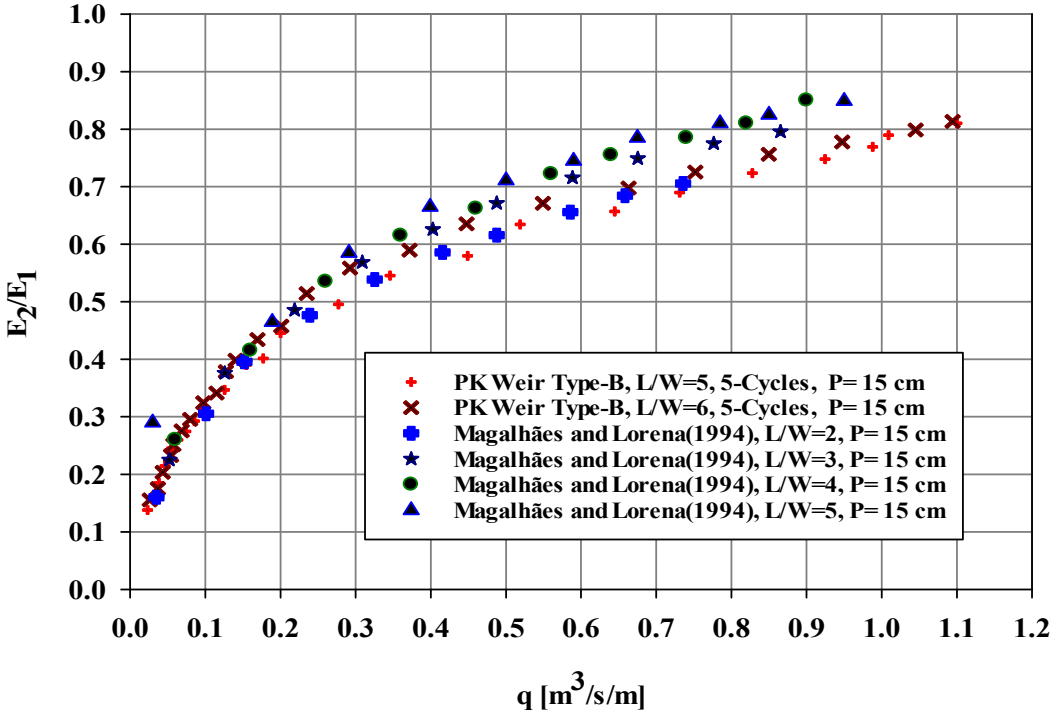

Figure: 4.23 (ii) (Relative residual energy [E_2/E_1] with respect to (a) the head water ratio [H_t/P] and (b) the unit discharge [q] for [L/W=5, 6]

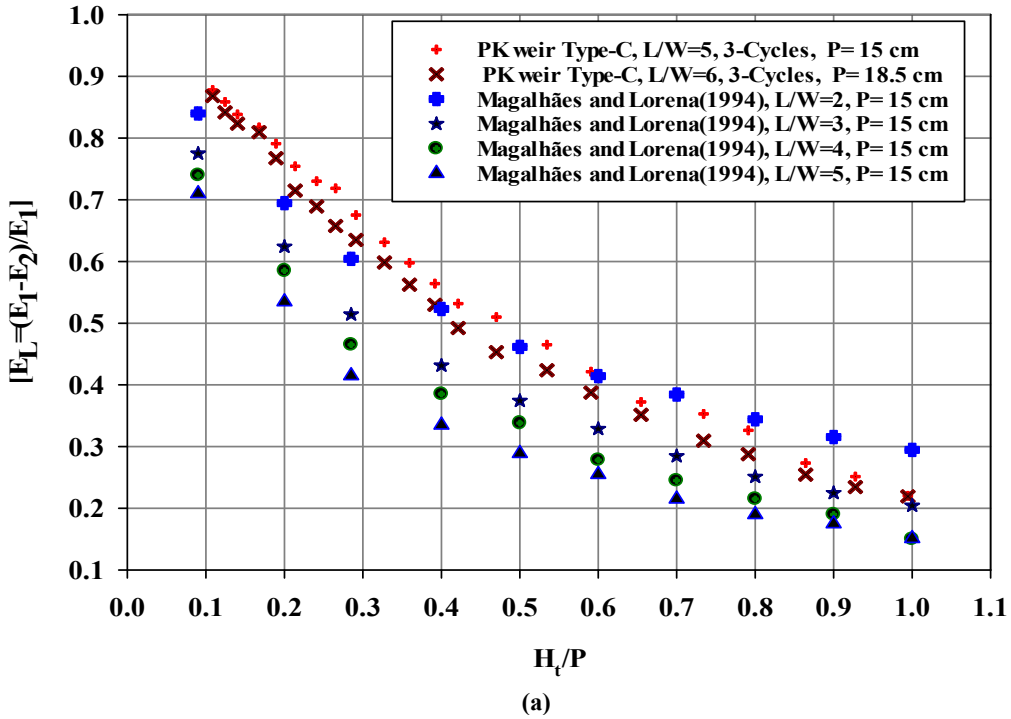

(a)

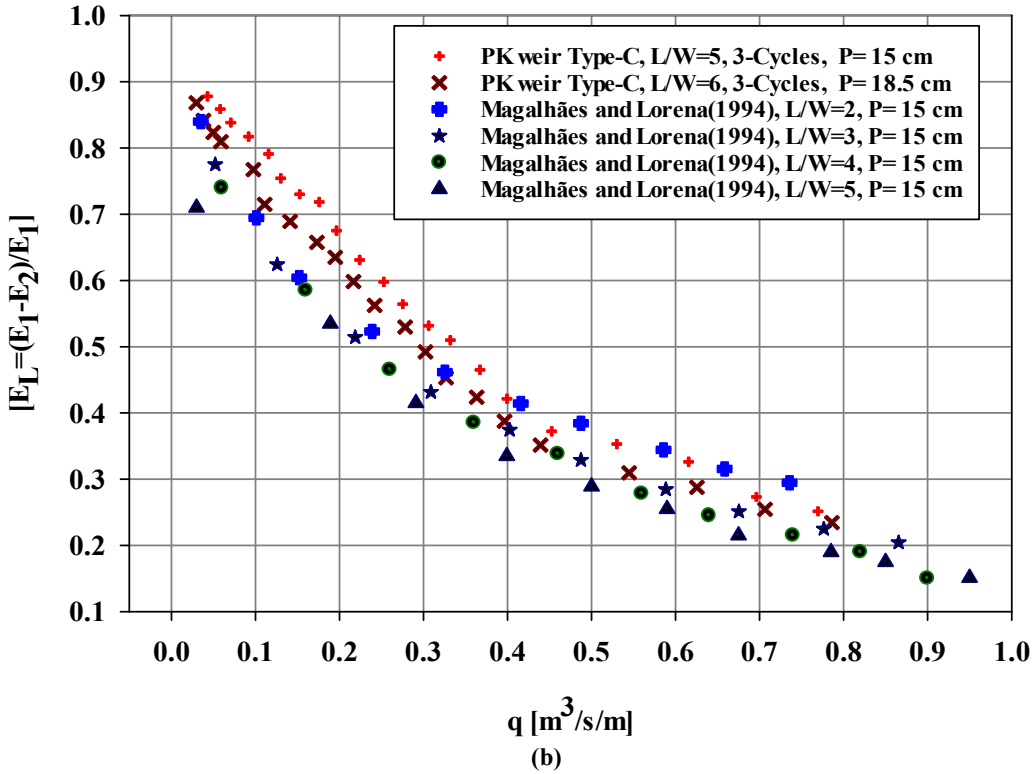

(b)

Figure: 4.24 (i) (Relative energy dissipation $[E_L=(E_1-E_2)/E_1]$ with respect to (a) the head water ratio $[H_t/P]$ and (b) the unit discharge [q] for [L/W=5, 6]

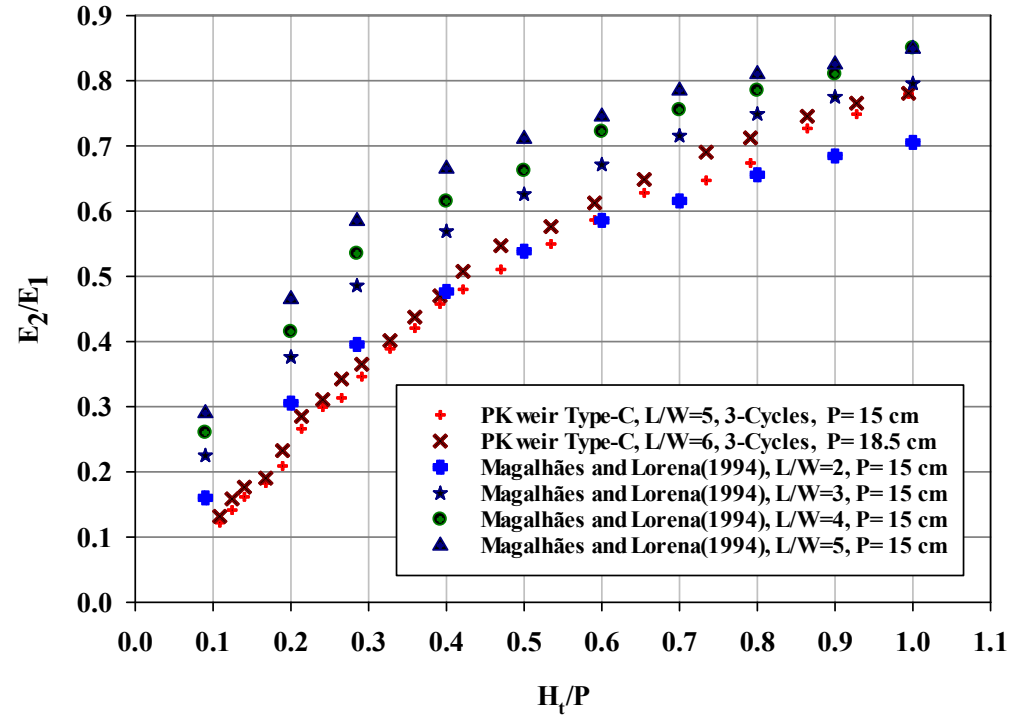

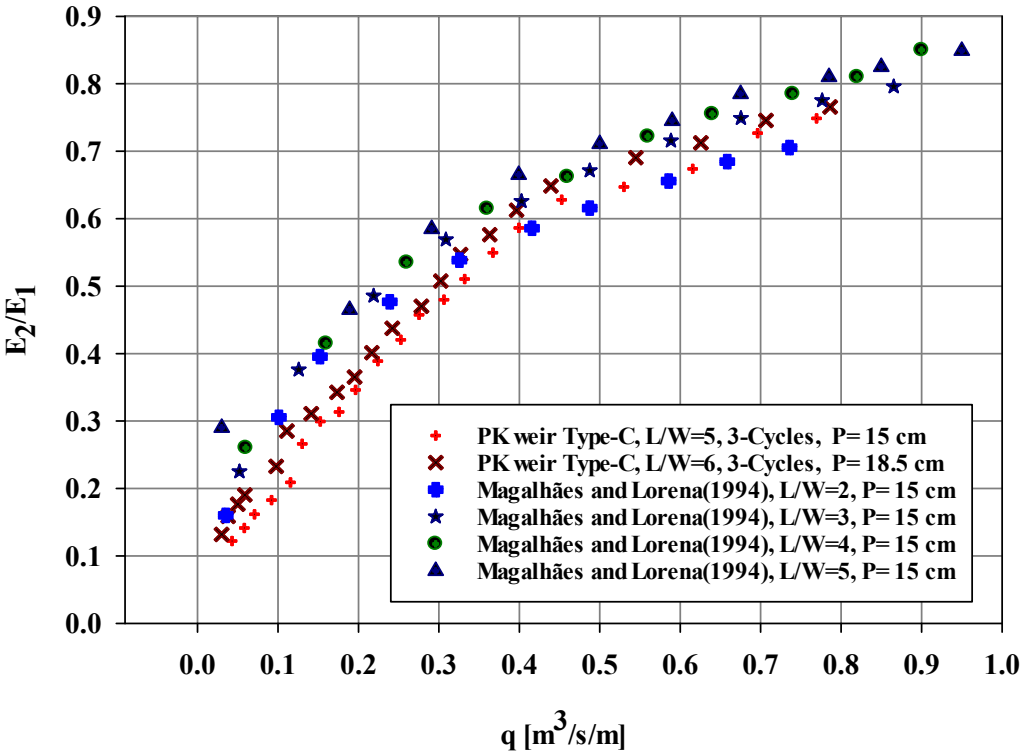

Figure: 4.24 (ii) (Relative residual energy [E_2/E_1] with respect to (a) the head water ratio [H_t/P] and (b) the unit discharge [q] for [L/W=5, 6]

Figures: 4.22, 4.23, and 4.24 depict that regardless of the magnification ratio (L/W), the relative energy dissipation [$E_L=(E_1-E_2)/E_1$]at the base of PKWs decreases with the relative total upstream head (H_t/P), especially for lesser values of the (H_t/P). The relative residual energy at the base of PKWs (E_2/E_1) increases with the magnification ratio (L/W), which was similar to **Magalhães and Lorena (1994).** According to the present study findings, type-A has 2-9 % more effective in dissipating energy than type B but 2-14% less effective than type C. As a result, type-C PKW is highly effective at dissipating energy, especially at low relative total upstream head (H_t/P) values, and the type-B PKW has the lowest efficiency.

Indeed, the L/W ratio demonstrates how effectively a design uses the available width W to maximize the crest length L. In order to maximize the crest discharge, the inlet cross-section must have a discharge capacity at each point that is at least equal to one of the downstream developed crest length sections. The outlet key is in charge of removing upstream streamwise flow and lateral overflow from the inlet key. The operation of the outlet determines the efficiency of a given PKW.

4.4.3 Effects of the relative width ratio(W_i/W_o) on energy dissipation

To provide additional insight and demonstrate the effects of different inlet-outlet key width ratios on energy dissipation. Following testing, the rating curves for each PKW were established, analyzed, and relative energy dissipations were compared. For comparison and reference, published data for trapezoidal labyrinth weirs (**Magalhães and Lorena, 1994)**; rectangular labyrinth weirs **(Merkel et al., 2018);** and PKW **(Eslinger and Crookston, 2020)** are included (**see Figure: 4.25 (i) & (ii))**. All the models showed very similar trends for relative energy dissipations, while their results were compared with previous studies within the accuracy of the measurement.

In this section of the present study, 10 PKW (5 type-A & 5 type-B) modes were tested and examined. The results indicate that all models relative energy dissipation patterns were almost identical. The energy dissipation rates for $H_t/P < 0.28$ (about for all type-A models) and $H_t/P < 0.27$ (approximate for all the type-B models) were found to be higher than in previously reported research (**see Figure: 4.25 (i) & (ii))**. The rate of relative energy dissipation was found to be lower when H_t/P was greater than 0.45 for type A and greater than 0.48 for type B, and the dissipation ($\Delta E/E_1$) rate between $0.28 \leq H_t/P \leq 0.45$ for type-A and $0.27 \leq H_t/P \leq 0.48$ for type-B were noticed intermixing in nature (**see Figure: 4.25 (i) & (ii)**).

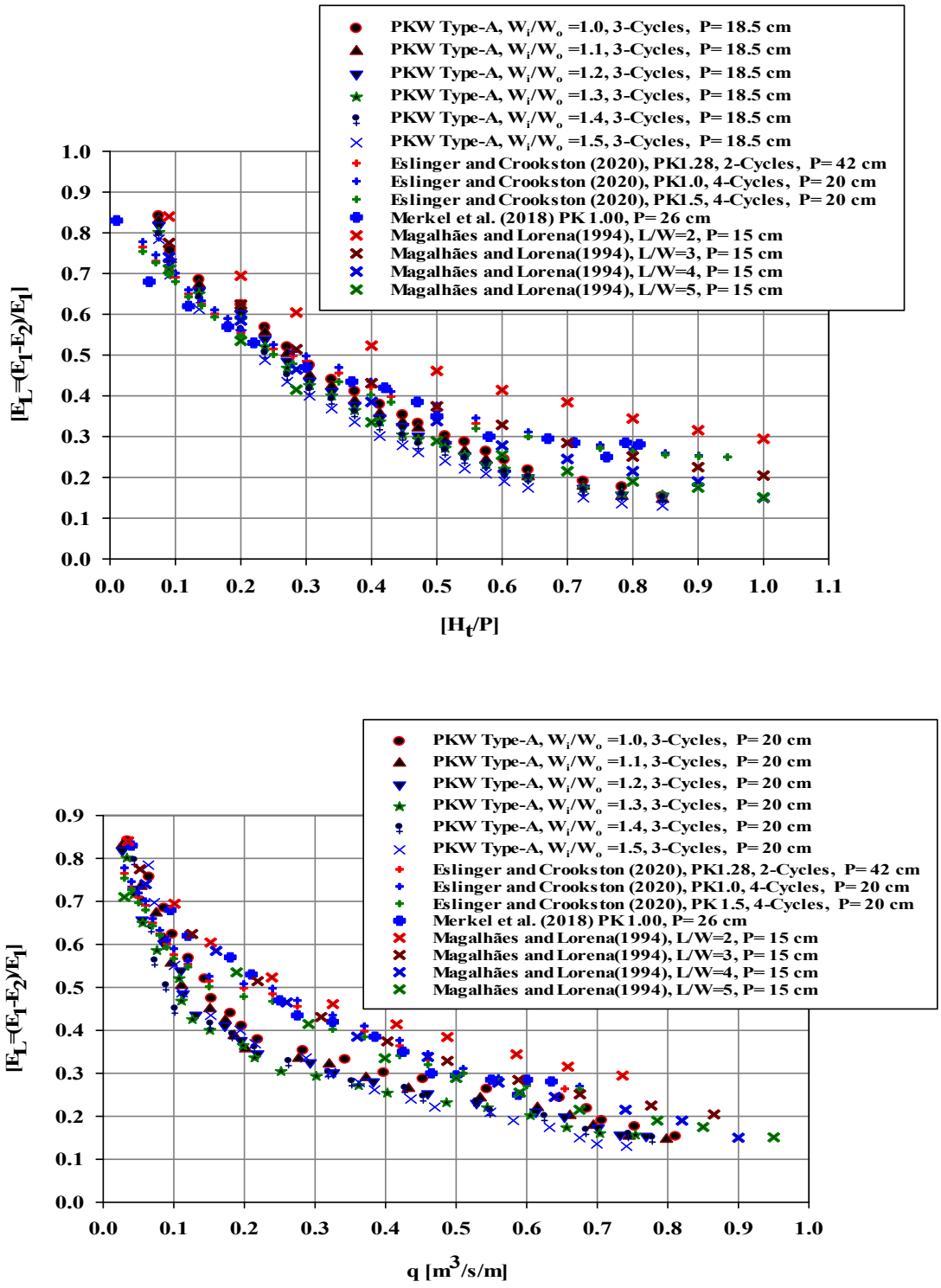

Figure: 4.25. (i) Relative energy dissipation [$E_L=(E_1-E_2)/E_1$] with respect to (a) the head water ratio [H_t/P] and (b) the unit discharge [q] for different W_i/W_o ratios for Type-A

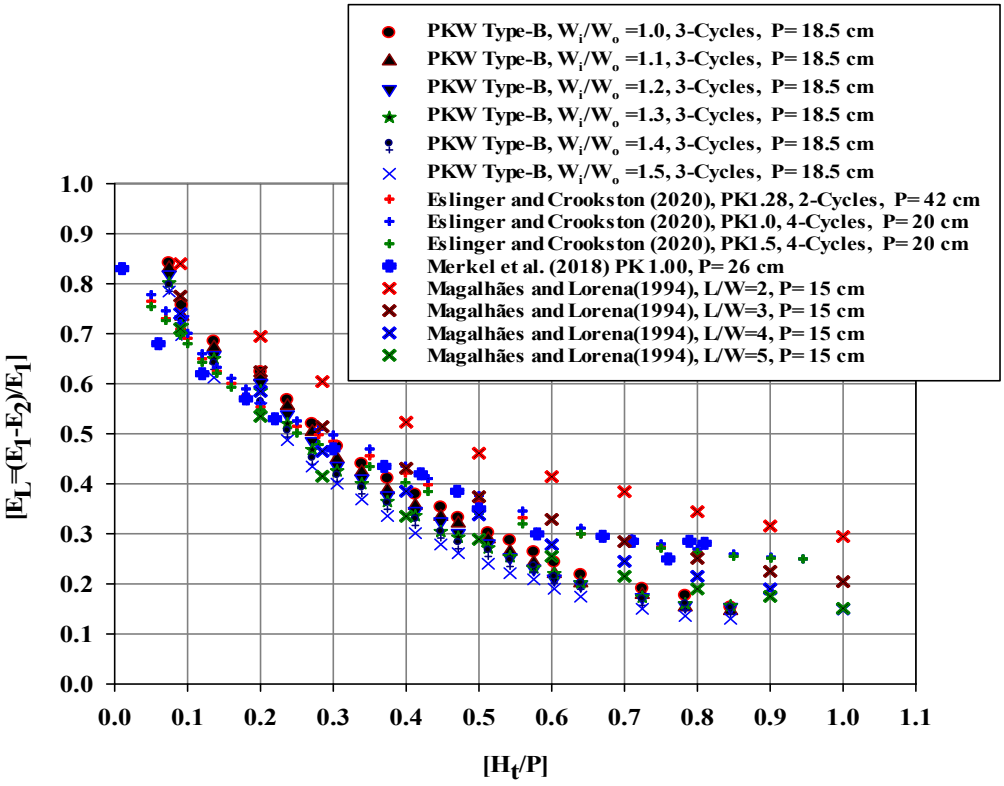

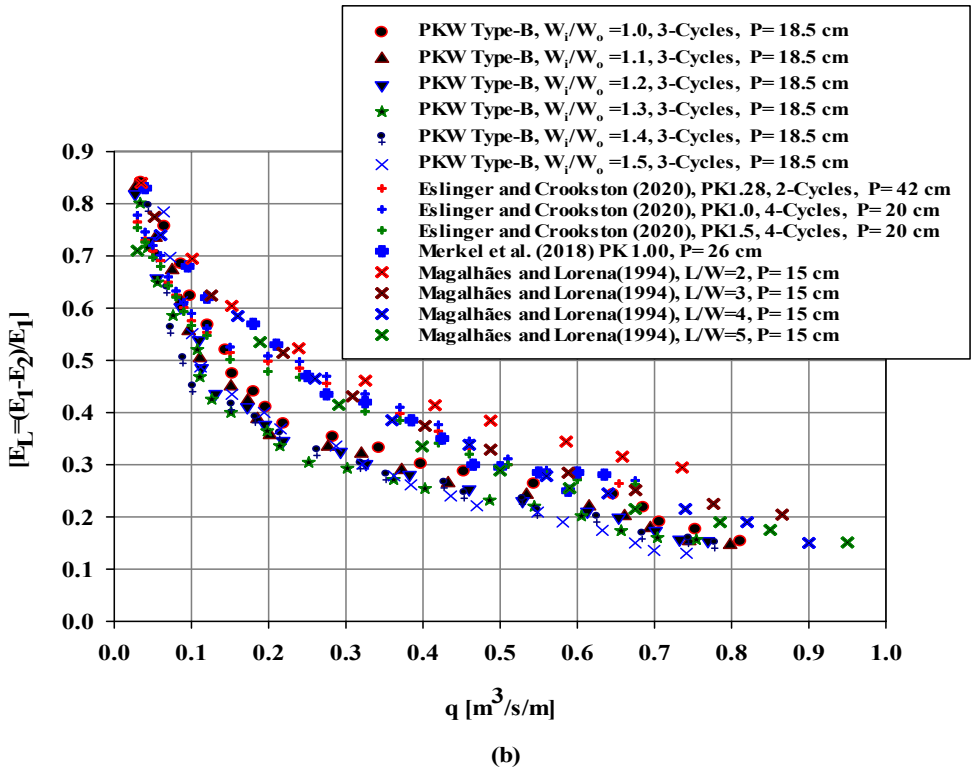

(b)

Figure: 4.25. (ii) Relative energy dissipation [$E_L=(E_1-E_2)/E_1$] with respect to (a) the head water ratio [H_t/P] and (b) the unit discharge [q] for different W_i/W_o ratios for Type-B

All types of PKW are less efficient at dissipating energy in higher heads, whereas all are the most effective at lower head levels. When $H_t/P < 0.18$ for type-A and 0.25 for type-B, even a little modification (in H_t/P) shows a noticeable variation in the energy dissipation. As H_t/P increases, the rate of ($\Delta E/E_1$) relative energy dissipation decreases steadily. At $H_t/P > 0.81$ for type-A and $H_t/P > 1.1$ for type-B results in constant relative energy dissipation, but between $0.18 \leq H_t/P \leq 0.81$ for type-A and $0.25 \leq H_t/P \leq 1.1$ for type-B, the relative energy dissipation rate ($\Delta E/E_1$) slowly reduces as H_t/P rises **(see Figure: 4.25 (i) and (ii))**. At low head levels or low discharges, the PKW dissipates energy more effectively; its relative dissipation decreases as it grows in head levels or discharges.This is because the energy is dissipated in the outlet key section for small discharges, and the nappes are aligned partially laterally and partially in the flow direction. The water level in the keys rises for higher discharges due to local submergence effects **(Crookston and Tulli, 2013)**, and the nappes are only aligned in the flow direction. As a result, energy dissipation decreases or remains nearly constant. This point concludes that the PKW represents the better relative energy dissipation efficiency at low discharges or low head level; an increasing the discharges or heads, its relative energy dissipation decreases gradually or sometimes rapidly.

Figures 4.25 (i) and (ii) show that the lowest value of W_i/W_o has the highest relative energy dissipation (i.e., $\Delta E/E_1$=.841 or 84.10 % for type-A, and 0.8313 or 83.13% of the type-B related W_i/W_o=1), and the highest value of W_i/W_o has the lowest energy loss ($\Delta E/E_1$=.784 and 78.40 percent for type-A and E_L= 0.772 or 77.20% for type-B related W_i/W_o=1.5). By increasing the W_i value, head losses caused by flow entering the inlet key are reduced, while the flow area is enhanced. A high W_i/W_o ratio in PKWs inlet keys optimizes flow approach and distribution, whereas a high W_i/W_o value in the outlet section promotes submergence influences. In the case of outlet sections, submergence effects may diminish the weir's discharge efficiency (areas where the weir crest height is higher than the flow depth in the outflow cycle).

4.4.4 Sensitivity Analysis

In this section, the sensitivity of the PKW has been assessed by constructing the steps at the outlet sections instead of the slanted floors (**See Figures: 4.26 (i) and (ii)**). The stepped spillway significantly dissipates the energy of passing flow and markedly reduces the occurrences of cavitation **(Chanson, 1994); (Parsaie et al., 2018)**. Hence, the current study has focused on the energy dissipation mechanism using the steps at the outlet key section of the PKWs.

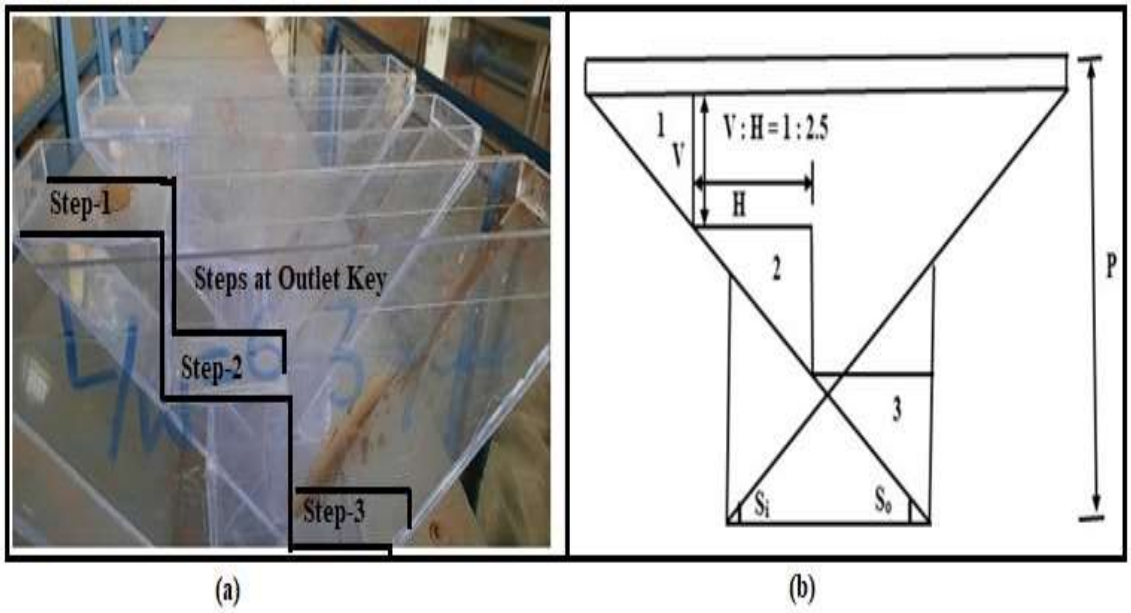

(i) Type-A

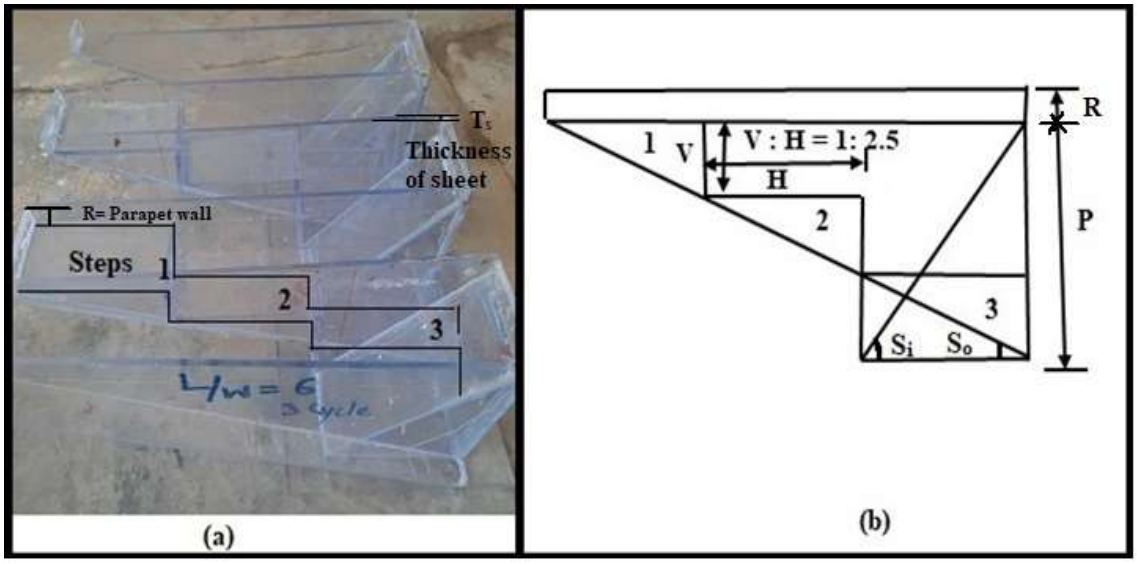

(ii) Type-B

Figure: 4.26 (i) & (ii) Type-A and Type-B PKW after using the steps at the outlet key, respectively (a) Laboratory model (b) Sectional view.

The flow configuration over stepped spillways can be classified into three types (napped flow, transition flow, and skimming flow) based on observation of the flow pattern **(see Figure: 4.27).** Napped flow condition occurs at low head/discharge values. In this condition, flow leaves the upper step and falls onto the lower stage **(Fen et al., 2016; Tobara et al., 2005; Chanson, 1996)**. During this condition, energy dissipation is caused by the

collision of a flow jet with steps and hydraulic jumps that may occur either entirely or partially.

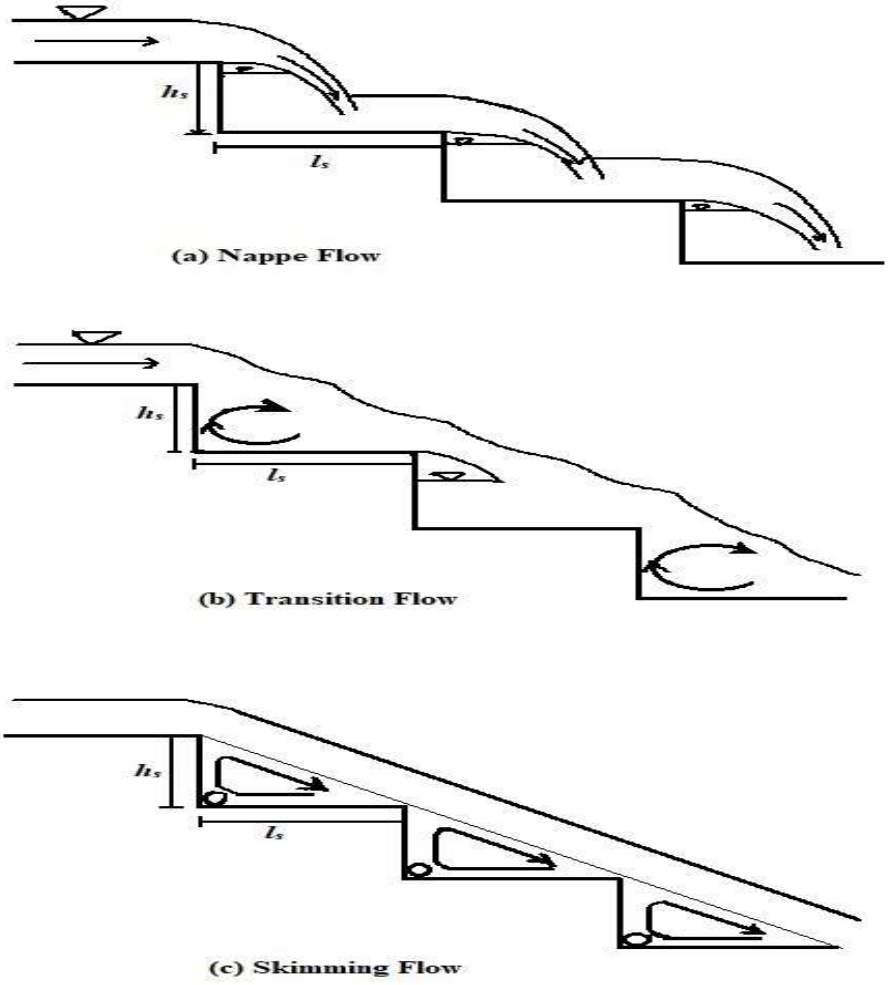

Figure: 4.27 Flow regimes above stepped weir: (a) Nappe Flow, (b) Transition Flow & (c) Skimming Flow

On the other hand, for large discharge values, a skimming flow condition occurs, and in this situation, a pseudo-bottom is created between steps and passing flow. In this case, a large amount of energy is dissipated in maintaining stable vortices beneath the pseudo-bottom formed by the external edges of the steps. The turbulent shear stresses between the skimming stream and the recirculating fluid strengthen the vortices **(Chanson, 1994)**. Notably, the turbulent kinetic energy dissipation above the steps must be precisely calculated, particularly for large discharges per unit width associated with the skimming flow regime. The high turbulence level and free-surface aeration characterize skimming flows **(Chanson and Toombes, 2002; Gonzalez and Chanson, 2008; Peyras et al., 1991; Rajaratnam, 1990)**. A transition regime is a condition between napped and skimming flow.

In order to determine the effect of the steps at the outlet key rather than on the sloping floor, four (2, type-A and 2, type-B) laboratory-scaled PKW models (with the specification L/W = 5, 3 cycles, P= 15 cm, and L/W = 6, 3 cycles, P = 15 cm) were modified using the three uniform steps (all with a slope of $1V$: $2.5H$) at outlet key, whereas all other geometric parameters were kept constant. The testing discharges were varied over the model between $0.05\ m^3/s \leq Q \leq 0.05\ m^3/s$.

To better understand the effect of steps at the outlet key, knowing the flow behavior over the PKW with or without steps is necessary. The steps significantly increase the energy dissipation rate along the face of the spillway and eliminate or significantly reduce the need for a large energy dissipator at the weir's toe **(Chanson, 1994)**. According to **Parsaie et al. (2018),** drop number, critical depth to the height of steps ratio, and Froude number are the most influential parameters on energy dissipation of flow over stepped spillways. The step's roughness also plays a vital role in energy dissipation over the stepped spillway by **Torabi et al. (2018).** According to the present study, energy dissipation rating curves followed the same pattern as the without using the steps at the outlet key but with steps showing higher energy dissipation. In the case of the stepped spillway, the chute slope and the size of the steps greatly influence the energy dissipation **(Parsaie and Haghiabi, 2019a, 2019b)**. A comparison of rating curves using steps at the outlet key and without using steps are shown in **Figures: 4.28 (i) and (ii).**

These results indicate a large proportion of the energy dissipated by water flowing over the steps at the outlet key rather than the sloping floor for all models. At a low head (H_t/P) ratio, the gain is approximately 5.60%-6.67% for type-A models, 5.67%, and 6.43 % for type-B models. In contrast, the decrease at a high H_t/P ratio is roughly 1.59 - 1.21 % for type-A and 2.05-1.67% for type-B, respectively (**see Figure: 4.28**). It partly may be the water flows down the steps as a coherent free stream at the low heads, skimming over the step edge's formed pseudo-bottom. The transmission of shear stress from the free stream maintains turbulent recirculation in the step cavities. The air at the free surface is constantly trapped and released. The water level in the outlet keys rises over the steps for higher heads or discharges due to local submergence effects. Consequently, a two-phase mixture interacts with flow turbulence, resulting in intricate air-water structures associated with complex energy dissipation mechanisms that reduce the energy dissipation capacity of the steeped weir.

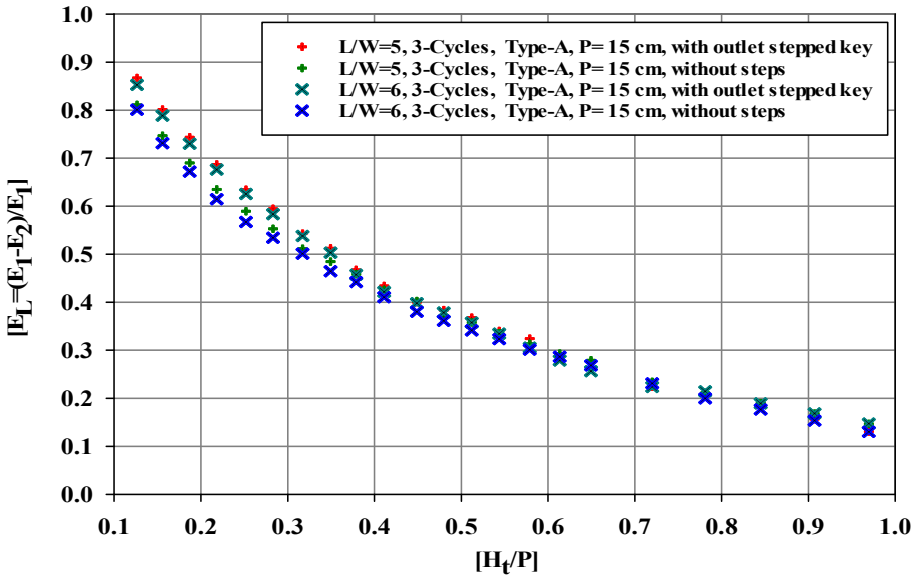

(a)

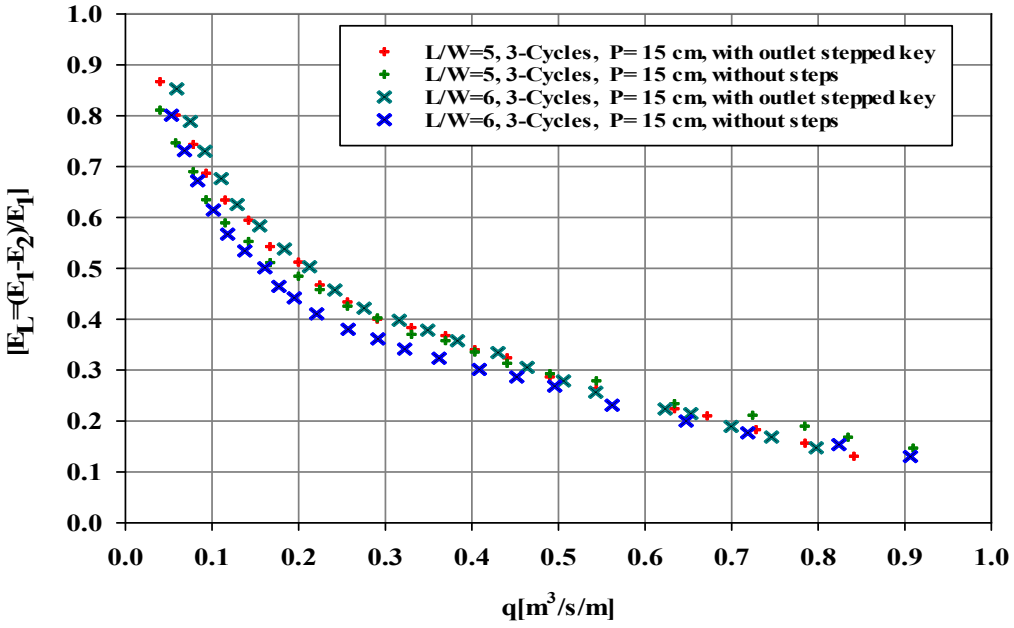

(b)

Figure: 4.28 (i) (Relative energy dissipation $[E_L=(E_1-E_2)/E_1]$ with respect to (a) the head water ratio $[H_t/P]$ and (b) the unit discharge [q] for type-A

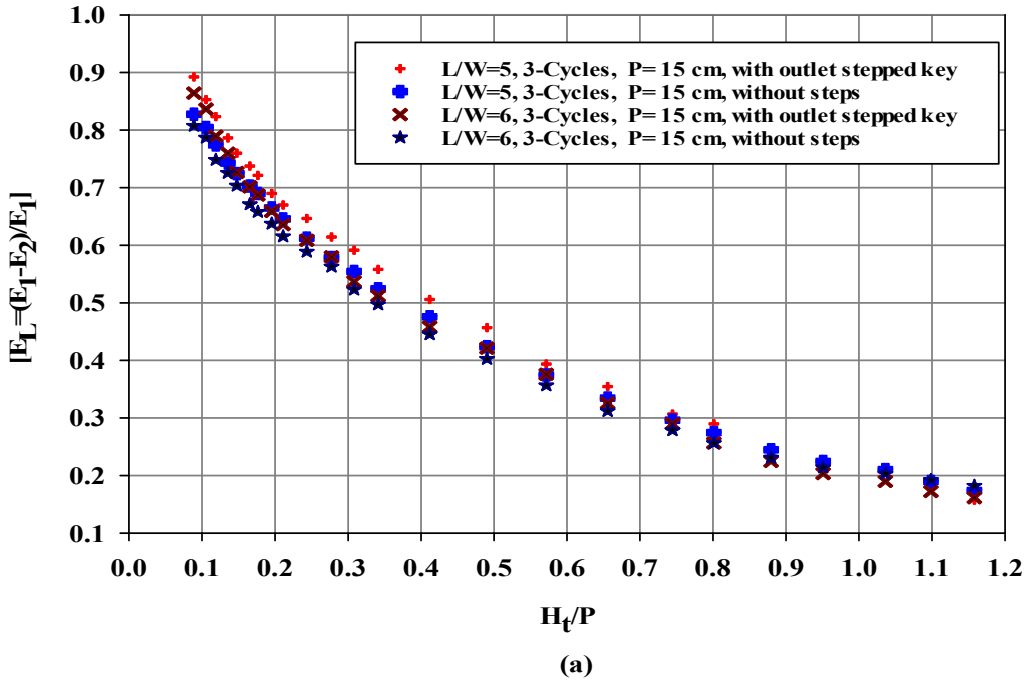

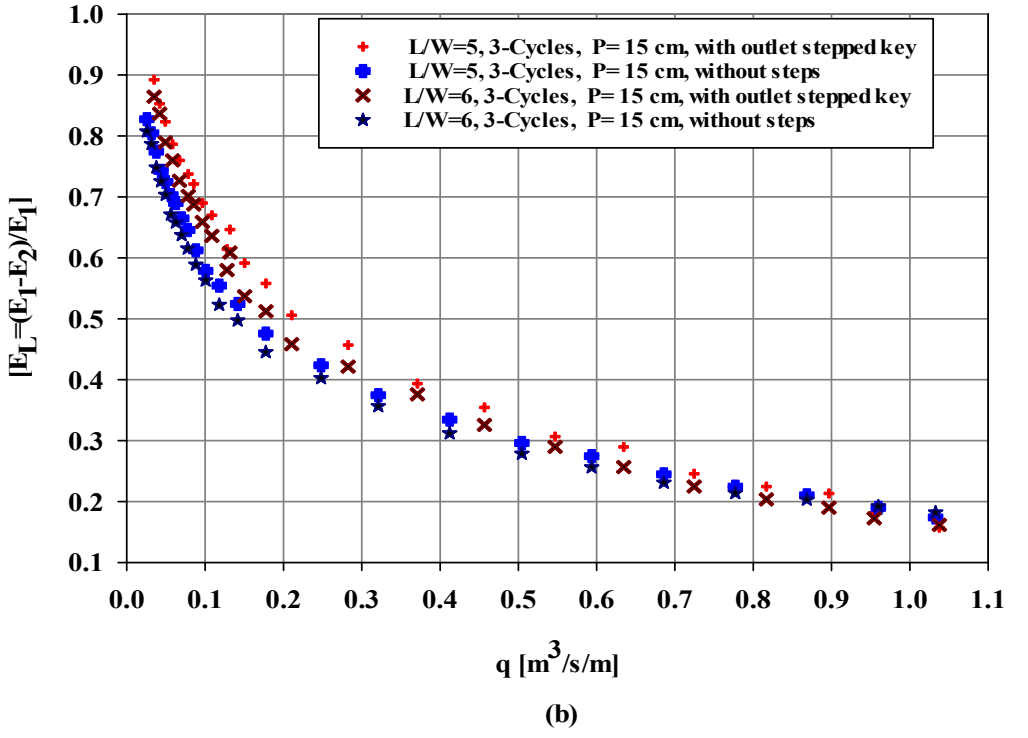

Figure: 4.28 (ii) (Relative energy dissipation $[E_L=(E_1-E_2)/E_1]$ with respect to (a) the head water ratio $[H_t/P]$ and (b) the unit discharge [q] for type-B

As a result, using the steps at the outlet key instead of the slanted floor increases the relative energy dissipation over the PKW for low head discharges while decreasing for higher

head discharges. It will help design energy-dissipative structures and reduce the downstream scour, the length of hydraulic jump and apron length for the weir, etc.

4.5 Aeration Capacity of the PKW

The main goal of this objective was to gather information on the aeration performance of the different types of PKW. To this end, three different laboratory-scale PKW models were built and tested to assess the aeration performance. The dissolved oxygen upstream and downstream of the PKWs was measured by DO meter, and the oxygen transfer rate/efficiency was assessed based on **Eqns. (3.27 to 3.30).** The experiments in this study were carried out or designed with the channel flow approach (i.e., experiments were carried out over PKW models in a laboratory flume); thus, this study's application consists primarily of PKWs set up at river barrages or as a control structure in a canal. The water jet from the test weir was directed into a downstream water pool, which was raised using a base/dam height mechanism (**see Figure: 4.29**). The depth in the downstream water pool was kept above the bubble penetration depth to ensure optimal aeration throughout the process. A calibrated "Thermo Scientific Orion Star A223 Dissolved Oxygen Portable Meter" was used to measure DO and temperature upstream and downstream of the PKW. The DO meter's calibration was calibrated using either water-saturated air or air calibration method, and calibration steps followed those recommended by the manufacturer. The calibration was carried out in humid air under ambient conditions. The flowing water over the weir was clean water. Each experiment was started by filling the storage tank with clean water.

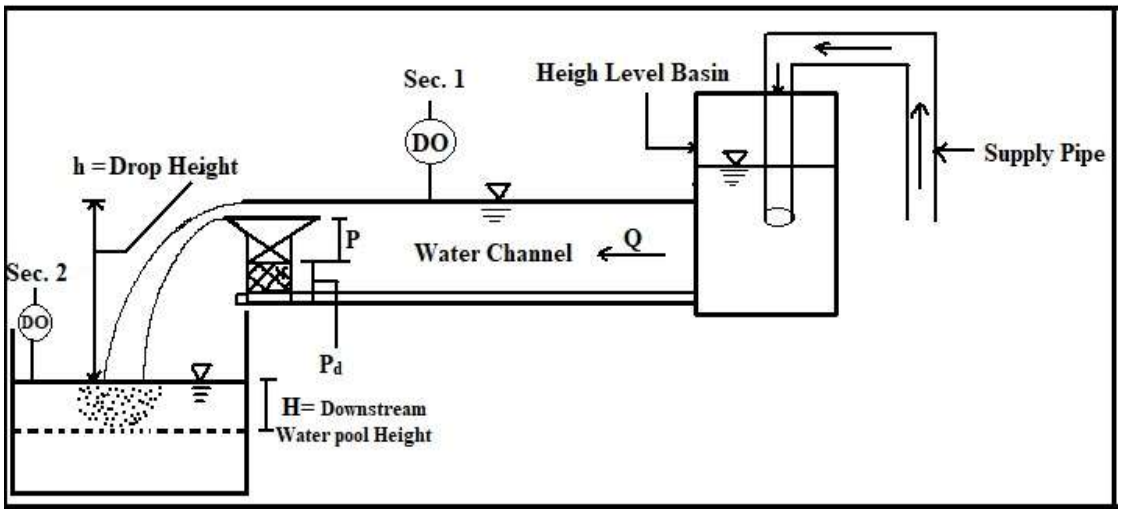

Figure: 4.29 Laboratory Schematic PKW Aeration Apparatus

The flow behaviour over the PKW is shown in **Figure: 4.30.** All three discharge parts interact, resulting in a complicated three-dimensional flow. With increasing head, water

spilled from the side crest enters the outlet key more readily, reducing hydraulic efficiency until the two discharging nappes clash and become one, resulting in the PKW assuming the characteristics of a linear weir. Water flowing over the crest of the sidewall revealed two nappes. In the first one, closer to the upstream side, there is no aeration. The second one is detached from the side crest and aerated, and the separation zone enhances as with discharge and moves downstream. **Figure: 4.30** shows that the flow across the PKW is immensely ventilated and three-dimensional, with splash and spray regions within the outlet keys and at the structure's bottom (**Singh and Kumar 2022c).**

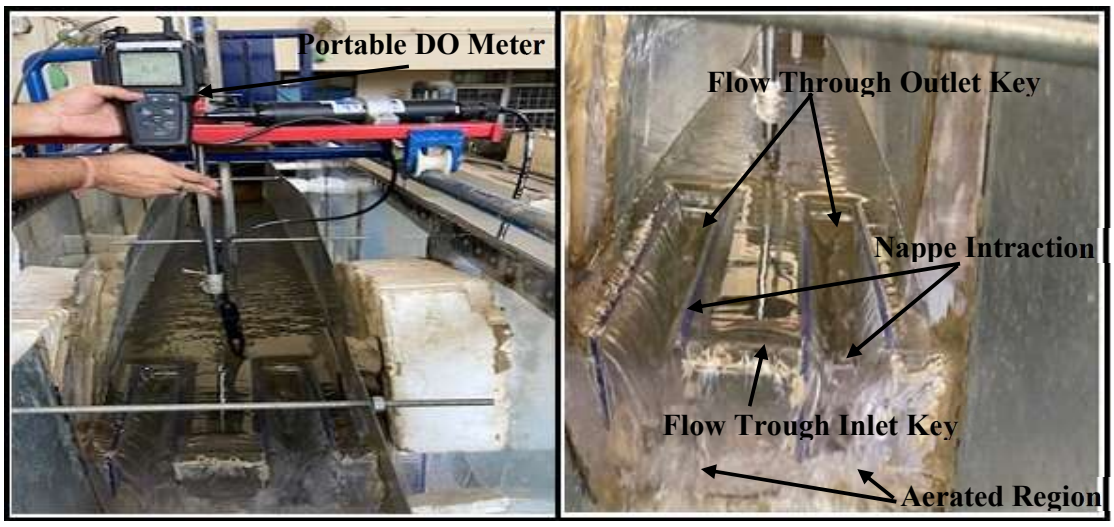

Figure: 4.30 Flow pattern over PKW.

As literature says, the aeration efficiency of the hydraulic structures depends on the flowing water temperature, water quality, tailwater depth, drop height, and water discharge. In the present study, it was seen that the drop height and discharge over the weir significantly affect the aeration efficiency of the weir. Greater time and longer path traveled by the air bubble in the downstream pool will increase the aeration efficiency. In order to achieve maximum aeration efficiency, **Avery and Novak (1978)** found that tailwater depth should equal 0.6 times drop height. Water quality is another crucial parameter affecting the aeration efficiency over the weir. If the water contains the active type of suspended solids, it will affect the aeration process. The dynamic suspended solids slow down the diffusion process and surface tension at the interface, affecting water's aeration. **Ervine and Elsawy (1975)** state the falling nappe's effects on the river aeration. In order to ensure optimal hydraulic performance while accounting for flow-induced vibrations, turbulence, noise, and flow surging **(Falvey, 1980)**.

In order to assess the aeration performance of different types of PKW, the testing model's configurations are as follows: the relative width ratio (W_i/W_o) is 1.28. The L/W ratio is 6, and the height of all models (P) is 20 cm. The inlet-outlet key slopes are 45^0 (S_i=S_o=1) for Type-A, S_i=1, & S_o=0.37 for Type-B, and S_i =1, & S_o =3.2 for Type-C. The two overhang portions are such that B_i=B_o, are alike for Type-A, whereas B_i=0, B_o= 2/3 B_b, for Type-B, and B_i=2/3 B_b, B_o=0, for Type-C. The testing discharges varied over the model between 0.003 $m^3/s \leq Q \leq 0.0155$ m^3/s on five different drop heights (20 cm, 25 cm, 30 cm, 35 cm, and 40 cm). The drop height is the difference between the water level upstream and downstream of the weir. (**see Figure: 4.29**). The data set collected in this study is shown in **Table: 4.10.**

Table: 4. 10 Ranges of data were collected for aeration performance of different types of PKWs.

Model Type	Range of Q (m^3/s)	$\frac{W_i}{W_o}$	W_i (m)	W_o (m)	P (m)	$\frac{L}{W}$	B (m)	B_i (m)	B_o (m)	Range of drop height h (m)	Range of Aeration efficiency (E_{20})	N (No. of cycles)
A	0.003-0.0155	1.28	0.088	0.069	0.2	6	0.43	0.142	0.142	0.20 -0.40	0.185-0.983	3
B	0.003-0.0155	1.28	0.088	0.069	0.2	6	0.43	0	0.285	0.20 -0.40	0.157-0.631	3
C	0.003-0.0155	1.28	0.088	0.069	0.2	6	0.43	0.285	0	0.20 -0.40	0.151-0.771	3

The experimental data results were documented and plotted for each PKW model with different characteristics (i.e., drop height and discharges). The results demonstrate that the aeration efficiency of PKW increases with the drop height but decreases with the flow rate over the weir.

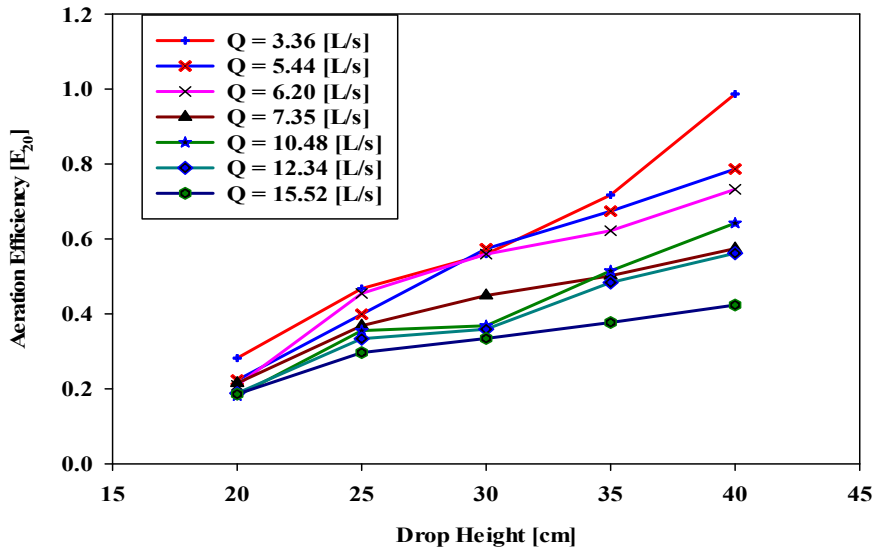

(a) Type-A

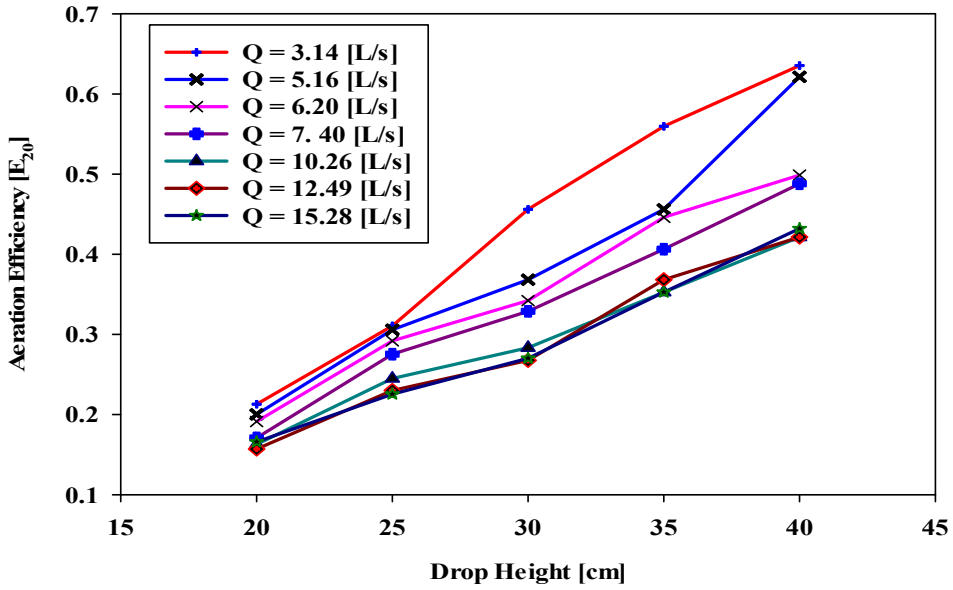

(b) Type-B

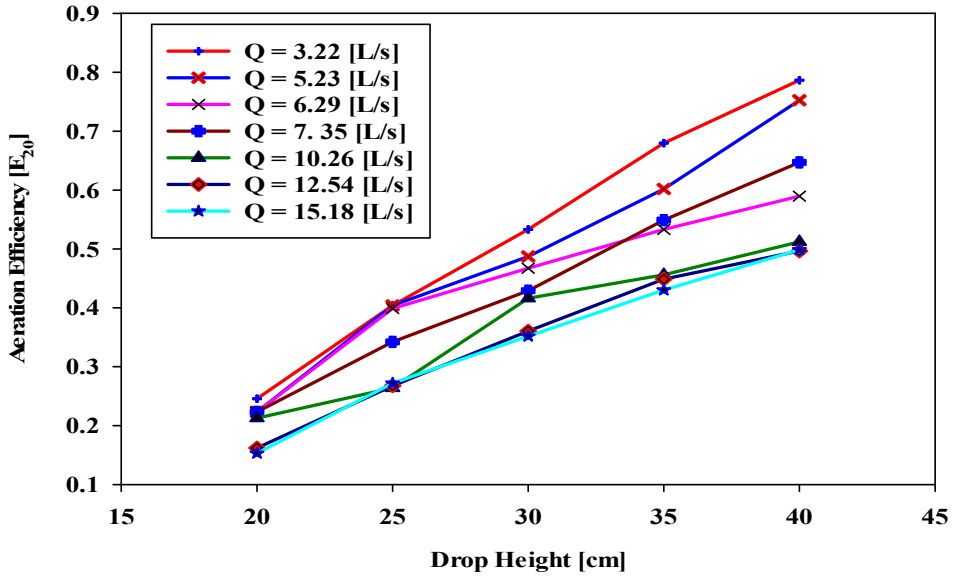

(c) Type-C

Figure: 4.31 Variation in Aeration Efficiency with Discharge and Drop height for (a)Type-A, (b) Type-B, and (c) Type-C Piano Key Weirs

Generally, a higher drop height may result in deep bubble insertion into the water pool and longer contact time, increasing the oxygen transfer rate. However, for the greater drop height, a collapse of the jet was observed. Because the jet eventually collides up into multiple droplets, the depth of bubble penetration and contact times decrease, enhancing the aeration efficiency. As discharge increases, bubble penetration and contact time in the downstream water pool decrease, reducing aeration efficiency. The results show that the type-B PKW

model yielded the lowest values of oxygen transfer efficiency. The maximum oxygen transfer efficiency of the type-B PKW model was 0.63, at a discharge of 0.00314 m^3/s and a fall height of 0.40 m. And the minimum aeration efficiency was observed at 0.15, corresponding to 0.0125 m^3/s discharge and fall height of 0.20 m. Thus the type-B PKW was found to be less effective as an aerator **(see Figure: 4.31 (b)).** The oxygen transfer efficiency values for the type-C PKW model were generally consistent with those for the type-A weir.

The greatest oxygen transfer efficiency of the type-C PKW model was 0.77, at a discharge of 0.0032 m^3/s and drop/fall height of 0.40 m, and the minimum aeration efficiency was observed at 0.151, corresponding to 0.0152 m^3/s flow rate and drop height of 0.20m **(see Figure: 4.31 (c))**.

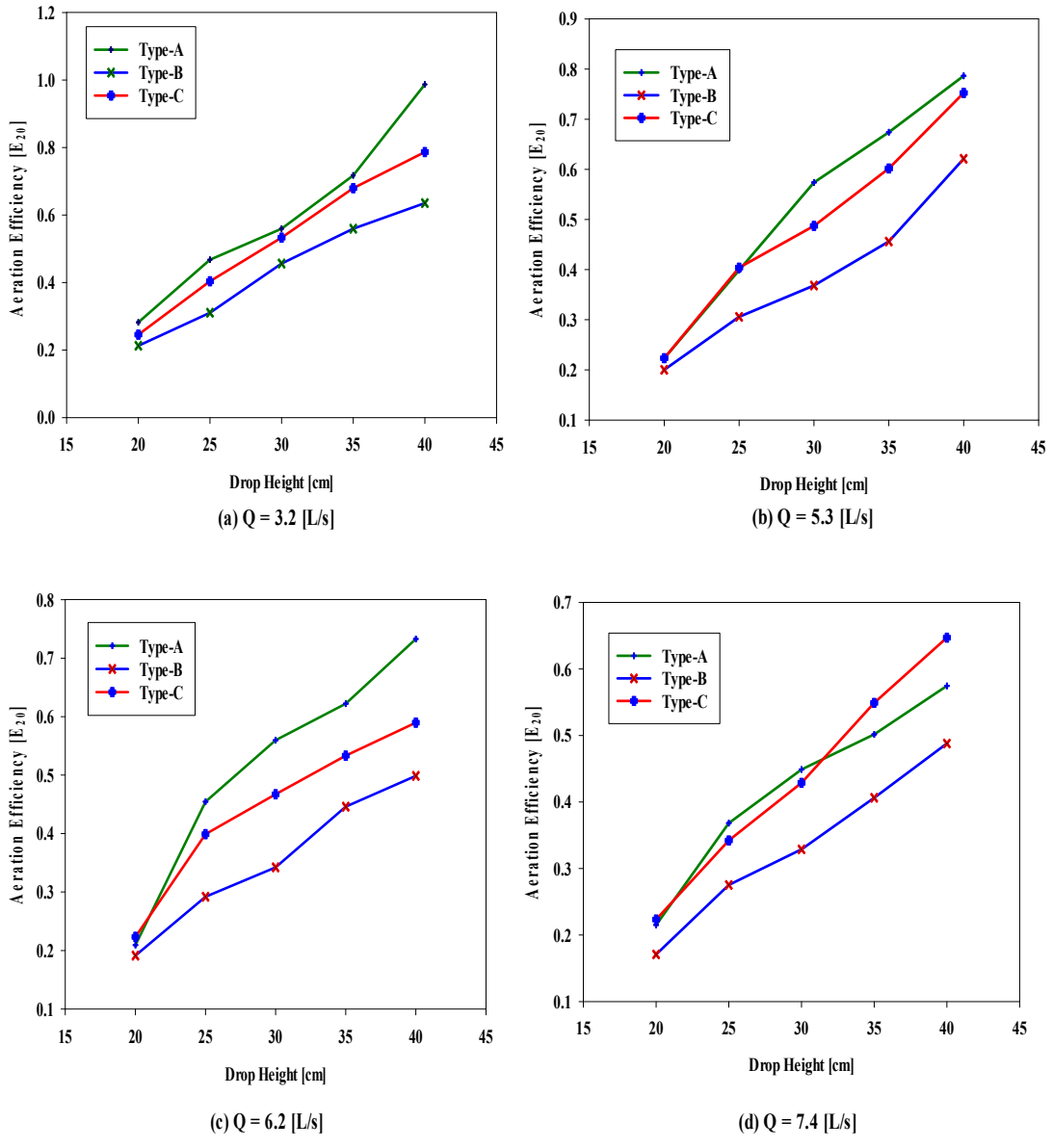

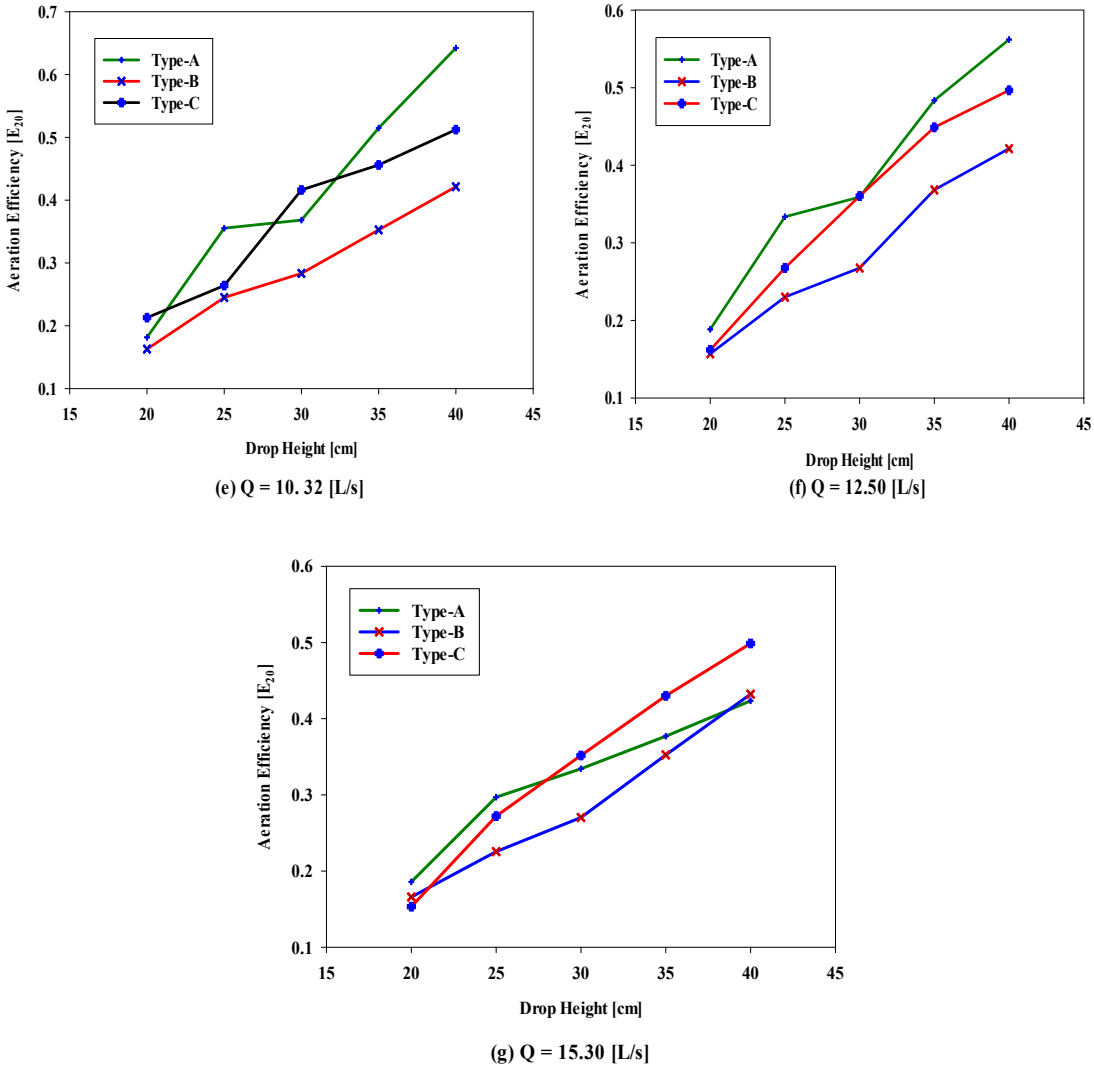

Figure: 4.32 Comparison of aeration efficiency curves of various PKWs models with drop heights

The oxygen transfer efficiency of the type-A PKW model was found to be most excellent. The maximum oxygen transfer efficiency of the type-A PKW model was 0.98, at a discharge of 0.0034 m^3/s and drop height of 0.40 m, and the minimum aeration efficiency was observed at 0.185, corresponding to 0.0155 m^3/s discharge and drop height of 0.20 m **(see Figure: 4.31 (a))**.

Figure: 4.32 shows the comparative aeration performances of different PKWs with different drop heights. From **Figure: 4.32**, it is clear that the aeration efficiency of all three models enhanced with the drop height but decreased with the increasing discharge. It concludes that the overall aeration performance of the type-B PKW is lesser than that of type-C. Type-A is more aeration performance than type-C for almost all the discharges.

The type-A PKW has shown a 22% - 28% higher aeration rate than the type-C at a drop height of 0.20 -0.40 m and a 23 to 56% higher aeration rate than type B at the same drop height. The type-A and type-C PKW models have downstream overhang portions of free jet formation. As a result of this free jet falling on the downstream pool of water, turbulent mixing and air entrainment occur, increasing oxygen transfer rates. In the downstream collection, more oxygen is transferred because the hydrostatic pressure on the air bubbles is greater. The overhangs of PKW were noticed to be a significant factor influencing aeration efficiency.

During the investigation, it was noticed that as the drop height increases, the aeration efficiency of all the weirs increases. However, increasing the discharge decrease the aeration efficiency of all weir shapes. A similar trend was observed by **Baylar and Bagatur (2000).** They presented the experimental results of aeration performance of different shapes of weirs, with flow rates Q varying from approximately 1.0 to 4.0 m^3/s. The drop height varied between 0.15 and 0.90 m. Therefore, the present experimental study herein shows good agreement with the published data.

4.6 Conclusion

The various parameters that affect the discharge carrying capacity of the multiple types of PKW are presented in this section. Furthermore, the energy dissipation across different types of PKW was investigated. The sensitivity of the type-A and type-B PKWs was then evaluated by building steps at the outlet key sections. Following that, the aeration performance of various PKW types was investigated. When comparing the various types of PKW, namely type-A, type-B, and type-C, the type-B PKW has the highest discharge carrying capacity but is the least effective in energy dissipation and has poor aeration performance. Type-C has the smallest discharge carrying capacity but the greatest energy dissipation. The type-A PKW has shown better energy dissipation and aeration performances than type-B but is less efficient in energy dissipation than type-C.

5.1 SUMMARY

Over the various dams and hydraulic structures, PKWs are the most cost-effective solution for rehabilitation and new dam construction. It has some advantages over the labyrinth and linear weir for the same crest length and width. PKW is less expensive than other rectilinear labyrinth weirs or nonlinear weir structures (i.e., small footprint, inclined key bottom slope, small reservoir level, high specific flood discharge). The basic concept of the flowing discharge over the PKW is that flow converges into the inlet key and diverges away from the outlet key. The total flowing discharge over the weir combines three discharges: discharge through the inlet keys, discharge through the outlet keys, and discharge through the side crest walls. All the three modes of the flow of discharges meet consequently in intricate and three-dimensional flow patterns in their vicinity. It acts in the same manner as a standard linear weir with a very long crest length at a low head, but at a slightly higher head, the additional velocity and longitudinal momentum of flow in the inlet key cause flow over the side crest to deviate from this normal vector.

The PKW is a complex structure involving many geometrical and hydraulic parameters that affect the hydraulic efficiency of the PKW. From the present study, the flow behavior of the PKW almost depends on the various dimensionless parameters (L/W, H_t/P, S_i/S_o, W_i/W_o, B_i/B_o ratios, parapet wall height, and the number of cycles (N)). And it was concluded that the discharge efficiency of the PKW increased or decreased with various geometrical variations. Further, the hydraulic performance of different types of PKW in energy dissipation and aeration performance was also assessed. It was found that type-C dissipates more energy than type-A & type-B, but type-A has a better aeration efficiency than type-B & type-C. However, type-B PKW has shown the most efficient PKW among the three.

Based on the results of this study, the following conclusions are made.

1. The magnification ratio (L/W) is the most significant parameter which directly influences PKW's discharge capacity. As the L/W ratio increases, the discharge carrying capacity of the PKW increases. Similar effects were observed by **Lempérière and Jun (2005), Machiels (2012), and Laugier *et al.* (2017).** For maximum discharge efficiency, the development crest length of the PKW should be several times the weir width. Indeed, this ratio demonstrates how effectively a design maximizes the crest length L by maximizing the available width W.

2. The weir height or inlet-outlet key's slope also plays a vital role in the discharge efficiency of the PKW and found that as the PKW sloped floors increase, the hydraulic efficiency of PKW increases to a certain slope then starts decreasing. In the present study, the PKW discharge efficiency increases at $H_t/P<0.24$ for all tested models, while decline trends were observed in almost all models at $H_t/P \geq 0.24$. However, the peak is ranged between $0.2 \leq H_t/P \leq 0.25$. The optimal range of the key slopes lies between 1 and 1.1 and shows better efficiency than the sharp-crested weir for all the tested model sets (i.e., $r \geq 1$ for each model). However, **Machiels et al. (2011c)** indicated that a further rise in the slope for a slope more than 1.2 (V: H) increases the slope and does not significantly change discharge efficiency.
3. Inlet and outlet key width ratio is another critical parameter that significantly influences the PKW's discharge efficiency. The optimal range of W_i/W_o for maximizing discharge efficiency is approximately 1.25 – 1.3, and the maximum efficiency observed corresponding to $W_i/W_o = 1.275 \approx 1.28$. This width ratio shows the 15% and 20 % higher efficiency than the $W_i/W_o = 1$ and $W_i/W_o = 1.5$. However, the result of maximum previous studies varies between ranges of 1-1.5 (**Anderson, 2011); (Anderson and Tullis, 2011); Machiels *et al.* (2011a)** and **Leite Ribeiro *et al.* (2012a)**. This is due to the balance of inlet cycle width to outlet cycle width concerning hydraulic capacity (ability to convey flow). As the inlet cycle width is increased, a reduction in energy loss as water enters the inlet keys, as well as an increase in inlet flow area, results in an increase in discharge capacity; but in consequence of the inlet key width increasing, the outlet key width is decreased (assuming $W_i + W_o$ = constant) resulting in an increase in local submergence of the outlet keys (particularly at the outlet key apexes) and a decrease in outlet key discharge capacity.
4. PKW overhangs result in a measurable increase in discharge efficiency relative. Type-B, PKW had shown maximum discharge efficiency from other PKW types. According to the present study findings, type-A has 5-13 % more effective than type C but 7-24% less effective than type B. However, **Cicero *et al.* (2016)** found that type-A is 15% more effective than type C but 5-15% less effective than type B. The PKW upstream overhang geometry increases the inlet flow area and wetter perimeter, reducing inlet velocities, flow contraction, and energy loss. This may explain, in part, why the PKW geometry Type-B (larger upstream overhangs) is

reported to have higher discharge efficiency than PKW geometry Type-A (smaller upstream overhangs). The PKW downstream overhang geometry results in a larger area and wetted perimeter in the outlet keys, resulting in a more efficient discharge outlet key exit.

5. The number of cycles or units represents the smallest extent of a complete structure and a critical parameter that enhances the energy dissipation over the PKW. As the number of cycles increases, the discharge efficiency decreases. For a specific channel width, total PKW length and discharge capacity/efficiency are maximized as the number of apexes and cycles is reduced. The maximum relative energy dissipation was observed in the present study corresponding to the highest cyclic count (i.e., $\Delta E/E_1$=.8831 or 88.31 percent for type-A and E_L= 0.8621 or 86.21% for type-B, which corresponds to L/W=5 and N=5). And the less energy dissipation for the lowest cyclic counts (i.e., E_L =.8210 and 82.10 % for type-A and E_L= .8077 or 80.77% for type-B, correspond to L/W=6, and N=3).
6. During the investigation, it was observed that as the L/W and W_i/W_o ratios increase, the energy dissipation at the base of the PKW shows a decreasing trend. But as the number of cycles increases, the energy dissipation downstream of the PKW increases. It means the discharge efficiency is inversely proportional to the energy dissipation.
7. The maximum relative energy dissipation was observed in the present study, corresponding to the lowest width ratio and the less energy dissipation for the highest width ratio. Increasing inlet key width reduces overall head losses due to the flow entering the inlet key. Increasing the inlet key flow area increases the flow carrying capacity of the key and reduces the energy dissipation over the weir. In comparison, Type-A has shown 2-9 % more effective in dissipating energy than type B but 2-14% less effective than type C. As a result, type-C PKW is highly effective at dissipating energy, especially at low relative total upstream head (H_t/P) values, and the type-B PKW has the lowest efficiency.
8. In comparing the labyrinth weir with different magnification ratios, all the types of PKW show a greater energy dissipation capacity than the labyrinth weir, except L/W = 2 of the trapezoidal labyrinth weirs **Magalhães and Lorena (1994)**, but it follows the same trend. This concludes that the energy dissipation over all the nonlinear types of weir (particularly for PKWs and labyrinth weirs) decreases as the magnification ratio increases.

9. The PKW has an excellent oxygen transfer efficiency than the linear one. The present study results demonstrate that the aeration efficiency of PKW increases with the drop height but decreases with the flow rate over the weir. Generally, a higher drop height may result in deep bubble insertion into the water pool and longer contact time, increasing the oxygen transfer rate. As discharge increases, bubble penetration and contact time in the downstream water pool decrease, reducing aeration efficiency.
10. The current study concludes that the overall aeration performance of the type-B PKW is the lowest; however, the Type-A PKW has the highest aeration performance for almost all discharges. The type-A PKW has shown a 22% - 28% higher aeration rate than the type-C at a drop height of 0.20 -0.40 m and a 23 to 56% higher aeration rate than type B at the same drop height.
11. The PKW has an excellent oxygen transfer efficiency than the linear one. The present study results demonstrate that the aeration efficiency of PKW increases with the drop height but decreases with the flow rate over the weir. Generally, a higher drop height may result in deep bubble insertion into the water pool and longer contact time, increasing the oxygen transfer rate. As discharge increases, bubble penetration and contact time in the downstream water pool decrease, reducing aeration efficiency. The current study concludes that the overall aeration performance of the type-B PKW is the lowest; however, the Type-A PKW has the highest aeration performance for almost all discharges. The type-A PKW has shown a 22% - 28% higher aeration rate than the type-C at a drop height of 0.20 - 0.40 m and a 23 to 56% higher aeration rate than type-B at the same drop height.

5.2 RECOMMENDATION FOR FURTHER WORK

In this study, we have tested the rectangular PKW; the different shapes of PKW may be further studied for the same parameters. The possible extension of this study could be to apply the economical design of various shapes of PKW for any rehabilitation and new dam construction, reservoir water storage, and increasing magnitudes of probable maximum storm events. The PKW has an excellent capability for energy dissipation across with or without using the steps at the outlet key instead of the slanting base, so additional research in this area is recommended to supplement the preliminary work. It can be constructed as an oxygen transfer structure to maintain and enhance the aeration performance of the stream/run of river cases.

LIST OF PUBLICATIONS

1. **Deepak Singh** and Munendra Kumar (2022) "Hydraulic Design and Analysis of Piano Key Weirs- A Review." *Arabian Journal for Science and Engineering,* https://doi.org/10.1007/s13369-021-06370-4 (***SCI-Expanded, Impact Factor-2.807)***
2. **Deepak Singh** and Munendra Kumar (2022) "Energy Dissipation of Flow Over the type-B Piano Key Weir." *Flow Measurement and Instrumentation.* https://doi.org/10.1016/j.flowmeasinst.2021.102109 (***SCI-Expanded, Impact Factor-2.420)***
3. **Deepak Singh** and Munendra Kumar (2022) "Study on Aeration performances of different types of Piano Key Weir." *Water supply, IWA Publishing.* https://doi.org/10.1016/j.flowmeasinst.2021.102109 (***SCI-Expanded, Impact Factor-1.768)***
4. **Deepak Singh** and Munendra Kumar (2022) "Gene expression programming for computing energy dissipation over type-B piano key weir." *Renewable Energy Focus.* https://doi.org/10.1016/j.flowmeasinst.2021.102109 (***ESCI- Impact Factor-4.081)***
5. **Deepak Singh** and Munendra Kumar (2022) "Computation of Energy Dissipation across the Type-A Piano Key Weir by using Gene Expression Programming technique."*Water supply, IWA Publishing.* https://doi.org/10.2166/ws.2022.255. (***SCI-Expanded, Impact Factor-1.768)***

LIST OF CONFERENCES

1. **Deepak Singh and** Munendra Kumar (2022). "Effects of Channel Bed Slope on Energy Dissipation of Different Types of Piano Key Weir." 110042(5), 142–147. **International Conference on "Water Resources Applications and Advances"** *organized by* **"World Academy of Science, Engineering and Technology**", Paris, France March, 2022.
2. **Deepak Singh** and Munendra Kumar (2020). "A Comparable Study on Aeration Performance of PK weir with its Alternatives." "Hydro-2020" **International Conference on Hydraulics, Water Resources, and Coastal Engineering**, organized by **NIT, NIT Rourkela on 26-28 March 2021.**

BOOK CHAPTER

1. Saurabh Sah, Munendra Kumar, **Deepak Singh** (2022). "Study of Flow Characteristic of Trapezoidal Labyrinth Weir." River Hydraulics. Water Science and Technology Library, vol 110. Springer, Cham. https://doi.org/10.1007/978-3-030-81768-8_20 (**Book Chapter**) **(Scopus).**

References

Abhash, A., and Pandey, K. K. (2020). "A review of Piano Key Weir as a superior alternative for dam rehabilitation A review of Piano Key Weir as a superior alternative for dam rehabilitation." *ISH Journal of Hydraulic Engineering*, Taylor & Francis, 00(00), 1–11.

Akbari, M., Salmasi, F., Arvanaghi, H., Karbasi, M., and Farsadizadeh, D. (2019). "Application of Gaussian Process Regression Model to Predict Discharge Coefficient of Gated Piano Key Weir." *Water Resources Management*, Water Resources Management, 33(11), 3929–3947.

Al-Hashimi, S. A. M., Madhloom, H. M., Nahi, T. N., and Al-Ansari, N. (2016). "Channel Slope Effect on Energy Dissipation of Flow over Broad Crested Weirs." *Engineering*, 08(12), 837–851.

Alizadeh Sanami, F., Saneie, M., and Afshar, M. H. (2021). "Experimental Study of the Hydraulic Performance of D-Type Triangular Piano Key Weirs." *International Journal of Civil Engineering*, Springer International Publishing, 19(10), 1209–1220.

Ali, M. S. and Mansoor, T. (2015). "Performance evaluation of piano key weir." "Hydro-2015" 20th international conference on hydraulics, water resources and river engineering. IIT Roorkee, India.

Al-Baghdadi Mohd. B (2019). "2D Visualization of flow phenomenon over individual inlet and outlet keys of piano key weir by CFD modeling." International Journal of Energy and Environment Volume 10, Issue 1, 2019 pp.15-24.

Anderson, R. M. (2011). "Piano Key Weir Head Discharge Relationships." All Graduate Theses and Dissertations, Paper 880, Utah State University.

Anderson, R. M. and Tullis B. P. (2011). "Influence of Piano Key Weir Geometry on Discharge." Proc. International Workshop on Labyrinth and Piano Key Weirs, Liège, Belgium.

Anderson, R.M. and Tullis, B.P. (2012). "Comparison of Piano Key and Rectangular Labyrinth Weir Hydraulics." J. Hydraulic Eng. ASCE, 138, 358-361

Anderson, R.M. and Tullis, B.P. (2012a). "Piano Key Weir: Reservoir versus Channel

Application." *J. Irrig. Drain Eng., ASCE, 138(8): 773-776.*

Anderson RM and Tullis B.P. (2013). "Piano Key Weir hydraulics and labyrinth weir comparison." Journal of Irrigation and Drainage Engineering, ASCE, 139(3), pp.246–253.

Avery, S., and Novak, P., (1978) "Oxygen Transfer at Hydraulic Structures." *Journal of Hydraulic Engineering, ASCE, Vol. 104, HY11, pp. 1521-1540.*

Azamathulla, H. M., Ahmad, Z., and Ab. Ghani, A. (2013). "An expert system for predicting Manning's roughness coefficient in open channels by using gene expression programming." *Neural Computing and Applications*, 23(5), 1343–1349.

Azamathulla, H. M., Rathnayake, U., and Shatnawi, A. (2018). "Gene expression programming and artificial neural network to estimate atmospheric temperature in Tabuk, Saudi Arabia." *Applied Water Science*, Springer International Publishing, 8(6), 1–7.

Bashiri, H., Dewals, B., Pirotton, M., Archambeau, P., and Erpicum, S. (2016). "Towards a new design equation for Piano Key weirs discharge capacity." *6th International Symposium on Hydraulic Structures: Hydraulic Structures and Water System Management, ISHS 2016*, 3310628160, 40–49.

Barcouda, M., Cazaillet, O., Cochet, P., Jones, B. A., Lacroix, S., Laugier, F., Odeyer, C., Vingny, J. P., (2006). "Cost-Effective Increase in Storage and Safety of Most Dams Using Fuse gates or PK Weirs." Proc. of the 22nd Congress of ICOLD., Barcelona, Spain.

Baylar A, and Bagatur, T. (2000). "Study of aeration efficiency at weirs." *Turk J. Eng Environ Sci 24(4):255–264*

Bekheet, A. A., AboulAtta, N. M., Saad, N. Y., and El-Molla, D. A. (2022). "Effect of the shape and type of piano key weirs on the flow efficiency." *Ain Shams Engineering Journal*, THE AUTHORS, 13(3).

Bieri M., Federspiel M., Boillat J., Houdant B. and Delorme F. (2009). "Spillway capacity upgrade of Gloriettes Dam: Environmental integration and energy dissipation." in

Proceedings of HYDRO 2009, Lyon, France.

Blanc P. and Lemperiere F. (2001). “Labyrinth spillways have a promising future.” *International Journal of Hydropower and Dams 8 (4), 129-131*.

Blancher, B., Montarros, F. and Laugier, F. (2011). “Hydraulic Comparison between Piano Key Weirs and Labyrinth Spillways.” Proceedings of the International Conference on Labyrinth and Piano Key Weirs (PKW 2011), pp. 141–150. CRC Press, Taylor & Francis Group.

Bremer, F. L., and Oertel, M. (2018). “Numerical uncertainty of piano key weir discharge coefficient estimations by means of 3D CFD modeling - A preliminary study.” *7th IAHR International Symposium on Hydraulic Structures, ISHS 2018*, 482–488.

Carollo, F. G., and Pampalone, V. (2021). “Testing the Stage-Discharge Relationship in Sloping SMBF Flumes.” *Journal of Irrigation and Drainage Engineering*, 147(5), 04021010.

Chanson, H. (1994). “Hydraulics of nappe flow regime above stepped chutes and spillways.” *Transactions of the Institution of Engineers, Australia. Civil engineering*, 36(1), 69–76.

Chanson, H. (1996). “Prediction of the transition nappe/skimming flow on a stepped channel.” *Journal of Hydraulic Research*, 34(3), 421–429.

Chanson H., and Toombes L. (2002). "Strong interactions between free-surface aeration and turbulence in an open channel flow." *Experimental Thermal and Fluid Science,* 2003, 27(5): 525-535.

Cicero, G.M., Menon, J.M., Luck, M., Pinchard, T. (2011). “Experimental study of side and scale effects on hydraulic performances of a Piano Key Weir.” *Proc. Int. Conf. Labyrinth and Piano Key Weirs Liège B, 167–172,* CRC Press, Boca Raton, FL.

Cicero G-M & Delisle JR (2013). “Effects of the crest shape on the discharge efficiency of a Type-A Piano Key weir.” Proceedings of the 2nd International Workshop on Labyrinth and Piano Key Weirs (PKW 2013), pp. 41–48. CRC Press, Taylor & Francis Group.

Cicero, G.M., Vermeulen, J. and Laugier, F. (2016). “Influence of Some Geometrical

Parameters on Piano Key Weir Discharge Efficiency." 6th International Symposium on Hydraulic Structures and Water System Management, Portland, Oregon, USA, 27-30 June 2016, ISBN 978-1-884575-75-4

Crookston, B.M. and Tullis, B.P. (2012). "Labyrinth weirs: Nappe interference and local submergence." *J. Irrig. Drain. Engr., ASCE, 138(8), 757-765.*

Crookston, B.M. and Tullis, B.P. (2012a). "Hydraulic design and analysis of labyrinth weirs. Part 1: Discharge relationships." *J. Irrig. Drain. Engr., ASCE, #(#). Posted ahead of print (date).*

Crookston, B.M. ASCE, A.M. and Tullis, B.P. (2012b). "Hydraulic design and analysis of Labyrinth weirs: Part-II: Nappe Aeration, Instability and Vibration." *J. Irrig. Drain. Engr., ASCE, 138(8), 757-765*.

Crookston, B. M., & Tullis, B. P. (2013). "Hydraulic Design and Analysis of Labyrinth Weirs. II: Nappe Aeration, Instability, and Vibration." *Journal of Irrigation and Drainage Engineering*, 139, 371 - 377.

Crookston, B., Anderson, R., and Tullis, B. (2018). "Free-flow discharge estimation method for Piano Key weir geometries." *J. Hydro. Environ. Res.*, 19, 160–167. doi:10.1016/j.jher.2017.10.003.

Crookston, B. M., Erpicum, S., Tullis, B. P., and Laugier, F. (2019). "Hydraulics of Labyrinth and Piano Key Weirs: 100 Years of Prototype Structures, Advancements, and Future Research Needs." *Journal of Hydraulic Engineering*, 145(12), 02519004.

Crookston, B. M. (2020). "A laboratory investigation on residual energy of nonlinear weirs." *Proceedings of the 8th IAHR International Symposium on Hydraulic Structures, ISHS 2020*.

Dabling, M.R. and Tullis, B.P. (2012). "Piano Key Weir submergence in channel applications." Proc. International Workshop on Piano Key Weir for In-Stream Storage and Safety, New Delhi, India. 13-23.

Denys, F. (2017). "Piano Key Weir spillway standard design principles and flow induced vibrations." (May), 0–15. *Proceedings of the 3rd International Workshop on Labyrinth and Piano Key Weirs (PKW 2017)*, pp. 119-126. CRC Press, Taylor & Francis Group.

Denys F, Basson G and Strasheim J (2017). “Fluid Structure Interaction of Piano Key Weirs.” Proceedings of the 3rd International Workshop on Labyrinth and Piano Key Weirs (PKW 2017), Qui Nhon, Vietnam, 119-126.

Denys F and Basson G (2018). “Transient Hydrodynamics of Piano Key Weirs.” 7th *International Symposium on Hydraulic Structures. Aachen, Germany*, 15-18 May 2018, ISBN 978-0-692-13277-7.

Dugue, V., Hachem, F., Boillat, J.-L., Nagel, V., Roca, J.-P., Laugier, F. (2011). “P. K. Weir and flap gate spillway for the Gage II Dam.” *Proc. Int. Conf. Labyrinth and Piano Key Weirs Liege B, 35–42, CRC Press, Boca Raton, FL.*

Elyass, Sahad Salim. 2012. *“*Effect of Channel Slope on Energy Dissipation of Flow for Single Step Broad – Crested Weirs, Introduction*:” 16(3): 91–103.Weirs Liege B, 35–42, CRC Press, Boca Raton, FL.*

Erpicum, S., Laugier, F., Boillat, J.L., Pirotton, M., Reverchon, B., and Schleiss, A.J. (2011). *Labyrinth and Piano Key Weirs - PKW 2011*. CRC Press, London, UK.

Erpicum, S., Machiels, O., Archambeau, P., Dewals, B., Pirotton, M. (2011a). “1D numerical modeling of the flow over a Piano Key Weir.” *Proc. Int. Conf. Labyrinth and Piano Key Weirs*”. Liege B, 151–158, CRC Press, Boca Raton, FL.

Erpicum, S., Laugier, F., Pfister, M., Pirotton, M., Cicero, G., and Schleiss, A.J. (2013). *Labyrinth and Piano Key Weirs II - PKW 2013*. CRC Press, London, UK.

Erpicum, S., Machiels, O., Dewals, B., Archambeau, P. and Pirotton, M. (2013a). “Considerations about the optimum design of PKW.” *Proceeding International conference Water Storage and Hydropower Development for Africa (Africa 2013)*. Addis Ababa, Ethiopia.

Erpicum, S., Archambeau, P., Pirotton, M. and Dewals, B.J. (2014). “Geometric parameters influence on Piano Key Weir hydraulic performances.” *5th International Symposium on Hydraulic Structures and Society*: Engineering Challenges and Extremes, Brisbane, Australia, 25-27 June 2014, ISBN 9781742721156.

Erpicum, S., Tullis, B. P., Lodomez, M., Archambeau, P., Dewals, B. J., & Pirotton, M. (2016). “Scale effects in physical piano key weir models.” *Journal of Hydraulic*

Research, 54(6), 692-698.

Erpicum, S., Laugier, F., Ho Ta Khanh, M., and Pfister, M. (2017). "*Labyrinth and Piano Key Weirs III - PKW 2017*." CRC Press, London, U.K.

Erpicum, S., Archambeau, P., Dewals, B. and Pirotton, M. (2017). "Hydraulics of Piano Key Weirs: A review." In Erpicum, S., Laugier, F., Ho Ta Khanh, M., and Pfister, M. (2017). *Labyrinth and Piano Key Weirs III - PKW 2017.* CRC Press, London, U.K., 27-36.

Ervine, D., and Elsawy, E. (1975). "The effect of a falling nappe on river aeration." Proc. 16th IAHR Congress, Sao Paulo, Brazil.

Eslinger, K. R., and Crookston, B. M. (2020). "Energy Dissipation of Type a Piano Key Weirs."

Falvey, H.T. (1980). "Air-water flow in hydraulic structures". NASA STI/ Recon Technical Report N, 81. Gabriel-Martin.

Falvey H.T. (2003). "Hydraulic design of labyrinth weirs." ASCE Press (*American Society of Civil Engineers*).

Fen, N., Kozlov, D.B., and Rumyantsev, I.S. (2016). "Hydraulic studies of stepped spillways of various design." *Power Technol. Eng.* 49, 337–344.

Ferreira, C. (2001). "Gene Expression Programming : A New Adaptive Algorithm for Solving Problems." 1–22.

Ferreira, C. (2001a). "Gene expression programming in problem-solving." In: 6th Online World Conference on Soft Computing in Industrial Applications (invited tutorial).

Ferreira, C. (2001b). "Gene expression programming: a new adaptive algorithm for solving problems." *Complex Systems* 13 (2), 87–129.

Gameson, A.L.H. (1957). "Weirs and aeration of rivers." *J. Inst Water Eng* 11(5), 477–490.

Gameson, A. L. H., Vandyke, K. G., and Ogden, C. G.(1958), *"*The Effect of Temperature on Aeration*", Water and Water Engineering, November 1958.*

Garg, S. K., (2010). Irrigation Engineering and Hydraulic Structures. *Khanna publishers,*

New-Delhi- 110002

Gebhardt, M., J. Herbst, J. Merkel, and F. Belzner. (2018). "Sedimentation at labyrinth weirs—An experimental study of the self-cleaning process." *J. Hydraul. Res.* 1–12. https://doi.org/10.1080/00221686.2018.1494053.

Ghaderi, A., Abbasi, S., Abraham, J., and Azamathulla, H. M. (2020). "Efficiency of Trapezoidal Labyrinth Shaped stepped spillways." *Flow Measurement and Instrumentation*, Elsevier Ltd, 72(February), 101711.

Ghanbari, R., and Heidarnejad, M. (2020). "Experimental and numerical analysis of flow hydraulics in triangular and rectangular piano key weirs." *Water Science*, Taylor & Francis, 00(00), 1–7.

Ghare, A. D., Mhaisalkar, V. A. & Porey, P. D., (2008). An Approach to Optimal Design of Trapezoidal Labyrinth Weirs. World Applied Sciences Journal 3, pp. 934- 938.

Gonzalez, C.A.; Chanson, H.: Turbulence and Cavity Recirculation in Air-Water Skimming Flows on a Stepped Spillway. *Journal of Hydraulic Research, IAHR, Vol.* 46, No. 1, *pp*. 65–72, (2008).

Gulliver J. S., Thene J .R. and Rindels, A. J. (1990). "Indexing gas transfer in self-aerated flows." *J. Environ." Eng., ASCE 116 (3) 503-523.*

Haghiabi, A. H., Ghaleh Nou, M. R., and Parsaie, A. (2021). "The energy dissipation of flow over the labyrinth weirs." *Alexandria Engineering Journal*, THE AUTHORS, 0–4.

Hien, T.C., Son, H.T., & Khanh, M.H.T. (2006). "Results of some piano keys weir hydraulic model tests in Vietnam". Proc. of the 22nd Congress of ICOLD, Barcelona, Spain.

Ho Ta Khanh, M., Sy Quat. D., and Xuan Thuy D., (2011). "PK weirs under design and construction in Vietnam (2010)." Labyrinth and piano key weirs-PKW 2011: 225-232. CRC Press: London.

Ho Ta Khanh, M. (2013). "The Piano KeyWeirs: 15 years of research & development – Prospect." Labyrinth and Piano Key weirs II – PKW2013, CRC Press, London, 3–14.

Ho Ta Khanh, M. (2017). "History and development of Piano Key Weirs in Vietnam from 2004 to 2016." In Erpicum, S., Laugier, F., Ho Ta Khanh, M., and Pfister, M. (2017).

Labyrinth and Piano Key Weirs III - PKW 2017. CRC Press, London, U.K., 3-16

Hotaki, A. and Hailkar, S.S. (2017). "Assessment of Discharge Enhancement of Piano Key and Rectangular Labyrinth Spillway and Hydraulic Comparison." International Journal for Research in Applied Science & Engineering Technology, ISSN: 2321-9653, Volume 5 Issue VII, July 2017

Hu, H., Qian, Z., Yang, W., Hou, D., and Du, L. (2018). "Numerical study of characteristics and discharge capacity of piano key weirs." *Flow Meas. Instrum.,* 62, 27–32. doi:10.1016/j.flowmeasinst.2018. 05.004

ICOLD 2010. ICOLD Bulletin 144: Cost Savings in Dams. Appendix 2. International Commission on Large Dams.

John, C. K., Pu, J. H., Pandey, M., and Hanmaiahgari, P. R. (2021a). "Sediment deposition within rainwater: Case study comparison of four different sites in ikorodu, Nigeria." Fluids, 6(3).

John, C. K., Pu, J. H., Pandey, M., and Moruzzi, R. (2021b). "Impacts of sedimentation on rainwater quality: Case study at Ikorodu of Lagos, Nigeria." Water Supply, 21(7), 3356–3369.

Jüstrich, S., Pfister, M., and Schleiss, A. J. (2016). "Mobile riverbed scour downstream of a piano key weir." *Journal of Hydraulic Engineering*, 142(11), 1–12.

Karbasi, M., and Azamathulla, H. M. (2016). "GEP to predict characteristics of a hydraulic jump over a rough bed." *KSCE Journal of Civil Engineering*, 20(7), 3006–3011.

Kabiri-Samani A & Javaheri A (2012). "Discharge coefficients for free and submerged flow over Piano Key weirs." J*ournal of Hydraulic Research*, *Taylor & Francis*, vol. 50, no. 1, pp. 114–120, February 2012.

Karimi, M., Attari, J., Saneie, M., and Ghazizadeh, M. R. J. (2018). "Side weir flow characteristics: Comparison of piano key, labyrinth, and linear types." *Journal of Hydraulic Engineering*, 144(12), 1–13.

Kashkaki, Z., Banejad, H., and Heydari, M. (2018). "Application of ANN in Estimating Discharge Coefficient of Circular Piano Key Spillways." *Soft Computing in Civil*

Engineering, 2(3), 39–49.

Khassaf, S. I., Aziz, L. J., and Elkatib, Z. A. (2015). "Hydraulic Behavior Of Piano Key Weir Type B Under Free Flow Conditions." *International Journal of Scientific & Technology Research*, 4(8), 158–163.

Kumar, B., Kadia, S., and Ahmad, Z. (2019). "Evaluation of discharge equations of the piano key weirs." *Flow Measurement and Instrumentation*, Elsevier Ltd, 68(February), 101577.

Kumar, B., and Ahmad, Z. (2020). "Experimental Study on Scour Downstream of a Piano Key Weir with Nose." (2019).

Kumar, B., Kadia, S., and Ahmad, Z. (2021). "Sediment Movement over Type A Piano Key Weirs." *Journal of Irrigation and Drainage Engineering*, 147(6), 04021018.

Kumar, B., and Ahmad, Z. (2022). "Scour Downstream of a Piano Key Weir with and without a Solid Apron." *Journal of Irrigation and Drainage Engineering*, 148(1), 1–12.

Lade, A., Jaltade, A., Kulkarni, J., Kokate, M., Lavate, A., and Harihar, R. (2015). "Experimental Study of Different Sill Geometries in Piano Key Weirs." *International Journal of Civil Engineering and Technology*, 6(2), 976–6308.

Laiadi, A.; Athmani, B.' Belaabed, F.; Ouamane, A. (2017) "The effect of the geometric shape of the alveoli on the performance of Piano Key Weirs." In Erpicum, S., Laugier, F., Ho Ta Khanh, M., and Pfister, M. (2017). *Labyrinth and Piano Key Weirs III - PKW 2017.* CRC Press, London, U.K., 27-36.

Lantz, W., Crookston, B. M., and Palermo, M. (2021). "Apron and cutoff wall scour protection for piano key weirs." *Water (Switzerland)*, 13(17).

Lantz, W. D., Crookston, B. M., and Palermo, M. (2022). "Evolution of local scour downstream of Type A PK weir in non-cohesive sediments." (2021), 103–113.

Laugier, F. (2007). "Design and construction of the first Piano Key Weir spillway at Goulours dam." *Intl. J. Hydropower & Dams*, 14(5), 94-100.

Laugier, F., Lochu, A., Gille, C., Leite Ribeiro, M., Boillat, J.-L. (2009). "Design and

construction of a labyrinth PKW spillway at St-Marc Dam, France." Intl. J. Hydropower Dams 15(5), 100–107.

Laugier F, Vermeulen J & Lefebvre V (2013). "Overview of Piano Key Weirs experience developed at EDF during the past few years." *Proceedings of the 2nd International Workshop on Labyrinth and Piano Key Weirs (PKW 2013)*, pp. 213-226. CRC Press, Taylor & Francis Group.

Laugier, F., Vermeulen, J., and Blancher, B. (2017). "Overview of design and construction of 11 piano key weir spillways developed in France by EDF from 2003 to 2006." In Erpicum, S., Laugier, F., Ho Ta Khanh, M., and Pfister, M. (2017). *Labyrinth and Piano Key Weirs III - PKW 2017*. CRC Press, London, U.K., 37-51.

Le Doucen, O., Leite Ribeiro, M., Boillat, J. L., Schleiss, A. and Laugier, F. (2009). "Etude parametrique de la capacite des PK-Weirs." Modeles physiques hydrauliques-outils indispensables du XXle siècle, Lyon: SHF.

Leite Ribeiro, M., Boillat, J.L., Schleiss, A., Laugier, F., and Albalat, C. (2007). "Rehabilitation of St-Marc dam – Experimental Optimization of a Piano Key Weir." Proc. of 32nd Congress of IAHR., Vince, Italy.

Leite Ribeiro, M., Bieri, M., Boillat, J., L., Schleiss, A., Delorme, F., and Laugier, F. (2009). "Hydraulic capacity improvement of existing spillways—Design of piano key weirs." *Proc., 23rd Congress of Large Dams. Question 90, Response 43 (CD-ROM), Int. Commission on Large Dams (ICOLD), Paris.*

Leite Ribeiro, M., Boillat, J.-L., and Schleiss, A.J. (2011). "Experimental parametric study for hydraulic design of PKWs." Proc. Int. Conf. Labyrinth and Piano Key Weirs, Liege B, 183–190, CRC Press, Boca Raton, FL.

Leite Ribeiro, M., Bieri, M., Boillat, J. L., Schleiss, A. J., Singhal, G., and Sharma, N. (2012). "Discharge capacity of piano key weirs." *Journal of Hydraulic Engineering*, 138(2), 199–203.

Leite Ribeiro M, Pfister M, Schleiss AJ, & Boillat J-L (2012a). "Hydraulic design of A-type Piano Key Weirs." Journal of Hydraulic Research, Taylor & Francis, Volume 50, Issue 4, pp. 400-408.

Leite Ribeiro, M., Pfister, M., Boillat, J. L., Schleiss, A.J., Laugier, F. (2012b). “Piano Key Weirs as efficient spillway Structure.” 24th ICOLD Congress Kyoto (Q94, R13), 1–10.

Leite Ribeiro, M. Pfister M. and Schleiss, A. J. (2013). “Overview of Piano Key weir prototypes and scientific model investigations.” Proceedings of the 2nd International Workshop on Labyrinth and Piano Key Weirs (PKW 2013), pp. 273–281. CRC Press, Taylor & Francis Group.

Lempérière, F. and Ouamane, A. (2003). “The piano keys weir: a new cost-effective solution for spillways, Hydropower and Dams”, 10(5):144-149.

Lempérière, F., and Jun G. (2005). “Low Cost Increase of Dams Storage and Flood Mitigation: The Piano Keys Weir.” Q.53 R. 2.06 International Commission on Irrigation and Drainage Nineteenth Congress Beijing.

Lempérière, F. (2009). “New Labyrinth weirs triple the spillways discharge.” <http://www.hydrocoop.org > (Feb. 8, 2010).

Lempérière, F. and Vigny, J. (2011). “General comments on labyrinth and Piano Keys Weirs–The future.” Labyrinth and Piano Key weirs-PKW 2011, 289–294.

Lempérière F, Vigny J. P. and Ouamane, A. (2011). “General comments on Labyrinth and Piano Key Weirs: The past and present.” Proceedings of the International Conference on Labyrinth and Piano Key Weirs (PKW 2011), pp. 17-24. CRC Press, Taylor & Francis Group.

Lempérière, F. (2013). New labyrinth weirs triple the spillways discharge. <http://www.hydrocoop.org>.

Li G., Li, S. and Hu, Y. (2019) “The effect of the inlet/outlet width ratio on the discharge of piano key weirs.” Journal of Hydraulic Research, 1686.

Lodomez, M., Pirotton, M., Dewals, B., Archambeau, P., & Erpicum, S. (2018). “Nappe oscillations on free-overfall structures: Experimental analysis.” Journal of Hydraulic Engineering, 144(3).

Lombaard, J. (2020). “Evaluation of the Influence of Aeration on the Discharge Capacity and Flow Induced Vibrations of Piano Key Weir Spillways.” (March) Masters of

Machiels, O., Erpicum, S., Archambeau, P., Dewals, B.J., & Pirotton, M. (2009). “Large scale experimental study of piano key weirs.” Proc. of 33rd of IAHR., Vancouver, Canada.

Machiels, O., Erpicum, S., Archambeau, P., Dewals, B.J., Pirotton, M. (2011a). “Influence of the Piano Key Weir height on its discharge capacity.” Proc. Int. Conf. Labyrinth and Piano Key Weirs Liege B, 59–66, CRC Press, Boca Raton, FL.

Machiels, O., Erpicum, S., Dewals, B.J., Archambeau, P., Pirotton, M. (2011b). “Influence of the alveoli slopes on the discharge capacity of Piano Key Weirs.” 34th IAHR World Congress, Brisbane, Australia.

Machiels, O., Erpicum, S., Archambeau, P., Dewals, B.J., Pirotton, M. (2011c). “Piano Key Weir preliminary design method – application to a new dam project.” Proc. Int. Conf. Labyrinth and Piano KeyWeirs Liège B, 199–206,CRC Press, Boca Raton, FL.

Machiels, O., Erpicum, S., Dewals, B.J., Archambeau, P., and Pirotton, M. (2011d). “Experimental observation of flow characteristics over a Piano Key Weir.” J. Hydraulic Res. 49(3), 359–366.

Machiels O. (2012). “Experimental study of the hydraulic behaviour of Piano Key Weirs.” Ph.D. Thesis ULgetd-09252012- 224610, University of Liege (Belgium).

Machiels, O., Erpicum, S., Archambeau, P., Dewals, B., and Pirotton, M. (2013). “Parapet wall effect on piano key weir efficiency.” *Journal of Irrigation and Drainage Engineering*, 139(6), 506–511.

Machiels, O., Pirotton, M., Archambeau, P., Dewals, B., and Erpicum, S. (2014). “Experimental parametric study and design of Piano Key Weirs.” Journal of Hydraulic Research, Taylor & Francs, 52(3), 326–335.

Magalhães, A.P., Lorena, M. (1994). "Perdas de Energiado do Escoamento Sobre Soleiras em Labirinto." (Energy Losses in Flow Over Labyrinth Weirs); SILUSBA: Lisboa, Portugal, pp. 203–211. (In Portuguese)

Mario Oertel, (2015). “Discharge coefficient of piano key weir from experimental and numerical models.” *E. proceedings of the 36th IAHR world congress*.

Mehboudi, A.; Attari, J. ; Hosseini, S. A.: Flow regimes over trapezoidal Piano Key Weirs. In Erpicum, S., Laugier, F., Ho Ta Khanh, M., and Pfister, M. (2017). Labyrinth and Piano Key Weirs III - PKW 2017. CRC Press, London, U.K., 65-74 (2017).

Mehri, Y., Esmaeili, S., and Soltani, J. (2020). "Experimental study and performance comparison on various types of rectangular piano key side weirs at a 120° section of a 180° curved channel." *Applied Water Science*, Springer International Publishing, 10(10), 1–13.

Merkel, J., Belzner, F., Gebhardt, M., and Thorenz, C. (2018). "Energy dissipation downstream of labyrinth weirs." *7th IAHR International Symposium on Hydraulic Structures, ISHS 2018*, 508–517.

Michael P. and Schleiss, A. J. (2013). "Estimation of A-type Piano Key weir rating curve." Proceedings of the 2nd International Workshop on Labyrinth and Piano Key Weirs (PKW 2013), pp. 139–147. CRC Press, Taylor & Francis Group.

Mishra, R. K., and Ahmad, Z. (2021). "DigitalCommons @ USU International Junior Researcher and Engineer Discharge Capacity of a Piano Key Weir with Curvilinear Keys Discharge Capacity of a Piano Key Weir with Curvilinear Keys."

Noseda, M., Stojnic, I., Pfister, M., and Schleiss, A. J. (2019). "Upstream Erosion and Sediment Passage at Piano Key Weirs." *Journal of Hydraulic Engineering*, 145(8), 04019029.

Noui, A. and Ouamane, A., (2011). "Study of optimization of the Piano Key Weir." Proceedings of the International Conference Labyrinth and Piano Key Weirs 2011, Liege, Belgium, CRC Press, London, pp. (175–182).

Noui, A., and Ouamane, A. (2013). "Study of optimization of the piano key weir." Labyrinth and piano key weirs II, CRC/ Balkema, Leiden, Netherlands, 175–182.

Novak, P., Guinot, V., Jeffrey, A., & Reeve, D. E. (2010). Hydraulic Modelling: An Introduction: Principles, methods, and applications.

Oertel, M., and Tullis, B., P. (2014). "Comparison of Piano Key Weir Discharge Coefficients from experimental and numerical models." Proc. 3rd IAHR Europe Congress, Porto, Portugal.

Oertel, M. (2016). “Sensitivity analysis for discharge coefficients of Piano Key Weirs.” *6th International Symposium on Hydraulic Structures: Hydraulic Structures and Water System Management, ISHS 2016*, 3330628160, 540–548.

Ouamane, A., Lempérière, F., (2006). “Design of a new economic shape of weir.” Proc. of the International Symposium of Dams in the Societies of the 21st Century, Barcelona, Spain, 463-470.

Pandey, M., Chen, S. C., Sharma, P. K., Ojha, C. S. P., and Kumar, V. (2019). “Local scour of armor layer processes around the circular pier in non-uniform gravel bed.” *Water (Switzerland)*, 11(7), 1–10.

Pandey, M., Oliveto, G., Pu, J. H., Sharma, P. K., and Ojha, C. S. P. (2020a). “Pier scour prediction in non-uniform gravel beds.” *Water (Switzerland)*, 12(6), 13–17.

Pandey, M., Zakwan, M., Khan, M. A., and Bhave, S. (2020b). “Development of scour around a circular pier and its modeling using genetic algorithm.” *Water Science and Technology: Water Supply*, 20(8), 3358–3367.

Pandey, M., Jamei, M., Karbasi, M., Ahmadianfar, I., and Chu, X. (2021). “Prediction of Maximum Scour Depth near Spur Dikes in Uniform Bed Sediment Using Stacked Generalization Ensemble Tree-Based Frameworks.” *Journal of Irrigation and Drainage Engineering*, 147(11), 04021050.

Pandey, M., and Md Azamathulla, H. (2021). “ Discussion of ‘Gene-Expression Programming, Evolutionary Polynomial Regression, and Model Tree to Evaluate Local Scour Depth at Culvert Outlets’ by Mohammad Najafzadeh and Ali Reza Kargar .” *Journal of Pipeline Systems Engineering and Practice*, 12(2), 07021001.

Parsaie, A., Haghiabi, A. H., Saneie, M., and Torabi, H. (2018). “Prediction of Energy Dissipation of Flow Over Stepped Spillways Using Data-Driven Models.” *Iranian Journal of Science and Technology - Transactions of Civil Engineering*, Springer International Publishing, 42(1), 39–53.

Parsaie, A., and Haghiabi, A. H.(2019a). "Inception point of flow aeration on quarter-circular crested stepped spillway." *Flow Measurement and Instrumentation*, 69 (August), 101618. https://doi.org/10.1016/j.flowmeasinst.2019.101618

Parsaie, A., and Haghiabi, A. H.(2019b). "The hydraulic investigation of circular crested stepped spillway." *Flow Measurement and Instrumentation*, 70 (August), 101624. https://doi.org/10.1016/j.flowmeasinst.2019.101624

Paxson, G. S, Tullis, B. P, and Hertel, D. J. (2013). "Comparison of Piano Key Weirs with labyrinth and gated spillways: Hydraulics, cost, constructability and operations." Proceedings of the 2nd International Workshop on Labyrinth and Piano Key Weirs (PKW 2013), pp. 123–130. CRC Press, Taylor & Francis Group.

Peyras, L., Royet, P., and Degoutte, G. (1991). "Ecoulement et Dissipation sur les Déversoirs en Gradins de Gabions." *Journal La Houille Blanche,* No. 1, pp. 37–47. in French).

Pfister, M., Capobianco, D., Tullis, B., Schleiss, A., (2013). "Debris-Blocking sensitivity of Piano Key weirs under reservoir-type approach flow." Journal of Hydraulic Engineering, Vol. 139, No. 11, pp. 1134-1141.

Pfister M, and Schleiss A.J. (2013a). "Comparison of hydraulic design equations for A-type Piano Key weirs." Proceeding International conference Water Storage and Hydropower Development for Africa (Africa 2013). Addis Ababa, Ethiopia.

Pfister, M., Schleiss, A. J., and Tullis, B. (2013b). "Effect of driftwood on hydraulic head of Piano Key weirs." Proceedings of the 2nd International Workshop on Labyrinth and Piano Key Weirs- PKW 2013, Paris, France, 20-22 november 2013, Erpicum et al. (Eds), CRC Press, Boca Raton, pp. 255-265.

Pfister M., Tullis B., ASCE M., Schleiss A. J. (2015). Closure to "Debris-Blocking Sensitivity of Piano Key Weirs under Reservoir-Type Approach Flow." by Michael Pfister, Damiano Capobianco, Blake Tullis, and Anton J. Schleiss. Journal of Hydraulic Engineering, 141(10).

Pfister M, Justrich, S. and Schleiss, A. J. (2017). "Toe scour formation at Piano Key weirs." In Erpicum, S., Laugier, F., Ho Ta Khanh, M., and Pfister, M. (2017). Labyrinth and Piano Key Weirs III - PKW 2017. CRC Press: Leiden.

Phillips MA and Lesleighter EJ (2013). "Piano Key Weir spillway: Upgrade option for a major dam." Proceedings of the 2nd International Workshop on Labyrinth and Piano Key Weirs (PKW 2013), pp. 159–168. CRC Press, Taylor & Francis Group.

Pralong, J., Vermeulen, J., Blancher, B., Laugier, F., Erpicum, S., MacHiels, O., Pirotton, M., Boillat, J. L., Leite Ribeiro, M., and Schleiss, A. J. (2011). "A naming convention for the Piano Key Weirs geometrical parameters." *Labyrinth and Piano Key Weirs - Proceedings of the International Conference on Labyrinth and Piano Key Weirs, PKW 2011*, 271–278.

Ranga Raju, K.G. *(2005). Flow-through open channels, Tata McGraw Hills, New Delhi, 194–196.*

Rajaratnam, N. (1990). "Skimming Flow in Stepped Spillways." J*ournal of Hydraulic Engineering, ASCE, Vol*. 116, *No*. 4, *pp*. 587–591.

Ramakrishna, K., Banupriya, R. and Rajashree, R., (2014). "Determination of coefficient of discharge for piano key weirs of varying geometry." Asian journal of applied science Volume, 7 (6): 499-509.

Saghari, A., Saneie, M. and Hosseini K.,(2019). "Experimental study of one- and two-cycle trapezoidal piano-key side weirs in a curved channel." Water Supply Press. IWA Publishing 2019.

Sancold, (1991). Safety Evaluation of Dams, Report No.4: Guidelines on Safety in Relation to Floods, s.l.: South African National Committee on Large Dams (SANCOLD).

Sangsefidi, Y., Tavakol-Davani, H., Ghodsian, M., Mehraein, M., and Zarei, R. (2021). "Hydrodynamics and free-flow characteristics of piano key weirs with different plan shapes." *Water (Switzerland)*, 13(15).

Schleiss A. J., (2011). "From Labyrinth to Piano Key Weirs - A historical review." Proceedings of the International Conference on Labyrinth and Piano Key Weirs (PKW 2011), pp. 3–15. CRC Press, Taylor & Francis Group.

Sharma, N. and Singhal, G. (2008). "A Dam Safety Solution by Piano Key Weir for enhanced spillway capacity." *Proceedings of the International Conference on Hydro Vision, July 14-18, 2008, Sacramento, CA., USA.*

Sharma, N. and Tiwari, H. (2013). "Experimental study on vertical velocity and submergence depth near Piano Key weir." Labyrinth and Piano Key Weirs II. –PKW 2013 – Erpicum et al. (eds) ©2014 Taylor & Francis Group, London, ISBN (pp. 93-100).

Silverstri, A., Erpicum, S., Archambeau, P., Dewals, B. and Pirotton, M. (2013a). “Stepped spillway downstream of a Piano Key weir- Critical length of uniform flow.” International Workshop on hydraulic structures. Bundesanstalt fur, Wasserbau, Karlsruhe, Germany, 99-107.

Silverstri, A., Archambeau, P., Pirotton, M., Dewals, B. and Erpicum, S. (2013b). “Comparative analysis of the energy dissipation on a stepped spillway downstream of a Piano Key weir.” Labyrinth and piano key weirs II-PKW 2013: 111-120. CRC Press, London.

Singh, D., and Kumar, M. (2021). “A Comparable Study on Aeration Performance of PK weir with its Alternatives.” “Hydro-2020” International Conference on Hydraulics, Water Resources, and Coastal Engineering, organized by NIT, NIT Rourkela on 26-28 March 2021.

Singh, D., and Kumar, M. (2022). “Hydraulic Design and Analysis of Piano Key Weirs : A Review.” *Arabian Journal for Science and Engineering*, Springer Berlin Heidelberg.

Singh, D., and Kumar, M. (2022a). “Energy dissipation of flow over the type-B Piano Key Weir.” *Flow Measurement and Instrumentation*, Elsevier Ltd, 83(November 2021), 102109.

Singh, D., and Kumar, M. (2022b). “Study on aeration performance of different types of piano key weir.” *Water Supply*, 00(0), 1–12.

Singh, D., and Kumar, M. (2022c). “Gene expression programming for computing energy dissipation over type-B piano key weir.” *Renewable Energy Focus*, Elsevier Ltd, 41, 230–235.

Subramanya, K., (2010). Flow in Open Channels. Tata McGraw Hill Education Private Limited, New Delhi.

Tabbara, M., Chatila, J., and Awwad, R. (2005). "Computational simulation of flow over stepped spillways." Comput. Struct. 83, 2215–2224, https://doi.org/10.1016/j. compstruc.2005.04.005.

Tiwari, H., and Sharma, N. (2017). “Turbulence study in the vicinity of piano key weir: relevance, instrumentation, parameters and methods.” *Applied Water Science*, Springer

Berlin Heidelberg, 7(2), 525–534.

Torabi, H., Parsaie, A., Yonesi, H., and Mozafari, E. (2018). "Energy Dissipation on Rough Stepped Spillways." *Iranian Journal of Science and Technology - Transactions of Civil Engineering*, Springer International Publishing, 42(3), 325–330.

Truong Chi, H. and Ho Ta Khanh, M., (2017). "Experimental study for energy dissipation using stilling basin downstream of a P. K. weirs type A." Labyrinth and piano key weirs III-PKW 2017 CRC Press: Leiden.

Tullis, B. P., Asce, M., Crookston, B. M., Asce, M., Brislin, J., Asce, S. M., and Seamons, T. (2020a). "Geometric Effects on Discharge Relationships for Labyrinth Weirs." 146(10), 1–10.

Tullis, B. P., Ph, D., Asce, M., Crookston, B. M., Ph, D., Asce, M., Young, N., and Asce, M. (2020b). "Scale Effects in Free-Flow Nonlinear Weir Head-Discharge Relationships." 146(2), 1–9.

Tullis, B. P., Jorgensen, T. J., and Crookston, B. M. (2021). "Effects of a Labyrinth Weir with Outlet Ramps on Downstream Steep-Stepped Chute Sidewall Height Requirements." *Journal of Irrigation and Drainage Engineering*, 147(12), 04021057.

Ujeniya, V. D., Mehta, K. G. and Khan, Mohd. (2016). "Optimization of Piano Key Weir for Dam." International Journal of Management, IT & Engineering, Vol. 6 Issue 9, ISSN: 2249-0558.

Ujeniya, V. D., Mehta, K. G. and Khan, Mohd. (2016a). "A Review of Perametric Studies of Piano Key Weir." International Journal of Research in Engineering and Applied Sciences, Vol. 6 Issue 7, July 2016, pp. 24-28 ISSN(O): 2249-3905, ISSN(P) : 2349-6525.

Vermeulen, J., Laugier, F., Faramond, L., Gille, C. (2011). "Lessons learnt from design and construction of EDF first Piano Key Weirs." Proc. Int. Conf. Labyrinth and Piano Key Weirs". Liège B, 215–224, CRC Press, Boca Raton, FL.

Vermeulen, J., Lassus, C., & Pinchard, T. (2017). "Design of a Piano Key Weir Aeration Network." Proceedings of the 3rd International Workshop on Labyrinth and Piano Key Weirs III - PKW 2017, Qui Nhon, Vietnam, 22-24 February 2017 (pp. 127-134).

London: Taylor & Francis Group.

Vischer, D. L. and Hager, W. H., (1998). Dam Hydraulics (1st ed.). Wiley.

Yazdi, A. M., Abbas Hoseini, S., Nazari, S., and Amanian, N. (2021). “Effects of weir geometry on scour development in the downstream of Piano Key Weirs.” *Water Science and Technology: Water Supply*, 21(1), 289–298.

Zhao, C., H. Fang, Y. Liu, S. Dey, and G. He. (2020). “Impact of particle shape on saltating mode of bedload transport sheared by turbulent flow.” J. Hydraul. Eng. 146 (5): 04020034. https://doi.org/10.1061/(ASCE) HY.1943-7900.0001735

Zounemat-Kermani, M., and Mahdavi-Meymand, A. (2019). “Hybrid meta-heuristics artificial intelligence models in simulating discharge passing the piano key weirs.” *Journal of Hydrology*, Elsevier, 569(November), 12–21.